# A COMPREHENSIVE STUDY OF RECYCLED CONCRETE AGGREGATES AS A DRAINABLE BASE LAYER FOR PAVEMENTS

by

JUAN BOSQUEZ JR.

Presented to the Faculty of the Graduate School of

The University of Texas at Arlington in Partial Fulfillment

of the Requirements

for the Degree of

DOCTOR OF PHILOSOPHY

THE UNIVERSITY OF TEXAS AT ARLINGTON

August 2009

ACKNOWLEDGEMENTS

The author would like to express his sincere appreciation to his advising professor, Dr. Anand J. Puppala, for providing guidance and encouragement throughout this research study. His knowledge and expertise have served as an invaluable resource for providing the necessary direction for the success of this dissertation.

The author would also like to convey his gratitude to Dr. Laureano R. Hoyos, Dr. Melanie L. Sattler, Dr. Mohammad Najafi, and Dr. Chien-Pai Han for their time and acceptance to be on the examination committee.

Most of all, the author would like to express his dearest appreciation to his wife, Judith, and daughter, Lauren, for their patience, understanding, and support throughout the course of his studies and research work.

July 15, 2009

ABSTRACT

A COMPREHENSIVE STUDY OF RECYCLED CONCRETE AGGREGATES

AS A DRAINABLE BASE LAYER FOR PAVEMENTS

Juan Bosquez Jr., PhD.

The University of Texas at Arlington, 2009

Supervising Professor: Anand J. Puppala

The use of recycled materials in construction is becoming increasingly popular due to the shortage of raw materials. Coupled with the environmental concerns surrounding the quarrying of natural minerals, waste materials are being considered as viable replacement sources. By recycling waste materials, available landfill space is increased and costs of transportation are reduced.

This dissertation study was conducted to evaluate the use of recycled concrete aggregates as flexible base as per the requirements of the Texas Department of Transportation (2004). Two sources of recycled aggregates and one source of natural limestone aggregate were collected from the Dallas/Fort Worth Area and used in the present study. The selected materials were evaluated in laboratory conditions, modeled in the use as base materials for flexible and rigid pavement structures, and compared in cost for their use in construction.

Laboratory testing was conducted to assess the physical, mechanical, and flow properties of the materials. The physical properties testing provided characterization of the materials that were used to ensure specification requirements. The major testing program was conducted to determine the small strain shear modulus ($G_{max}$) using bender elements. In doing so, the $G_{max}$ results were used to estimate the modulus of elasticity of the materials. Unconfined compressive strengths (UCS) were also determined for the materials. Both $G_{max}$ and UCS were measured at varying moisture contents at 7-day and 28-day curing periods. The moisture contents represented a dry, optimum, and wet of optimum conditions related to 95% optimum dry density conditions. Results from the study show UCS to be highest at optimum moisture content-dry density condition and to increase with curing time. Results from the study also show $G_{max}$ to decrease with an increase in moisture content and increase with curing time. Permeability of all three materials met the requirements for drainage of base courses. The recycled aggregates demonstrated a decrease in permeability with an increase in moisture content.

Flexible and rigid pavement tables were prepared for varying traffic and materials conditions. The determined modulus of elasticity was employed into the design of the pavement structures. Based on the design of pavement structures for flexible pavements, base course layer thickness using recycled aggregates were greater in poor subgrade conditions and high traffic volume conditions. The rigid pavement design structures showed no effects due to base course layer thickness.

The cost analysis for the use of recycled materials concurs that savings can be expected during the construction. Maintenance and rehabilitation costs were not included in the analysis as both types of materials showed similar properties and hence are expected to perform similarly. The use of recycled aggregates can produce positive impacts on engineering, economic, and social environments.

TABLE OF CONTENTS


| | |
|---|---|
| ACKNOWLEDGEMENTS…… | iii |
| ABSTRACT…… | iv |
| LIST OF ILLUSTRATIONS…….. | x |
| LIST OF TABLES…….. | xix |
| Chapter | Page |
| 1. INTRODUCTION…… | 1 |
| 1.1 Recycled Aggregates…… | 1 |
| 1.1.1 Demolition of Reinforced Concrete Structures and Pavements…..……. | 2 |
| 1.1.2 Use of Crushing Plant Operation for Recycling Concrete…….. | 2 |
| 1.1.3 Natural Aggregates…..…….. | 3 |
| 1.1.4 Use of Recycled Aggregates in Flexible Pavement……. | 3 |
| 1.1.5 Use of Recycled Aggregates in Rigid Pavement……..….. | 4 |
| 1.2 Research Objective……..…… | 5 |
| 2. LITERATURE REVIEW…… | 6 |
| 2.1 Recycled Materials Applications..…….. | 6 |
| 2.1.1 Use of Recycled Materials in Transportation..…… | 6 |
| 2.1.1.1 Blast Furnace Slag..……. | 6 |
| 2.1.1.2 Steel Slag...…….……. | 7 |
| 2.1.1.3 Waste Tires……..……. | 7 |
| 2.1.1.4 Carpet Fiber Waste..……. | 8 |
| 2.1.1.5 Glass Cullet……..……. | 9 |

2.1.1.6 Hydrated Fly Ash……. 10

2.1.1.7 Cement Kiln Dust……. 11

2.1.1.8 High-Density Polyethylene……. 11

2.1.1.9 Recycled Asphalt Pavement……. 12

2.2 Recycled Aggregates Testing…….. 13

2.2.1 Use of Recycled Aggregates from Crushed Concrete…… 13

2.2.1.1 Use of Recycled Aggregates as a Base Course…… 14

2.2.1.2 Use of Recycled Aggregates in Portland Cement Concrete……. 20

2.3 Bender Element Testing…….. 23

2.3.1 Theory of Bender Elements…….. 23

2.3.2 Interpretation of Bender Elements Results…….. 27

2.4 Pavement Design…….. 30

2.4.1 Flexible Pavement Design..…….. 31

2.4.2 Rigid Pavement Design……..…….. 33

2.5 Summary…….. 38

3. EXPERIMENTAL PROGRAM……. 39

3.1 Introduction……..…….. 39

3.2 Properties of Testing Materials..……..…….…. 39

3.2.1 Gradation of Materials……..……..…… 42

3.2.2 Compaction Moisture Content – Dry Density Curves…….. 47

3.2.3 Plasticity Index……..……..…… 52

3.2.4 pH and Specific Gravity…..……..……..…… 53

3.2.5 Shear Modulus Testing Using Bender Elements…… 54

3.2.6 Unconfined Compression Strength Testing…..…… 62

3.2.7 Permeability Testing..…….……..…… 65

3.3 Summary……..…….…….…….. 66

4. MECHANICAL AND FLOW PROPERTIES OF RECYCLED CONCRETE AGGREGATES…….…….. 67

4.1 Introduction…….. 67

4.2 Engineering Properties…….…… 67

4.2.1 Unconfined Compression Strength (UCS) Test…….. 68

4.2.1.1 Effects of Moisture Content on Unconfined Compression Strength…….……. 77

4.2.1.2 Effects of Curing Period on Unconfined Compression Strength…….……. 81

4.2.2 Small Strain Shear Modulus $G_{max}$ Determination Using Bender Element Testing……. 87

4.2.2.1 Effects of Moisture Content on Small Strain Shear Modulus $G_{max}$....…….……. 96

4.2.2.2 Effects of Curing Period on Small Strain Shear Modulus $G_{max}$....…….. 100

4.2.3 Determination of Coefficient of Permeability..……. 105

4.2.3.1 Effects of Moisture Content on Permeability…… 110

4.3 Statistical Analysis…….…… 115

4.3.1 Statistical Analysis Within Materials……. 115

4.3.1.1 Statistical Analysis of Unconfined Compression Strength……..…. 115

4.3.1.2 Statistical Analysis of Small Strain Shear Modulus $G_{max}$……..……. 118

4.3.1.3 Statistical Analysis of Permeability...……. 121

4.3.2 Statistical Analysis Between Materials……. 122

4.3.2.1 Statistical Analysis of Unconfined Compression Strength……...…….……. 123

4.3.2.2 Statistical Analysis of Small Strain Shear Modulus $G_{max}$.....……. 124

4.3.2.3 Statistical Analysis of Permeability..... 126

4.4 Summary..... 127

5. FLEXIBLE AND RIGID PAVEMENT DESIGN..... 128

5.1 Introduction..... 128

5.2 Modulus of Elasticity..... 128

5.3 Flexible Pavement Design..... 129

5.4 Flexible Pavement Design Comparisons..... 166

5.5 Rigid Pavement Design..... 176

5.6 Rigid Pavement Design Comparisons..... 211

5.7 Benefits of Using Recycled Aggregates..... 221

5.8 Summary..... 221

6. COST ANALYSIS..... 222

6.1 Introduction..... 222

6.2 Life Cycle Cost Analysis (LCCA)..... 222

6.3 Construction Costs..... 223

6.4 Sustainability of Recycled Aggregates..... 231

6.5 Summary..... 232

7. SUMMARY OF FINDINGS AND FUTURE RESEARCH DIRECTION..... 233

7.1 Introduction..... 233

7.2 Summary of Findings..... 233

7.3 Future Recommendations..... 237

APPENDIX

A. PHOTOS OF LABORATORY SAMPLES AND TESTING..... 238

B. PHOTOS OF CONCRETE RECYCLING EQUIPMENT..... 243

REFERENCES..... 245

BIOGRAPHICAL INFORMATION..... 249

LIST OF ILLUSTRATIONS


| Figure | | Page |
|---|---|---|
| 2.1 | Resilient modulus variation according to Two-Parameter Model (Nataatmadja and Tan, 2001)…… | 17 |
| 2.2 | Results from repeated load triaxial tests after different storing time (Arm, 2001)…..…….. | 18 |
| 2.3 | Comparison of resilient modulus between crushed concrete and granite (Arm, 2001)…..……. | 19 |
| 2.4 | Series connected piezo-ceramic bender element (Dyvik and Madshus, 1986).……..…….. | 24 |
| 2.5 | Parallel connected piezo-ceramic bender element (Dyvik and Madshus, 1986)……..…… | 25 |
| 2.6 | Schematic for bender element (Baig and Nazarian, 1995)..……..…… | 26 |
| 2.7 | Variations of different methods for determining travel time of shear wave (Kung et al., 2004)…….……. | 28 |
| 2.8 | Variations of shear wave velocity $V_s$ versus $L_{tt}/\lambda$ (Kung et al., 2004)…….. | 29 |
| 2.9 | Variations of shear wave velocity $V_s$ versus $\lambda/L_b$ (Kung et al., 2004)……..…… | 30 |
| 2.10 | Design chart for flexible pavements (AASHTO, 1993)…… | 35 |
| 2.11 | Design chart for rigid pavements – Segment 1 (AASHTO, 1993)…….. | 36 |
| 2.12 | Design chart for rigid pavements – Segment 2 (AASHTO, 1993)…….. | 37 |
| 3.1 | Crushed limestone aggregate test material…….…… | 40 |
| 3.2 | Recycled concrete aggregate RC1 test material…….. | 41 |
| 3.3 | Recycled concrete aggregate RC2……..… | 41 |
| 3.4 | Sieve analysis test results for crushed concrete aggregate RC1.....…….. | 43 |
| 3.5 | Sieve analysis test results for crushed concrete aggregate RC2…….……. | 44 |
| 3.6 | Sieve analysis test results for crushed limestone aggregate…..……..….. | 45 |

3.7 Sieve Analysis test results for all three materials…… 46

3.8 Density curve for recycled aggregate RC1……..…… 49

3.9 Density curve for recycled aggregate RC2…… 50

3.10 Density curve for limestone aggregate……..…. 51

3.11 Linear bar shrinkage test for samples…… 53

3.12 40 MHz Arbitrary Waveform Generator…….. 55

3.13 Pico Technology oscilloscope…….. 56

3.14 End cap with piezo-ceramic bender element…….. 56

3.15 Specimen in triaxial chamber with bender elements…… 58

3.16 Small strain shear modulus $G_{max}$ value for limestone at varying confining pressure……..……. 59

3.17 Small strain shear modulus Gmax value for recycled concrete aggregate RC1 varying confining pressure…..…… 60

3.18 Unconfined bender element experiment instrumentation set up……... 61

3.19 Shear wave measurement of crushed limestone aggregate for a 7-day curing period……..…….…… 62

3.20 Four-inch diameter specimen in compression with digital displacement recorder……..…. 63

3.21 Test Mark CM-3000 compression machine with digital Loading indicating system……. 64

3.22 Falling-head permeameter testing apparatus set up……..……. 65

4.1 Unconfined compression strength of recycled concrete aggregate RC1 at different moisture content after 7 days of curing…….. 71

4.2 Unconfined compression strength of recycled concrete aggregate RC1 at different moisture content after 28 days of curing…….. 72

4.3 Unconfined compression strength of recycled concrete aggregate RC2 at different moisture content after 7 days of curing…….. 73

4.4 Unconfined compression strength of recycled concrete aggregate RC2 at different moisture content after 28 days of curing……... 74

4.5 Unconfined compression strength of limestone aggregate at different moisture content after 7 days of curing…….. 75

4.6 Unconfined compression strength of limestone aggregate at different moisture content after 28 days of curing…….. 76

4.7 Average values of unconfined compression strength for recycled concrete aggregate RC1 at different moisture content for 7 and 28 day curing……. 78

4.8 Average values of unconfined compression strength for recycled concrete aggregate RC2 at different moisture content for 7 and 28 day curing……. 79

4.9 Average values of unconfined compression strength for limestone aggregate at different moisture content for 7 and 28 day curing…… 80

4.10 Ratio of 28-day to 7-day for average values of unconfined compression strength for recycled concrete aggregate RC1…….. 83

4.11 Ratio of 28-day to 7-day for average values of unconfined compression strength for recycled concrete aggregate RC2…….. 84

4.12 Ratio of 28-day to 7-day for average values of unconfined compression strength for crushed limestone aggregate…….. 85

4.13 Ratio of 28-day to 7-day for average values of unconfined compression strength for all three materials…….. 86

4.14 Average values of small strain shear modulus $G_{max}$ of recycled concrete aggregate RC1 for 7 day curing……. 90

4.15 Average values of small strain shear modulus $G_{max}$ of recycled concrete aggregate RC1 for 28 day curing……. 91

4.16 Average values of small strain shear modulus $G_{max}$ of recycled concrete aggregate RC2 for 7 day curing……. 92

4.17 Average values of small strain shear modulus $G_{max}$ of recycled concrete aggregate RC2 for 28 day curing……. 93

4.18 Average values of small strain shear modulus $G_{max}$ of limestone aggregate for 7 day curing……. 94

4.19 Average values of small strain shear modulus $G_{max}$ of limestone aggregate for 28 day curing……. 95

4.20 Average values of small strain shear modulus $G_{max}$ of recycled concrete aggregate RC1 for 7 and 28 day curing……. 97

4.21 Average values of small strain shear modulus $G_{max}$ of recycled concrete aggregate RC2 for 7 and 28 day curing……. 98

4.22 Average values of small strain shear modulus $G_{max}$ of limestone aggregate RC1 for 7 and 28 day curing……. 99

4.23 Ratio of 28-day to 7-day for average values of small strain $G_{max}$ for recycled concrete aggregate RC1…….…….. 101

4.24 Ratio of 28-day to 7-day for average values of small strain $G_{max}$ for recycled concrete aggregate RC2…….…….. 102

4.25 Ratio of 28-day to 7-day for average values of small strain $G_{max}$ for crushed limestone aggregate…….…….. 103

4.26 Ratio of 28-day to 7-day for average values of small strain $G_{max}$ for all three materials…….…….. 104

4.27 Coefficient of permeability of recycled concrete aggregate RC1 for varying moisture content……..….. 107

4.28 Coefficient of permeability of recycled concrete aggregate RC2 for varying moisture content……..….. 108

4.29 Coefficient of permeability of limestone aggregate for varying moisture content……..….. 109

4.30 Average values for coefficient of permeability of all three materials for varying moisture content……..….. 111

4.31 Comparison for coefficient of permeability of all three materials for varying moisture content……..….. 112

4.32 Recycled concrete aggregate RC1 at wet density condition during compaction…… 113

4.33 Compacted recycled concrete aggregate RC1 at wet density condition…… 114

5.1 Design chart for determining thickness of base layer for interstates using recycled concrete aggregate RC1……..…….. 139

5.2 Design chart for determining thickness of base layer for interstates using recycled concrete aggregate RC1…….……..…. 140

5.3 Design chart for determining thickness of base layer for interstates using recycled concrete aggregate RC1…….……..…. 141

5.4 Design chart for determining thickness of base layer for state highways using recycled concrete aggregate RC1…….……..…. 142

5.5 Design chart for determining thickness of base layer for state highways using recycled concrete aggregate RC1…….……..…. 143

5.6 Design chart for determining thickness of base layer for state highways using recycled concrete aggregate RC1…….……..…. 144

5.7 Design chart for determining thickness of base layer for city roads using recycled concrete aggregate RC1…….……..……..…. 145

5.8 Design chart for determining thickness of base layer for city roads using recycled concrete aggregate RC1……..…….…. 146

5.9 Design chart for determining thickness of base layer for city roads using recycled concrete aggregate RC1……..…….…. 147

5.10 Design chart for determining thickness of base layer for interstates using recycled concrete aggregate RC2……..…….. 148

5.11 Design chart for determining thickness of base layer for interstates using recycled concrete aggregate RC2……..…. 149

5.12 Design chart for determining thickness of base layer for interstates using recycled concrete aggregate RC2……..…. 150

5.13 Design chart for determining thickness of base layer for state highways using recycled concrete aggregate RC2……..…. 151

5.14 Design chart for determining thickness of base layer for state highways using recycled concrete aggregate RC2……..…. 152

5.15 Design chart for determining thickness of base layer for state highways using recycled concrete aggregate RC2……..…. 153

5.16 Design chart for determining thickness of base layer for city roads using recycled concrete aggregate RC2……..…….…. 154

5.17 Design chart for determining thickness of base layer for city roads using recycled concrete aggregate RC2……..…….…. 155

5.18 Design chart for determining thickness of base layer for city roads using recycled concrete aggregate RC2……..…….…. 156

5.19 Design chart for determining thickness of base layer for interstates using limestone aggregate……..…….…. 157

5.20 Design chart for determining thickness of base layer for interstates using limestone aggregate……..…….…. 158

5.21 Design chart for determining thickness of base layer for interstates using limestone aggregate……..…….…. 159

5.22 Design chart for determining thickness of base layer for state highways using limestone aggregate……..…….…. 160

5.23 Design chart for determining thickness of base layer for state highways using limestone aggregate……..…….…. 161

5.24 Design chart for determining thickness of base layer for state highways using limestone aggregate……..…….…. 162

5.25 Design chart for determining thickness of base layer for city roads using limestone aggregate……..…….…. 163

5.26 Design chart for determining thickness of base layer for city roads using limestone aggregate…. 164

5.27 Design chart for determining thickness of base layer for city roads using limestone aggregate…. 165

5.28 Comparison of base layer thickness between recycled aggregates and limestone aggregates for interstate traffic conditions…… 167

5.29 Comparison of base layer thickness between recycled aggregates and limestone aggregates for interstate traffic conditions…... 168

5.30 Comparison of base layer thickness between recycled aggregates and limestone aggregates for interstate traffic conditions…... 169

5.31 Comparison of base layer thickness between recycled aggregates and limestone aggregates for highway traffic conditions…... 170

5.32 Comparison of base layer thickness between recycled aggregates and limestone aggregates for highway traffic conditions…... 171

5.33 Comparison of base layer thickness between recycled aggregates and limestone aggregates for highway traffic conditions…... 172

5.34 Comparison of base layer thickness between recycled aggregates and limestone aggregates for city traffic conditions…... 173

5.35 Comparison of base layer thickness between recycled aggregates and limestone aggregates for city traffic conditions…... 174

5.36 Comparison of base layer thickness between recycled aggregates and limestone aggregates for city traffic conditions…... 175

5.37 Design chart for determining rigid pavement thickness for interstates using recycled concrete aggregate RC1…... 184

5.38 Design chart for determining rigid pavement thickness for interstates using recycled concrete aggregate RC1…... 185

5.39 Design chart for determining rigid pavement thickness for interstates using recycled concrete aggregate RC1…... 186

5.40 Design chart for determining rigid pavement thickness for state highways using recycled concrete aggregate RC1…… 187

5.41 Design chart for determining rigid pavement thickness for state highways using recycled concrete aggregate RC1…… 188

5.42 Design chart for determining rigid pavement thickness for state highways using recycled concrete aggregate RC1…… 189

5.43 Design chart for determining rigid pavement thickness for city roads using recycled concrete aggregate RC1…… 190

5.44 Design chart for determining rigid pavement thickness for city roads using recycled concrete aggregate RC1……..…..…..……..…. 191

5.45 Design chart for determining rigid pavement thickness for city roads using recycled concrete aggregate RC1……..…..…..……..…. 192

5.46 Design chart for determining rigid pavement thickness for interstates using recycled concrete aggregate RC2….....…..……..…. 193

5.47 Design chart for determining rigid pavement thickness for interstates using recycled concrete aggregate RC2….....…..……..…. 194

5.48 Design chart for determining rigid pavement thickness for interstates using recycled concrete aggregate RC2….....…..……..…. 195

5.49 Design chart for determining rigid pavement thickness for state highways using recycled concrete aggregate RC2……..…..……..…. 196

5.50 Design chart for determining rigid pavement thickness for state highways using recycled concrete aggregate RC2……..…..……..…. 197

5.51 Design chart for determining rigid pavement thickness for state highways using recycled concrete aggregate RC2……..…..……..…. 198

5.52 Design chart for determining rigid pavement thickness for city roads using recycled concrete aggregate RC2……..…..…..……..…. 199

5.53 Design chart for determining rigid pavement thickness for city roads using recycled concrete aggregate RC2……..…..…..……..…. 200

5.54 Design chart for determining rigid pavement thickness for city roads using recycled concrete aggregate RC2……..…..…..……..…. 201

5.55 Design chart for determining rigid pavement thickness for interstates using limestone aggregate…….....…..……..…. 202

5.56 Design chart for determining rigid pavement thickness for interstates using limestone aggregate…….....…..……..…. 203

5.57 Design chart for determining rigid pavement thickness for interstates using limestone aggregate…….....…..……..…. 204

5.58 Design chart for determining rigid pavement thickness for state highways using limestone aggregate…….....…..……..…. 205

5.59 Design chart for determining rigid pavement thickness for state highways using limestone aggregate…….....…..……..…. 206

5.60 Design chart for determining rigid pavement thickness for state highways using limestone aggregate…….....…..……..…. 207

5.61 Design chart for determining rigid pavement thickness for city roads using limestone aggregate…….....…..……..…. 208

5.62 Design chart for determining rigid pavement thickness for city roads using limestone aggregate……..... 209

5.63 Design chart for determining rigid pavement thickness for city roads using limestone aggregate……..... 210

5.64 Comparison of CRCP pavement thickness with aggregate base layer for interstate traffic conditions……..... 212

5.65 Comparison of CRCP pavement thickness with aggregate base layer for interstate traffic conditions……..... 213

5.66 Comparison of CRCP pavement thickness with aggregate base layer for interstate traffic conditions……..... 214

5.67 Comparison of CRCP pavement thickness with aggregate base layer for highway traffic conditions……..... 215

5.68 Comparison of CRCP pavement thickness with aggregate base layer for highway traffic conditions……..... 216

5.69 Comparison of CRCP pavement thickness with aggregate base layer for highway traffic conditions……..... 217

5.70 Comparison of CRCP pavement thickness with aggregate base layer for city traffic conditions……..... 218

5.71 Comparison of CRCP pavement thickness with aggregate base layer for city traffic conditions……..... 219

5.72 Comparison of CRCP pavement thickness with aggregate base layer for city traffic conditions……..... 220

6.1 Comparison in cost of limestone and recycled aggregates as flexible base material……..... 226

6.2 Total cost for flexible base construction of a 381.0 mm (15-inch) lift……..... 229

LIST OF TABLES


| | Table | Page |
|---|---|---|
| 2.1 | Aggregate Specification Requirements for Flexible Base (TxDOT, 2004)…… | 14 |
| 2.2 | Comparisons of Performance Using Two-Parameter Model (Nataatmadja and Tan, 2001)…… | 16 |
| 2.3 | Properties of Natural Aggregate (Poon and Chan, 2006)…… | 20 |
| 2.4 | Properties of Recycled Concrete Aggregates (Poon and Chan, 2004)…… | 20 |
| 2.5 | Effect of RCA on Mechanical of Concrete (FHWA, 2007)…… | 22 |
| 2.6 | Effect of RCA on Fresh Concrete Properties (FHWA, 2007)…… | 22 |
| 2.7 | Effect of RCA on Concrete Durability (FHWA, 2007)…… | 23 |
| 3.1 | Percent Retained for Sieve Analysis Gradation Requirements and Material Results…… | 42 |
| 3.2 | Percent Finer for Materials at Three Point Location on Grain Size Distribution Curve…… | 47 |
| 3.3 | Compaction Parameters…… | 48 |
| 3.4 | Summary of Optimum Dry Density and Optimum Moisture Content…… | 48 |
| 3.5 | Plasticity Index Testing Results…… | 52 |
| 3.6 | pH Measurements of Materials…… | 54 |
| 3.7 | Specific Gravity of Materials…… | 54 |
| 4.1 | Results for Unconfined Compression Strength of Recycled Concrete Aggregate RC1…… | 69 |
| 4.2 | Results for Unconfined Compression Strength of Recycled Concrete Aggregate RC2…… | 70 |
| 4.3 | Results for Unconfined Compression Strength of Limestone Aggregate…… | 70 |

4.4 Results of Small Strain Shear Modulus $G_{max}$ for Recycled Concrete Aggregate RC1……..……..……..... 88

4.5 Results of Small Strain Shear Modulus $G_{max}$ for Recycled Concrete Aggregate RC2……..... 88

4.6 Results of Small Strain Shear Modulus $G_{max}$ for Limestone Aggregate……..……..……..... 89

4.7 Small Strain Shear Moduli from Resonant Column Tests (Hoyos et al. 2009)……..……..... 89

4.8 Results for Permeability of Recycled Concrete Aggregates RC1……..……..……..……..... 106

4.9 Results for Permeability of Recycled Concrete Aggregates RC2……..……..……..... 106

4.10 Results for Permeability of Limestone Aggregates……..... 106

4.11 UCS t-test Results for Recycled Concrete Aggregate RC1 at 7 days……..……..... 116

4.12 UCS t-test Results for Recycled Concrete Aggregate RC1 at 28 days……..……..... 116

4.13 UCS t-test Results for Recycled Concrete Aggregate RC1 for 7 day to 28 day Comparison……..……..... 116

4.14 UCS t-test Results for Recycled Concrete Aggregate RC2 at 7 days……..……..... 117

4.15 UCS t-test Results for Recycled Concrete Aggregate RC2 at 28 days……..……..... 117

4.16 UCS t-test Results for Recycled Concrete Aggregate RC2 for 7 day to 28 day Comparison……..……..... 117

4.17 UCS t-test Results for Limestone Aggregate at 7 days…..……..... 117

4.18 UCS t-test Results for Limestone Aggregate at 28 days...…….... 118

4.19 UCS t-test Results for Limestone Aggregate for 7 day to 28 day Comparison……..……..... 118

4.20 $G_{max}$ t-test Results for Recycled Concrete Aggregate RC1 at 7 days……..……..... 119

4.21 $G_{max}$ t-test Results for Recycled Concrete Aggregate RC1 at 28 days……..……..... 119

4.22 $G_{max}$ t-test Results for Recycled Concrete Aggregate RC1 for 7 day to 28 day Comparison……..……..... 119

4.23 $G_{max}$ t-test Results for Recycled Concrete Aggregate RC2 at 7 days…… 120

4.24 $G_{max}$ t-test Results for Recycled Concrete Aggregate RC2 at 28 days…… 120

4.25 $G_{max}$ t-test Results for Recycled Concrete Aggregate RC2 for 7 day to 28 day Comparison…… 120

4.26 $G_{max}$ t-test Results for Limestone Aggregate at 7 days…… 120

4.27 $G_{max}$ t-test Results for Limestone Aggregate at 28 days…… 121

4.28 $G_{max}$ t-test Results for Limestone Aggregate for 7 day to 28 day Comparison…… 121

4.29 Permeability t-test Results for Recycled Concrete Aggregate RC1…… 122

4.30 Permeability t-test Results for Recycled Concrete Aggregate RC2…… 122

4.31 Permeability t-test Results for Limestone Aggregate…… 122

4.32 t-test Comparison of Materials for Unconfined Compression Strength…… 123

4.33 t-test Comparison of Materials for Unconfined Compression Strength…… 124

4.34 t-test Comparison of Materials for Unconfined Compression Strength…… 124

4.35 t-test Comparison of Materials for Small Strain $G_{max}$…… 125

4.36 t-test Comparison of Materials for Small Strain $G_{max}$…… 125

4.37 t-test Comparison of Materials for Small Strain $G_{max}$…… 125

4.38 t-test Comparison of Materials for Coefficient of Permeability…… 126

4.39 t-test Comparison of Materials for Coefficient of Permeability…… 126

4.40 t-test Comparison of Materials for Coefficient of Permeability…… 126

5.1 Modulus of Elasticity and Structural Coefficient for Recycled Concrete Aggregate RC1…… 130

5.2 Modulus of Elasticity and Structural Coefficient for Recycled Concrete Aggregate RC2…… 130

5.3 Modulus of Elasticity and Structural Coefficient for Limestone Aggregate…… 131

5.4 Traffic Variables for Type of Highway System…… 131

5.5 Material Variables for Type of Highway System…… 132

5.6 Design Table for Interstate Traffic Conditions with Recycled Concrete Aggregate RC1 as Base Material…… 134

5.7 Design Table for Highway Traffic Conditions with Recycled Concrete Aggregate RC1 as Base Material…… 134

5.8 Design Table for City Road Traffic Conditions with Recycled Concrete Aggregate RC1 as Base Material…… 135

5.9 Design Table for Interstate Traffic Conditions with Recycled Concrete Aggregate RC2 as Base Material…… 135

5.10 Design Table for Highway Traffic Conditions with Recycled Concrete Aggregate RC2 as Base Material…… 136

5.11 Design Table for City Road Traffic Conditions with Recycled Concrete Aggregate RC2 as Base Material…… 136

5.12 Design Table for Interstate Traffic Conditions with Limestone Aggregate as Base Material…… 137

5.13 Design Table for Highway Traffic Conditions with Limestone Aggregate as Base Material…… 137

5.14 Design Table for City Road Traffic Conditions with Limestone Aggregate as Base Material…… 138

5.15 Traffic Variables for Type of Highway System…… 177

5.16 Material Variables for Type of Highway System…… 177

5.17 Design Table for Interstate Traffic Conditions with Recycled Concrete Aggregate RC1 as Base Material CRCP Layer Thickness…… 179

5.18 Design Table for Highway Traffic Conditions with Recycled Concrete Aggregate RC1 as Base Material CRCP Layer Thickness…… 179

5.19 Design Table for City Road Traffic Conditions with Recycled Concrete Aggregate RC1 as Base Material CRCP Layer Thickness…… 180

5.20 Design Table for Interstate Traffic Conditions with Recycled Concrete Aggregate RC2 as Base Material CRCP Layer Thickness…… 180

5.21 Design Table for Highway Traffic Conditions with Recycled Concrete Aggregate RC2 as Base Material CRCP Layer Thickness……..……..…..…..… 181

5.22 Design Table for City Road Traffic Conditions with Recycled Concrete Aggregate RC2 as Base Material CRCP Layer Thickness……..…..…..… 181

5.23 Design Table for Interstate Traffic Conditions with Limestone Aggregate as Base Material CRCP Layer Thickness……..……..……..…..…. 182

5.24 Design Table for Highway Traffic Conditions with Limestone Aggregate as Base Material CRCP Layer Thickness ……..……..…..…..…. 182

5.25 Design Table for City Road Traffic Conditions with Limestone Aggregate as Base Material CRCP Layer Thickness ……..……..……..…..…. 183

6.1 Cost for Use of Flexible Base per Square Meter..…..……..…. 225

6.2 Cost for Use of Flexible Base per Square Meter…...…….……..…. 225

6.3 Example Cost Analysis for Flexible Base Requirement….……..…. 228

# CHAPTER 1

# INTRODUCTION

## 1.1 Recycled Aggregates

Use of recycled materials in construction is becoming increasingly popular due to the lack of available raw materials, and current environmental and economic concerns (Abou-Zeid & McCabe, 2002). With the creation of slow-decaying and non-decaying materials, waste disposal landfills are rapidly being consumed. In addition, the amount of waste being generated increases with the growth of the world population (Schroeder, 1994).

There are other factors that make the use of recycled materials a necessity. In some areas of the United States, the large amounts of waste materials that have been produced have cause a reduction in the amount of available landfill space. It is estimated that building demolition alone produces 123 million tons of construction waste per year (FHWA, 2004). The current production of concrete waste is mainly attributed to the demolition of structures and roadways. With the aging of roadways in the United States, the demolition and replacement of concrete pavements is increasing. The recycling of waste materials, especially demolished concrete, can increase the available landfill space and lessens the amount of raw materials needed for construction. The cost benefits for using recycled concrete aggregates in some regions of the United States may materialize into a savings of 20% to 30% less than natural aggregates (ReTAP, 1998). The Federal Highway Administration has noted that many states have high tipping fees for the disposal of recycled concrete aggregates (FHWA, 2004).

### *1.1.1 Demolition of Reinforced Concrete Structures and Pavements*

The demolition of concrete structures that are considered relatively young has occurred due to the loss of their intended function. Concrete structures, in existence for as little as twenty years, have been demolished in order to expand and modernize facilities. These demolished structures normally consist of concrete and steel. The steel materials are salvaged and delivered to metal scrap plants. However, the concrete rubble from these demolished structures is delivered to landfills.

Similarly, concrete pavements are being replaced due to the growth of populations and increased vehicular traffic. There has also been an increase in heavy truck traffic that has caused concerns due to damage inflicted on pavements. Therefore, the increase in traffic volume and heavy traffic loads have required for pavements to be expanded or replaced. As in concrete structures, demolished concrete pavements consist of steel materials that are salvaged and concrete rubble that is delivered to landfills.

### *1.1.2 Use of Crushing Plant Operation for Recycling Concrete*

The recycling of demolished concrete by using a concrete crushing operation is an alternative for wasting. At this time, there are several mobile crushing plants available suitable for this operation. Mobile plants are easy to transport, set up on site quickly, and can effectively convert rubble to base aggregate (Landers, 2004). Through proper planning and permitting, a mobile crushing plant can be set on site or close to the site in which a concrete demolition is occurring. The type of crusher, primary impactor or jaw crusher, and the screening design can affect the versatility and function of the concrete crushing plant. Moreover, the screening allows for different size aggregate materials to be separated and discharged through conveyor belts.

During the demolition of reinforced concrete, most of the steel reinforcement separates from the concrete. This allows for minimal steel to be loaded with the concrete rubble that is delivered to the concrete crushing plant. The steel reinforcement that remains with the concrete rubble is separated at the crushing plant through a mechanical method with the use of magnets.

The concrete can be crushed into different particle sizes and separated by screening. By using proper screening, the crushed concrete can be produced to meet an array of different gradations. This allows for the demolished concrete to be processed similarly to natural aggregates.

### *1.1.3 Natural Aggregates*

Over two billion tons of natural aggregates are produced in the United States for use in construction (FHWA, 2004). These natural aggregates are obtained by the method of quarrying. Quarrying processes however, require a vast amount of land and cause several environmental concerns. The environmental effects of quarrying include the continual noise and dust pollution (Chini & Monteiro, 1999). The large amounts of water use have also caused concerns for depletion of water supply and runoff management. The growth of cities have caused for the quarries to relocate into areas further away from metropolitan areas in order to meet stricter environmental regulations. This in turn has increased the cost of the transportation from these remote locations. In addition, an increasing cost of fuel has added to an increased cost for delivery of the materials.

Natural aggregates are facing other problems. There has been an ongoing shortage of natural resources of aggregates used for concrete and as backfill for structures (Aqil, Tatsuoka, & Uchimura, 2005). The limited supply of natural aggregates in many areas of the United States has compounded the already increased costs in the delivery of the materials. This has served as an incentive for many states to develop or adopt the use of recycled aggregates.

### *1.1.4 Use of Recycled Aggregates in Flexible Pavement*

In Texas, a granular base is used in the construction of highways and has traditionally consisted of aggregates derived from crushed stone. Recently, allowances have been made for the use of crushed concrete as a granular base. The crushed concrete recycled for use as a

granular base must meet stringent requirements as required by the Texas Standard Specifications (2004).

The structure of a flexible pavement normally consists of a subgrade, subbase, granular base, and asphalt-concrete surface. The subbase is regularly omitted when the subgrade is found to meet or exceed the requirements of the subbase. The base course or granular base is considered to be the structural portion of the flexible pavement and lies directly under the surface course (Merritt, Loftin, & Ricketts, 1996). Its primary function is to increase the load capacity of the pavement and to distribute the applied load to avoid damage to the subgrade (Chini & Monteiro, 1999). Therefore, the specifications for the base course layer are therefore more stringent than those of a subbase. These specifications for the granular base include the properties of strength, stability, hardness, aggregate types, and gradation.

Use of recycled aggregates as a base course in flexible pavements is a viable alternative to wasting demolished concrete. By evaluating the properties of recycled aggregates, efficient flexible pavement designs can be determined. In doing so, the high cost of transporting is reduced and the need of landfill space is eliminated.

### *1.1.5 Use of Recycled Aggregates in Rigid Pavement*

As in flexible pavement, recycled aggregates can be used as a layer of granular base or subbase material in the pavement structure. The rigid pavement structure normally consists of a portland-cement concrete slab resting on a base or subbase that rests on a subgrade. This base or subbase layer can be that of a compacted granular material that provides a uniform, stable, and permanent support for the concrete pavement. In many cases, this layer of granular base or subbase can help increase the modulus of subgrade reaction, improves the effects of frost, and prevents the pumping of subgrade soils along the joints, cracks, and edges of the pavement (Merritt, Loftin, & Ricketts, 1996).

## 1.2 Research Objective

The main objective of this research is to characterize and evaluate the use of recycled concrete aggregates as a base course layer in pavement structures. The engineering properties of recycled concrete aggregates are compared to that of a natural aggregate that is commonly used as a base course aggregate. As non-destructive laboratory testing, bender elements are used due to their ability to measure dynamic shear moduli properties at small strains (less than $10^{-3}$ %). At very small shear strain levels, the shear modulus is maximum and nearly constant with shear strain. At large strains, shear modulus becomes a function of shear strain and is more complex to determine. The secondary objective of this research is to evaluate pavement structure layer thickness with the use of recycled aggregates and natural aggregate as base course layers. The objectives are to be completed by performing the following tasks:

- Review literature on recycled aggregates, natural aggregates, bender element testing, and pavement design concepts
- Use two sources of recycled aggregates and one of the natural aggregate
- Develop density curves and evaluate compacted samples of recycled aggregates and natural aggregate at dry, optimum, and wet moisture levels
- Perform bender elements tests to determine shear modulus at 7-day and 28-day curing periods
- Perform unconfined compression strength tests at 7-day and 28-day curing periods
- Determine the coefficient of permeability for the materials at different moisture content levels
- Determine and model the Resilient Modulus of a base course for the recycled aggregates and natural aggregate from test results
- Develop design thickness of base course layers for pavement structures
- Perform cost analysis for alternate pavement designs

# CHAPTER 2

# LITERATURE REVIEW

## 2.1 Recycled Materials Applications

Recycled materials have been successfully utilized in various construction projects. Particularly, there are many studies that have been conducted for the application of recycled materials in highway construction. These studies have been reviewed in order to obtain knowledge of the most advanced use of recycled materials.

### *2.1.1 Use of Recycled Materials in Transportation*

In recent years, the increasing problem with the disposal of waste materials has led to studies for the recycling and reusing of waste materials. Many studies conducted have produced acceptable recycled and reusable materials. Among the many materials studied, blast furnace slag, steel slag, rubber tires, carpet fibers, glass cullet, hydrated fly ash, cement kiln dust, high-density polyethylene, and recycled asphalt pavements have proven to be applicable materials in construction. The studies of these materials demonstrate the continual search for applications in which waste materials can be reused and not wasted.

#### 2.1.1.1 Blast Furnace Slag

As a by-product of iron in a blast furnace, slag consists mainly of silicates and aluminosilicates of lime (Schroeder, 1994). Three types of blast furnace can be produced depending on the cooling method. The different types of slag produced are air-cooled, expanded, and granulated. As many as 14 million metric tons of blast furnace slag have been sold in the United States in a year (Schroeder, 1994). Currently, air cooled slag in the United States has many uses in highway construction. The slag can be used as an additive in

concrete and asphalt mix, fill material in embankments, road base material, and as treatments for the improvement of soils.

Cervantes and Roesler (2007) describe that air-cooled slag binds well with Portland cement and asphalt mixtures due to the slag's rough finish and larger surface area in comparison to other aggregates. It is also noted that Ground Granulated Blast Furnace Slag (GGBFS) has a positive effect on the flexural and compressive strength of concrete. The increase in strength is most notable after 28 days.

2.1.1.2 Steel Slag

Steel slag is a by-product from steel making. The steel slag is produced in one of three furnace types: Open Hearth, Basic Oxygen or Electric Arc Furnace. The Electric Arc Furnace is the furnace type mostly used in the production of steel slag. With its significant amount of iron, steel slag is a very dense and hard material. Molten steel is solidified by cooling at atmospheric conditions. Further cooling of steel slag can be accomplished by the addition of water once solidification has occurred.

Steel slag also has several uses in highway construction similar to those of blast furnace. Most of its uses have been concentrated as road base material and fill material. Steel slag can at times possibly contain free lime. This will cause the steel slag material to become expansive. Therefore, proper selection is required in its application. Recently, steel slag has been used as a substitute for coarse aggregates in asphalt mixes to improve resistance to rutting and skid resistance (Huang, Bird, & Heidrich, 2007). However, the high specific gravity of steel can increase the density of the asphalt mix and cause an increase in the cost of transportation.

2.1.1.3 Waste Tires

Every year in the United States, about 279 million waste tires are disposed (Takallou & Takallou, 1991). The stockpiling of rubber tires has prompted the development of new ways to recycle and reuse waste tires. Due to the synthetic elastomers found in some tires, reclaiming of tires has become a more costly and complex process. Currently, scrap tires buried in landfills

account for about 75-80% of tire waste. In most landfills, tires must be shredded before they are accepted. In order to help alleviate some of the disposal and stockpiling of waste tires, several studies have been conducted to properly recycle waste tires into applicable materials in highway construction.

Due to the bulkiness of tires and tendency to float to the surface with time, rubber tires are best applied in soils after being shredded. The waste tires have to be shredded into small strips that are placed in embankments in an effort to help strengthen the soil. In other applications, tire chips are created and used in landscaping as substitute for mulch. The chips trap the moisture and prevent weeds from growing. As a whole, tires have had some limited success in building artificial reefs, breakwaters, dock bumpers, soil erosion control mats, and playground equipment. Tire rubber has also been used in asphalt rubber mixers. Most of the success of tire rubber in asphalt has been shown to occur in the open graded friction course. The tire rubber reduces cracking, improves the durability and reduces tire noise (Huang et al., 2007).

The application of shredded tires has been evaluated on materials handling, compaction, and environmental impact. Shredded tires do not present any major handling and placement problems in construction. Leachate analysis indicates little or no likelihood of adverse affects on groundwater (Eldin & Senouci, 1992). In sand, the addition of tire strips has shown an increase in the shear strength of the soil material. Mixtures of shredded tires and soil can be useful in highway fills that require a lightweight fill.

2.1.1.4 Carpet Fiber Waste

About 70 percent of carpet produced in the United States is used to replace existing carpets. This in turn produces approximately 1.2 million tons of carpet waste every year (Schroeder, 1994). In order to help alleviate some of the waste generated from the existing carpet disposal, several research studies are being conducted to determine the feasibility of using recycled fibers from carpet waste. These studies include the use of carpet fibers mixed in concrete, asphalt, and soils to provide improvements in the strength of these materials.

In concrete, fibers have been added to increase the toughness of the concrete and increase its tensile properties (Wang, Wu, & Li, 2000). Other benefits of fiber reinforced concrete include reduction of shrinkage, and improved fatigue strength, wear resistance, and durability. As in concrete, fibers in asphalt have been used to increase the toughness and fracture resistance (Putnam and Amirkhanian, 2004). The fibers are also used as a stabilizer in preventing draindown of the asphalt binder (Hansen, McGennis, Prowell, & Stonex, 2000). In soils, addition of carpet waste fibers to sands has improved the shear strength of the sand (Hossein, Poorebrahim, & Gray, 2004).

2.1.1.5 Glass Cullet

Glass is a municipal waste that comprises about 7 percent of municipal solid waste in the United States (Schroeder, 1994). This amounts to a total of approximately 12 million tons on an annual basis. Glass cullet (broken glass) has been extensively collected through recycling programs in many parts of the United States. Glass cullet is primarily reused to manufacture glass containers. Glass cullet, which has a relatively high density, is collected and transported to glass manufacturers.

The use of glass cullet is very limited. Currently, there is only one well established market. The glass container industry uses glass cullet in their glass production. In order to avoid color contamination, extensive sorting is required. The process of sorting is an involved process that makes the reuse of glass cullet to be very expensive. In addition, the high cost for transportation of this relatively high-density material has caused it to be an unpopular alternative. For these reasons, studies have been conducted in using glass cullet for other applications. These applications include that of roadway construction.

Glass cullet has been extensively evaluated in laboratory tests for different blends of cullet and soils for the Texas Department of Transportation (Nash et al., 1995). In this study, compaction tests for glass cullet in limestone did not have any noticeable effect on optimum moisture content and dry density of the blended material. The Texas Triaxial Tests had no appreciable change in the maximum corrected stress for the blended samples. It was

concluded that glass cullet, up to 20% by weight, may be mixed with granular material in structural fills without compromising the strength of the material. Permeability tests also show that glass cullet can be blended with limestone to provide a filter material.

Other studies have concentrated on using glass as an aggregate of asphalt mixes. Asphalt surface course pavement containing 10-15% of glass with a gradation of less than 4.75 mm have resulted in satisfactory performance (Huang, Bird, and Heidrich, 2007). Recycling glass for highway construction has become more popular when compared with the high costs of transporting the glass to recycling centers and manufacturing plants that can reuse the glass.

2.1.1.6 Hydrated Fly Ash

Fly ash is a by-product of coal combustion and is defined as the fine gas-borne particles of noncombustible material. The state of Texas generates over 50% of its electricity from coal burning plants, therefore producing millions of tons of by products on a yearly basis. According to the Texas Department of Transportation (2000), approximately 2.4 million tons of coal combustion products out of 12.8 million tons produced were used in construction for the year of 1996.

Coal power plants produce powdered fly ash that is cured with moisture. The cured stiffened fly ash is known as hydrated fly ash. Fly ash with natural reactivity can set in stockpiles without organized curing. The stiffened fly ash can attain compressive strengths as high as 15,000 kPa (Nash et al., 1995).

Fly ash is currently used mainly in conjunction with cement in Portland cement concrete. The use of fly ash in Portland cement concrete allows for more efficient mix designs to be developed. Even with the high usage of fly ash in concrete, large quantities of fly ash are still available. Recent focus has included the use of fly ash as an aggregate and as a roadway fill. The aggregate is created by crushing the stiffened fly ash. Properly processed hydrated fly ash will continue to gain strength after placement due to hydration. Low moisture contents provide higher strengths while a dried material may experience shrinkage.

#### 2.1.1.7 Cement Kiln Dust

Cement kiln dust (CKD) is produced as a by-product from the manufacturing of Portland cement. Annually, million of tons of kiln dust are collected and removed from the cement manufacturing process. The cement kiln dust is considered to pose a health hazard, and creates storage and disposal problems (Bagdadi et al., 1995).

Cement kiln dust is collected and removed as an industrial waste. This dust has no recycling or reuse plan available. The potential application of treating marginal soils in construction can help alleviate potential health hazards associated with the disposal of cement kiln dust.

Laboratory tests conducted of sand treated with cement kiln dust have shown compressive strength increases with the amount of cement kiln dust and curing duration. High temperatures also increase the compressive strength of sand. The dry density increases with the increase of cement kiln dust up to 50% (Baghdadi, Fatani, & Sabban, 1995). The increase in density can be attributed to the fines of the cement kiln dust filling the voids of the sand.

#### 2.1.1.8 High-Density Polyethylene

Polyethylene (plastics) exists in many forms. High-density polyethylene (HDPE) is used more frequently for the storage of various liquids. Many of these liquids are major household products. There are recycling and reuse programs for high-density polyethylene. Due to involved process of cleansing these containers, the programs have had limited success.

Secondary markets for the use of recycled high-density polyethylene have not developed. Due to its low melting point, reclaimed polyethylene is prohibited from being used to produce containers for consumption, drugs, or cosmetics (Benson & Khire, 1994). As with tires, high-density polyethylene strips are being added to soil embankments to improve soil strength characteristics.

Testing of soils reinforced with strips of reclaimed high-density polyethylene has found that strength and resistance to deformation are enhanced in sand. Sand specimens reinforced with high-density polyethylene have a higher resilient modulus and shear strength.

Reinforcement of the soil is determined to be affected by the aspect ratio (length/width) of the strips (Benson & Khire, 1994). The most significant increases in measured strength have occurred in specimens with a higher aspect ratio.

2.1.1.9 Recycled Asphalt Pavement

Recycled Asphalt Pavement (RAP) has been used for many years in Texas Department of Transportation (TxDOT) projects. RAP is produced by roto-milling existing asphalt pavement. The process of roto-milling, is widely used in construction in the state of Texas. With the more stringent environmental regulations in disposal of solid wastes, recycling of asphalt pavements is a more feasible option.

In 2007, TxDOT presented data showing that approximately 15 million tons of HMA were produced for TxDOT in the year of 2006. During this same year, approximately 3.2 million tons of RAP were recovered. Of the Rap recovered in 2006:

13% was reused in Hot Mix Asphalt HMA

24% was donated to Texas County governments

6% was used to backfill pavement edges

9% was used to rework base

4% was used as a base course

44% was used by TxDOT Maintenance or not formally accounted for

Additionally, there are still many uses for the RAP in TxDOT construction projects. In many instances, RAP has been used as a stabile material for temporary driveways. In doing so, the use of RAP is economical when it is produced on site and reused. On SH 360 in Grand Prairie, Texas, RAP has been used in a test section as a subbase for a concrete pavement structure.

Rathje, Trejo, and Folliard (2006) evaluated the used of RAP as a backfill for mechanically stabilized earth walls. The RAP was evaluated for gradation and compaction, strength, drainage, collapse potential, pullout, creep, and corrosion. The RAP was determined to have favorable gradation, strength, and drainage properties. However, corrosion and

potential for creep deformations did not allow the RAP to be recommended as a suitable material for backfill.

## 2.2 Recycled Aggregates Testing

In this study, crushed concrete aggregate material is evaluated for the purpose of determining its effectiveness as a granular base course for concrete and asphalt pavements. In order to accomplish this, an extensive background search and evaluation was conducted on previous studies in the use of recycled concrete aggregates. The research into the studies conducted on recycled concrete aggregates produced a wide array of information. The most beneficial studies found, compared crushed concrete aggregates to that of a material normally used as a base course. However, no information was found that shows the material to have been evaluated for $G_{max}$ using bender elements and its application in pavement designs.

### *2.2.1 Use of Recycled Aggregates from Crushed Concrete*

In 2004, the Federal Highway Administration (FHWA) projected that the production of aggregates is to increase to over 2.5 billion tons per year by the year of 2020. The FHWA conducted a review to capture the most advanced uses of recycled concrete aggregate (RCA) applicable to transportation use in the United States. The overall findings of the FHWA review presented RCA as a valuable resource when properly administered in engineering applications. In addition, there are other studies that have been conducted for the use of RCA outside of the transportation applications.

#### 2.2.1.1 Use of Recycled Aggregates as a Base Course

With the shortage of raw materials and the abundance of demolished concrete, studies have been conducted into recycling concrete waste materials. The demolished concrete that is converted into reusable aggregates through the process of crushing has been studied in highway applications as a base course. The use of recycled aggregates as a base course requires that the specifications applicable to other materials used as base course must be met

by the recycled materials. The properties that determine the use of a material in lieu of traditional materials are gradation, liquid limit, plasticity index, wet ball mill, and compressive strength (Standard Specifications for Construction and Maintenance of Highways, Streets, and Bridges, 2004). These specifications are presented on Table 2.1. Soundness requirements were found by Richardson and Jordan (1994) to have little effect on the strength of the samples. Permeability of a base course, however, plays an important part in providing a drainable material that helps prevent pavement failures.

Table 2.1 Aggregate Specification Requirements for Flexible Base (TxDOT, 2004)

**Table 1**
**Material Requirements**

| Property | Test Method | Grade 1 | Grade 2 | Grade 3 | Grade 4 |
|---|---|---|---|---|---|
| Master gradation sieve size (% retained) | Tex-110-E | | | | As shown on the plans |
| 2-1/2 in. | | – | 0 | 0 | |
| 1-3/4 in. | | 0 | 0–10 | 0–10 | |
| 7/8 in. | | 10–35 | – | – | |
| 3/8 in. | | 30–50 | – | – | |
| No. 4 | | 45–65 | 45–75 | 45–75 | |
| No. 40 | | 70–85 | 60–85 | 50–85 | |
| Liquid limit, % max.[1] | Tex-104-E | 35 | 40 | 40 | As shown on the plans |
| Plasticity index, max.[1] | Tex-106-E | 10 | 12 | 12 | As shown on the plans |
| Plasticity index, min.[1] | | As shown on the plans | | | |
| Wet ball mill, % max.[2] | Tex-116-E | 40 | 45 | – | As shown on the plans |
| Wet ball mill, % max. increase passing the No. 40 sieve | | 20 | 20 | – | |
| Classification[3] | Tex-117-E | 1.0 | 1.1–2.3 | – | As shown on the plans |
| Min. compressive strength[3], psi | | | | | As shown on the plans |
| lateral pressure 0 psi | | 45 | 35 | – | |
| lateral pressure 15 psi | | 175 | 175 | – | |

1. Determine plastic index in accordance with Tex-107-E (linear shrinkage) when liquid limit is unattainable as defined in Tex-104-E.
2. When a soundness value is required by the plans, test material in accordance with Tex-411-A.
3. Meet both the classification and the minimum compressive strength, unless otherwise shown on the plans.

With the versatility of crushing and screening, the demolished concrete can meet the gradation of most base course requirements. The largest aggregate size must pass through a 2.5 inch sieve. Many states have performed studies and some have incorporated the use of recycled aggregates in highway construction. In Texas, the placement of recycled concrete aggregates (RCA) as a base has produced some knowledge on the behavior of the material. TxDOT determined that excessive working of RCA base created segregation and that the RCA base should be in a saturated state to achieve a homogeneous mix of the fines (FHWA, 2004). The Virginia Department of Transportation (VDOT) also concluded in their experience with the RCA base that the material should be compacted in a saturated state. The state of California uses most of the demolished concrete from existing streets and highways as aggregate base. Additionally, the California Department of Transportation allows any mixture of recycled concrete aggregate as a base material (FHWA, 2004).

The use of RCA as base has produced excellent results as noted by the state agencies in Texas, Virginia, Minnesota, and California. All of these states have noticed improved strength of the RCA base over the virgin aggregate normally used. Minnesota and California determined that the residual cementitious material helped provide the RCA with bonding that does not occur in the natural aggregate (FHWA, 2004; Arm, 2001). This characteristic along with the high angularity of the aggregate allows optimum grading and densification of the RCA material. Hence, a higher than normal stiffness of the material is achieved.

Nataatmadja and Tan (2001) tested recycled aggregates obtained from crushed concrete. From these results, the resilient modulus was concluded to be higher under low deviator stresses when compared to other base materials. A two-parameter model previously developed by Nataatmadja (1992) was used in the evaluation of the recycled concrete aggregates,

$$M_r = (\Phi/q_r)(A+Bq_r) \qquad (2.1)$$

in which $M_r$ is the resilient modulus, $\Phi$ is the sum of principal stresses, $q_r$ is the repeated deviator stress, and A and B are experimental coefficients. These results are presented on Table 2.2 and correspond to Figure 2.1.

Table 2.2 Comparisons of Performance Using Two-Parameter Model (Nataatmadja and Tan, 2001)

| Aggregate | *A* (kPa) | *B* | $r^2$ |
|---|---|---|---|
| AF RCA | 69,872 | 510 | 0.9777 |
| 18.5 MPa RCA | 110,372 | 628 | 0.9198 |
| 49 MPa RCA | 112,963 | 711 | 0.9781 |
| 75 MPa RCA | 80,084 | 514 | 0.9814 |
| Hicks' base course (Nataatmadja and Parkin 1989) | 20,420 | 412 | 0.9691 |
| Dry rhyolite (Nataatmadja and Parkin 1989) | 24,200 | 560 | 0.9801 |
| Uzan's dense graded aggregate (Nataatmadja and Parkin 1989) | 38,310 | 445 | 0.9500 |
| Sandstone subbase (Nataatmadja 1994) | 44,300 | 350 | 0.9593 |

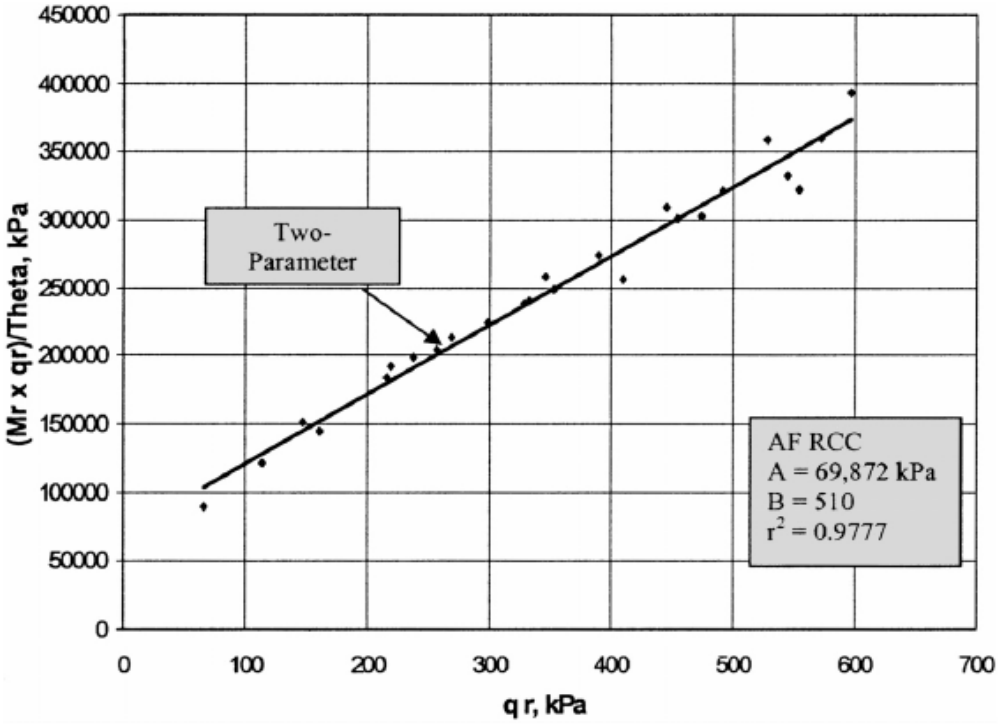


Figure 2.1 Resilient modulus variation according to Two-Parameter Model (Nataatmadja and Tan, 2001)

In the experiment, it was noted that the original strength, amount of soft material in the RCA, and the flakiness index of the RCA had a significant effect on the resilient modulus. Therefore, it was recommended that RCA can be used as a base or subbase if the material can be produced consistently to meet quality standards.

Specific testing of recycled aggregates as road base provides a basis for their applications. Arm (2001) reported that the crushed concrete from structures resulted in an optimum water content of 9.4% and a maximum dry density of 2.0 t/m$^3$. The results from repeated load triaxial testing show an increase in layer moduli with time for the crushed concrete aggregates. These repeated load triaxial results are presented on Figure 2.2.

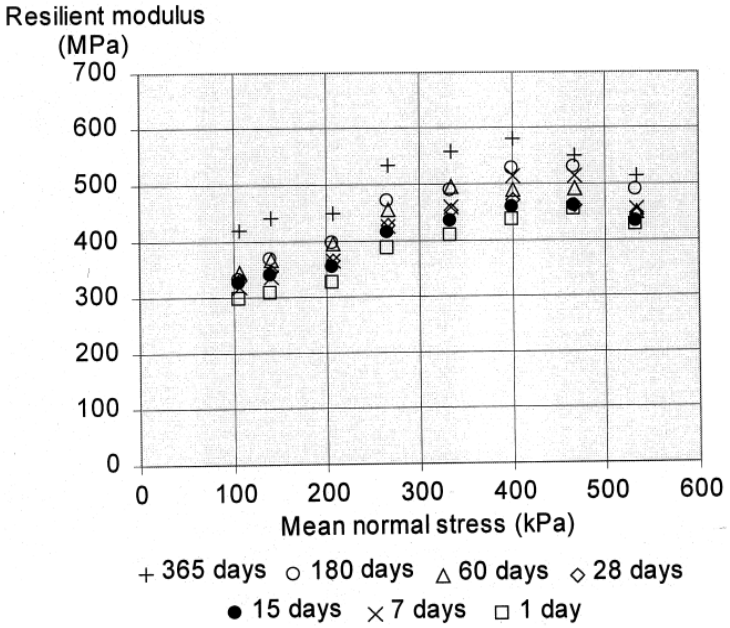


Figure 2.2 Results from repeated load triaxial tests after different storing time (Arm, 2001).

The comparison by Arm (2001) between the crushed concrete and natural aggregate (granite) shows a higher resilient modulus with time for the crushed concrete at all stress levels. Arm also concludes that the crushed concrete is less stress dependent than the natural aggregate (granite). The comparison of the resilient modulus between the crushed concrete and granite are presented on Figure 2.3.

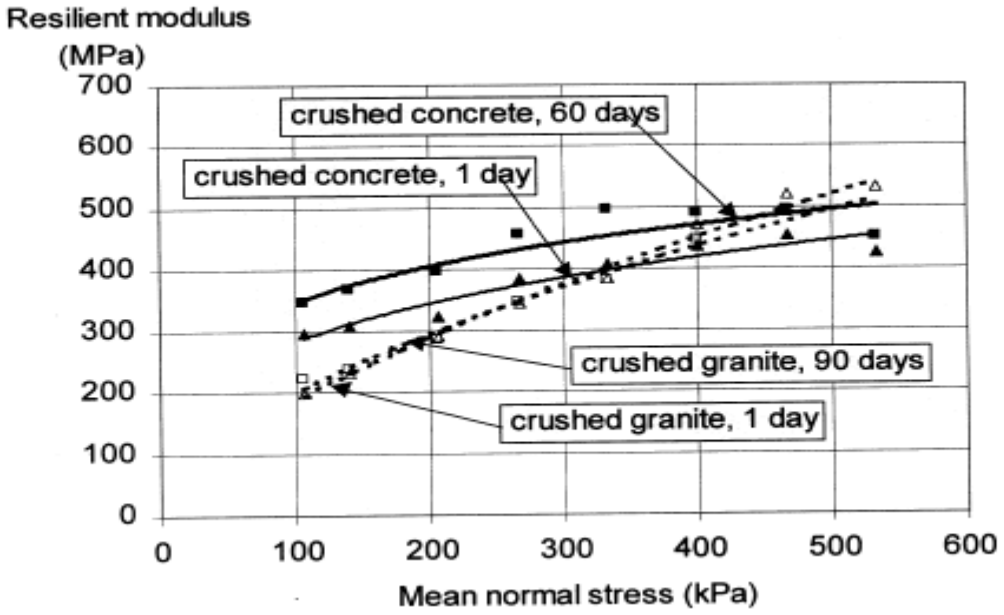


Figure 2.3 Comparison of resilient modulus between crushed concrete and granite (Arm, 2001)

Poon and Chan (2006) compared a natural aggregate (granite) with recycled concrete aggregates. In their study of the material properties, they concluded the natural aggregate had a higher density that the recycled concrete aggregates. The soundness tests for both materials were similar as presented on Table 2.3 for the natural aggregate and Table 2.4 for the recycled concrete aggregates.

Table 2.3 Properties of Natural Aggregate (Poon and Chan, 2006)

Properties of natural aggregates

| Properties | Aggregate size | | | | Test method |
|---|---|---|---|---|---|
| | 40 mm | 20 mm | 10 mm | <5 mm | |
| Density-SSD (kg/m$^3$) | 2622 | 2660 | 2577 | 2579 | BS 812 Part 2 |
| Density-oven-dry (kg/m$^3$) | 2594 | 2644 | 2562 | 2492 | |
| Water absorption (%) | 1.06 | 0.57 | 0.59 | 3.51 | |
| Ten percent fines – dry (kN) | – | 190 | – | – | BS 812 Part 111 |
| Ten percent fines – soaked (kN) | – | 190 | – | – | |
| Water-soluble sulphate content (g/L) | – | – | – | 0.025 | BS 1377 Part 3 |
| Soundness % | – | 97.5 | – | – | BS 812 Part 121 |
| Particle size distribution (mm) | Percent passing (%) | | | | |
| 50.0 | 100 | – | – | – | BS 812: 103.1 |
| 37.5 | 96.9 | 100 | – | – | |
| 20.0 | 2.09 | 92.1 | – | – | |
| 14.0 | 0.1 | 36.0 | 100 | – | |
| 10.0 | – | 8.35 | 95.9 | – | |
| 5.0 | – | 0.41 | 13.5 | 97.3 | |
| 2.36 | – | – | 1.18 | 77.7 | |
| 1.18 | – | – | – | 58.0 | |
| 0.6 | – | – | – | 41.9 | |
| 0.3 | – | – | – | 19.2 | |

Table 2.4 Properties of Recycled Concrete Aggregates (Poon and Chan, 2006)

Properties of recycled concrete aggregates

| Properties | Aggregate size | | | | Test method |
|---|---|---|---|---|---|
| | 40 mm | 20 mm | 10 mm | <5 mm | |
| Density-SSD (kg/m$^3$) | 2487 | 2546 | 2580 | 2310 | BS 812 Part 2 |
| Density-oven-dry (kg/m$^3$) | 2411 | 2493 | 2523 | 2093 | |
| Water absorption (%) | 3.17 | 2.17 | 2.29 | 10.3 | |
| Ten percent fines – dry (kN) | – | 146 | – | – | BS 812 Part 111 |
| Ten percent fines – soaked (kN) | – | 109 | – | – | |
| Water-soluble sulphate content (g/L) | – | – | – | 0.032 | BS 1377 Part 3 |
| Soundness % | – | 96.3 | – | – | BS 812 Part 121 |
| Particle size distribution (mm) | Percent passing (%) | | | | |
| 50.0 | 100 | – | – | – | BS 812: 103.1 |
| 37.5 | 96.4 | 100 | – | – | |
| 20.0 | 3.98 | 98.4 | – | – | |
| 14.0 | 0.23 | 31.4 | 100 | – | |
| 10.0 | – | 4.73 | 93.8 | – | |
| 5.0 | – | 0.18 | 7.6 | 100 | |
| 2.36 | – | – | 1.6 | 73.6 | |
| 1.18 | – | – | – | 48.3 | |
| 0.6 | – | – | – | 31.1 | |
| 0.3 | – | – | – | 17.7 | |

2.2.1.2 Use of Recycled Aggregates in Portland Cement Concrete

In another aspect, studies for the use of the recycled aggregates from crushed concrete in Portland cement concrete have been conducted. The recycled aggregates have been incorporated as a coarse aggregate in concrete mix designs. The results provided by the

Federal Highway Administration (2004), do not show much success in this application. Several issues were noted with the use of recycled aggregates from crushed concrete in Portland cement concrete.

TxDOT (FHWA, 2004) identified an increase in creep and shrinkage in concrete when RCA's were used in concrete. This can be a major issue when concrete is used in structural applications. The Michigan Department of Transportation (FHWA, 2004) has limited RCA used in concrete mix designs mainly to flatwork and temporary pavements. The Minnesota Department of Transportation (FHWA, 2004) requires the washing of aggregates used in Portland cement concrete pavements to eliminate excess fines. The process of washing aggregates when using mobile crushing plants is not very feasible due to limited space. The California Department of Transportation (FHWA, 2004) is developing specifications for used of RCA in Portland cement concrete for non-structural applications.

In conjunction with many states, the Federal Highway Administration has issued a Technical Advisory T 5040.37 (2007) that provides guidance on the use of recycled concrete pavement as aggregate in Portland cement concrete used for pavements. With this guidance, the FHWA has provided information on the effects of RCA's on mechanical properties of concrete, fresh concrete properties, and concrete durability. The effects of RCA on the mechanical properties are presented on Table 2.5. The effects of RCA on fresh concrete properties are presented on Table 2.6. The effects of RCA on concrete durability are presented on Table 2.7.

Table 2.5 Effect of RCA on Mechanical Properties of Concrete (FHWA, 2007)

| Property | Range of expected changes from similar mixtures using virgin aggregates. (ACI 555R) | |
|---|---|---|
| | Coarse RCA only | Coarse and Fine RCA |
| Compressive Strength | 5% to 24% less | 15% to 40% less |
| Strength Variation | Slightly greater | Slightly greater |
| Modulus of Elasticity | 10% to 33% less | 25% to 40% less |
| Creep | 30% to 60% greater | 30% to 60% greater |
| Tensile Strength | 10% less | 10% to 20% less |
| Permeability | 200% to 500% greater | 200% to 500% greater |
| Thermal Expansion | Somewhat less than expected for coarse aggregate used | Somewhat less than expected for coarse aggregate used |
| Specific Gravity | 5% to 10% lower | 5% to 10% lower |

Table 2.6 Effect of RCA on Fresh Concrete Properties (FHWA, 2007)

| Property | Range of expected changes from similar mixtures using virgin aggregates. (ACI 555R) | |
|---|---|---|
| | Coarse RCA only | Coarse and Fine RCA |
| Water Demand | Greater | Much greater |
| Drying Shrinkage | 20% to 50% more | 70% to 100% more |
| Finishability | More difficult | More difficult |

Table 2.7 Effect of RCA on Concrete Durability (FHWA, 2007)

| Property | Range of expected changes from similar mixtures using virgin aggregates. (ACI 555R) | |
|---|---|---|
| | Coarse RCA only | Coarse and Fine RCA |
| Corrosion Rate | May be faster | May be faster |
| Freeze-thaw Durability | Dependent on air void system | Dependent on air void system |
| Carbonization | 65% greater | 65% greater |
| Sulfate Resistance | Dependent on mixture | Dependent on mixture |

Restricting the use of RCA in Portland cement concrete to only certain applications may not be economical for ready mix concrete suppliers. The management of separate stockpiles for RCA materials can be difficult due to the small quantities required, frequency of usage, and the cost for preparation and maintenance of the stockpiles. In order for recycled materials to be attractive to the private industry, they must require minimal maintenance costs.

## 2.3 Bender Element Testing

In order to develop an effective experiment design, an extensive review of bender element testing methods was conducted. This review was performed to establish the most effective use of bender elements for recycled aggregates derived from crushed concrete. The review of previous bender element testing did not produce any applications to recycled concrete aggregates.

### *2.3.1 Theory of Bender Elements*

Bender elements have become useful in non-destructive testing methods for soils. Bender elements are thin sheets of piezo-ceramics inserted into soils specimens. The piezo-ceramic bender element is capable of converting mechanical energy to or from electrical energy (Dyvik & Madshus, 1986). The piezo-ceramic sheets are configured into what is known as a transmitting and a receiving bender element. This is accomplished by bonding together two

piezo-ceramic plates in a series or parallel configuration as presented on figure 2.4 and figure 2.5, respectively.

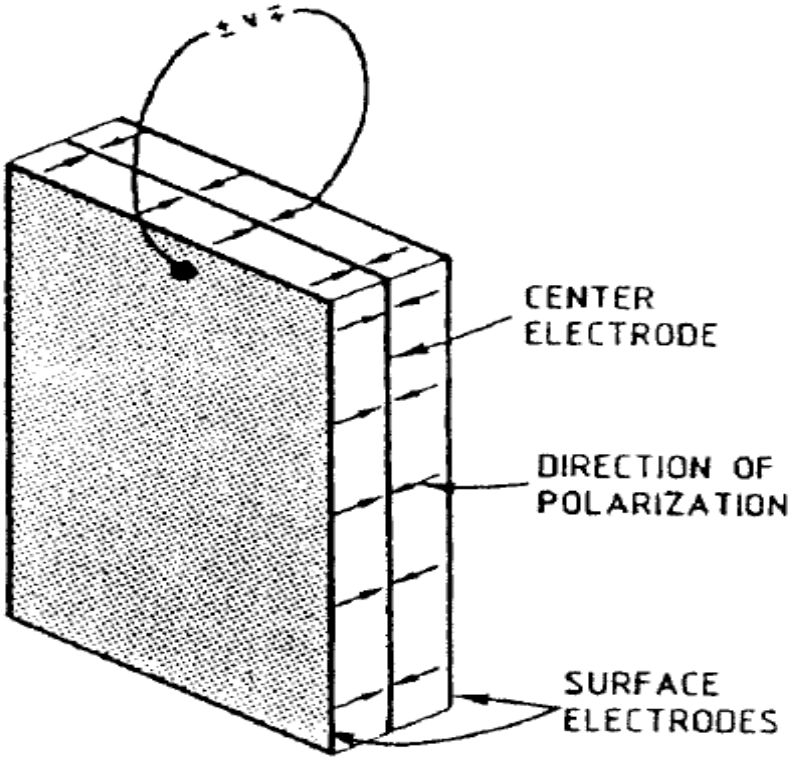


Figure 2.4 Series connected piezo-ceramic bender element (Dyvik & Madshus, 1986)

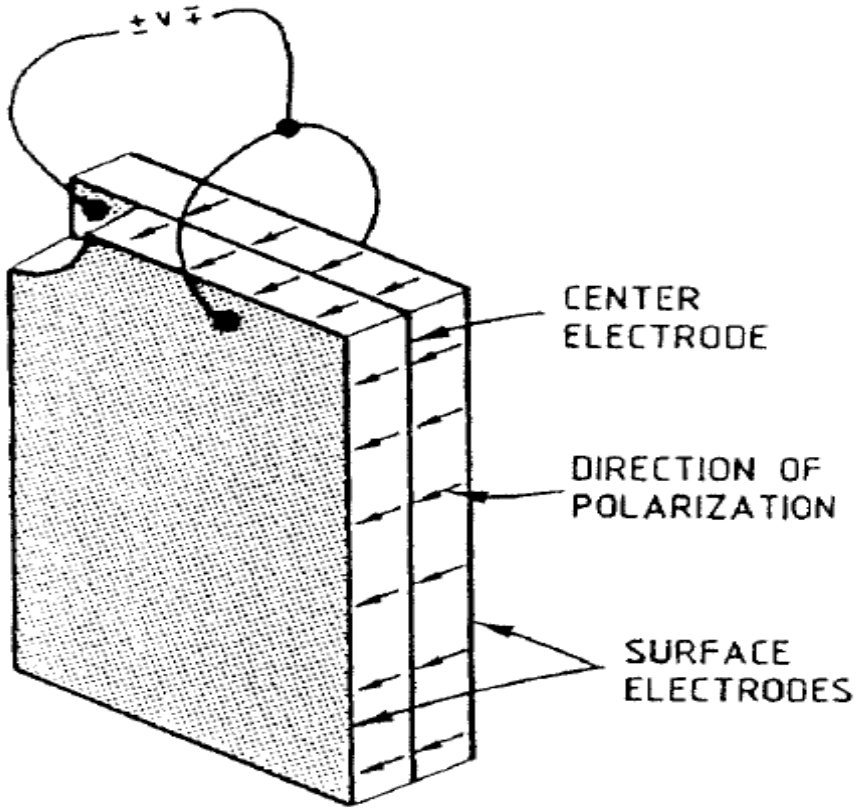


Figure 2.5 Parallel connected piezo-ceramic bender element (Dyvik & Madshus, 1986)

The series configuration has been known to be more effective as a receiver and the parallel configuration more effective as a transmitter. When a current is applied, a mechanical wave is transmitted through the soil specimen by the transmitter bender element. At the receiving end of the specimen, the mechanical wave is detected by the receiver bender element. By measuring the speed of a bender shear-wave through the soil specimen, and knowing the total mass density of the soil (ρ), the Shear Modulus ($G_{max}$) for that soil can be calculated as shown on equation 2.2. The velocity of the shear-wave is determined by measuring the distance ($L_{tt}$) between bender elements in soil and dividing by the measured time (t) for the wave through this distance.

$$G_{max} = \rho V_s^2 \qquad (2.2)$$

Since the development of this application in laboratory tests (Shirley and Hampton, 1978), the use of bender elements has provided researchers with a consistent method of measuring the shear modulus of a soil. In turn, the Young's Modulus (E), which is comparable to the resilient modulus of soils in pavement design, can be calculated as presented on equation 2.3 with the use of a known Poisson's Ratio (μ).

$$E = 2(1+ \mu)G_{max} \qquad (2.3)$$

Figure 2.6 presents a typical schematic diagram of an assembled testing device use by researchers in measuring the Shear Modulus for soil specimens.

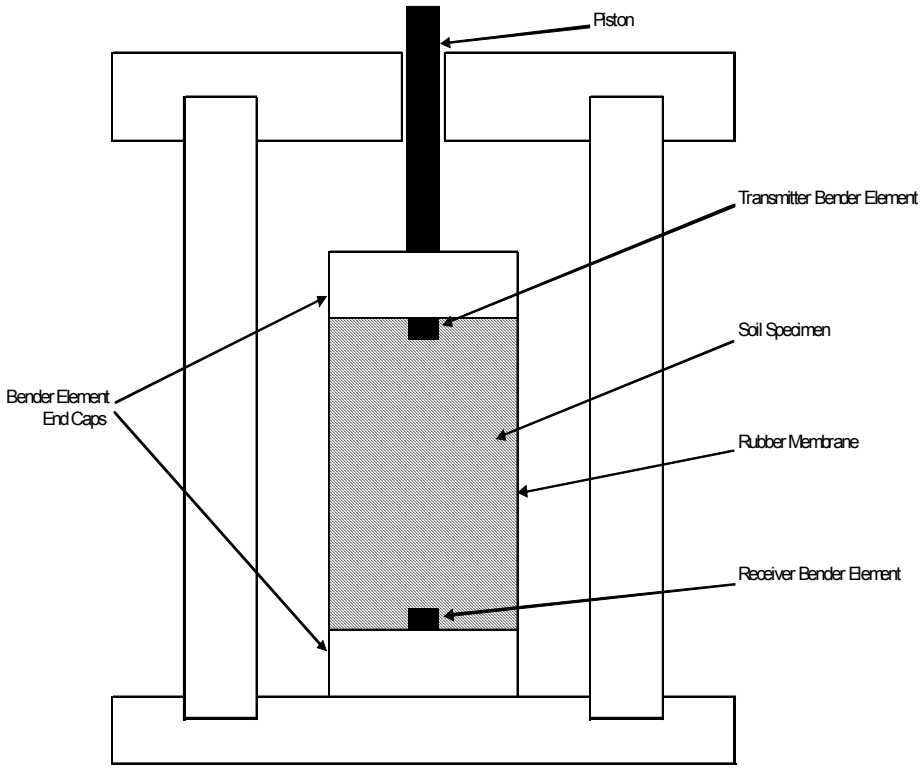


Figure 2.6 Schematic for bender element test setup (Baig & Nazarian, 1995)

*2.3.2 Interpretation of Bender Elements Results*

Many studies have been conducted to better interpret the results produced from the use of bender elements. It is attributed to previous research findings, (Lohani & Imai, 1999; Kung, Ou, & Hsieh, 2004; Leong, Yeo, & Rahardjo, 2005; Dyvik & Madshus, 1986; Jovicic, Coop, and Simic, 1996; Viggiani and Atkinson, 1995) that has allowed for the use of bender element testing in providing effective and properly interpreted results. Lohani and Imai (1999) concluded that a sine wave input resulted with clearer and more distinct arrival points than that of a square wave. The use of a resonance frequency eliminates inaccuracies in the measurement of the time of travel of the shear wave. The use of resonance frequency is described by Kung, Ou, and Hsieh (2004). The use of resonance frequency is based on worked conducted by Jovicic, Coop, and Simic (1996). By conducting testing above resonance frequency, it is shown that near field effects are avoided. When the testing frequency is at or above resonance frequency, the time of travel of the shear wave becomes consistent regardless of the method used as presented on figure 2.7. Therefore, the velocity also becomes consistent as shown by Kung, Ou, and Hsieh (2004).

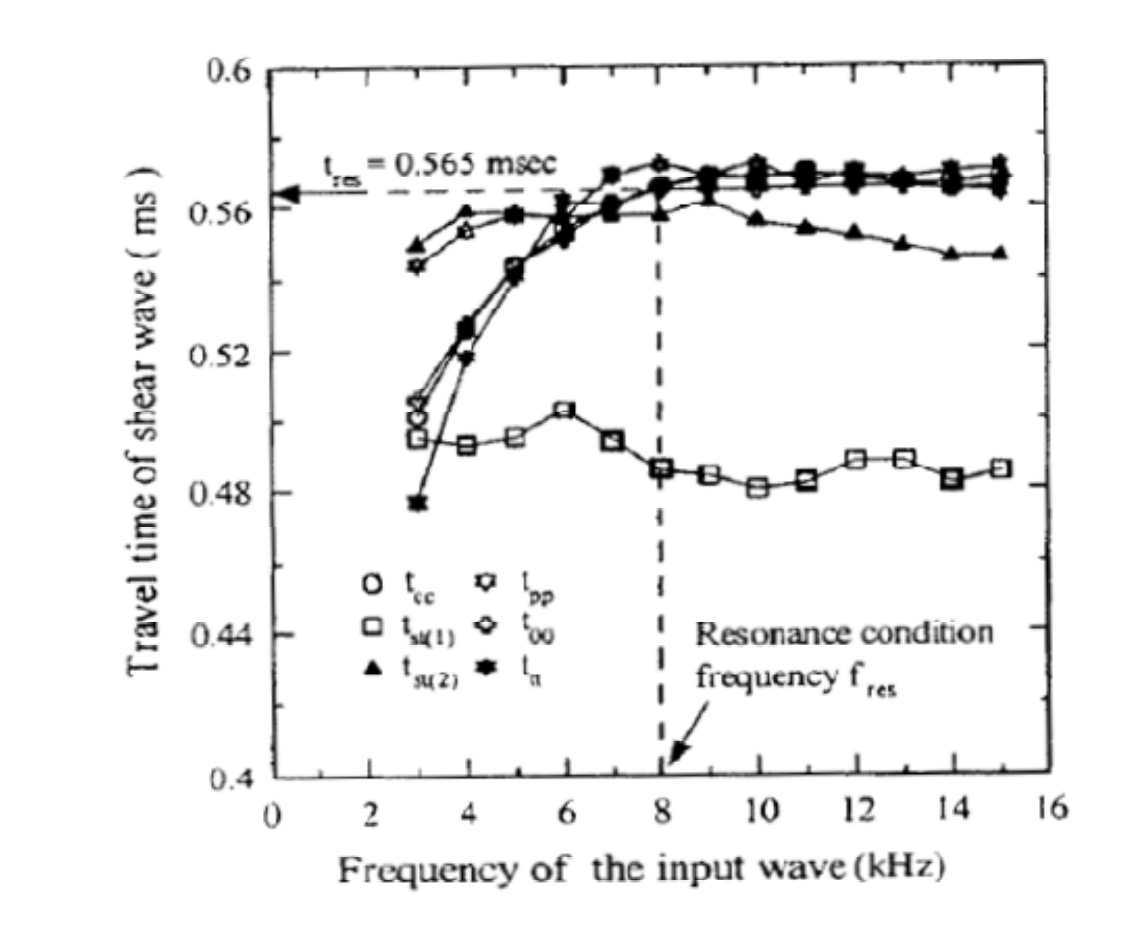


Figure 2.7 Variations of different methods for determining travel time of shear wave (Kung et al., 2004)

The selection of the frequency has been shown to have an effect on the measurement of the shear wave velocity through a soil. Therefore, it is important to determine the resonance frequency for each of the soil samples. Also, it is important to review the wave path length (tip-to-tip of bender elements) to the wavelength ratio ($L_{tt}/\lambda$). As the frequency ($f$) is increased, the wavelength ($\lambda$) decreases. By using a frequency higher than the determined resonance frequency, the wave path length to wavelength ratio increases. This will ensure that the near field effects errors can be avoided as presented on figure 2.8. In addition to the near field effects, Arulnathan, Boulanger, and Riemer (1998) attributed the $\lambda/L_b$ to effects of wave interference at the end caps. Kung, Ou, & Hsieh (2004) also discussed the use of the ratio

between wavelength and length of bender element ($\lambda/L_b$). In this relationship, the ratio of $\lambda/L_b$ used must be less than that at resonance $(\lambda/L_b)_{res}$ to eliminate the end cap effects. However, the use of a frequency above the resonant frequency ensures that the ratio $\lambda/L_b$ is less than that at resonance frequency as presented on figure 2.9.

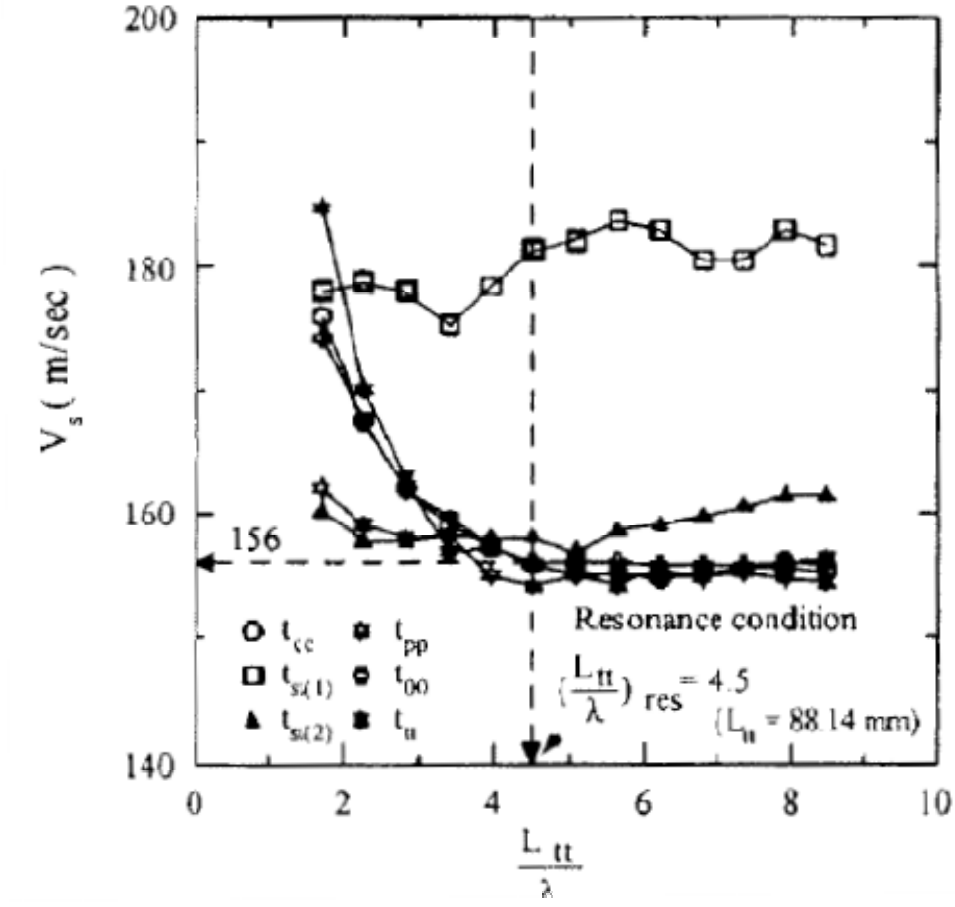


e

Figure 2.8 Variations of shear wave velocity $V_s$ versus $L_{tt}/\lambda$ (Kung et al., 2004)

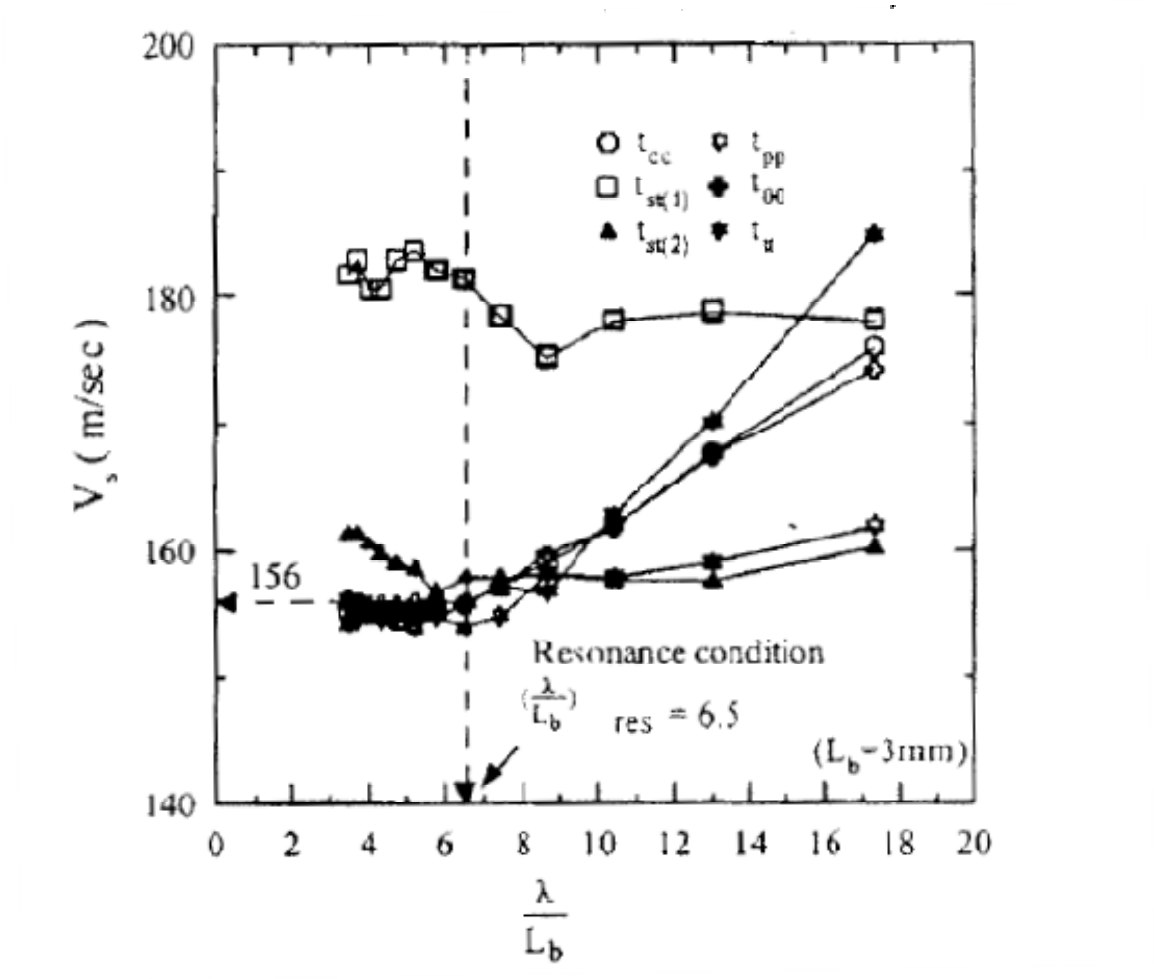


Figure 2.9 Variations of shear wave velocity $V_s$ versus $\lambda/L_b$ (Kung et al., 2004)

## 2.4 Pavement Design

In the design of both flexible and rigid pavements, the AASHTO *Guide for Design of Pavement Structures* addresses pavement performance, traffic volume, subgrade soils, construction materials, environment, drainage, reliability, life cycle costs, and shoulder design. The primary focus is the functional and structural performance of the pavements. In doing so, the performance serviceability is used to evaluate the functional performance of the pavement. The structural performance relates to the physical condition and load-carrying ability of the pavement structure.

*2.4.1 Flexible Pavement Design*

The first objective in flexible pavement design is to determine the structural number (SN) required for the specific conditions. Once the structural number is determined, it can be used in developing the pavement structure thickness for each layer as shown in equation 2.4.

$$SN = a_1D_1 + a_2D_2m_2 + a_3D_3m_3 \quad (2.4)$$

The layer coefficients $a_1$ (surface), $a_2$ (base), and $a_3$ (subgrade) are combined with the corresponding thickness ($D_{1,2,3}$) and drainage coefficient ($m_{2,3}$) for each layer of the pavement structure. This allows for various pavement designs to be evaluated and optimized for the most practical and economical use.

In determining the structural number, specific parameters must be known. The following parameters allow for the use of an established nomograph found in the AASHTO *Guide for Design of Pavement Structures*:

Estimated future traffic, $W_{18}$, is the cumulative expected 18-kip equivalent single axle loads (ESAL). The predicted traffic is determined by equation 2.5,

$$W_{18} = D_D \text{ X } D_L \text{ X } w_{18} \quad (2.5)$$

where $D_D$ is the directional distribution factor that account for ESAL in opposite direction, $D_L$ is the lane distribution factor that accounts for traffic distribution when more than one lane exists, and $w_{18}$ is the cumulative two directional 18-kip ESAL unit predicted for the roadway.

Reliability, R, provides a predetermined level of assurance that pavements will survive their intended design period. The reliability is a function of the overall standard deviation.

Overall standard deviation, $S_o$, accounts for chance variation in traffic condition and normal variation in pavement performance.

Resilient Modulus, $M_R$, characterizes the roadbed soil as a measure of the elastic property of the soil. Laboratory resilient modulus tests (AASHTO T 274) are performed on representative samples of the roadbed soil. Seasonal moduli may also be determined to quantify the relative damage experienced by the pavement due to seasonal changes.

Serviceability loss, $\Delta PSI$, signifies the total change of the serviceability of the roadway. The primary measure for serviceability is the Present Serviceability Index (PSI). The PSI is rated from values of 0 to 5. The PSI value of 0 is the poorest condition and the PSI value of 5 the best condition for a roadway. The serviceability loss is determined from the difference of the PSI values at the initial serviceability and the terminal serviceability of the pavement.

Once the above parameters are established, the structural number (SN) is determined from the Equation 2.6 or from the use of the AASHTO nomograph for flexible pavements shown in figure 2.10.

$$\text{Log}_{10}W_{18} = Z_R * S_o + 9.36 * \log_{10}(SN+1) - 0.20 + [\log_{10}(\Delta PSI/(4.2-1.5))]/[0.40+1094/(SN+1)^{5.19}] + 2.32 * \log_{10}M_R - 8.07 \quad (2.6)$$

The structural number (SN) is then used in the Equation 2.4 to determine the pavement structure thickness for each of the material layers. The approach is that of a trial an error until the most economical pavement structure is determined.

*2.4.2 Rigid Pavement Design*

The primary focus in rigid pavement design as described in the AASHTO *Guide for Design of Pavement Structures* begins with identification of an effective modulus of subgrade (k-value) reaction. The effective k-value is dependent on several factors outside that of the roadbed soil resilient modulus and therefore must be adjusted to account for the effects of these factors. These factors include the subbase type, subbase thickness, loss of support, and depth of rigid foundation.

In determining the slab thickness of the rigid pavement, specific parameters must be established similarly to the flexible pavement design parameters previously described. These parameters are the estimated future traffic, the reliability, the overall standard deviation, and design serviceability. In addition to these parameters, rigid pavement design requires the following parameters to be determined.

Concrete elastic modulus, $E_c$, is recommend by American Concrete Institute to be determined by the correlation for normal weight Portland cement concrete shown in equation 2.7,

$$E_c = 57{,}000\ (f'_c)^{0.5} \tag{2.7}$$

where $f'_c$ is the compressive strength of Portland cement concrete in psi.

Concrete modulus of rupture, $S'_c$, is the mean value determined for 28-day flexural strength tests using third-point loading.

Load transfer coefficient, J, is a factor used to account for the ability of a pavement structure to transfer loads across discontinuities such as joints and cracks.

Drainage Coefficient, $C_d$, is a factor that is used to account for the quality of drainage and the percent of time that a pavement is expose to moisture levels approaching saturation.

Once the above parameters are established, the slab thickness for a rigid pavement is determined by equation 2.8 or from the use of the AASHTO nomograph for rigid pavements shown in figures 2.11 and 2.12.

$$Log_{10}W_{18}=Z_R*S_o + 7.35*\log_{10}(D+1) - 0.06 + [\log_{10}(\Delta PSI/(4.5-1.5))]/1 + (1.624*10^7/((D+1)^{8.46} + (4.22-0.32p_t)*\log_{10}[(S'_c*C_d(D^{0.75}-1.132))/(215.63*J(D0.75-(18.42/(E_c/k)^{0.25})))] \quad (2.8)$$

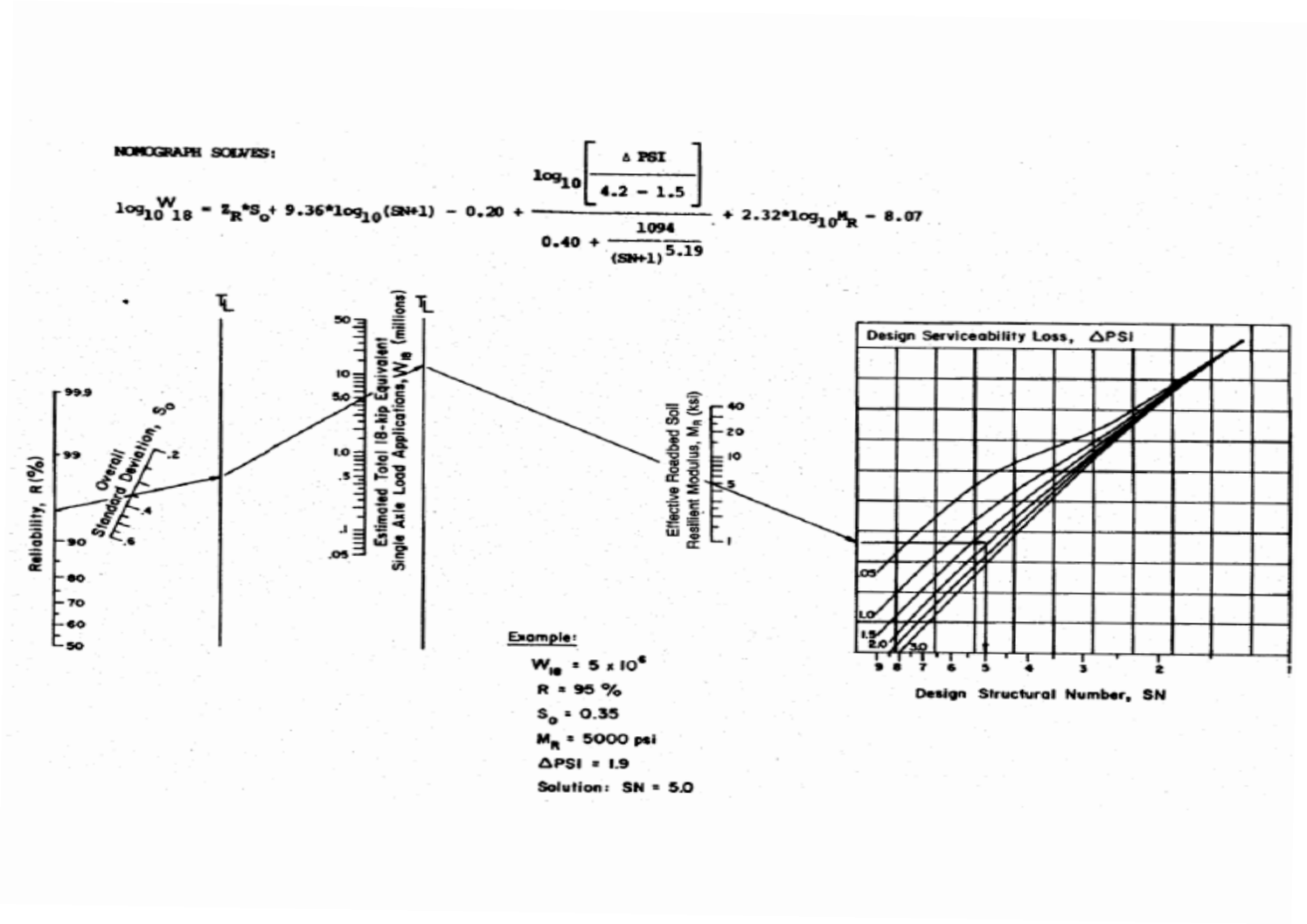


Figure 2.10 Design chart for flexible pavements (AASHTO, 1993)

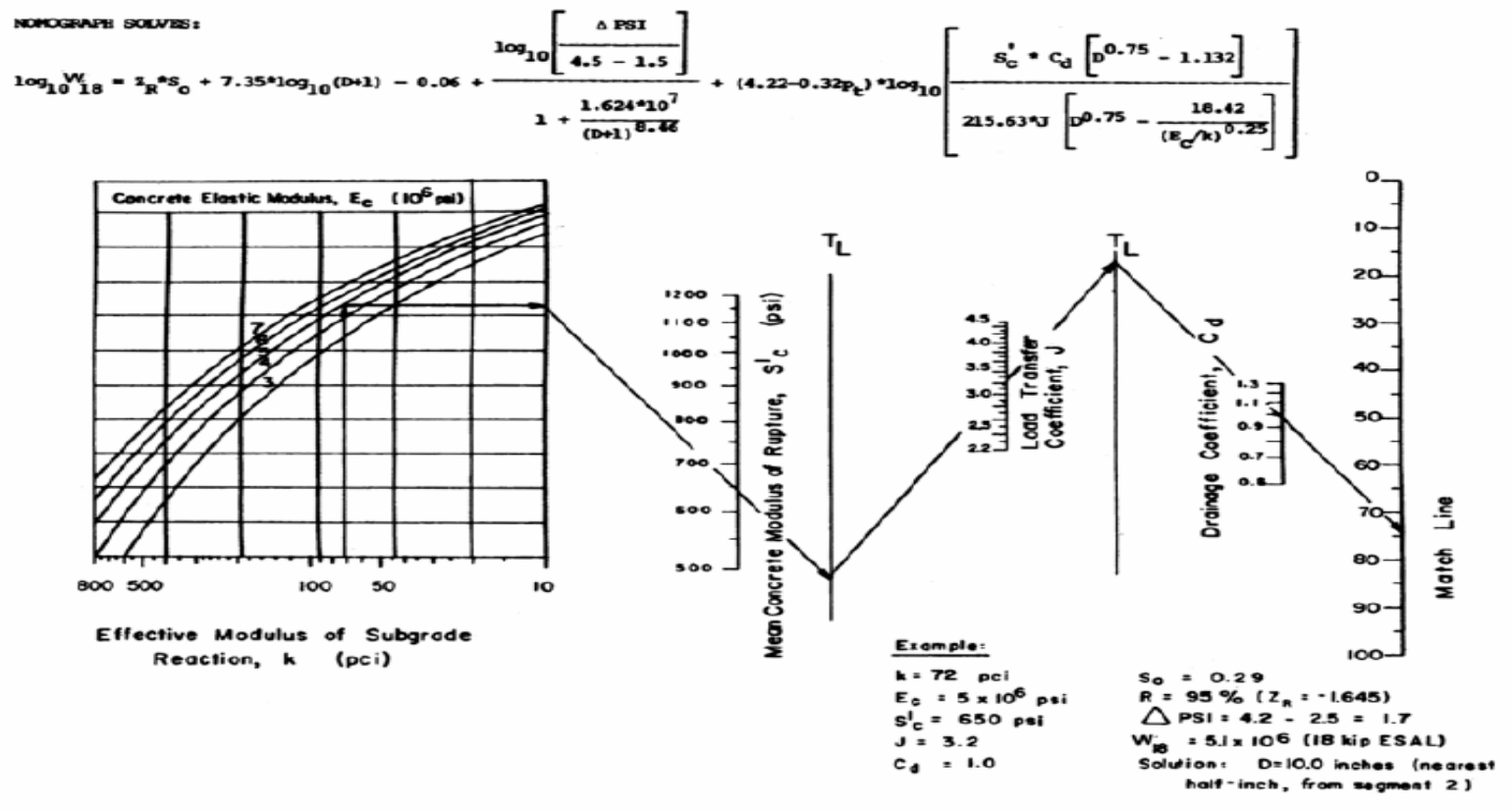


Figure 2.11 Design chart for rigid pavements - Segment 1 (AASHTO, 1993)

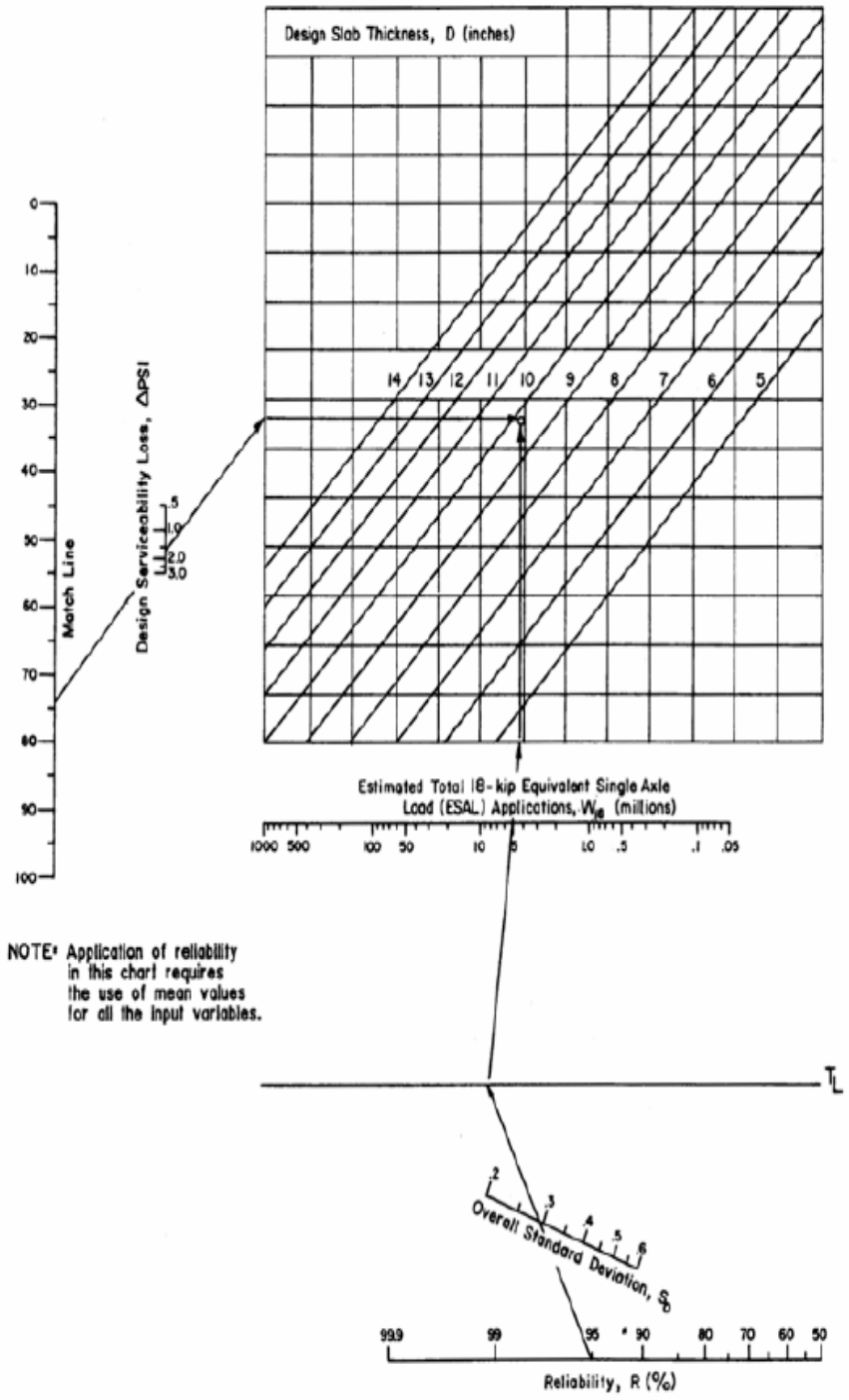


Figure 2.12 Design chart for rigid pavements - Segment 2 (AASHTO, 1993)

## 2.5 Summary

In the review, it was noted that several studies have concluded that similarities exists between the engineering properties of recycled concrete aggregates and natural aggregates. The feasibility of using recycled aggregates in lieu of natural aggregates along with the effective use of bender elements in determining the shear modulus of soil materials allows for the development of pavement structure designs. With this in mind, it has become apparent that the recycled aggregates can be used effectively in pavement design structures.

# CHAPTER 3

# EXPERIMENTAL PROGRAM

## 3.1 Introduction

The experimental program was designed and conducted to determine and compare the shear and elastic moduli properties of a natural aggregate with that of recycled concrete aggregates at different moisture content levels. In order to accomplish this, the small strain shear modulus $G_{max}$ was determined at a dry, optimum, and wet condition for the materials on 7-day and 28-day curing periods for each of the natural aggregate and recycled concrete aggregate materials. In addition to the shear modulus, pertinent physical and chemical properties of the materials were determined through laboratory testing. The following sections describe the physical and chemical properties of the natural aggregate and of the recycled concrete aggregates, types of laboratory tests performed, testing equipment, and methods for the testing performed.

## 3.2 Properties of Testing Materials

The materials used in this research are that of a crushed natural limestone that is predominantly used in the Dallas/Fort Worth area and recycled concrete aggregates. The recycled concrete aggregates were derived from the crushing of demolished concrete pavement (RC1) and bridge structures (RC2) collected from Dallas County, Texas. Both the natural limestone and recycled concrete aggregates were similarly graded to produce comparable materials as required for flexible base (Flex Base) material standards and specifications as per Texas Department of Transportation. The materials for crushed limestone aggregate, recycled concrete aggregates RC1, and recycled concrete aggregate RC2 are shown in figures 3.1, 3.2, and 3.3, respectively. Compaction moisture content - dry density curves were developed for each of the materials to determine the moisture content and dry density of each material at their

dry, optimum, and wet conditions. At 7-day and 28-day curing periods, the material small strain $G_{max}$ of the material was determined. The materials were also tested to determine their specific gravity, pH, and permeability in order to further characterize the materials and evaluate their suitability as base course materials. These results are summarized in the following sections.

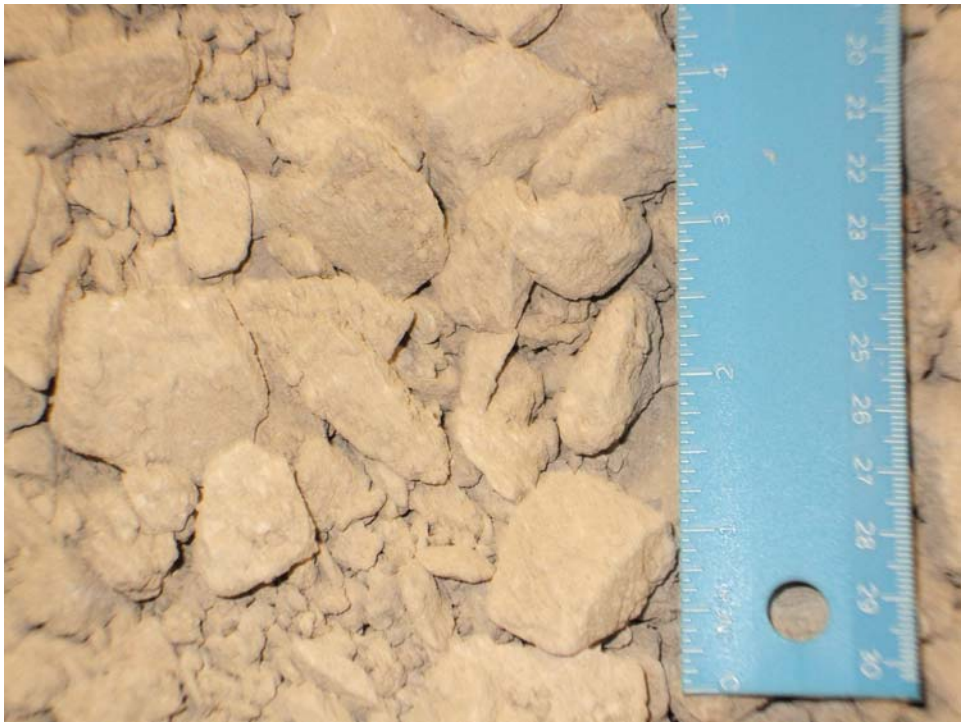

Figure 3.1 Crushed limestone aggregate test material

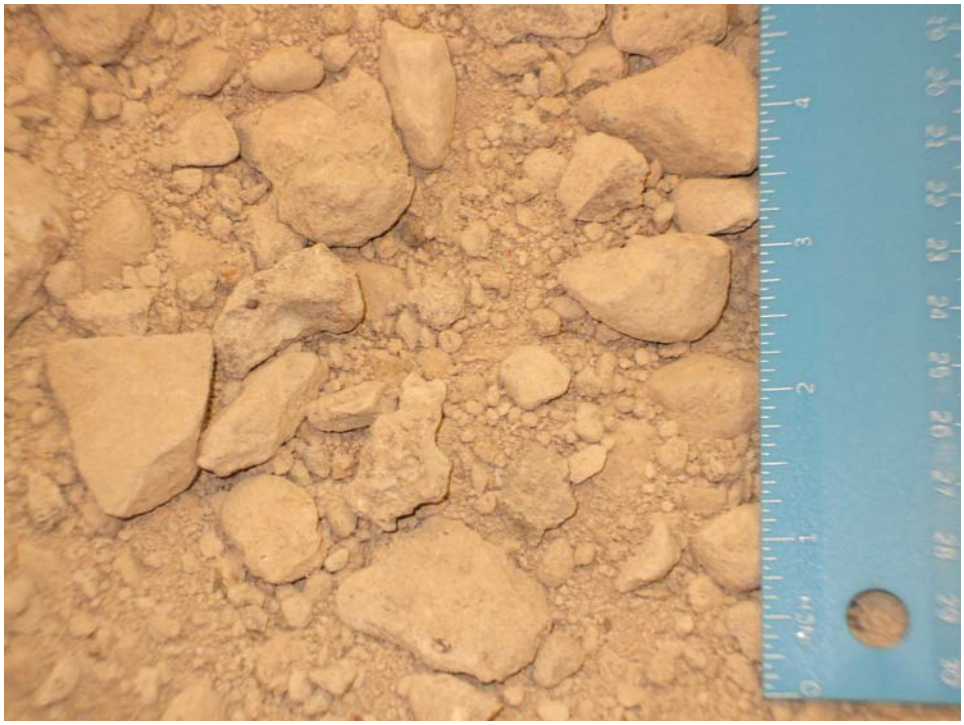

Figure 3.2 Recycle concrete aggregate RC1 test material

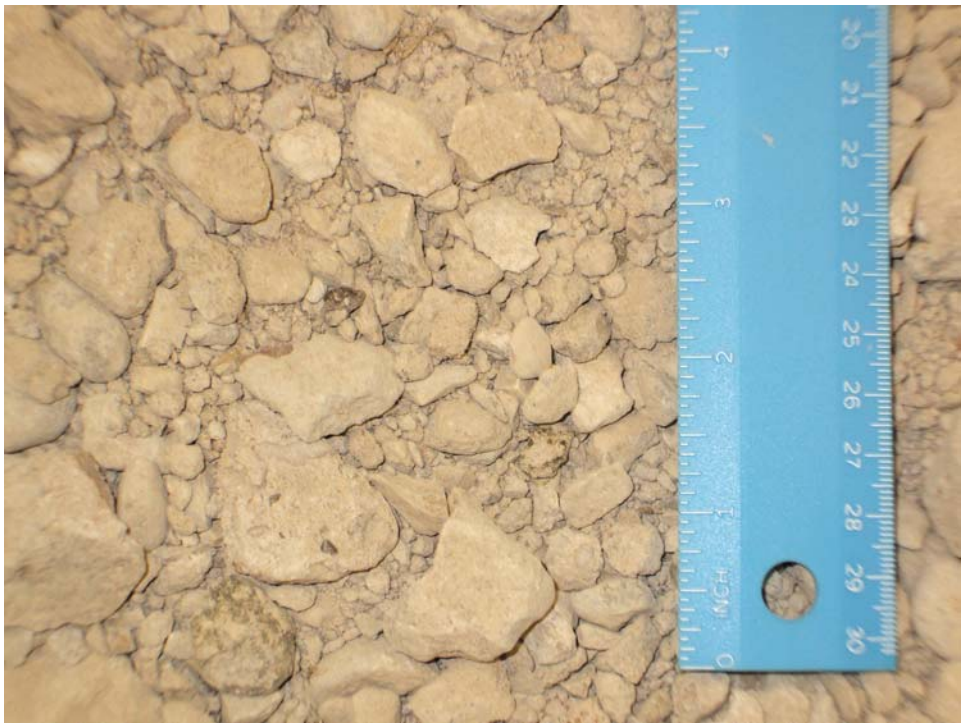

Figure 3.3 Recycle concrete aggregate RC2 test material

*3.2.1 Gradation of Materials*

The particle size distribution of the materials used was determined at the beginning of the experimental program. This was achieved by performing sieve analysis as per TxDOT gradation specifications for flex base materials. The sieve analysis results indicate that all material gradations were consistent with that of a Grade 1 flex base. The sieve analysis consisted of using the 2-1/2", 1-3/4", 7/8", 3/8", No. 10, No. 4, and No. 40 sieves. Figures 3.4, 3.5, and 3.6 present the grain size distribution curve for each of the materials. Figure 3.7 shows the grain size distribution comparison of all three materials. All three materials resulted having binder (material passing a No. 40 sieve) ranging between 15 and 17 percent. The results of the sieve analysis are shown on Table 3.1 and compared with the gradation requirements as per Texas Department of Transportation standards and specifications. Based on sieve analysis results, all three materials met the Grade 1 gradation requirements. Table 3.2 shows the similarities for the percentage of materials finer at grain sizes of 10 mm, 1mm, and 0.1 mm.

Table 3.1 Percent Retained for Sieve Analysis Gradation Requirements and Material Results

| Sieve No. | Flex Base Gradation Requirements | | | Materials for Experiment | | |
|---|---|---|---|---|---|---|
| | Grade 1 | Grade 2 | Grade 3 | RC1 | RC2 | Limestone |
| 2-1/2" | | 0 | 0 | | | |
| 1-3/4" | 0 | 0-10 | 0-10 | | | |
| 7/8" | 10-35 | | | 11.48 | 11.38 | 10.10 |
| 3/8" | 30-50 | | | 33.80 | 33.03 | 30.05 |
| No. 4 | 45-65 | 45-75 | 45-75 | 48.94 | 48.85 | 46.01 |
| No. 40 | 70-85 | 60-85 | 50-85 | 84.72 | 83.46 | 84.42 |

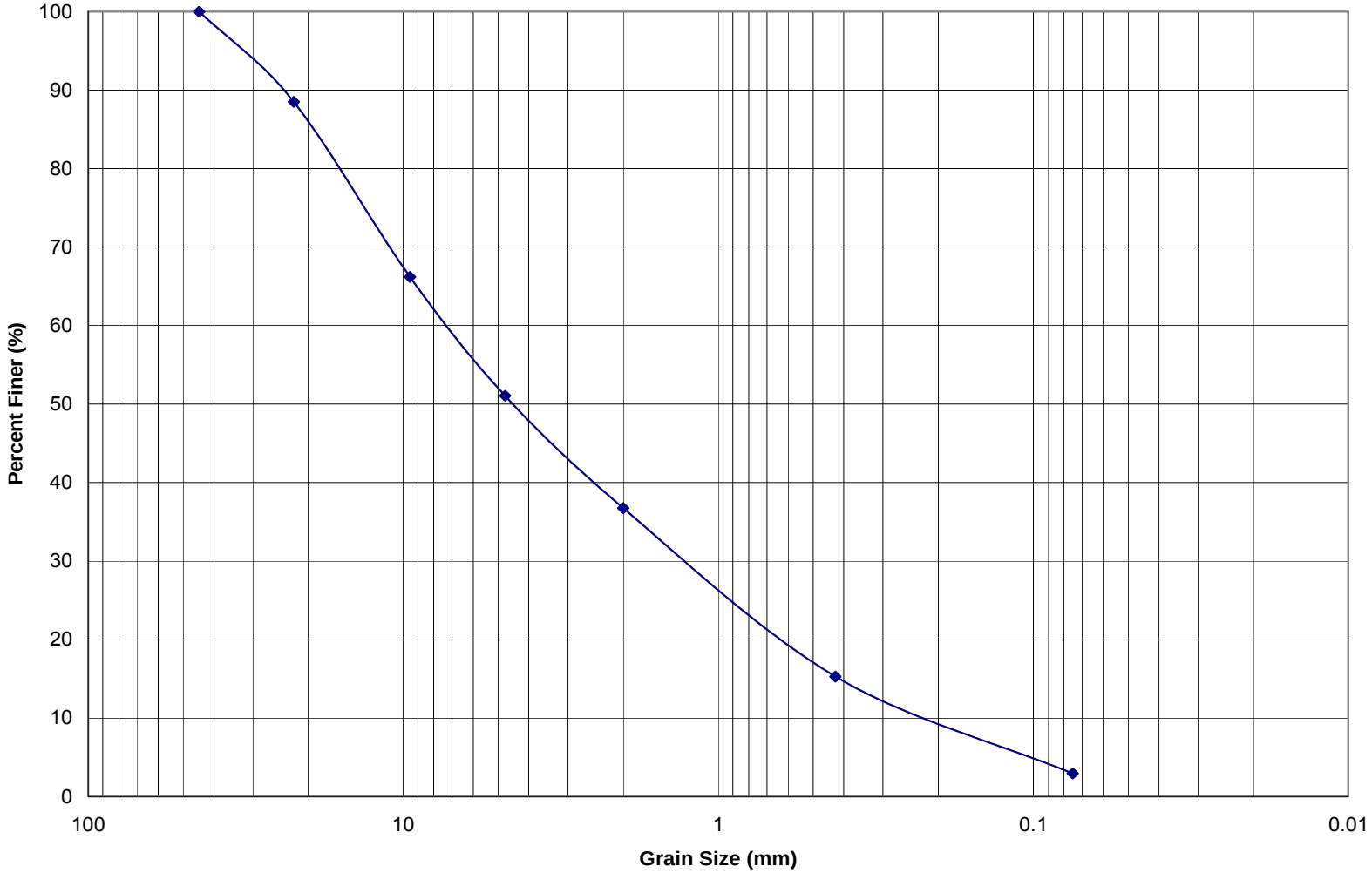


Figure 3.4 Sieve analysis test results for crushed concrete aggregate RC1

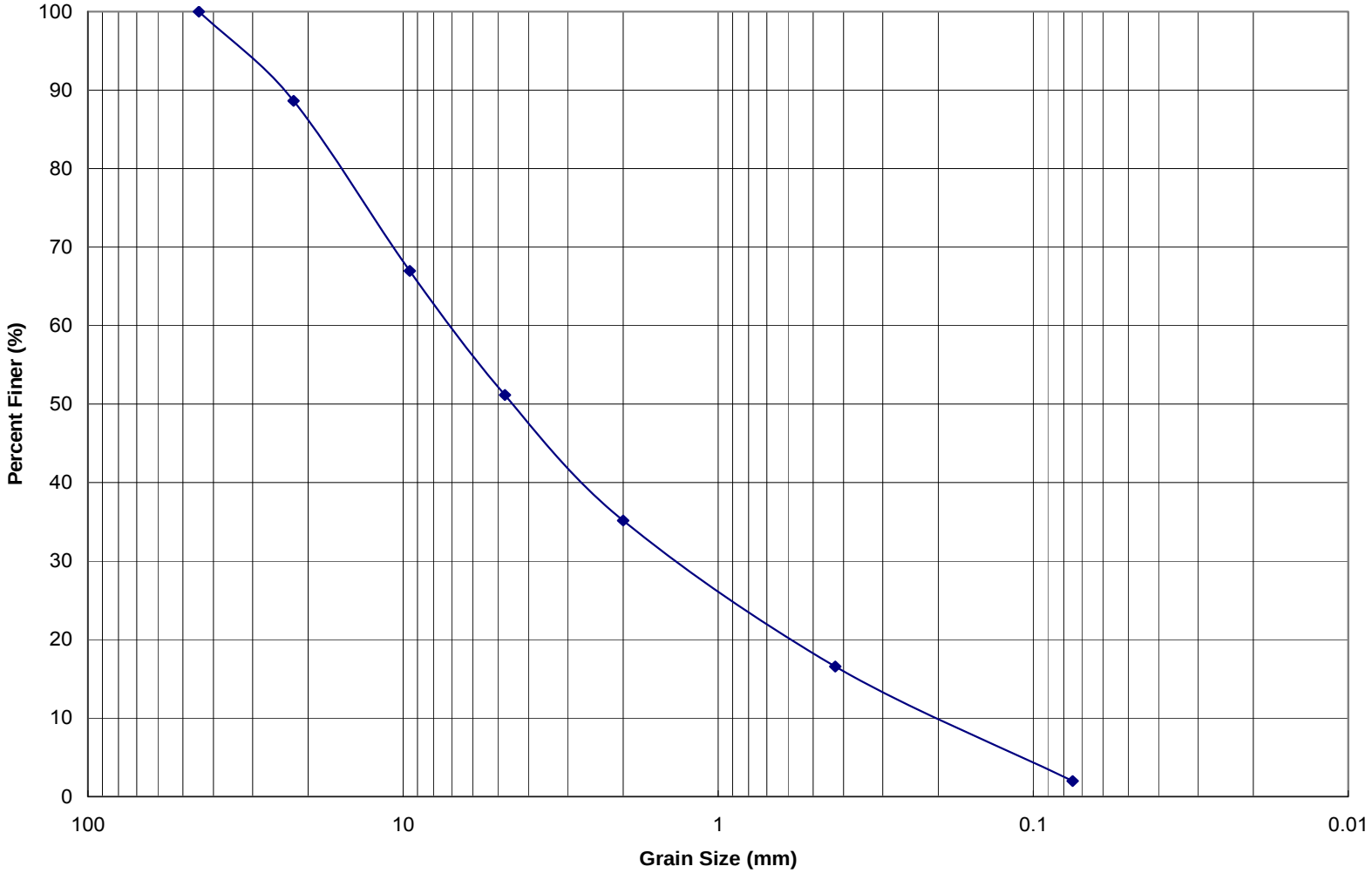


Figure 3.5 Sieve analysis test results for crushed concrete aggregate RC2

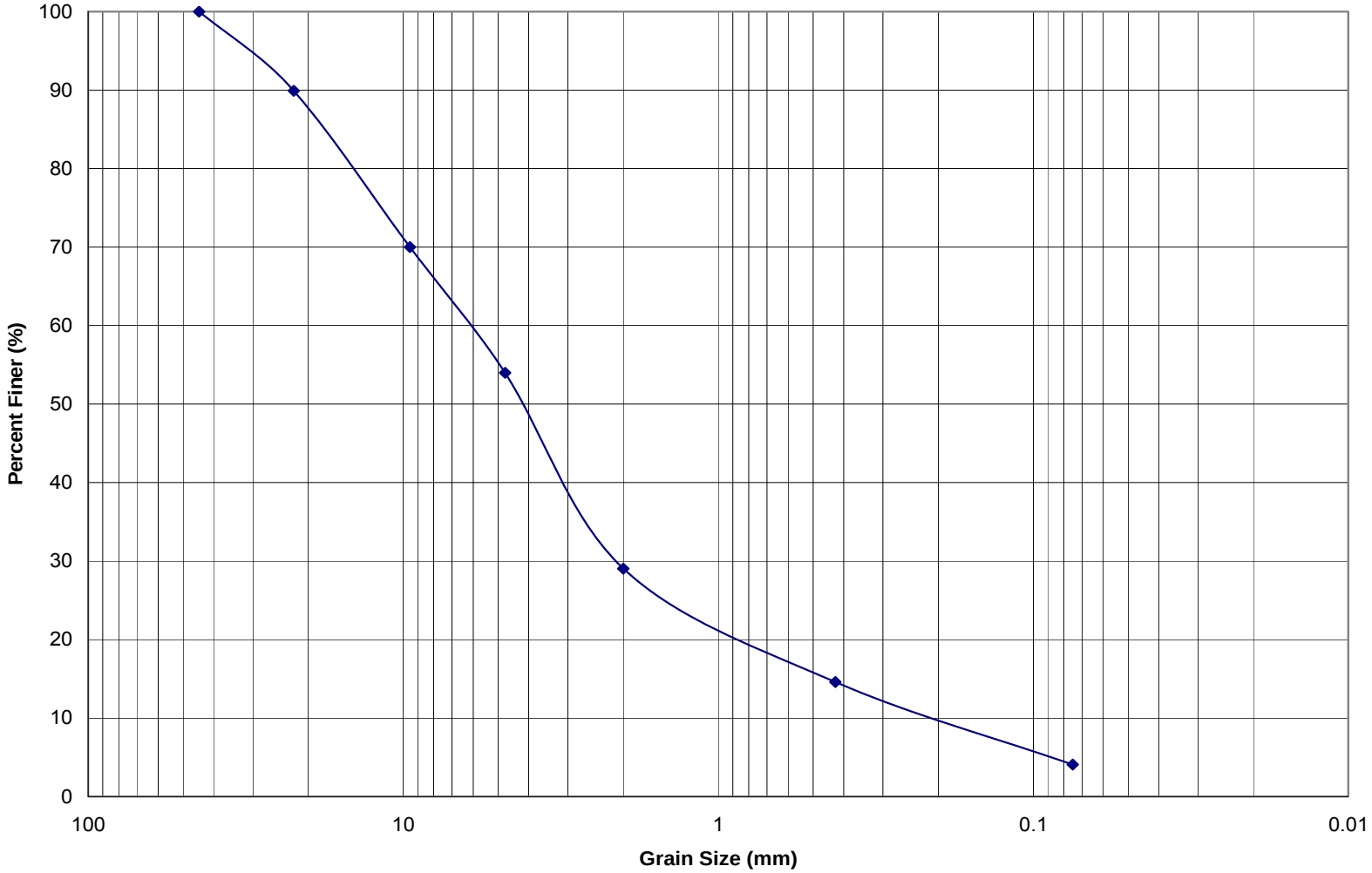


Figure 3.6 Sieve analysis test results for crushed limestone aggregate

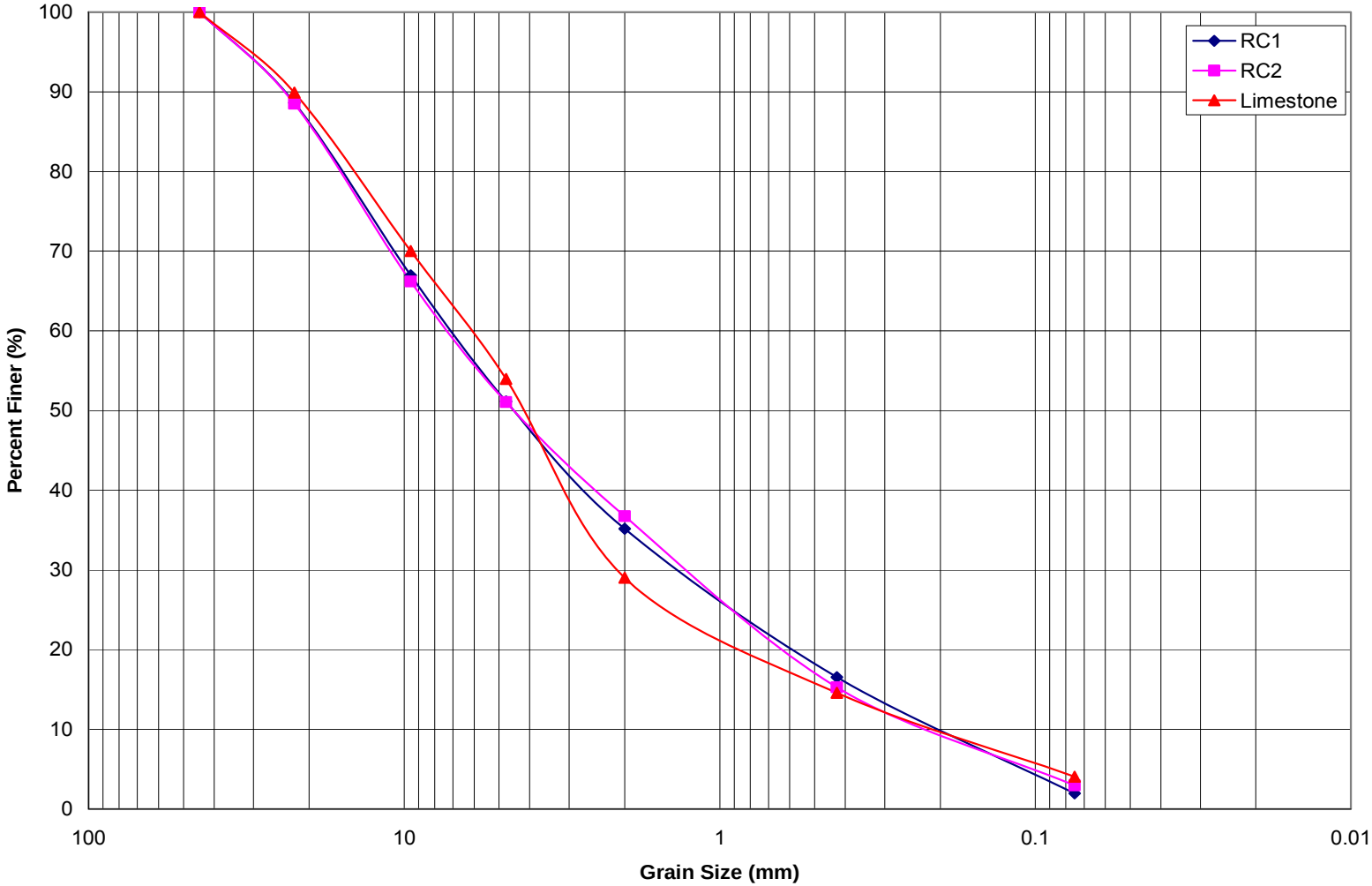


Figure 3.7 Sieve analysis test results for all three materials

Table 3.2 Percent Finer for Materials at Three Point Locations on Grain Size Distribution Curve

| Grain Size Opening (mm) | 10 | 1 | 0.1 |
|---|---|---|---|
| RC1 | 68 | 26 | 4 |
| RC2 | 69 | 27 | 5 |
| Limestone | 71 | 21 | 6 |

*3.2.2 Compaction Moisture Content – Dry Density Curves*

Soil compaction tests were conducted to establish the optimum moisture content and dry densities for each of the three materials. The ASTM D 1557 modified proctor test procedure was used for determining the laboratory moisture-density relationships. This procedure requires a compactive effort of 2694 kJ/m$^3$ (56,000 ft-lbf/ft$^3$). This requirement is met by using a 4.54 kg (10-lbf) rammer that is dropped from a height of 45.72 cm (1.5 ft). As per ASTM D 1557 method, it was determined that Method C would be used to meet gradation requirements. In this method, a 152.4mm (6.0-inch) diameter specimen with a height of 114.3 mm (4.5 in.) was prepared with material passing a 19.0 mm (3/4 in.) sieve. The compaction of each material was accomplished in five layers with a 56 blow count per layer with the rammer at the height described previously. Table 3.3 summarizes the compaction parameters used for the samples. Figures 3.8, 3.9, and 3.10 present the compaction dry unit weight and moisture content relationships for the crushed concrete aggregates and crushed limestone aggregate. It was determined from the compaction tests that the natural limestone has a higher optimum dry density than the recycled concrete aggregates. The optimum density in the limestone occurs at a percent moisture level equal to about one-half that of the recycled concrete aggregates. Table 3.4 shows the summary of optimum dry density and optimum moisture content for the materials.

Table 3.3 Compaction Parameters

| Property | Value |
|---|---|
| Required Compactive Effort (J/cm$^3$) | 2.69 |
| Weight of Hammer (kg) | 4.54 |
| Height of Drop (cm) | 45.72 |
| Diameter of Sample (cm) | 15.24 |
| Height of Sample (cm) | 4.58 |
| Volume of Molded Specimen (cm$^3$) | 17.78 |
| No. of Layers for Molding Sample | 5 |
| Drops per Layer | 56 |
| Applied Compactive Effort (J/cm$^3$) | 2.69 |

Table 3.4 Summary of Optimum Dry Density and Optimum Moisture Content

| Material | Optimum Dry Density kN/m$^3$ | Optimum Moisture Content % |
|---|---|---|
| RC1 | 18.54 | 14 |
| RC2 | 19.17 | 12 |
| Limestone | 22.25 | 6 |

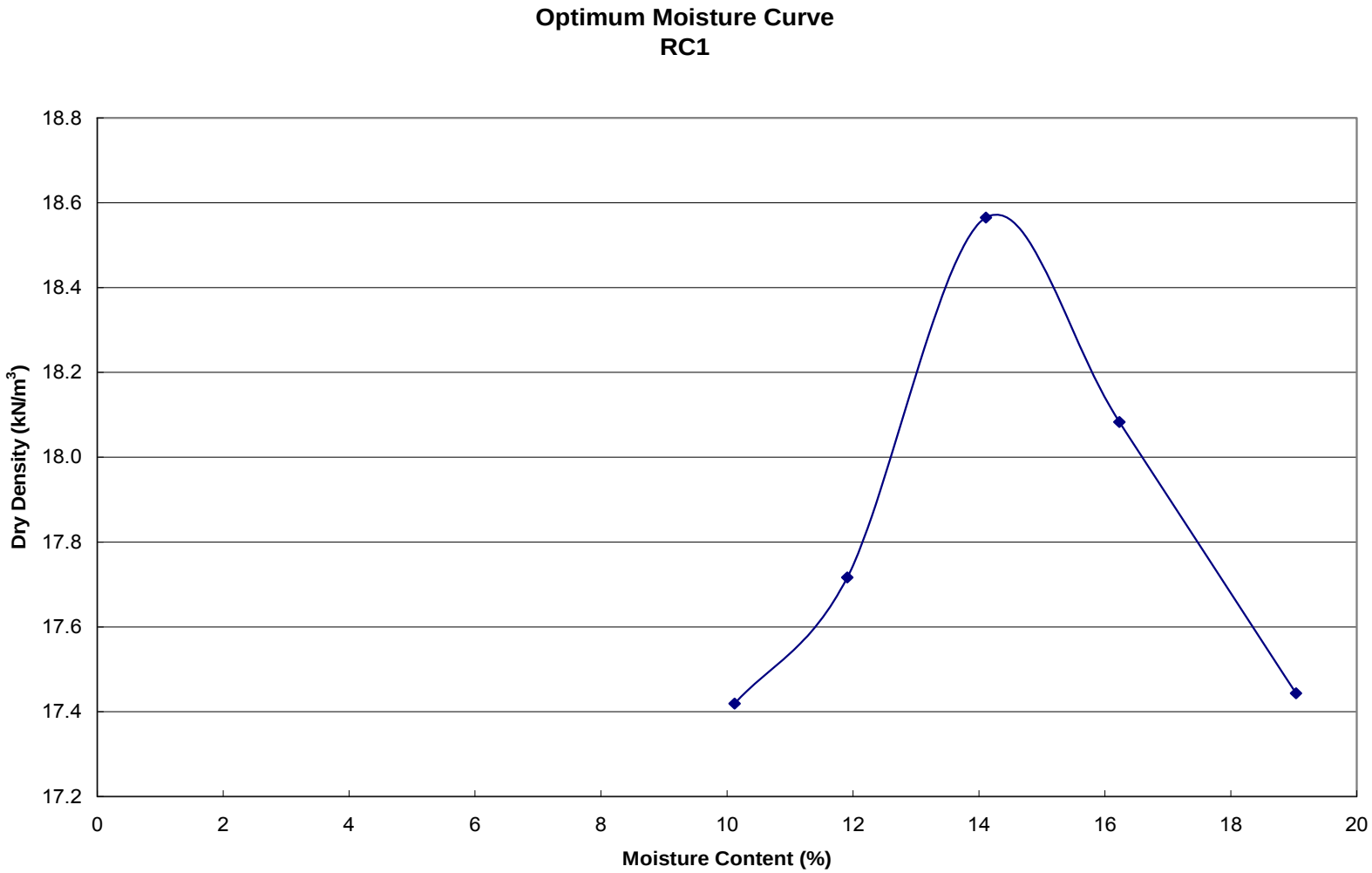


Figure 3.8 Density curve for recycled aggregate RC1

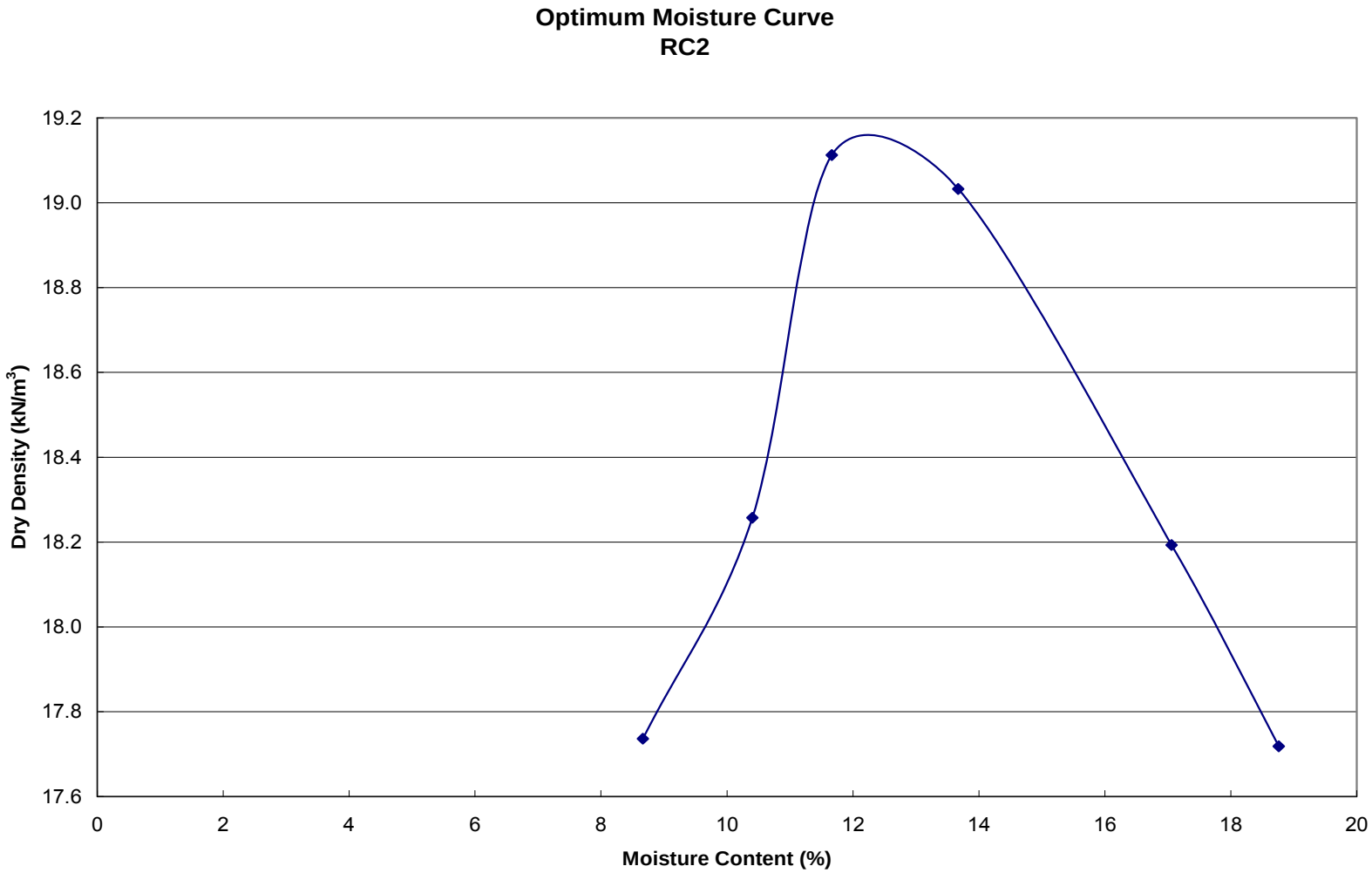


Figure 3.9 Density curve for recycled aggregate RC2

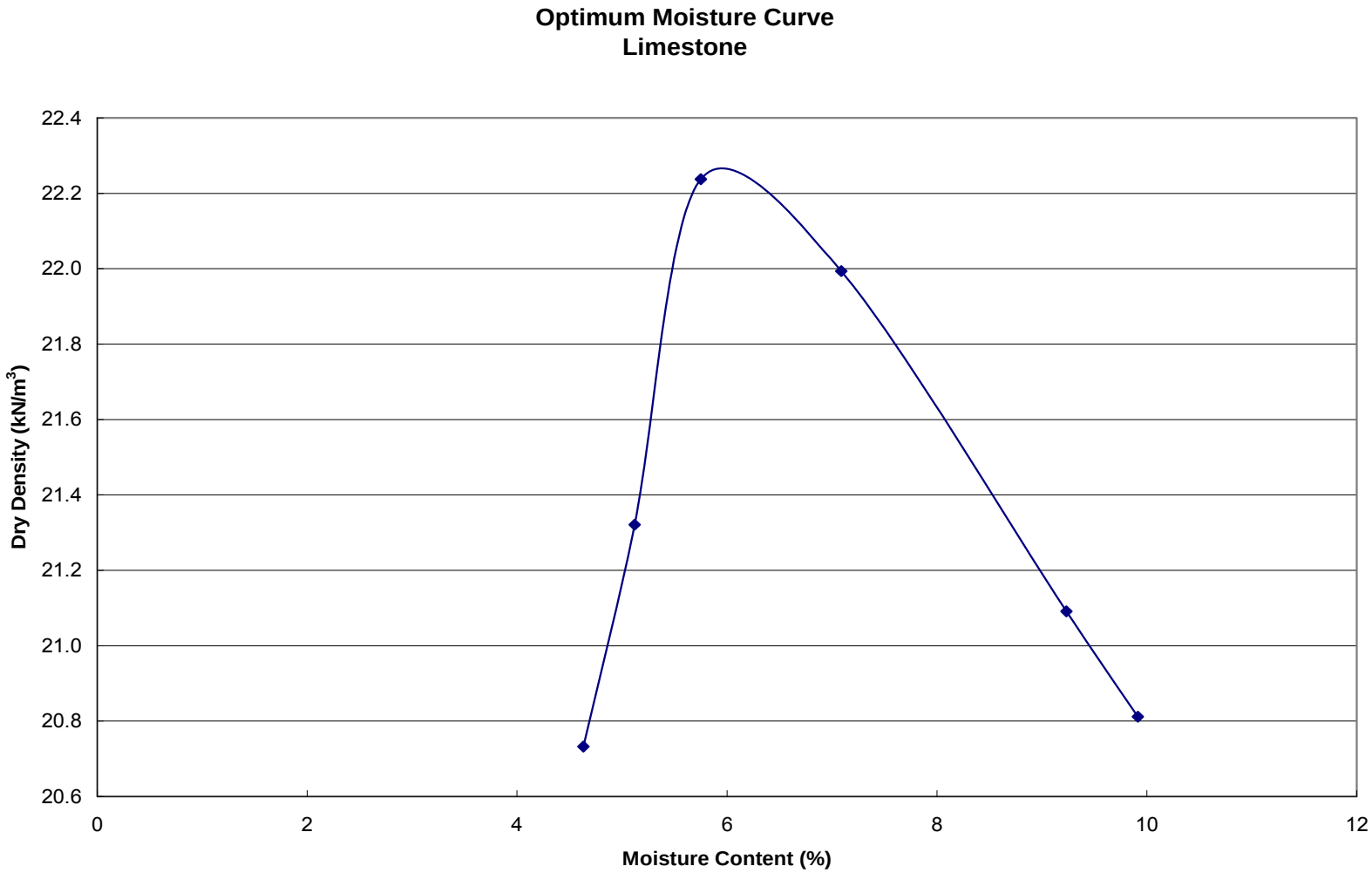


Figure 3.10 Density curve for limestone aggregate

*3.2.3 Plasticity Index*

The plasticity indices of the material samples were determined as per Texas Department of Transportation testing procedures. The procedures Tex-104-E tested for liquid limit, Tex-105-E tested for plastic limit, and Tex-107-E for the bar linear shrinkage. The plasticity index for the natural aggregate material was determined from the results of the liquid limit and the plastic limit. The plasticity index for the crushed concrete aggregates was determined from the linear bar shrinkage as described in Tex-104-E procedure. The liquid limit and plastic limit tests were inconclusive for the recycled concrete aggregates. Table 3.5 shows the results from these testing procedures. Figure 3.11 shows the test samples for the linear bar shrinkage test from left to right for the RC1, Limestone, and RC2 samples, respectively.

Table 3.5 Plasticity Index Testing Results

| Material Sample | LL | PL | PI |
|---|---|---|---|
| RC1 | - | - | NP |
| Limestone | 18 | 12 | 6 |
| RC2 | - | - | NP |

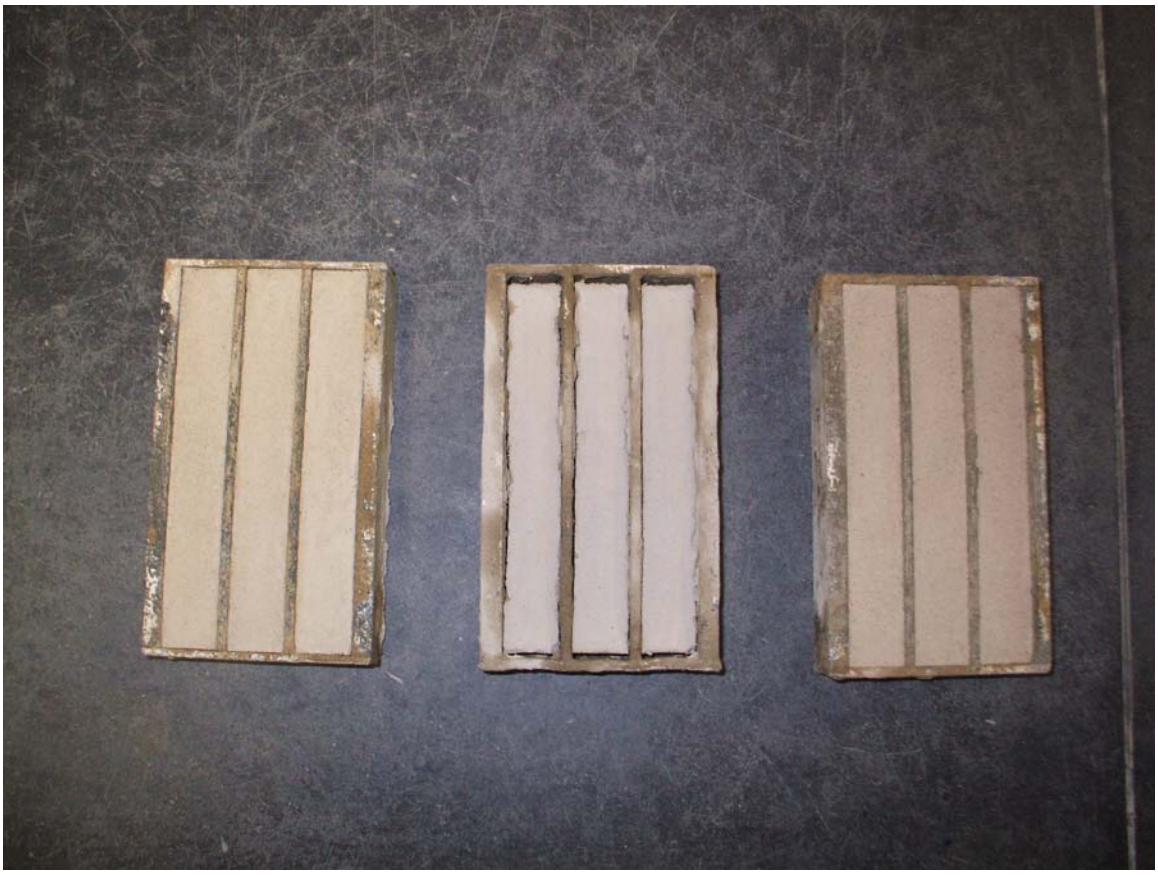

Figure 3.11 Linear bar shrinkage tests for samples

*3.2.4 pH and Specific Gravity*

The pH of all three materials was determined by using method ASTM D 4972-01. The material that was used for this testing passed a No. 10 sieve and the pH measurement was determined with a pH meter. As per ASTM D 4972-01, the pH measurements of the soils were taken in both water and in the solution of calcium chloride. The results of the pH measurements and temperatures recorded during testing are shown on Table 3.6.

The specific gravity of all three materials was determined by using method ASTM D 854-02. The material used in this procedure passed a No. 4 sieve. The results of the specific gravity results are shown on Table 3.7

Table 3.6 pH Measurements of Materials

| Material Samples | $H_2O$ | $^oC$ | $CaCl_2$ | $^oC$ |
|---|---|---|---|---|
| RC1 | 8.5 | 24.6 | 8.5 | 24.6 |
| RC2 | 8.3 | 24.6 | 8.2 | 24.6 |
| Limestone | 8.0 | 24.6 | 7.9 | 24.6 |

Table 3.7 Specific Gravity of Materials

| Material Sample | Specific Gravity |
|---|---|
| RC1 | 2.63 |
| RC2 | 2.66 |
| Limestone | 2.81 |

*3.2.5 Shear Modulus Testing Using Bender Elements*

The soil samples for the bender element testing were compacted to represent the moisture-density curves developed from the modified compaction testing for the materials. In place of the 152.4 mm (6.0-inch) diameter specimens, 101.6 mm (4.0-inch) diameter specimens were used. As in the development of the moisture-density curves, material passing a 19.0 mm (3/4 in.) sieve was used for preparing the specimens. In order to meet the same compaction effort used in moisture-density tests, the 101.6 mm (4.0-inch) samples were compacted in 5 layers with 25 blows per layer with a 4.54 kg (10.0 lbf) hammer. The soil samples were compacted into specimen molds that measured 101.6 mm (4.0-inch) diameter by 120.7 mm (4.75 in.) in length and represented the density compaction curves. For each of the three different materials, samples were molded to represent a dry, optimum, and wet condition on the moisture-density relationship. Samples for wet moisture-density conditions remained in the

mold for at least four days before being extracted. This allowed the samples from being damaged. The shear wave velocity through each of the samples was determined using a waveform generator and bender elements. These same samples were then used to determine the compressive strengths.

The bender element instrumentation used in the experiment consisted of a 40 MHz Arbitrary Waveform Generator, oscilloscope, and bender element transmitter and receiver caps as shown on Figure 3.12, Figure 3.13, and Figure 3.14, respectively. The oscilloscope was interfaced with a desktop computer and software to receive and capture the data for the testing. The bender elements are embedded into 101.6 mm (4-inch) diameter end caps with the transmitter on the top end cap and the receiver on the bottom end cap.

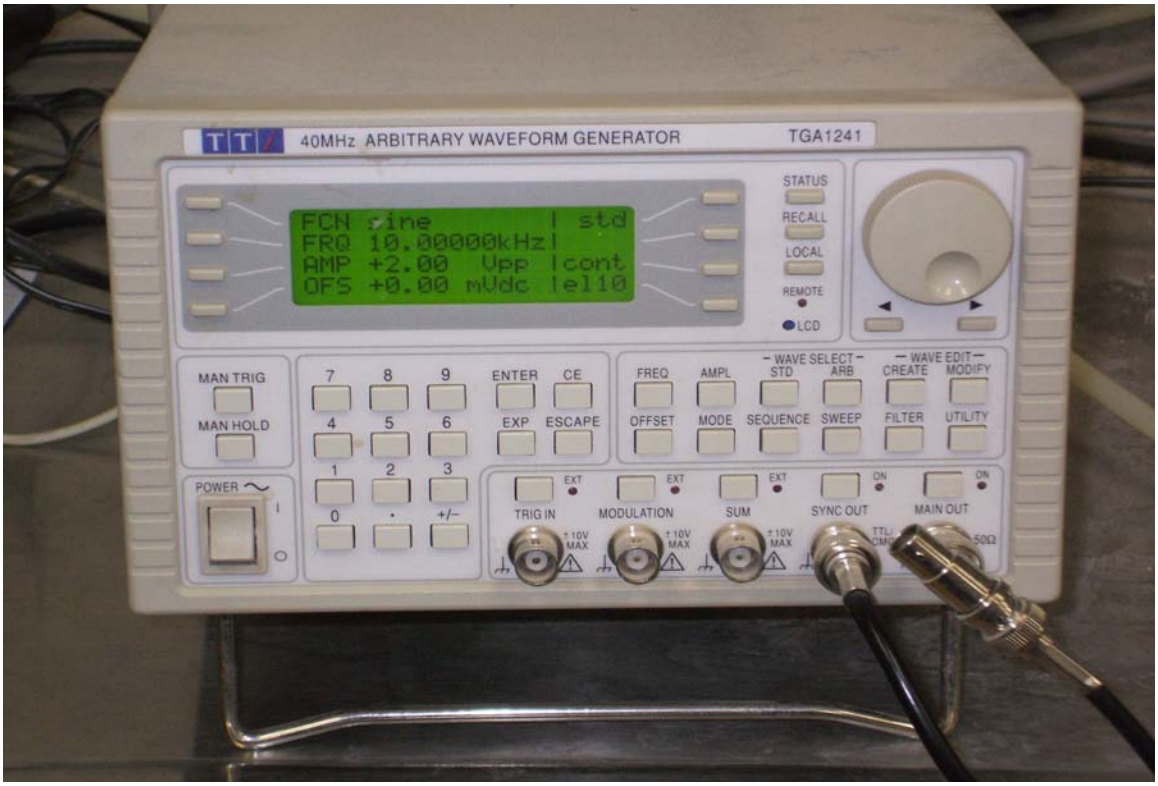


Figure 3.12 40 Mhz Arbitrary Waveform Generator


Figure 3.13 Pico Technology oscilloscope

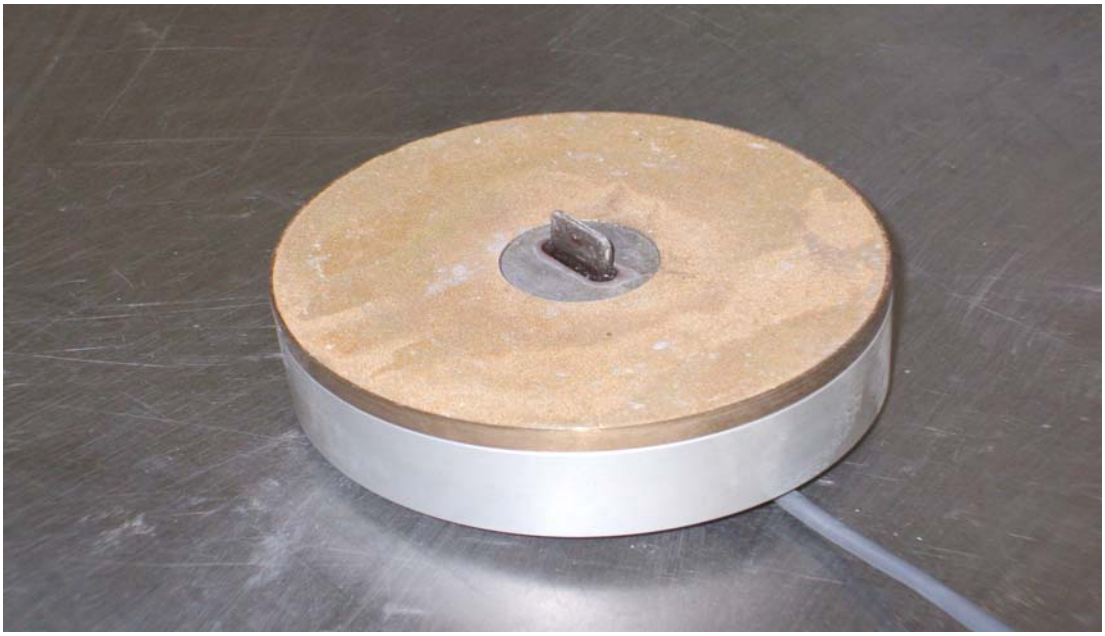

Figure 3.14 End cap with piezo-ceramic bender element

Initially, compacted samples were placed in a triaxial chamber with a bender element transmitter and receiver as shown in Figure 3.15. The confining pressure of the triaxial chamber was varied using 0 kPa (0 psi), 20.68 kPa (3 psi), 41.37 kPa (6 psi), and 82.74 kPa (12 psi). There were no variations in shear wave velocity measurements for the specimens due to the varying confining pressure as shown in Figures 3.16 and 3.17. Therefore, the shear wave measurements used for this study to determine the Shear Modulus were performed under unconfined conditions.

Figure 3.18 shows the instrumentation and set-up used for the experiment in unconfined conditions. Between the end caps and the soil sample, a foam board cut out at a 101.6 mm (4.0-inch) diameter and 2.0 mm thickness was used to create a level surface for the specimens. The foam board included cut-out sections in the center to allow the bender element to penetrate into the samples. Due to the hardness of the specimens and inclusion of aggregates, the specimens cannot be trimmed as can be done with most other cohesive soils. The indentions into the sample specimens are created to insert the bender elements to allow readings for shear wave velocity. The indentions on each end of the sample specimens accounted for the thickness of the foam board and the length of the bender element.

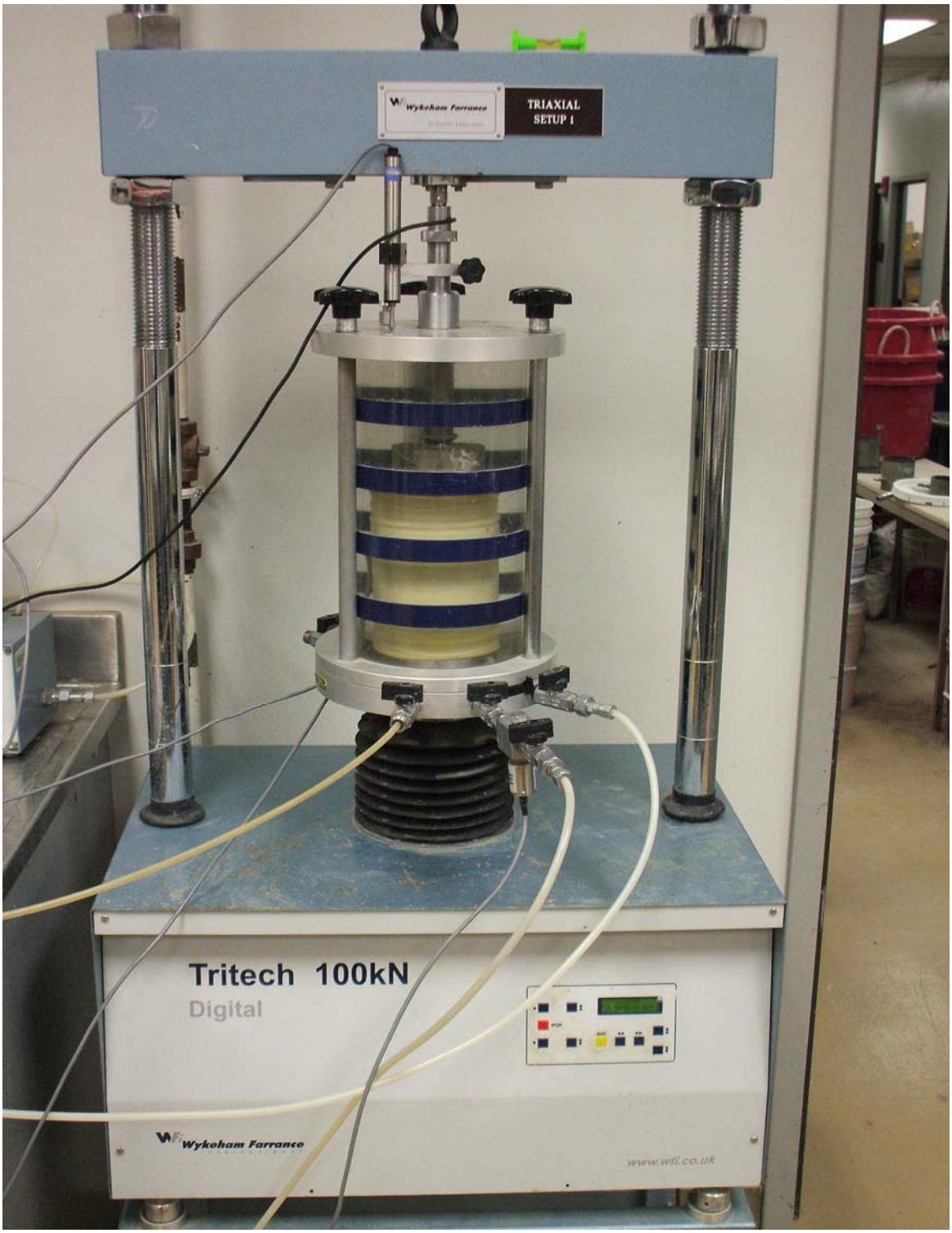

Figure 3.15 Specimen in triaxial chamber with bender elements

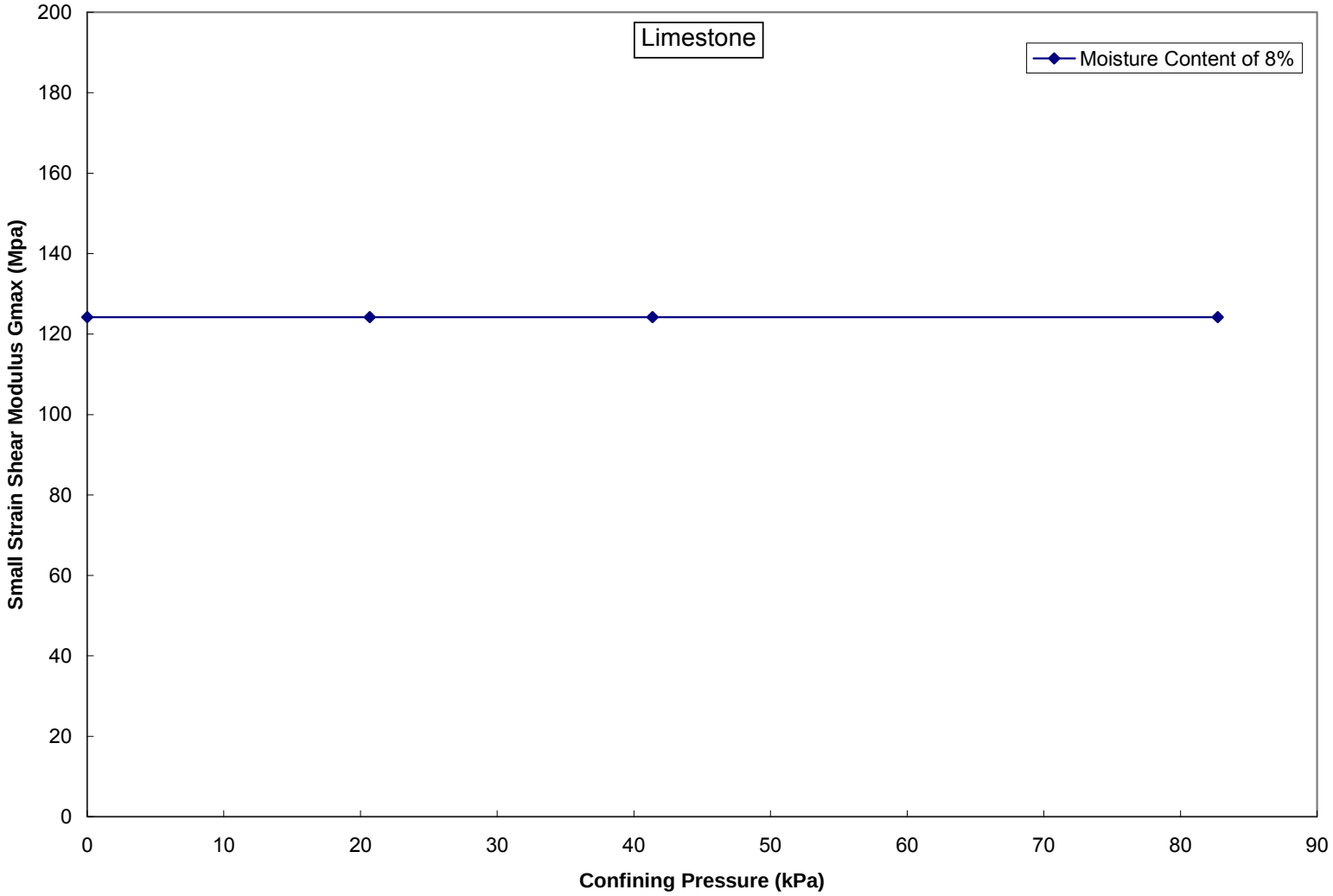


Figure 3.16 Small strain shear modulus $G_{max}$ value for limestone at varying confining pressure

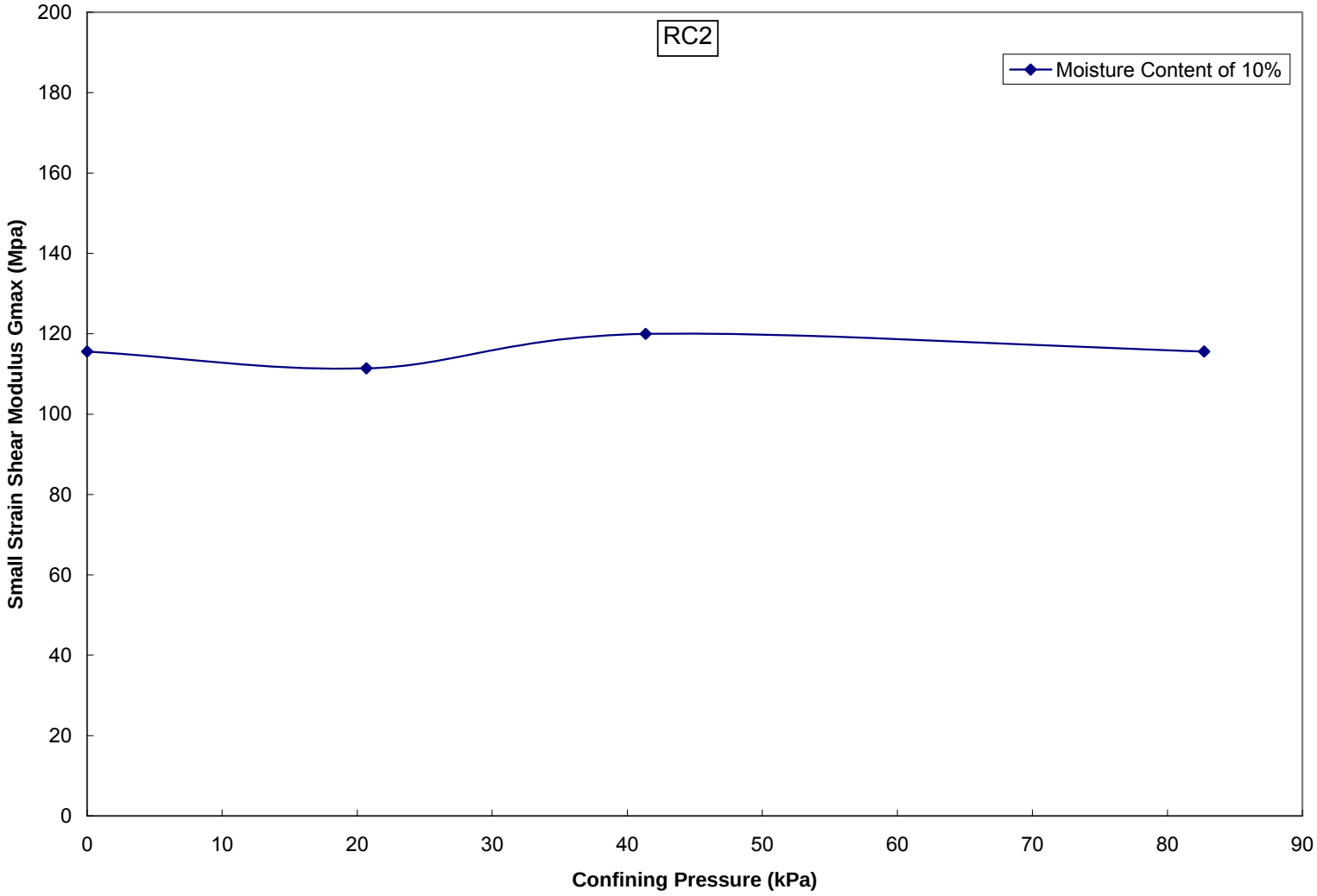


Figure 3.17 Small strain shear modulus $G_{max}$ value for recycled concrete aggregate RC2 at varying confining pressure

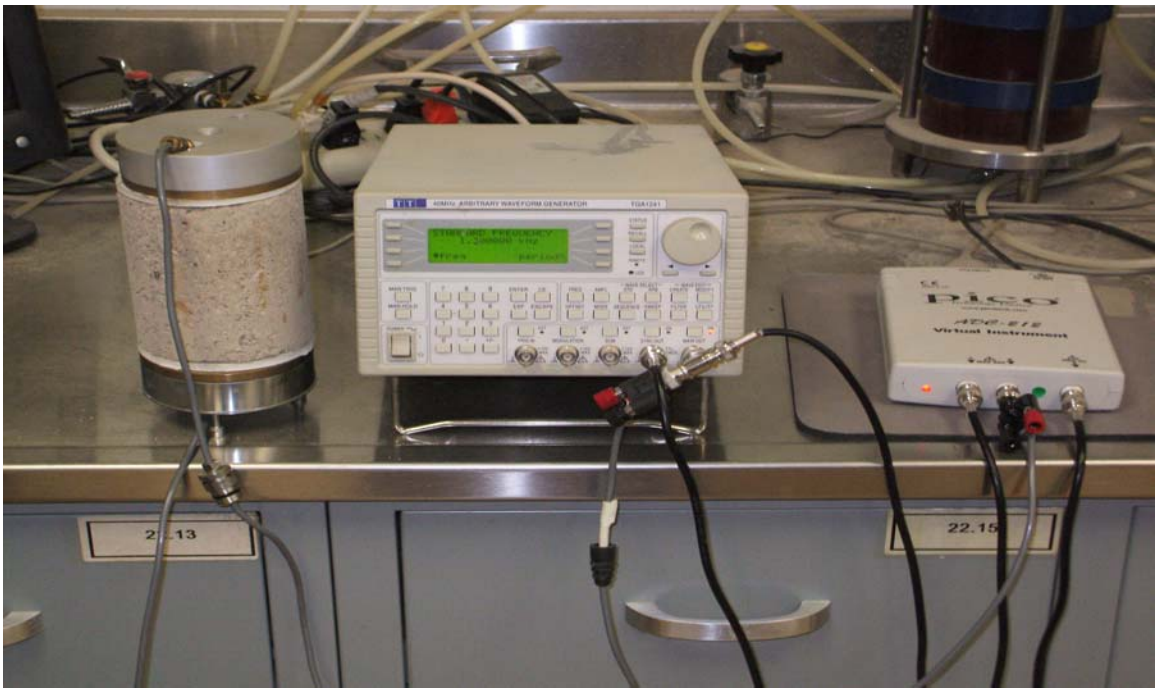


Figure 3.18 Unconfined bender element experiment instrumentation set up

In the measurement of the shear wave velocity, each sample was tested to determine the resonant frequency. This was accomplished by measuring the travel time of the shear wave while increasing the frequency of the wavelength. Once the resonant frequency is reached the time of travel does not vary as the frequency is increased. The shear wave time of travel for the specimens was determined at a frequency higher than the determined resonant frequency. The distance for time of travel was measured from the originating point of the sending wave (blue) to the first reverse point in the receiving wave (red) as shown on Figure 3.19. The originating point and point of receiving are marked with vertical lines labeled with ‘x’ and ‘o’. The time of travel is labeled as ‘xo’ and measured in seconds. The measured time of travel was used for calculating the shear wave velocity based on measured distance between the tips of the bender element piezo-ceramics.

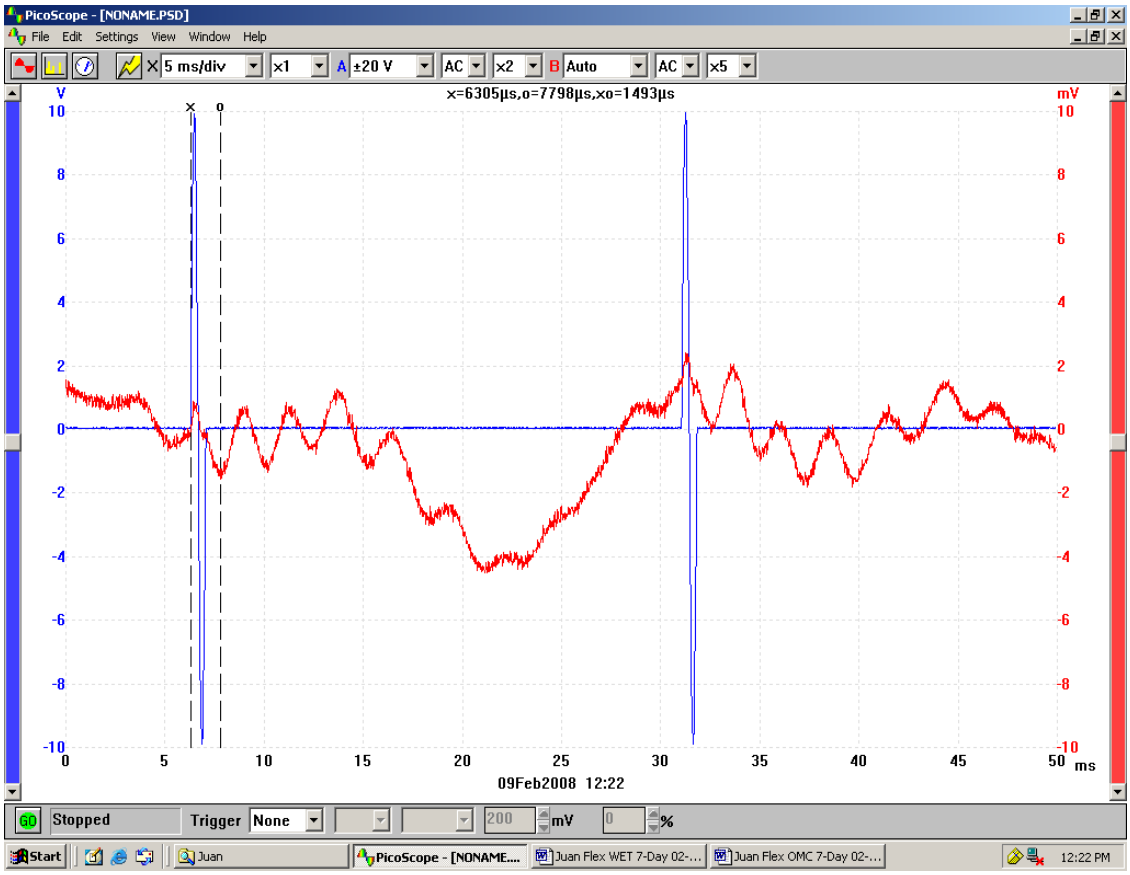


Figure 3.19 Shear wave measurement of crushed limestone aggregate for a 7-day curing period

*3.2.6 Unconfined Compression Strength Testing*

After the measurement of the shear wave velocity, the specimens were tested for their unconfined compression strengths. This was performed in a Test Mark CM-3000 compression testing machine that was controlled through a digital load indicating system. The specimens initial height and failure height were recorded using a digital recorder. This allowed the axial deformation to be determined. The compressive axial stress was determined using the corrected cross sectional area. The compressive strengths were determined using the specimens compacted as explained in the bender element test related specimens. Figure 3.20

and 3.21 show the testing equipment and sample setup for the unconfined compression strength tests.


Figure 3.20 Four-inch diameter specimen in compression with digital displacement recorder


Figure 3.21 Test Mark CM-3000 compression machine with digital loading indicating system

*3.2.7 Permeability Testing*

The soil specimens used in the permeability tests were derived from excess samples from the bender element and compression testing. The samples were saturated for a period of 24 hrs. The tests results were determined by taking an average of four readings. The readings were collected only after verifying that the sample had been properly saturated. These samples were used in a falling head permeameter that consisted of a burette on the water supply end to measure the head difference, and porous stones on each end of the sample. Figure 3.22 shows the testing apparatus used for the permeability testing.

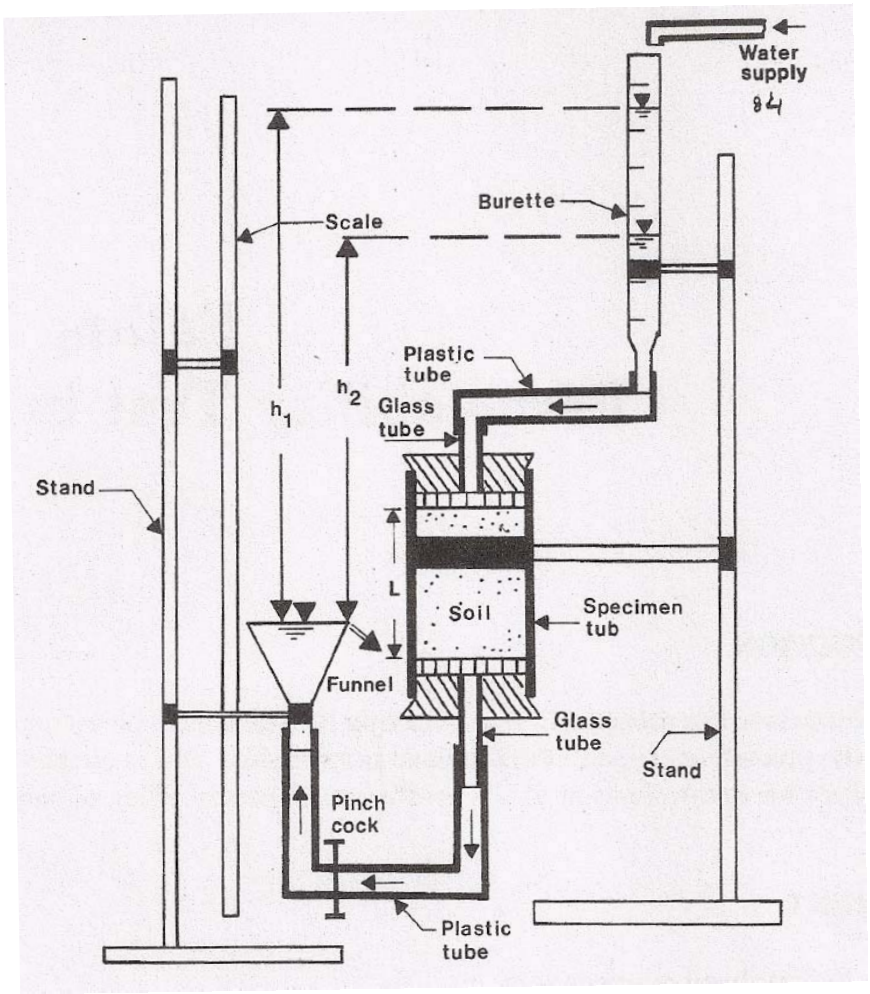


Figure 3.22 Falling-head permeameter testing apparatus setup (Das, 1989)

## 3.3 Summary

This chapter presented the experimental program, testing methods and process for determining the properties of the natural aggregates and recycled concrete aggregates. Also, several photographs of actual testing were presented in the test sections. Specifically, the method for determination of the shear modulus from the use of bender elements and measuring shear wave velocity was presented.

# CHAPTER 4

# MECHANICAL AND FLOW PROPERTIES OF RECYCLED CONCRETE AGGREGATES

## 4.1 Introduction

This chapter presents the analysis of the test results for the small strain shear modulus, unconfined compression strength, and permeability or hydraulic conductivity properties of the two recycled concrete aggregates used in this study. For comparisons, the same properties of a base aggregate were used. The specimens were tested at three compaction moisture contents that represent each a dry, optimum, and wet of optimum conditions related to 95% and optimum dry density conditions. The individual moisture contents were presented in the previous chapter. These tests were conducted for each material. Tests were conducted at 7-day and a 28-day curing periods to monitor any significant changes that may have occurred due to curing conditions. Analyses of these test results including statistical analyses are covered.

## 4.2 Engineering Properties

This section provides analyses of the test data resulting from various material properties. The results of the testing are presented for each material. The material properties are compared to show their similarities and differences at the varying moisture content – dry density conditions and curing periods.

The recycled concrete aggregate RC1 was molded into 101.6 mm (4.0 in.) diameter specimens with a height of 120.7 mm (4.75 in.). Moisture content selected for the specimens represent a dry, optimum, and wet condition on the compaction moisture content – dry density curve. The corresponding percent moisture contents are 12 %, 14%, and 18%, respectively. A minimum of two samples were used for each compaction condition and each curing period. The

maximum dry density determined was 1890 kg/m$^3$ (118 lb/ft$^3$). These values are consistent with testing data obtained from tests performed on other recycled concrete aggregates by the Texas Department of Transportation (2001).

The recycled concrete aggregate RC2 was molded into 101.6 mm (4.0 in.) diameter specimens with a height of 120.7 mm (4.75 in.). Moisture content selected for the specimens represent a dry, optimum, and wet condition on the compaction moisture content – dry density curve. The corresponding percent moisture contents are 10%, 12%, and 17%, respectively. A minimum of two samples were used for each compaction condition and each curing period. The maximum dry density determined was 1954 kg/m$^3$ (122 lb/ft$^3$). These values are consistent with testing data obtained from tests performed on other recycled concrete aggregates by the Texas Department of Transportation (2001).

The crushed limestone aggregate was molded into 101.6 mm (4.0 in.) diameter specimens with a height of 120.7 mm (4.75 in.). Moisture content selected for the specimens represent a dry, optimum, and wet condition on the compaction moisture content – dry density curve. The corresponding percent moisture contents are 5%, 6%, and 8%, respectively. A minimum of two samples were used for each compaction condition and each curing period. The maximum dry density determined was 2259 kg/m$^3$ (141 lb/ft$^3$). These values are consistent with testing data obtained from tests performed on other limestone aggregates by the Texas Department of Transportation (2001).

In addition, pH tests were conducted on the material specimens, and these results showed that the recycled concrete aggregates tested here were similar to the results of the crushed limestone aggregates. The values of all three materials were measured to be at approximately a pH of 8. This presents an opportunity that can allow the use of recycled concrete aggregates in applications that have restrictions due to high pH values.

*4.2.1 Unconfined Compression Strength (UCS) Test*

The material specimens molded as described previously were tested in unconfined conditions for compression strength and corrected for axial deformation. The specimens were loaded at a uniform rate not to exceed a vertical strain greater than 2% per minute. The corrected values for the measured compression strength are provided in figure 4.1 through figure 4.6 for all three materials. The figures show the measured values and the average value determined from the measurements for each material at the specified percent moisture content and curing period.

In order to evaluate the testing procedure for the measurement of the unconfined compression strength, the results were analyzed for each material and assessed for repeatability and reliability. The analyses of the materials are presented in tables 4.1, 4.2, and 4.3. The standard deviation for the unconfined compression strength tests ranged from 3.25 kPa to 56.27 kPa. The coefficient of variation remained small for each of the materials tested, indicating that the test results obtained were repeatable.

Table 4.1 Results for Unconfined Compression Strength of Recycled Concrete Aggregate RC1

| Cure Time | Moisture Content | Unconfined Compressive Strength | Unconfined Compressive Strength | Mean | Variance | Standard Deviation | Coefficient of Variation |
|---|---|---|---|---|---|---|---|
| Days | % | kPa | kPa | kPa | $(kPa)^2$ | kPa | % |
| 7 | 12 | 163.96 | 143.41 | 153.69 | 211.23 | 14.53 | 9.46 |
| 28 | 12 | 438.79 | 400.34 | 419.57 | 739.40 | 27.19 | 6.48 |
| 7 | 14 | 235.42 | 193.58 | 214.50 | 875.30 | 29.59 | 13.79 |
| 28 | 14 | 578.35 | 589.60 | 583.98 | 63.31 | 7.96 | 1.36 |
| 7 | 18 | 132.44 | 121.84 | 127.14 | 56.10 | 7.49 | 5.89 |
| 28 | 18 | 361.14 | 347.91 | 354.52 | 87.50 | 9.35 | 2.64 |

Table 4.2 Results for Unconfined Compression Strength of Recycled Concrete Aggregate RC2

| Cure Time | Moisture Content | Unconfined Compressive Strength | Unconfined Compressive Strength | Mean | Variance | Standard Deviation | Coefficient of Variation |
|---|---|---|---|---|---|---|---|
| Days | % | kPa | kPa | kPa | $(kPa)^2$ | kPa | % |
| 7 | 10 | 107.09 | 102.34 | 104.71 | 11.25 | 3.35 | 3.20 |
| 28 | 10 | 469.32 | 456.21 | 462.76 | 85.97 | 9.27 | 2.00 |
| 7 | 12 | 153.99 | 163.68 | 158.83 | 46.93 | 6.85 | 4.31 |
| 28 | 12 | 544.88 | 531.66 | 538.27 | 87.37 | 9.35 | 1.74 |
| 7 | 17 | 95.15 | 105.19 | 100.17 | 50.39 | 7.10 | 7.09 |
| 28 | 17 | 418.18 | 404.08 | 411.13 | 99.38 | 9.97 | 2.42 |

Table 4.3 Results for Unconfined Compression Strength of Limestone Aggregate

| Cure Time | Moisture Content | Unconfined Compressive Strength | Unconfined Compressive Strength | Mean | Variance | Standard Deviation | Coefficient of Variation |
|---|---|---|---|---|---|---|---|
| Days | % | kPa | kPa | kPa | $(kPa)^2$ | kPa | % |
| 7 | 5 | 205.07 | 283.55 | 244.31 | 3079.41 | 55.49 | 22.71 |
| 28 | 5 | 505.68 | 489.54 | 497.61 | 130.25 | 11.41 | 2.29 |
| 7 | 6 | 336.69 | 352.87 | 344.78 | 130.98 | 11.44 | 3.32 |
| 28 | 6 | 547.21 | 572.23 | 559.72 | 313.00 | 17.69 | 3.16 |
| 7 | 8 | 330.29 | 250.72 | 290.50 | 3166.13 | 56.27 | 19.37 |
| 28 | 8 | 430.91 | 456.11 | 443.51 | 317.52 | 17.82 | 4.02 |

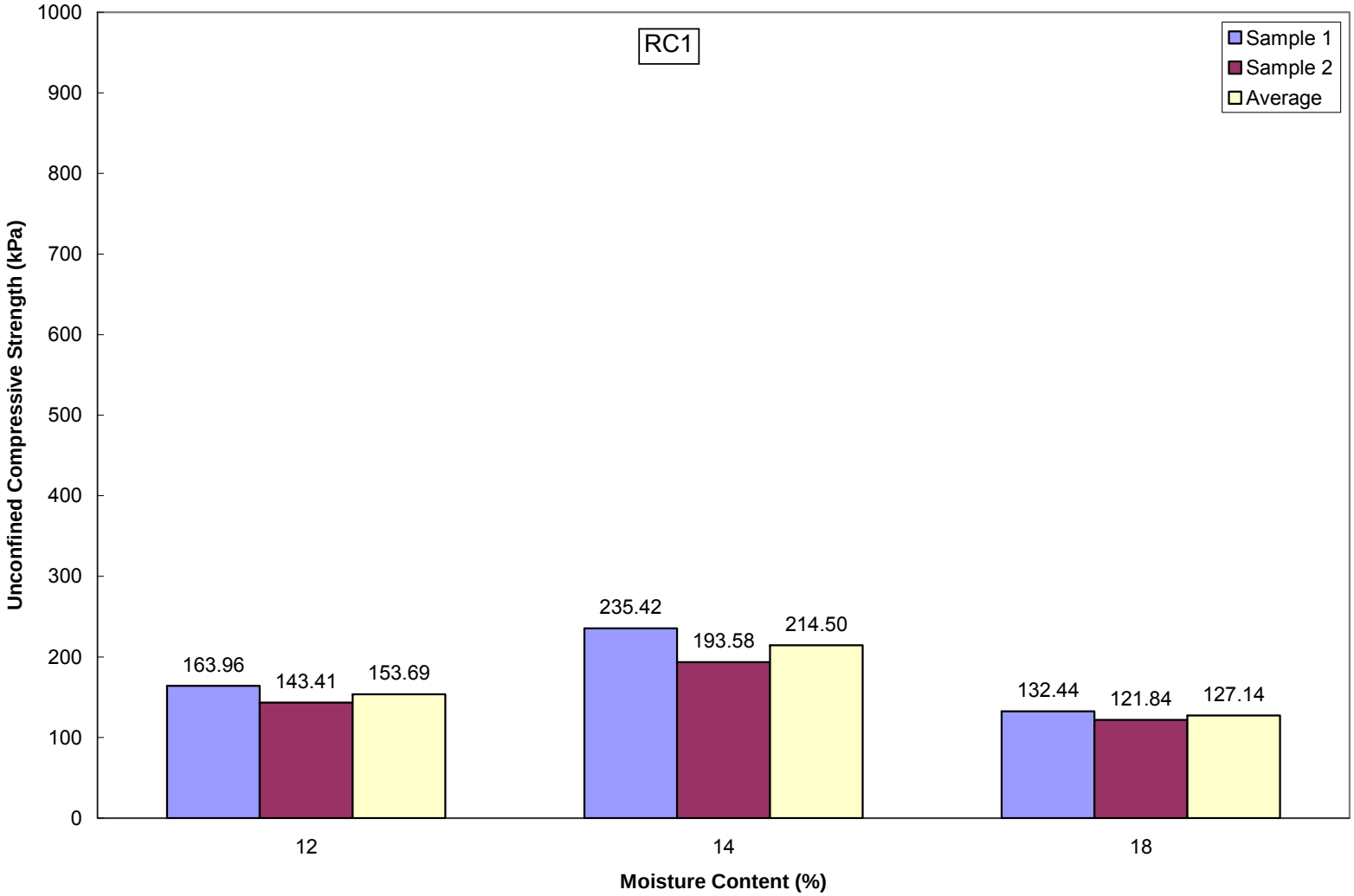


Figure 4.1 Unconfined compression strength of recycled concrete aggregate RC1 at different moisture content after 7 days of curing

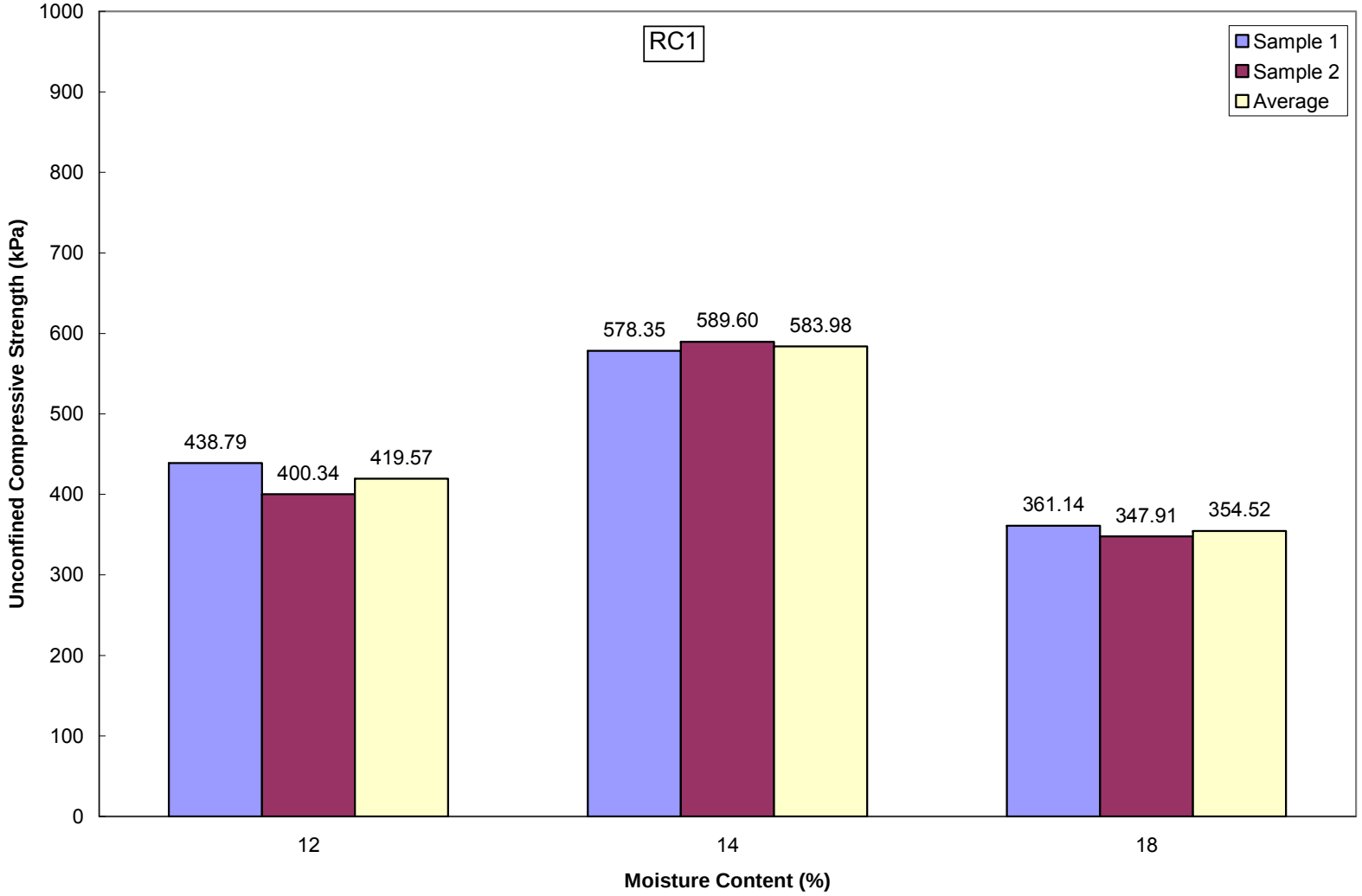


Figure 4.2 Unconfined compression strength of recycled concrete aggregate RC1 at different moisture content after 28 days of curing

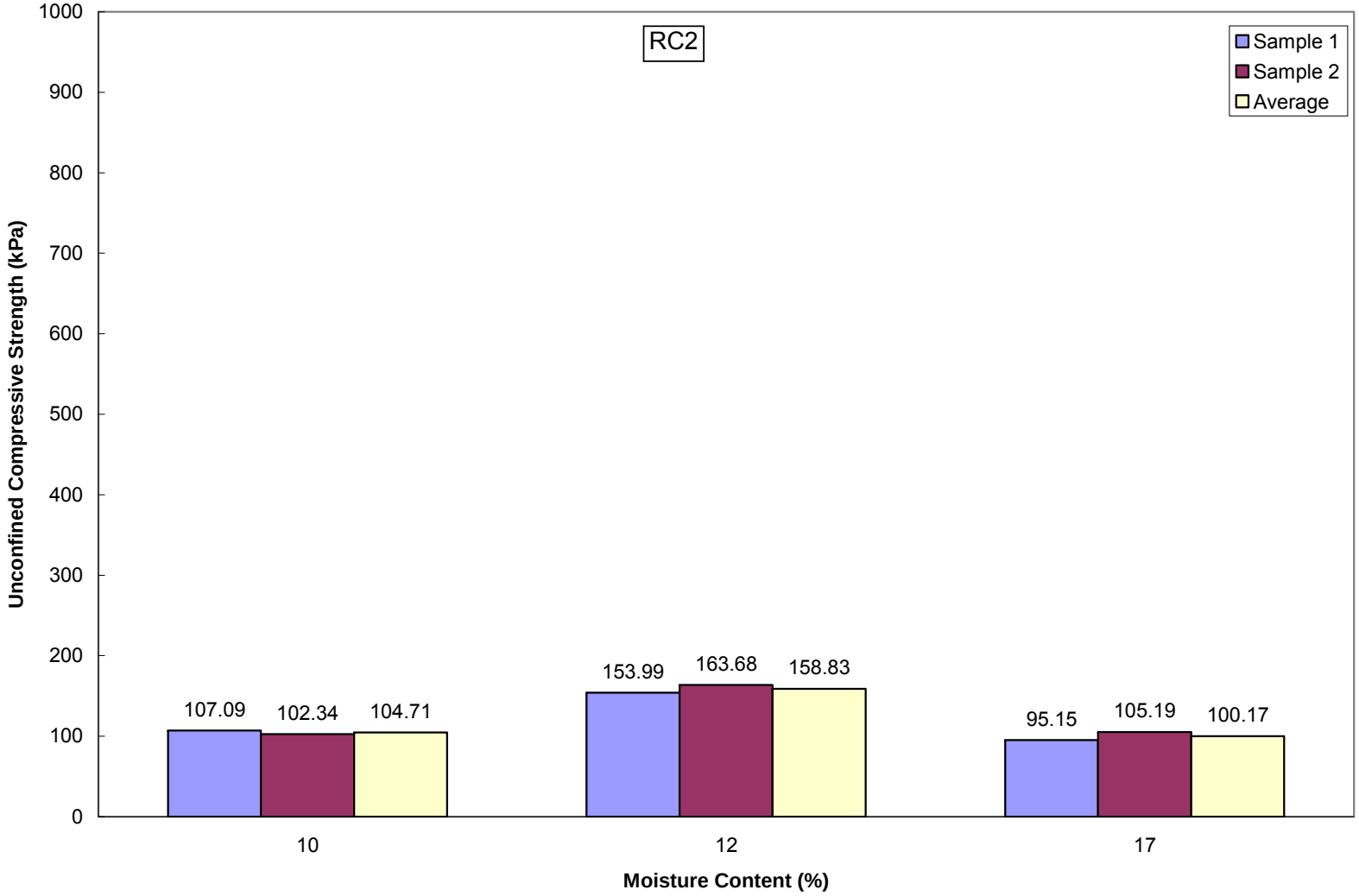


Figure 4.3 Unconfined compression strength of recycled concrete aggregate RC2 at different moisture content after 7 days of curing

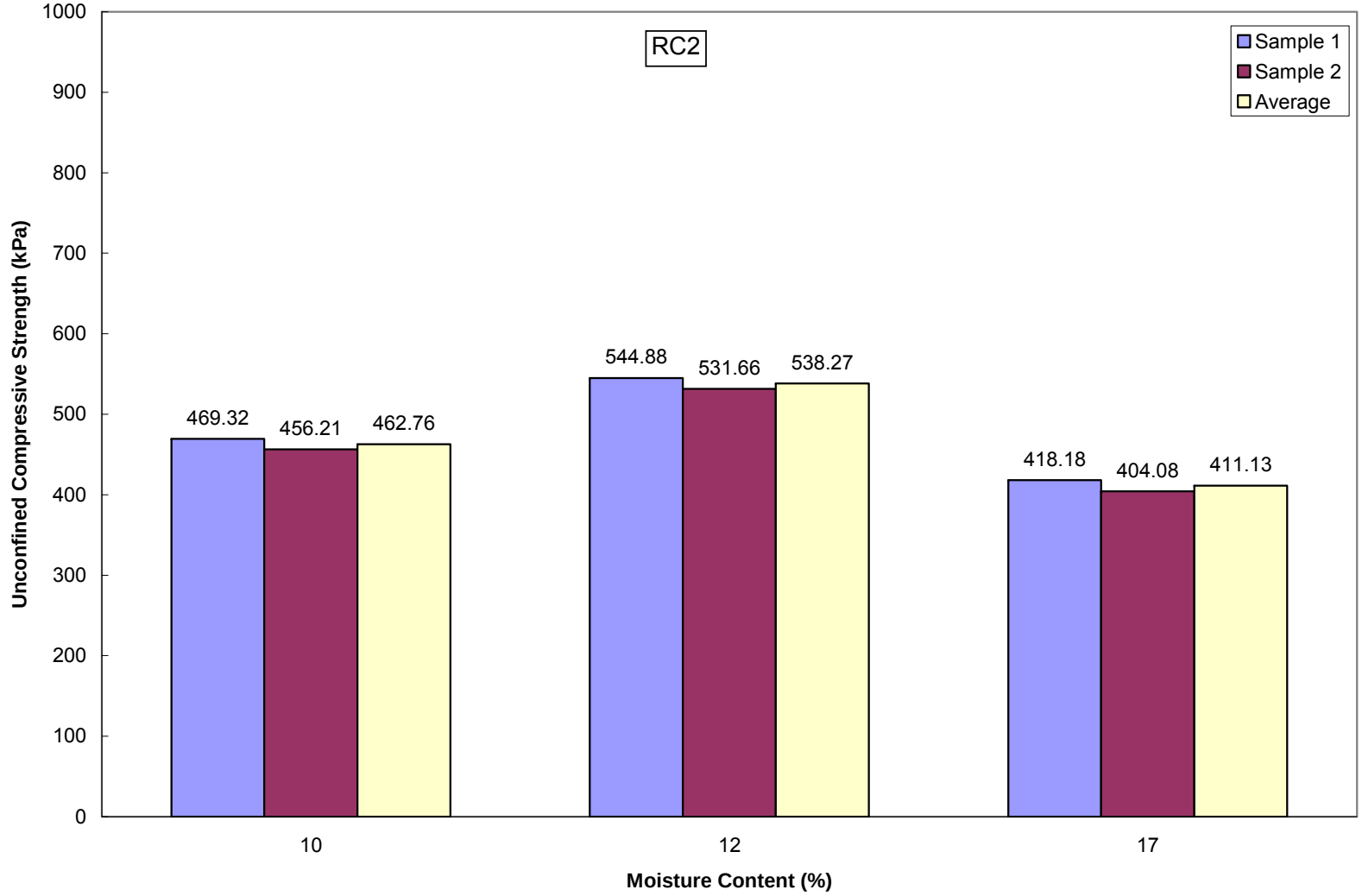


Figure 4.4 Unconfined compression strength of recycled concrete aggregate RC2 at different moisture content after 28 days of curing

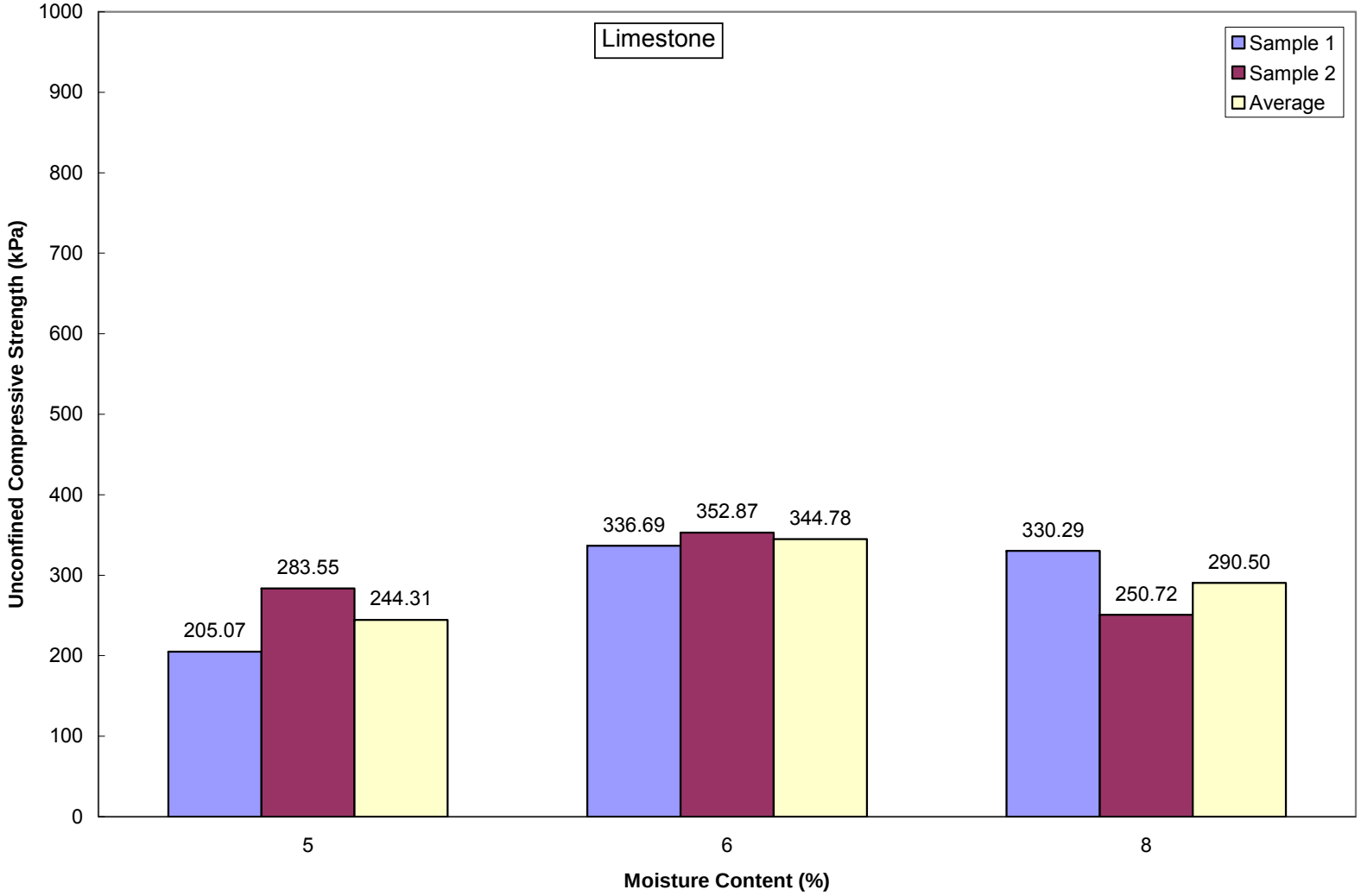


Figure 4.5 Unconfined compression strength of limestone aggregate at different moisture content after 7 days of curing

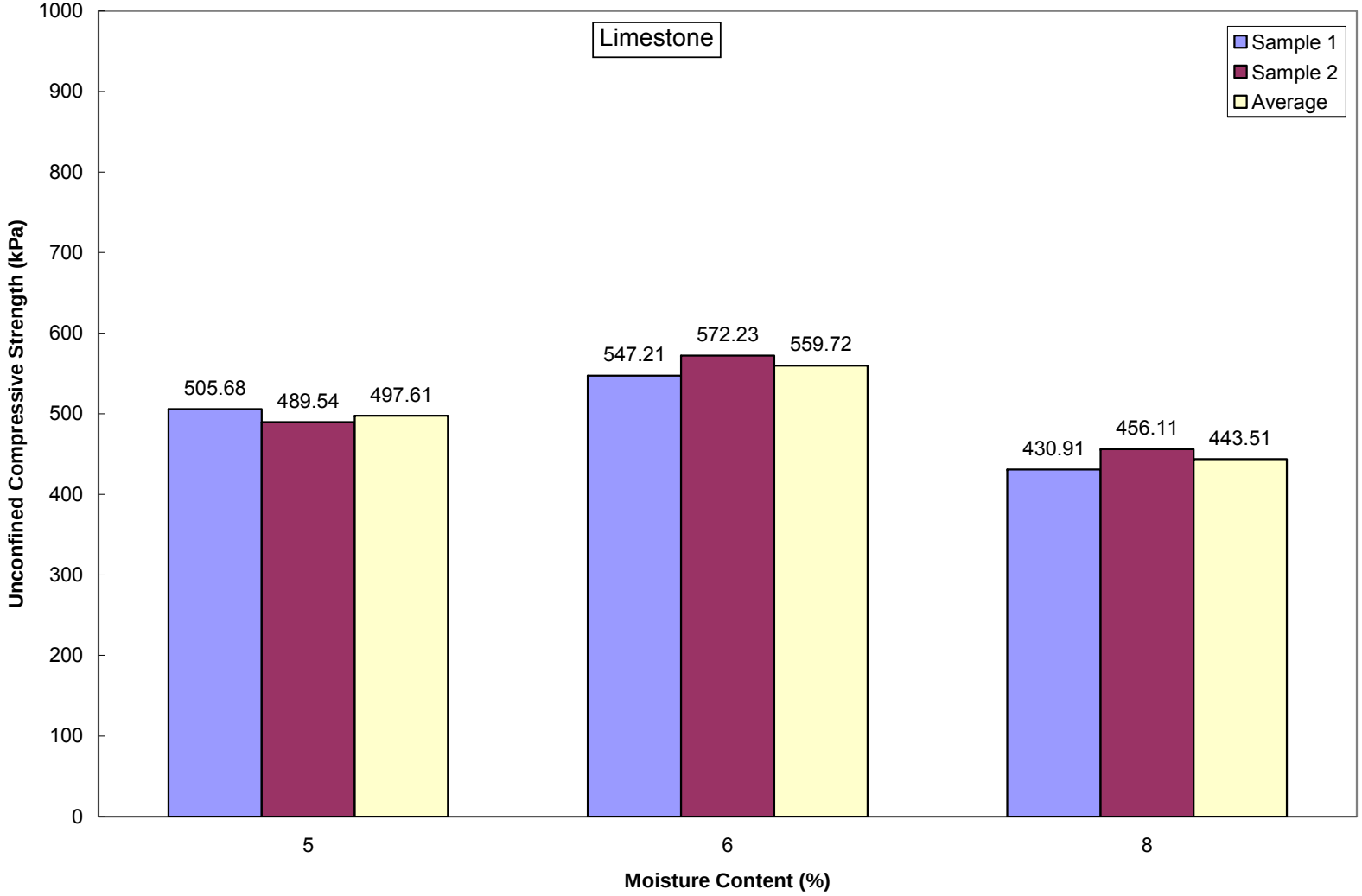


Figure 4.6 Unconfined compression strength of limestone aggregate at different moisture content after 28 days of curing

#### 4.2.1.1 Effects of Moisture Content on Unconfined Compression Strength

The average unconfined compression strength values determined for each material are presented in figures 4.7, 4.8, and 4.9. In reviewing the results, all three materials showed that the unconfined compression strength for all three materials was highest at the optimum moisture content – dry density condition. The second highest strength measurements occurred at the dry of optimum moisture content condition for each material.

The lowest strengths were consistently found to occur on the wet side of optimum moisture content condition. The density of each material coincides with the results of the unconfined compression strength from dry to optimum conditions. High strength at optimum moisture content was attributed to closer and compacted structures of the aggregate specimens. The increased moisture content on the wet side of optimum moisture content condition resulted in low strength due to moderate softening of the bonds between particles. Overall, the strength decrease is small and this could be attributed to a small increase in compaction moisture content of a relatively coarse to medium sized particles of the base mixtures of both recycled concrete aggregates and conventional flex base aggregates.

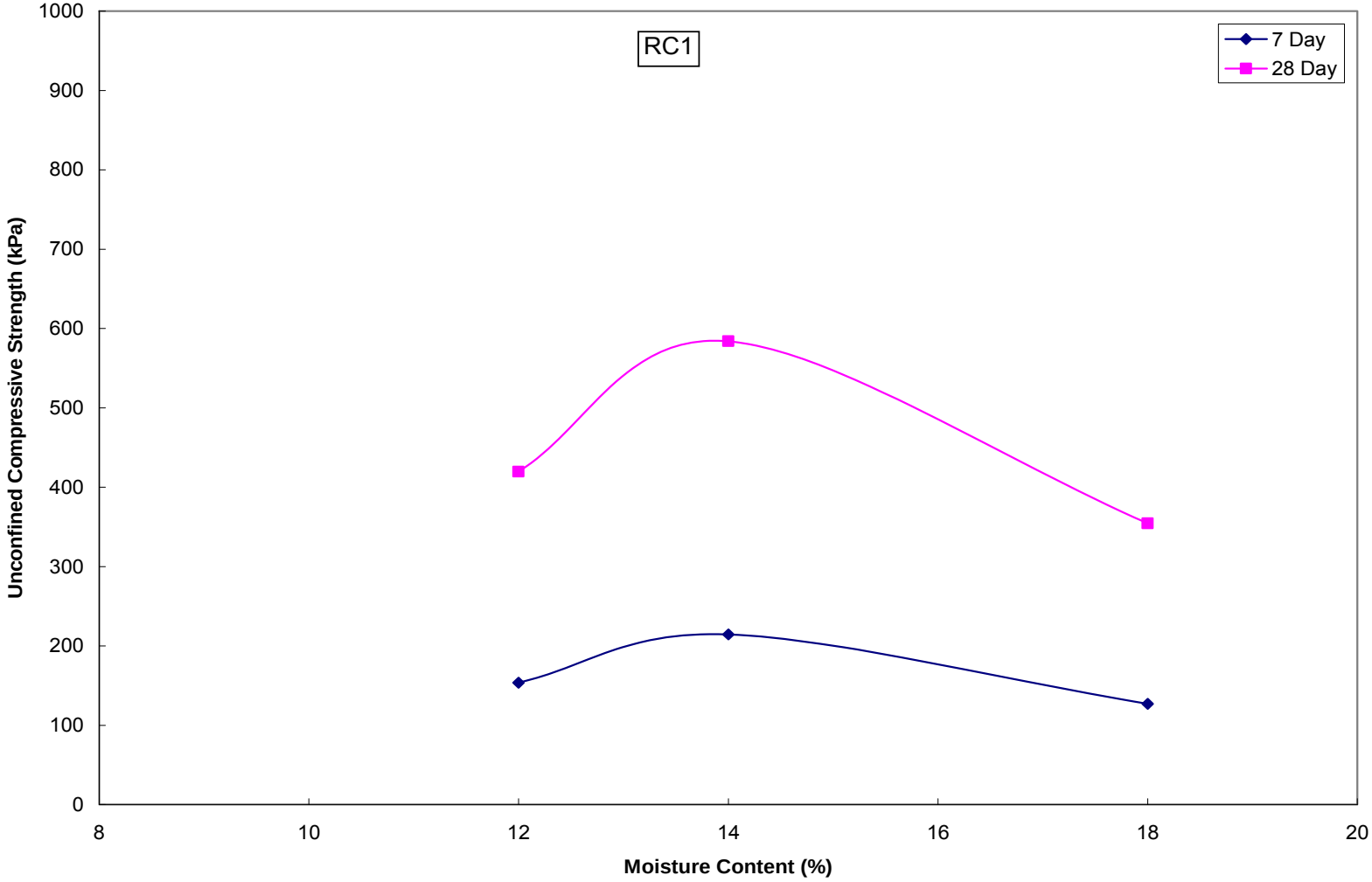


Figure 4.7 Average values of unconfined compression strength for recycled concrete aggregate RC1 at different moisture content for 7 and 28 day curing

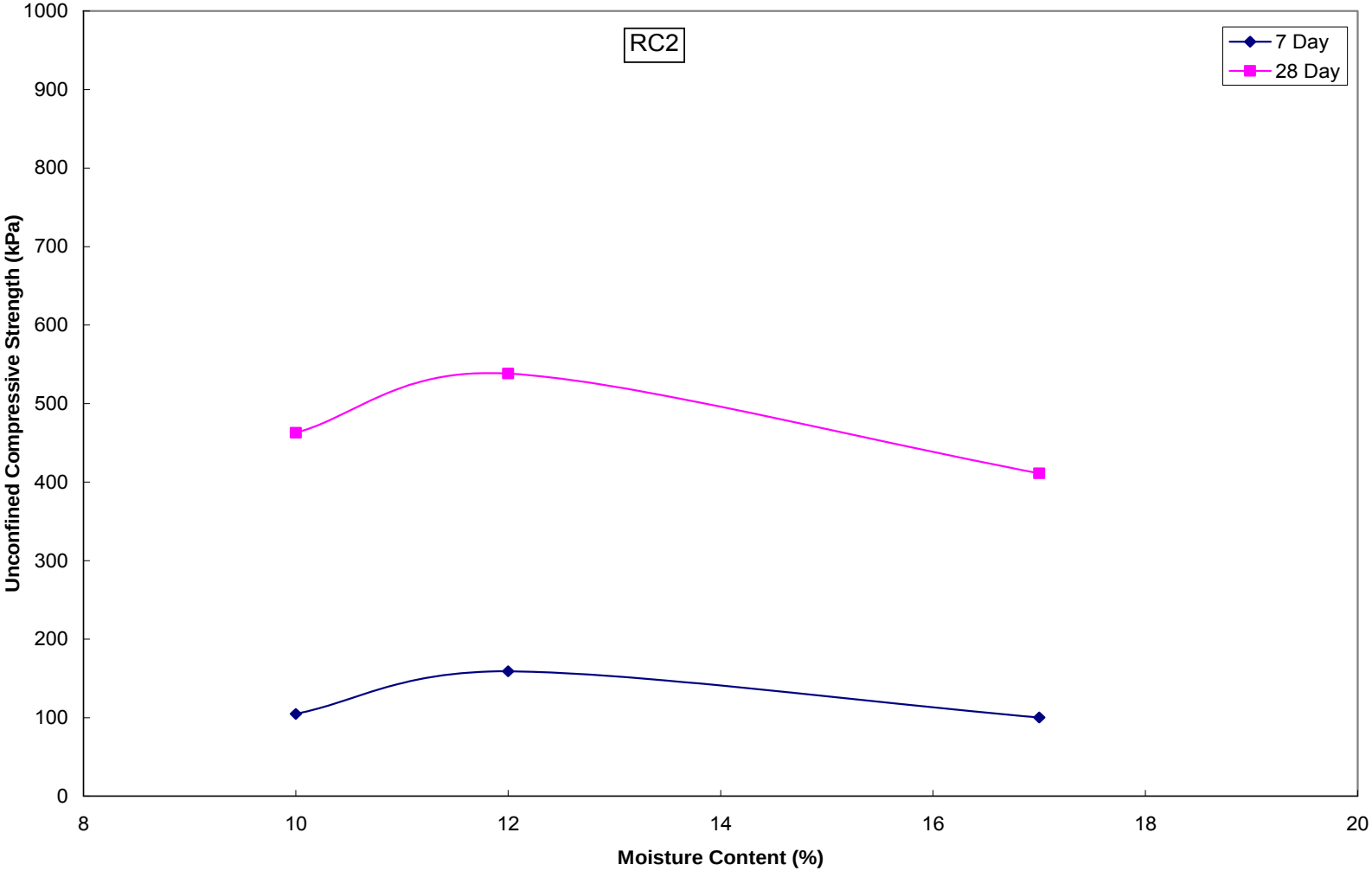


Figure 4.8 Average values of unconfined compression strength for recycled concrete aggregate RC2 at different moisture content for 7 and 28 day curing

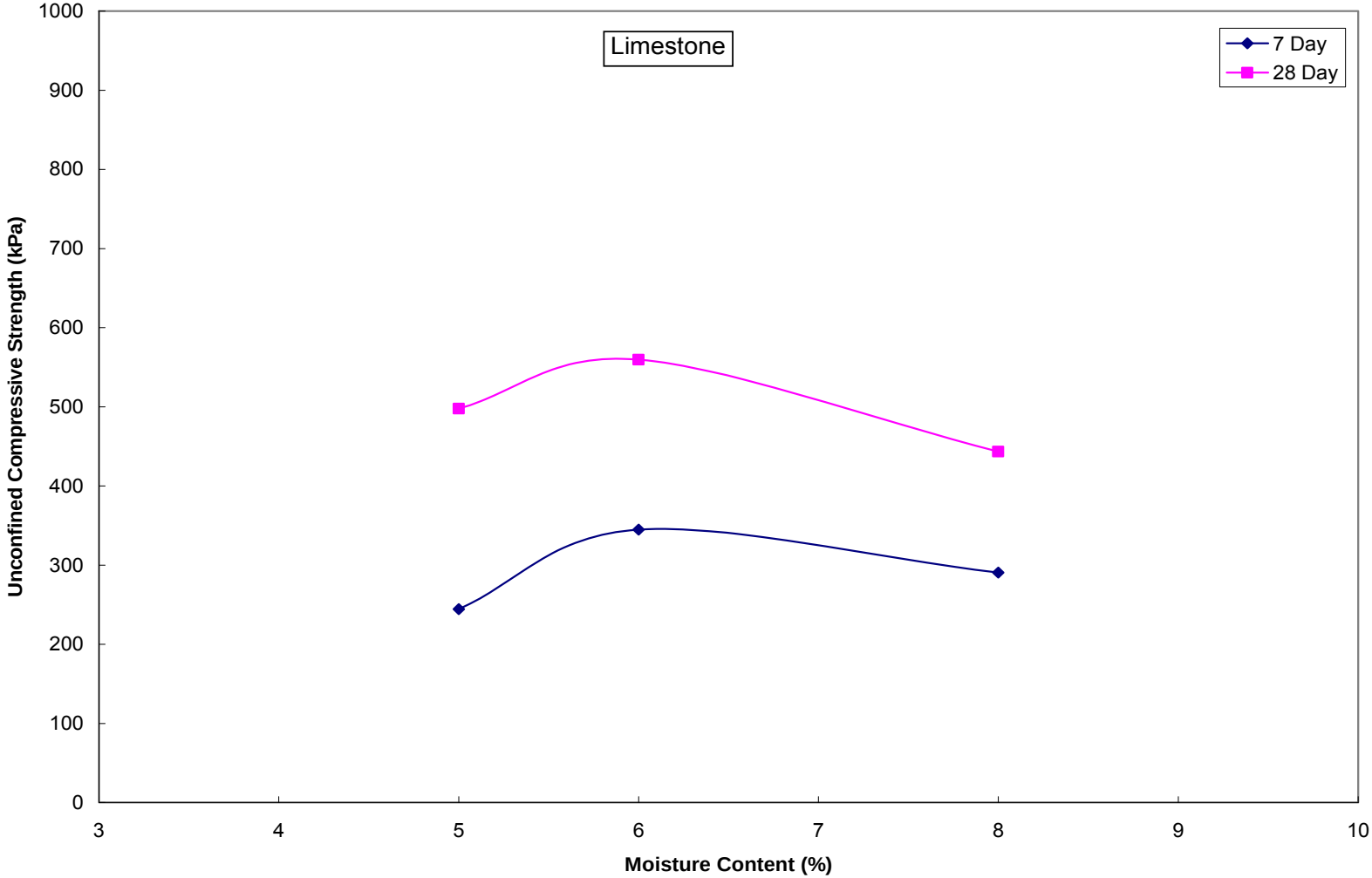


Figure 4.9 Average values of unconfined compression strength for limestone aggregate at different moisture content for 7 and 28 day curing

#### 4.2.1.2 Effects of Curing Period on Unconfined Compression Strength

The unconfined compression strength average for each material is compared between the curing periods in the following figures. Figures 4.10, 4.11, and 4.12 show the ratio of unconfined compression strength at 28 days to that of 7 days for the three varying moisture contents of each material. The results of all three materials show that the unconfined compression strength increased with the curing time. The increase in the unconfined compression strength of the recycled concrete aggregates is expected due to the activation of cementitious material resulting from the crushing of the Portland cement concrete. However, the increase in unconfined compression strength in the crushed limestone aggregate was unexpected and requires further evaluation to explain the increase.

The largest increases in unconfined compression strength between the curing periods occurred for the recycled aggregate RC2 as shown in figure 4.13. The 7-day to 28-day increase in strength of 4.42 times occurred on the dry of optimum moisture content condition for recycled concrete RC2 The wet side of optimum moisture content exhibited a similar increase of 4.10 times from the 7-day to 28-day strength. The optimum shows the increase in strength to be 3.39 times from the 7-day to 28-day strength. The higher increases could be attributed to the cement content available in recycled concrete aggregate RC2.

The recycled concrete aggregate RC1 experienced increases in unconfined compression strength from the 7-day to the 28-day measurement. However, the increase was lower than the increase seen in recycled concrete aggregate RC2 and more consistent between the varying moisture contents of the material. The 7-day to 28-day unconfined compression strength ratio resulted in 2.73, 2.72, and 2.79 times in increases for the dry, optimum, and wet of optimum density conditions, respectively.

The unexpected increase in the strength of the crushed limestone aggregate shows a 7-day to 28-day increase of 2.04, 1.62, and 1.53 times for the dry, optimum, and wet of optimum density conditions, respectively. The increase could be attributed to the loss of moisture from

the samples. Therefore, the samples with the greater percentage loss of moisture demonstrated a higher increase.

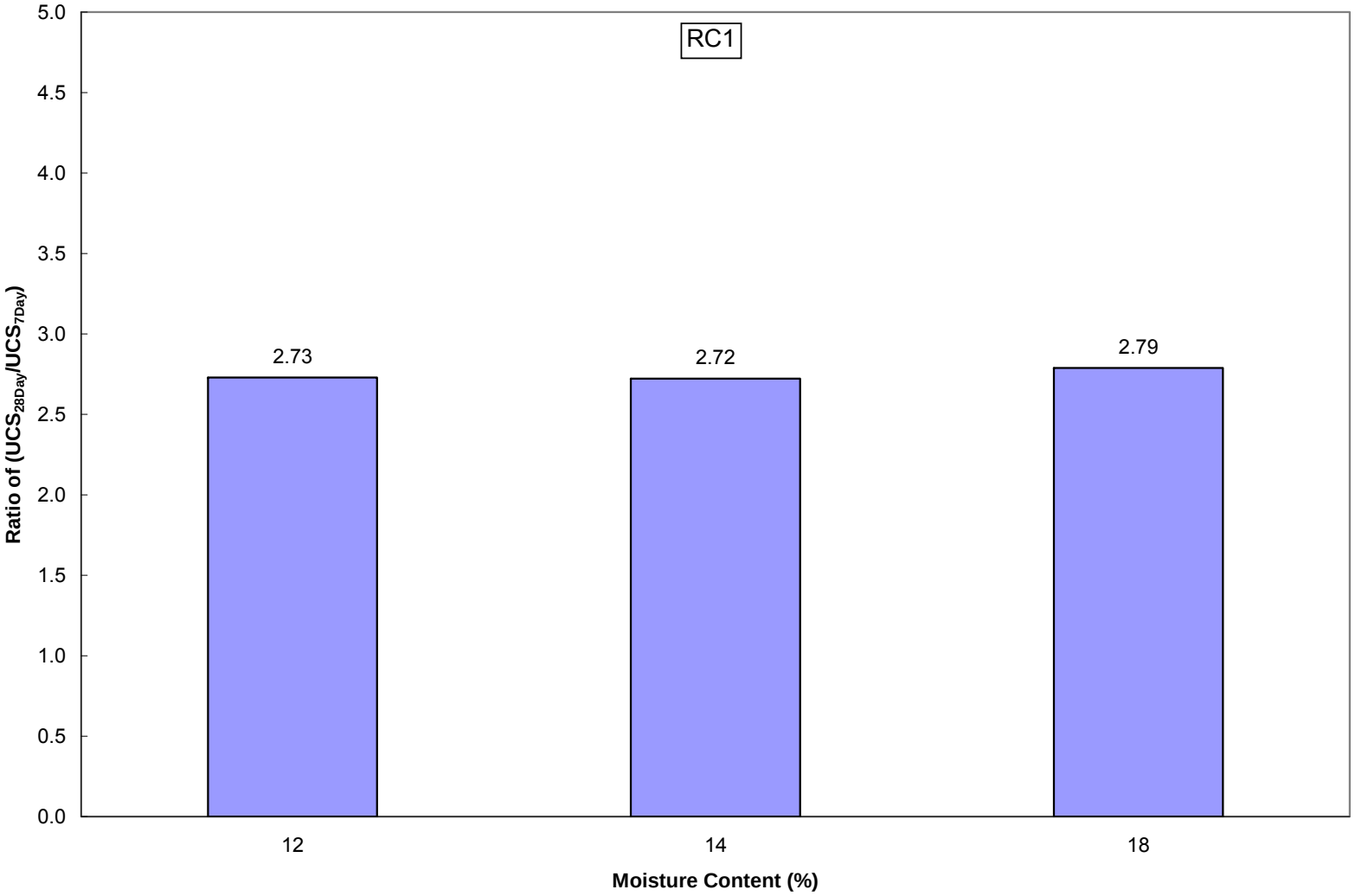


Figure 4.10 Ratio of 28-day to 7-day for average values of unconfined compression strength for recycled concrete aggregate RC1

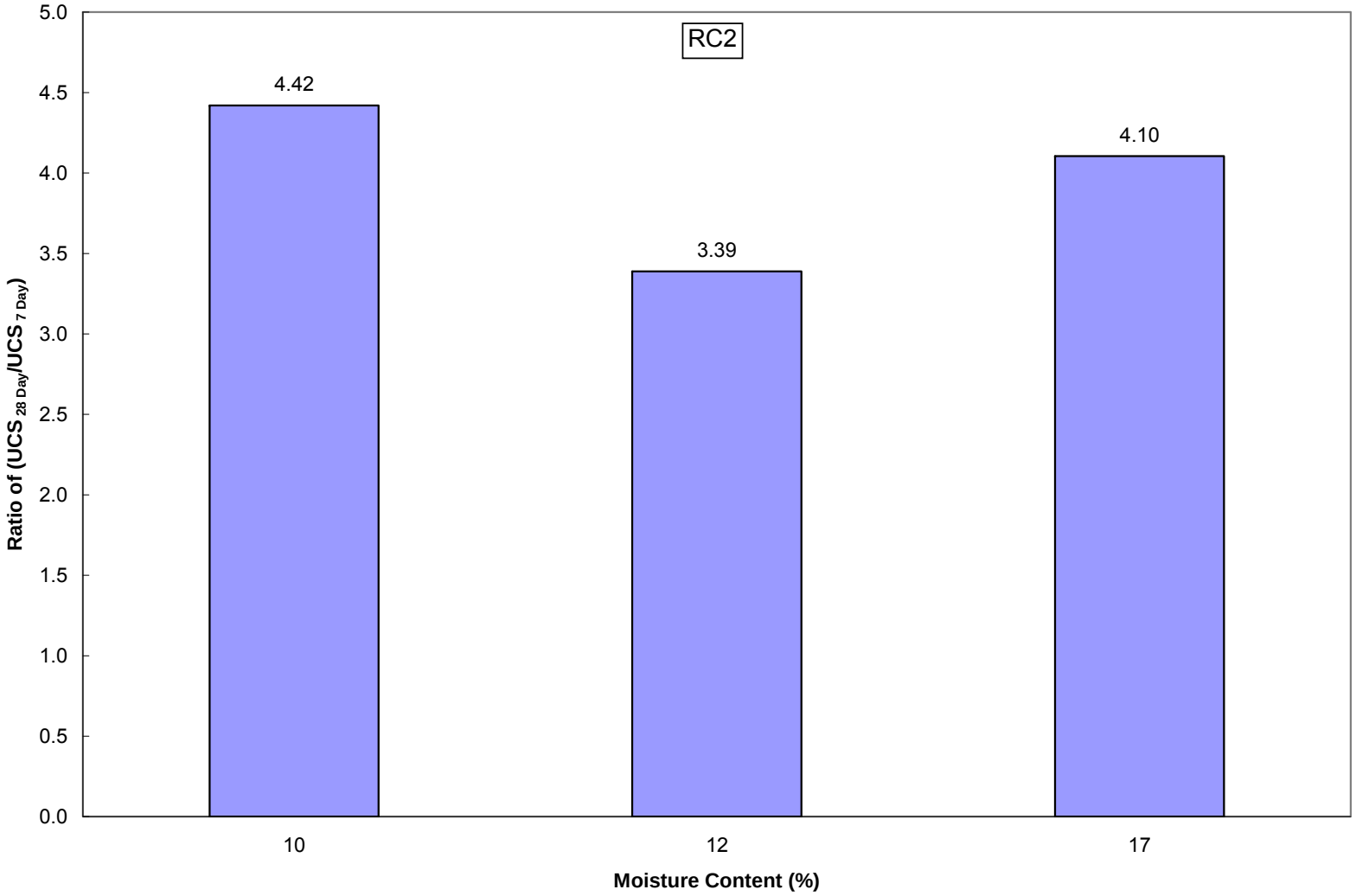


Figure 4.11 Ratio of 28-day to 7-day for average values of unconfined compression strength for recycled concrete aggregate RC2

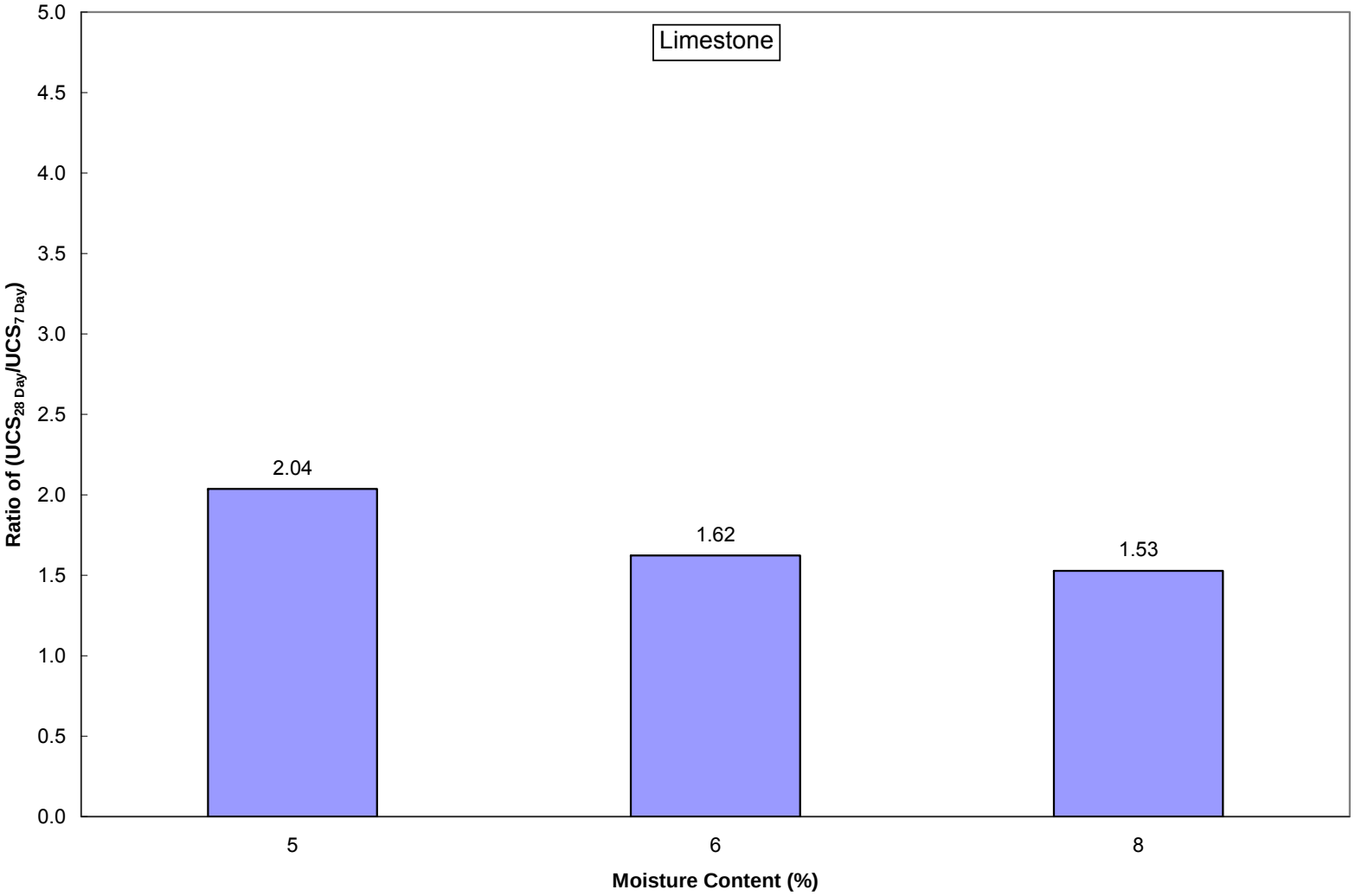


Figure 4.12 Ratio of 28-day to 7-day for average values of unconfined compression strength for crushed limestone aggregate

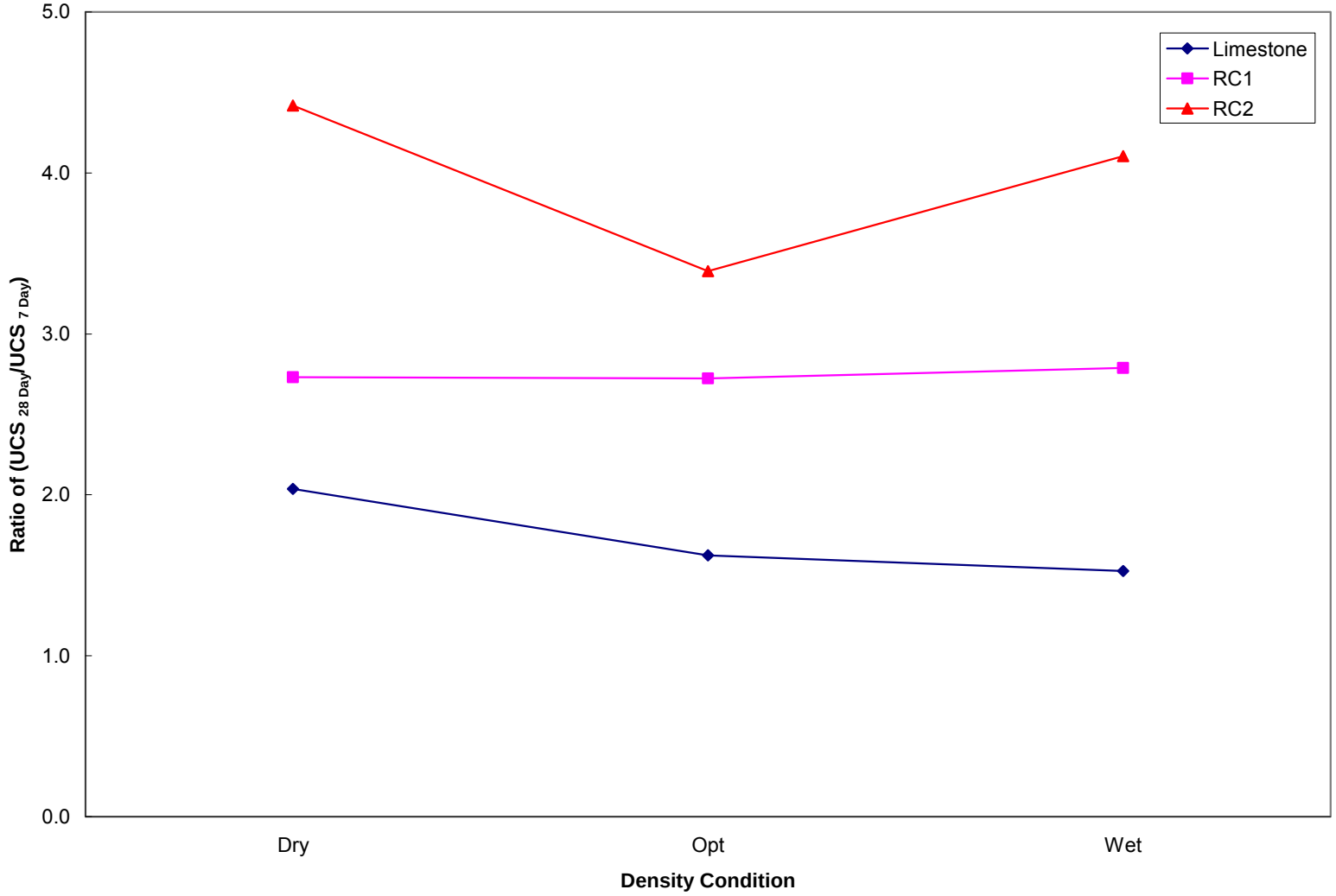


Figure 4.13 Ratio of 28-day to 7-day for average values of unconfined compression strength for all three materials

*4.2.2 Small Strain Shear Modulus $G_{max}$ Determination Using Bender Element Testing*

Bender elements were used to measure the shear wave velocity through the material specimens. The measured shear wave velocity of the samples was then used to determine the small strain shear modulus $G_{max}$ of the materials at the specified moisture content. These moduli can be used to estimate the resilient moduli with an assumed poisson's ratio and can also be indirectly used to estimate the subgrade modulus parameter.

Three specimens were used to represent each moisture content condition with a 28-day curing period and two specimens to represent each material moisture content condition with a 7-day curing period. The $G_{max}$ results calculated from the measured shear wave velocity are presented in the following figures. Figures 4.14 through 4.19 show the calculated $G_{max}$ of each specimen and average $G_{max}$ for each moisture content condition and curing period.

In order to evaluate the testing procedure for the measurement of the shear wave velocity and determination of small strain $G_{max}$, the measured results were assessed for repeatability and reliability. The analyses of the materials are presented in tables 4.4, 4.5, and 4.6. The standard deviation for $G_{max}$ ranged between 0.32 MPa to 18.48 MPa. The coefficient of variation remained low for each of the materials tested, indicating the procedure followed to measure shear wave velocities and moduli and the specimens used have yielded repeatable results.

In comparison of the moduli with those of cement treated RAP material mixtures presented in table 4.7 as conducted by Hoyos et al., (2008), the present results are closer in agreement with those of RAP mixtures with zero to low cement dosages (less than 2%). Much higher moduli were reported for 6% cement treated RAP mixtures. This is expected as the mix design in that case was done on an optimized mixture of RAP aggregates and cement additives. It should be noted here that the RC1 and RC2 were not conventionally treated in this research, the original cementing particles of the recycled cement concrete aggregates have provided the moderate pozzolanic activity in the present mixtures.

Table 4.4 Results of Small Strain Shear Modulus $G_{max}$ for Recycled Concrete Aggregate RC1

| Cure Time | Moisture Content | Small Strain Shear Modulus $G_{max}$ | Small Strain Shear Modulus $G_{max}$ | Small Strain Shear Modulus $G_{max}$ | Mean | Variance | Standard Deviation | Coefficient of Variation |
|---|---|---|---|---|---|---|---|---|
| Days | % | MPa | MPa | MPa | MPa | $(MPa)^2$ | MPa | % |
| 7 | 12 | 113.17 | 93.00 | | 103.08 | 203.37 | 14.26 | 13.83 |
| 28 | 12 | 111.31 | 105.07 | 104.86 | 107.08 | 13.41 | 3.66 | 3.42 |
| 7 | 14 | 99.59 | 100.05 | | 99.82 | 0.10 | 0.32 | 0.32 |
| 28 | 14 | 105.52 | 104.68 | 103.58 | 104.59 | 0.94 | 0.97 | 0.93 |
| 7 | 18 | 98.71 | 80.76 | | 89.73 | 161.11 | 12.69 | 14.15 |
| 28 | 18 | 97.58 | 92.51 | 94.57 | 94.89 | 6.49 | 2.55 | 2.69 |

Table 4.5 Results of Small Strain Shear Modulus $G_{max}$ for Recycled Concrete Aggregate RC2

| Cure Time | Moisture Content | Small Strain Shear Modulus $G_{max}$ | Small Strain Shear Modulus $G_{max}$ | Small Strain Shear Modulus $G_{max}$ | Mean | Variance | Standard Deviation | Coefficient of Variation |
|---|---|---|---|---|---|---|---|---|
| Days | % | MPa | MPa | MPa | MPa | $(MPa)^2$ | MPa | % |
| 7 | 10 | 108.90 | 98.48 | | 103.69 | 54.26 | 7.37 | 7.10 |
| 28 | 10 | 117.23 | 115.99 | 119.63 | 117.62 | 3.42 | 1.85 | 1.57 |
| 7 | 12 | 93.51 | 97.68 | | 95.59 | 8.72 | 2.95 | 3.09 |
| 28 | 12 | 112.56 | 117.20 | 114.17 | 114.64 | 5.55 | 2.36 | 2.05 |
| 7 | 17 | 80.51 | 88.66 | | 84.58 | 33.17 | 5.76 | 6.81 |
| 28 | 17 | 110.94 | 106.47 | 104.48 | 107.30 | 10.94 | 3.31 | 3.08 |

Table 4.6 Results of Small Strain Shear Modulus $G_{max}$ for Limestone Aggregate

| Cure Time | Moisture Content | Small Strain Shear Modulus $G_{max}$ | Small Strain Shear Modulus $G_{max}$ | Small Strain Shear Modulus $G_{max}$ | Mean | Variance | Standard Deviation | Coefficient of Variation |
|---|---|---|---|---|---|---|---|---|
| Days | % | MPa | MPa | MPa | MPa | $(MPa)^2$ | MPa | % |
| 7 | 5 | 124.07 | 128.40 | | 126.24 | 9.35 | 3.06 | 2.42 |
| 28 | 5 | 127.63 | 123.00 | 136.57 | 129.07 | 47.65 | 6.90 | 5.35 |
| 7 | 6 | 159.44 | 133.30 | | 146.37 | 341.44 | 18.48 | 12.62 |
| 28 | 6 | 139.81 | 160.37 | 164.28 | 154.82 | 172.85 | 13.15 | 8.49 |
| 7 | 8 | 99.77 | 100.86 | | 100.32 | 0.59 | 0.77 | 0.76 |
| 28 | 8 | 118.50 | 113.69 | 119.42 | 117.20 | 9.46 | 3.08 | 2.62 |

Table 4.7 Small Strain Shear Moduli from Resonant Column Tests (Hoyos et al., 2008)

| Material | Cement dosage (%) | Shear modulus, $G_{max}$ (ksi) | | |
|---|---|---|---|---|
| | | $\sigma_3$ = 0 psi | $\sigma_3$ = 3 psi | $\sigma_3$ = 6 psi |
| Cement treated RAP | 0 | 6.4 | 10.6 | 18.3 |
| | 2 | 25.1 | 35.5 | 53.6 |
| | 4 | 55.7 | 68.0 | 82.3 |
| Cement-fiber treated RAP | 2 | 18.3 | 28.1 | 37.4 |
| | 4 | 38.0 | 80.6 | 105.7 |
| | 6 | 68.0 | 97.2 | 115.0 |
| RAP core sample | 6 | 116.1 | 124.2 | 126.0 |

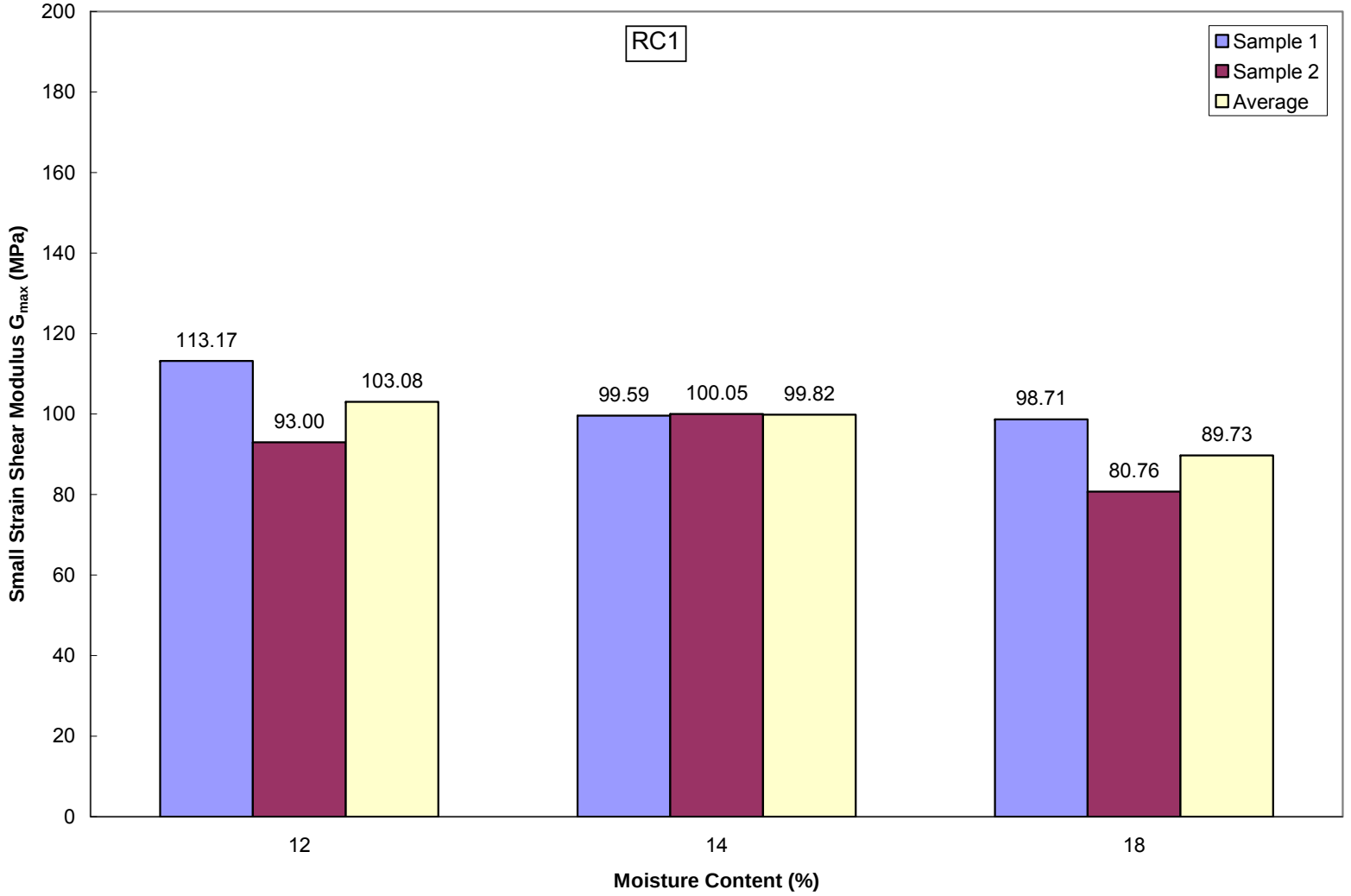


Figure 4.14 Average values of small strain shear modulus $G_{max}$ of recycled concrete aggregate RC1 for 7 day curing

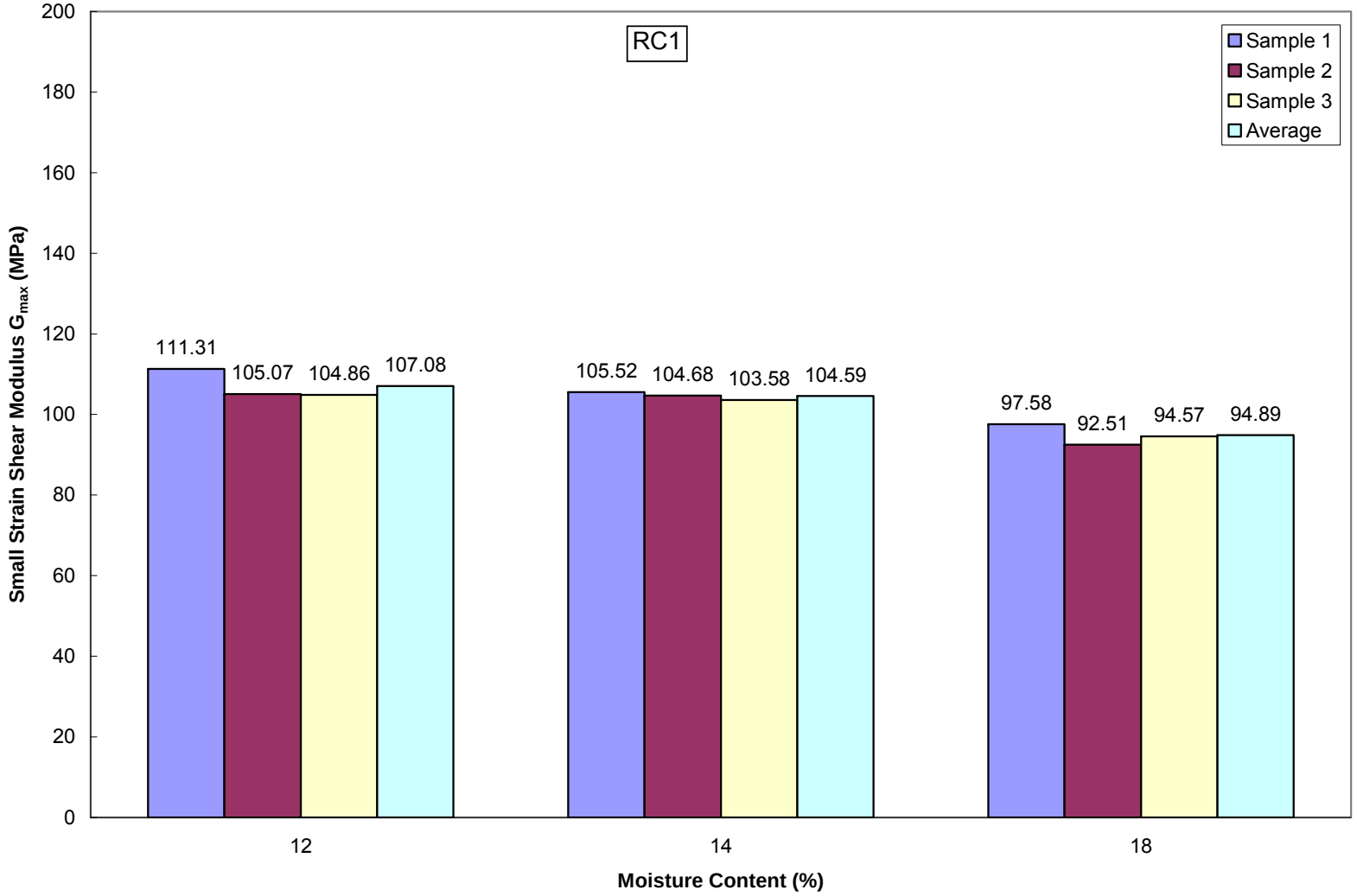


Figure 4.15 Average values of small strain shear modulus $G_{max}$ of recycled concrete aggregate RC1 for 28 day curing

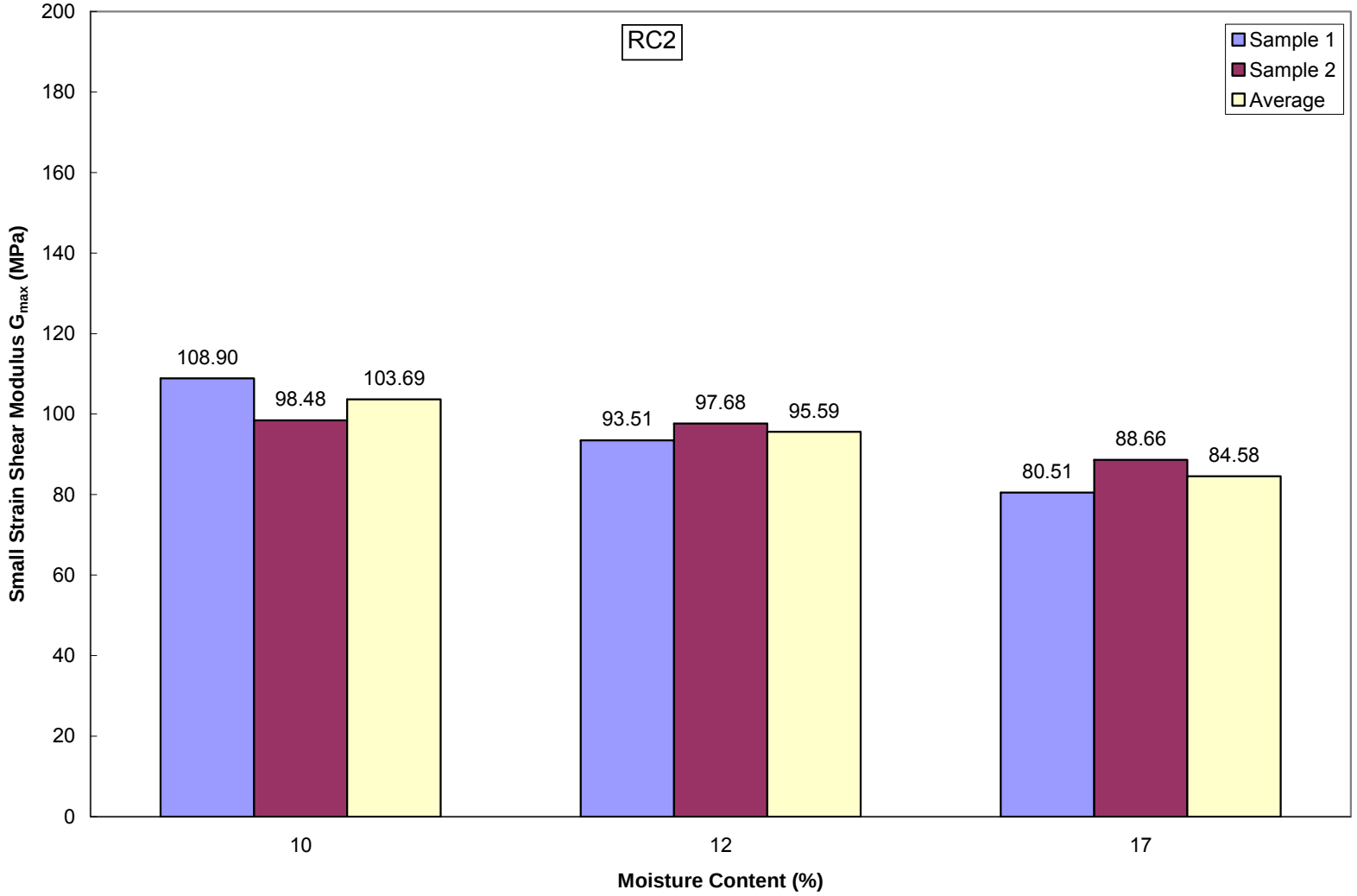


Figure 4.16 Average values of small strain shear modulus $G_{max}$ of recycled concrete aggregate RC2 for 7 day curing

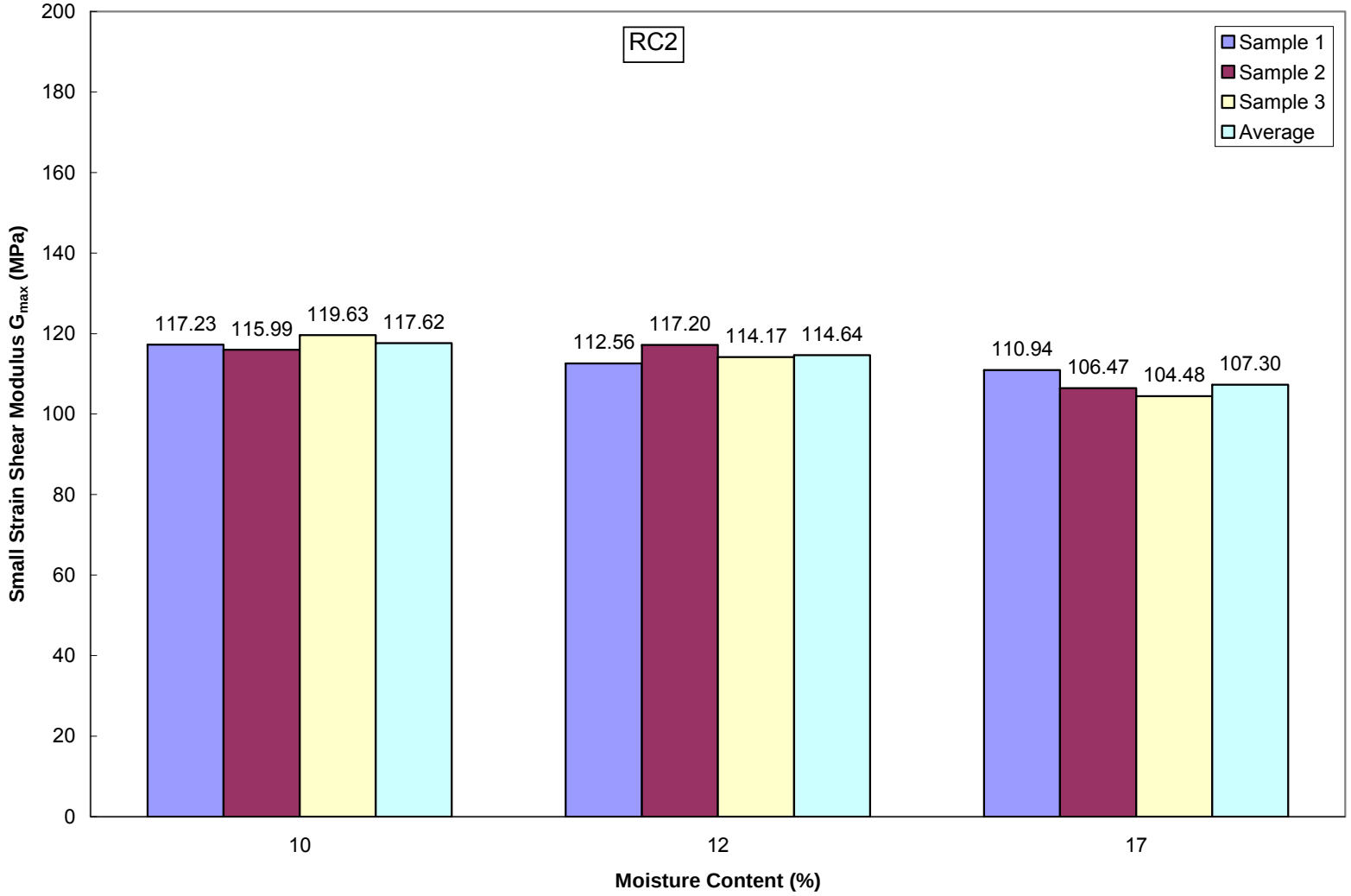


Figure 4.17 Average values of small strain shear modulus $G_{max}$ of recycled concrete aggregate RC2 for 28 day curing

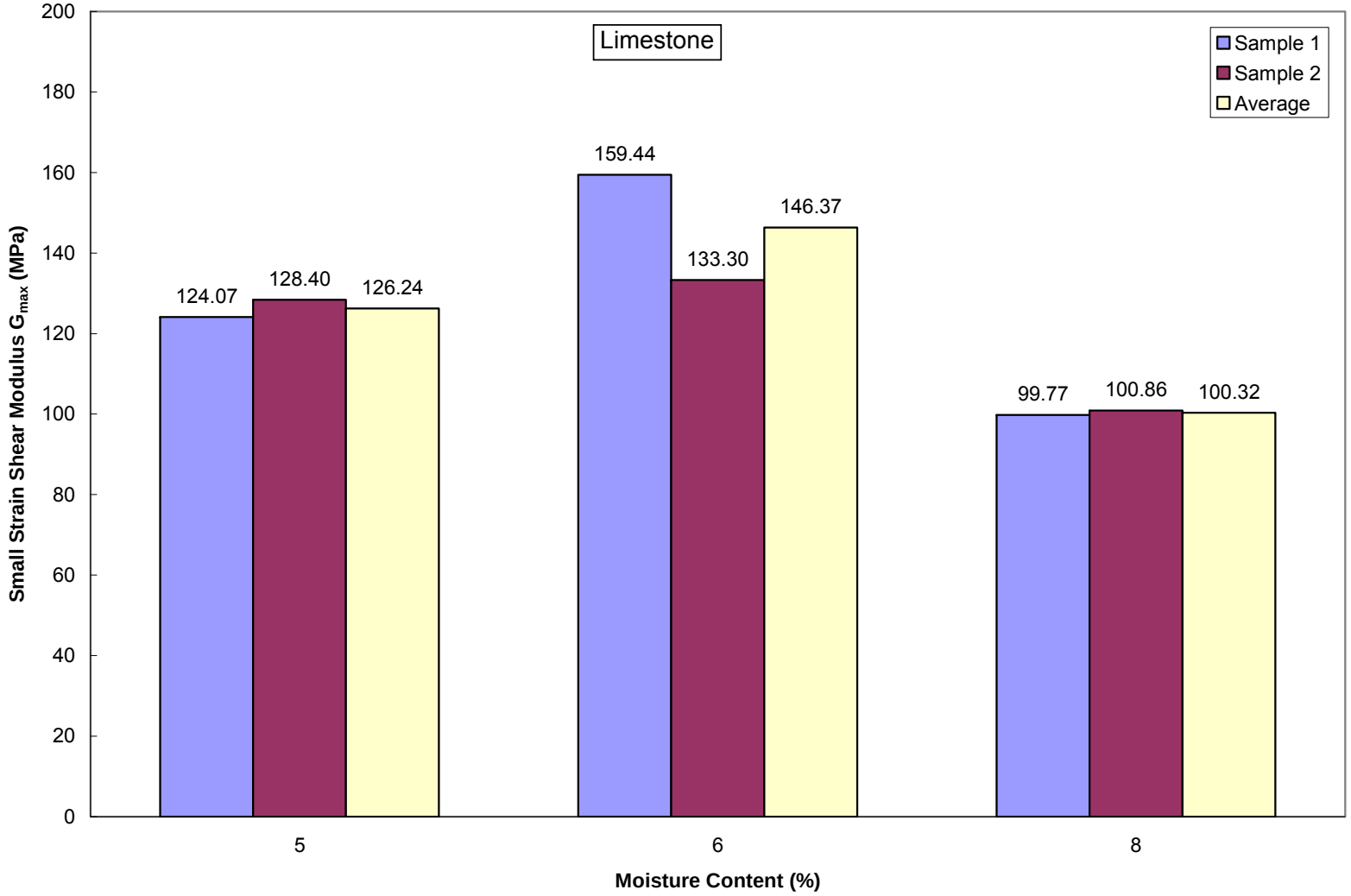


Figure 4.18 Average values of small strain shear modulus $G_{max}$ of limestone aggregate for 7 day curing

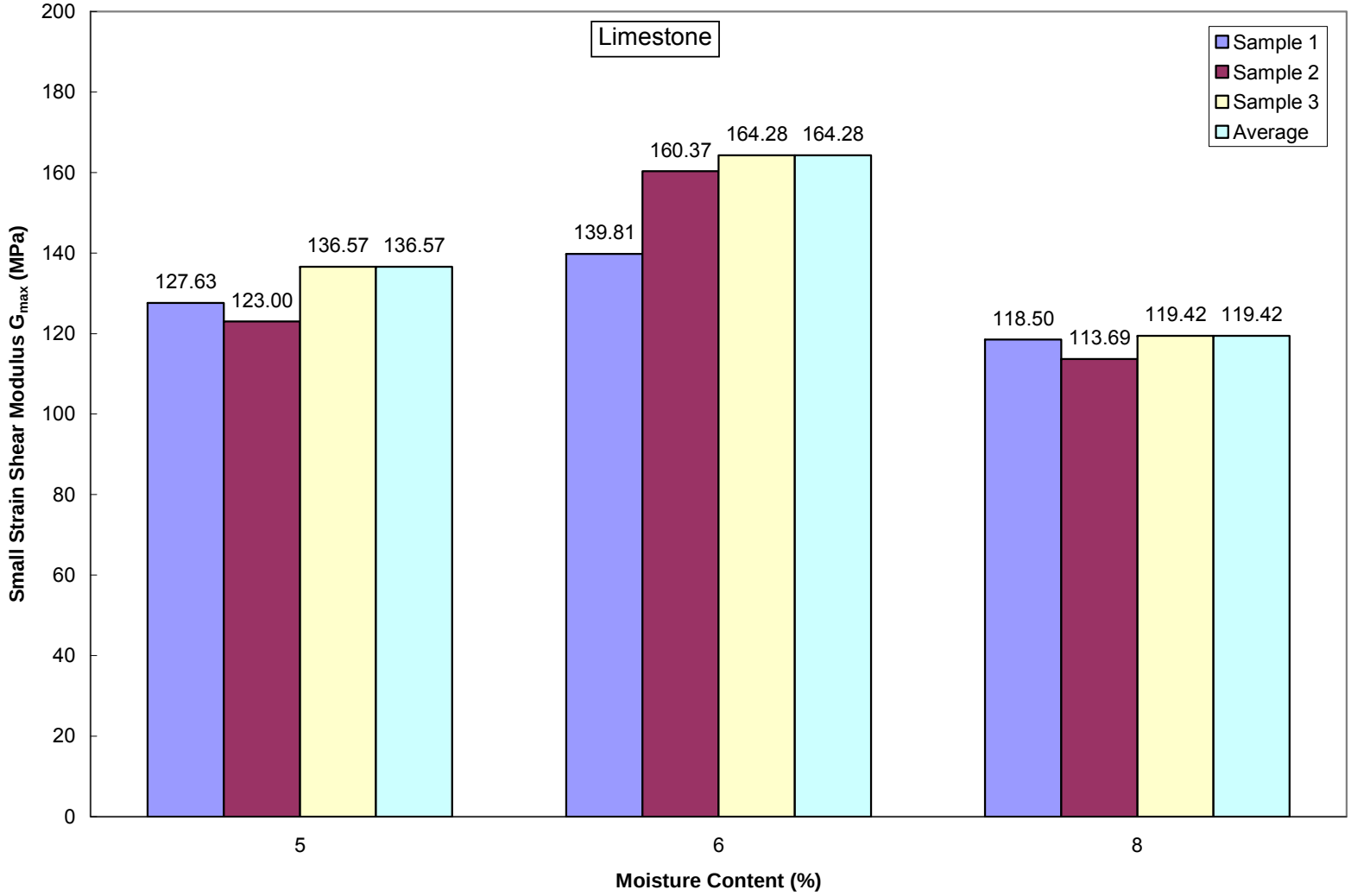


Figure 4.19 Average values of small strain shear modulus $G_{max}$ of limestone aggregate RC2 for 28 day curing

4.2.2.1 Effects of Moisture Content on Small Strain Shear Modulus $G_{max}$

The average $G_{max}$ value determined for each material is presented in figures 4.20, 4.21, and 4.22. The figures show the average $G_{max}$ value at the different moisture content conditions for each material. The results for the recycled aggregates yield similar results. The values of $G_{max}$ decrease with the increase in compaction moisture content. The decrease in $G_{max}$ from the dry of optimum and optimum moisture content density condition is slight. However, the decrease from the optimum moisture content density condition to the wet of optimum moisture content condition is more apparent.

The crushed limestone aggregate varies from the recycled concrete aggregates in that the higher $G_{max}$ values occur at the optimum moisture content density condition. The dry of optimum moisture content condition follows with the second highest values of $G_{max}$ while the lowest are seen at the wet of optimum moisture content condition. The $G_{max}$ values determined at the wet of optimum moisture content condition are similarly lowest in all materials. The $G_{max}$ values of the crushed limestone aggregates are also much higher than the recycled concrete aggregates.

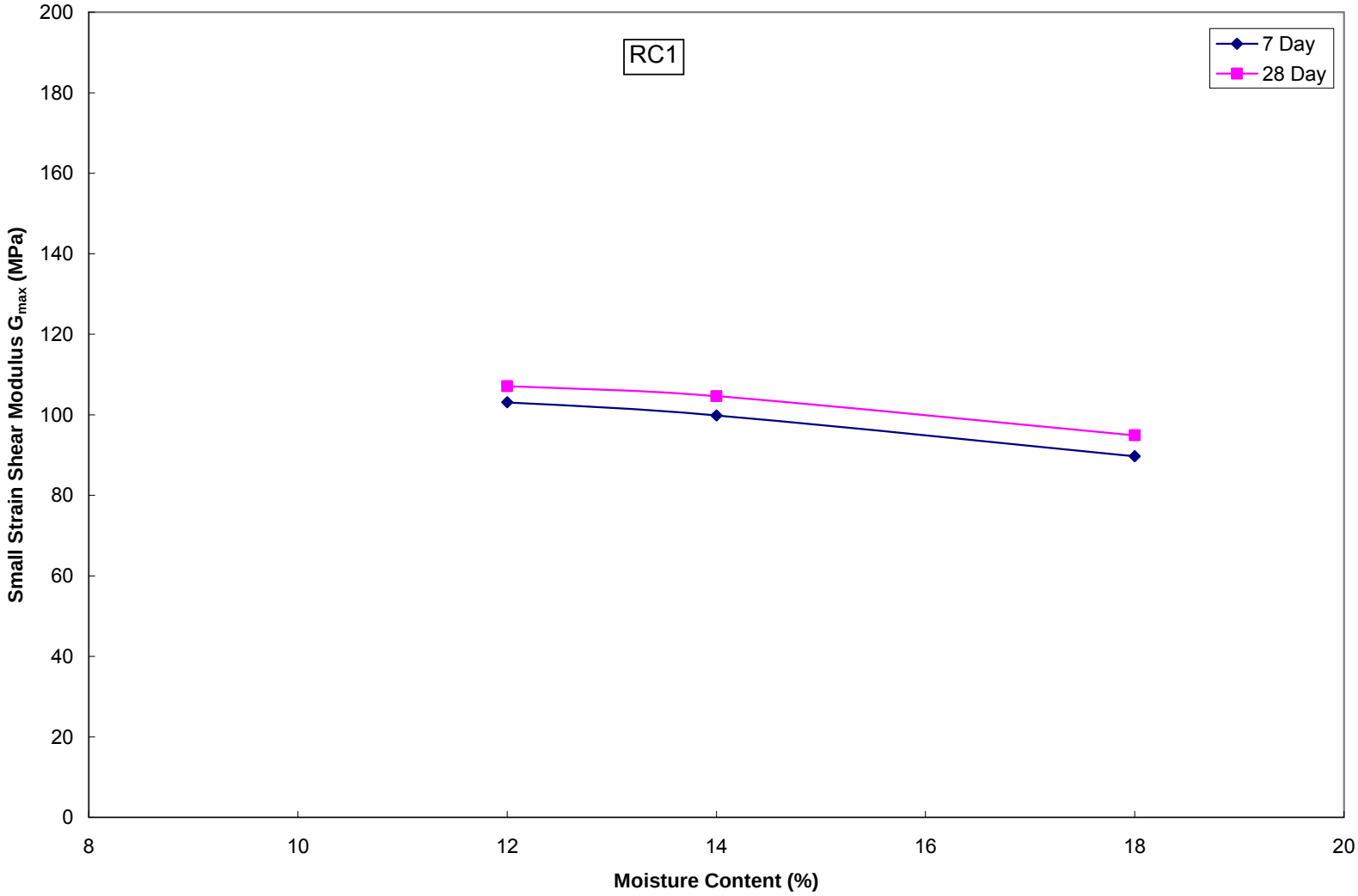


Figure 4.20 Average values of small strain shear modulus $G_{max}$ of recycled concrete aggregate RC1 for 7 and 28 day curing

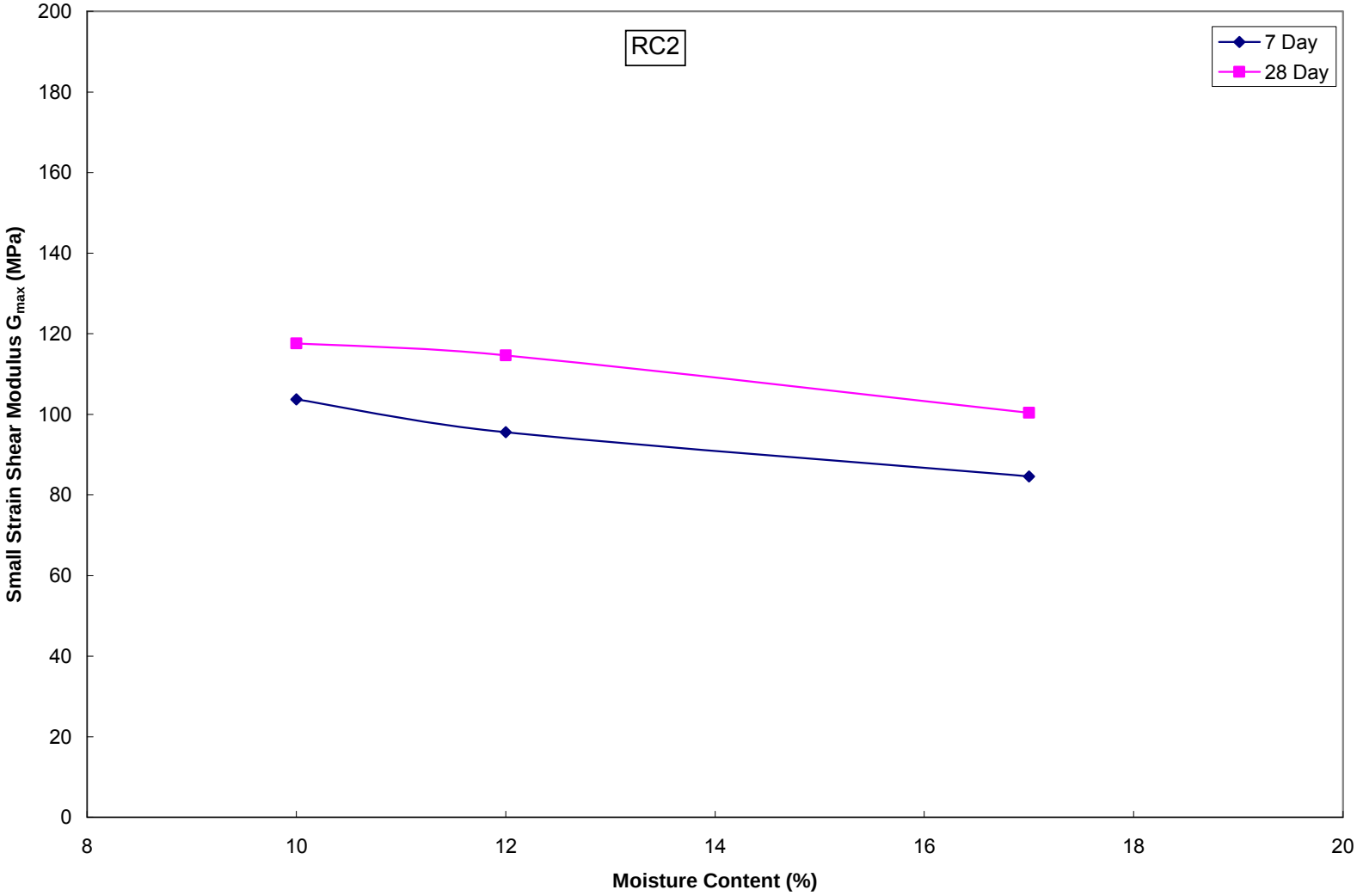


Figure 4.21 Average values of small strain shear modulus $G_{max}$ of recycled concrete aggregate RC2 for 7 and 28 day curing

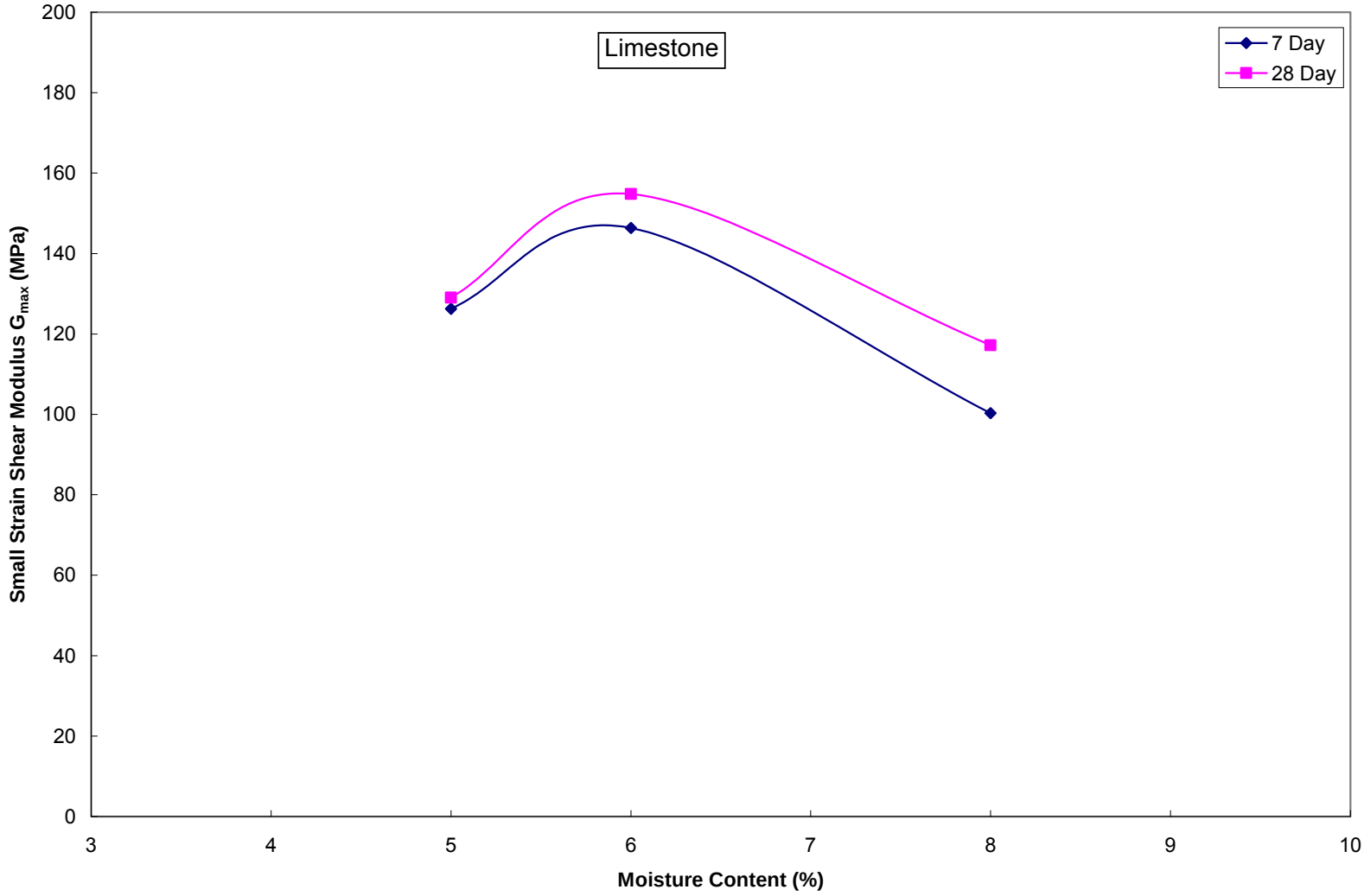


Figure 4.22 Average values of small strain shear modulus $G_{max}$ of limestone aggregate for 7 and 28 day curing

4.2.2.2 Effects of Curing Period on Small Strain Shear Modulus $G_{max}$

The ratio for the average $G_{max}$ value for 28-day to 7-day curing period for each material is presented in the following figures. Figures 4.23, 4.24, and 4.25 show the 28-day to 7-day ratio for each material at the different moisture content conditions. The results for all three materials show that the average $G_{max}$ value increases with the curing time. Similar to the unconfined compression strength, a slight increase was expected on the recycled concrete aggregates but not on the crushed limestone aggregate. The increase in the crushed limestone requires further investigation to explain this occurrence.

The largest increases in shear modulus $G_{max}$ between the curing periods occurred for the recycled aggregate RC2 as shown in figure 4.26. The increase of 20% in the shear modulus for recycled aggregate RC2 occurred on the optimum moisture content condition. The wet side of optimum moisture content exhibited a similar increase of 19%. The dry side of optimum moisture content shows the increase in shear modulus to be 13%. The higher increases could be attributed to the cement content available in recycled concrete aggregate RC2.

The recycled concrete aggregate RC1 experienced increases in shear modulus $G_{max}$ from the 7-day to the 28-day measurement. However, the increase was lower than the increase seen in recycled concrete aggregate RC2 and more consistent between the varying moisture contents of the material. The 28-day to 7-day shear modulus $G_{max}$ ratio resulted in 4%, 5%, and 6% increases for the dry, optimum, and wet of optimum density conditions, respectively.

The unexpected increase in the strength of the crushed limestone aggregate shows a 28-day to 7-day ratio increase of 2%, 6%, and 17% for the dry, optimum, and dry of optimum density conditions, respectively.

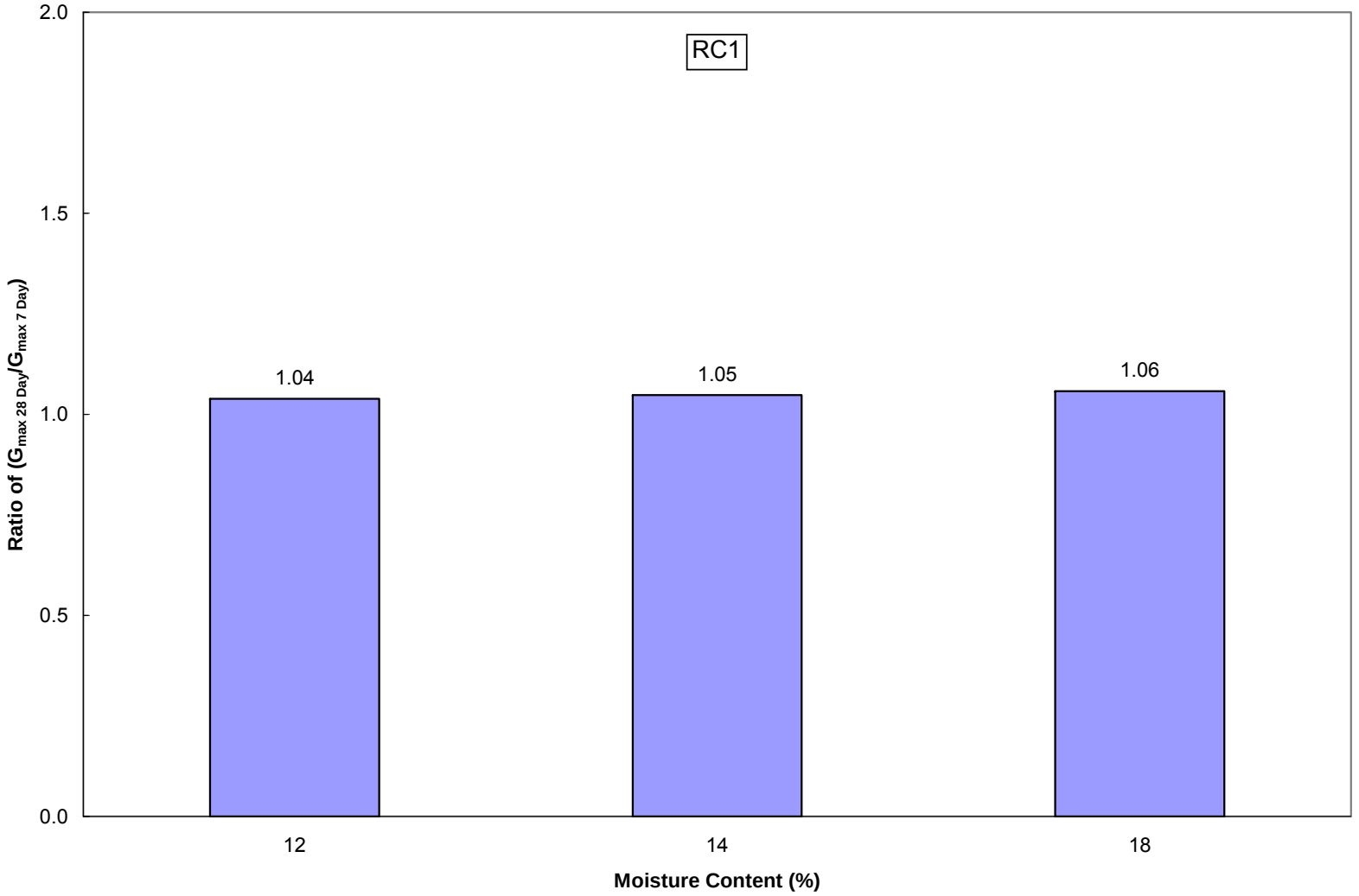


Figure 4.23 Ratio of 28-day to 7-day for average values of small strain $G_{max}$ for recycled concrete aggregate RC1

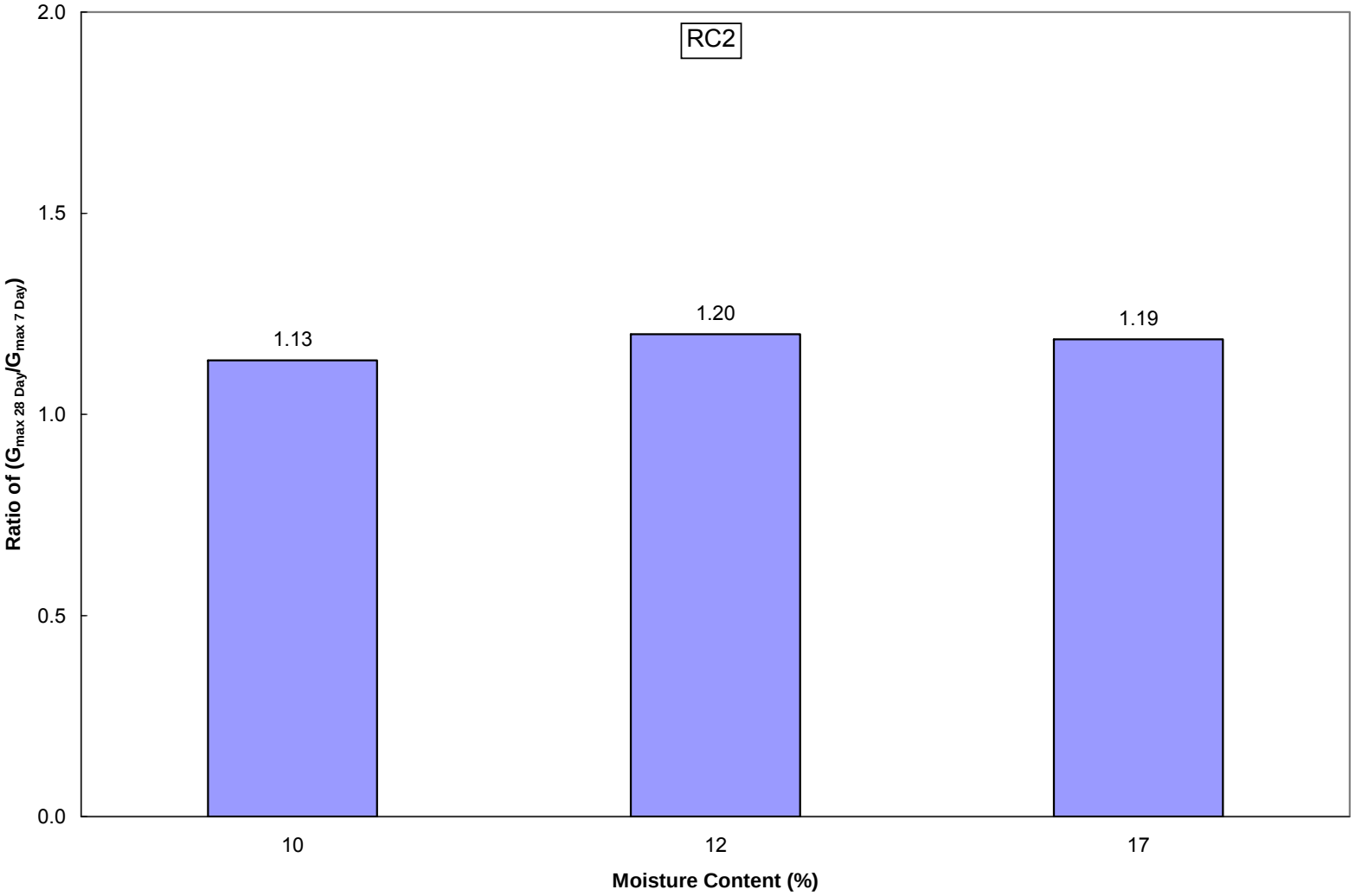


Figure 4.24 Ratio of 28-day to 7-day for average values of small strain $G_{max}$ for recycled concrete aggregate RC2

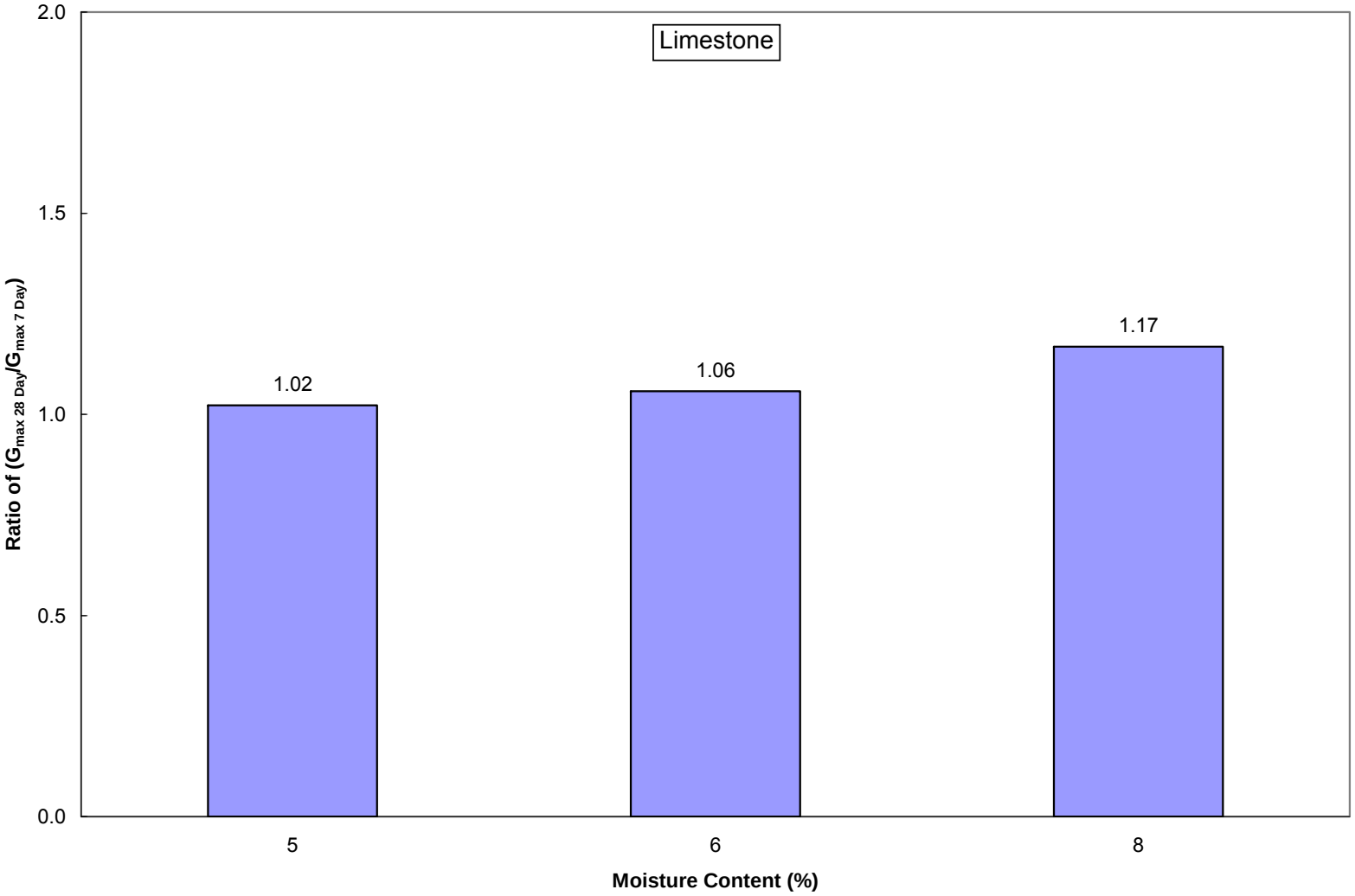


Figure 4.25 Ratio of 28-day to 7-day for average values of small strain $G_{max}$ for crushed limestone aggregate

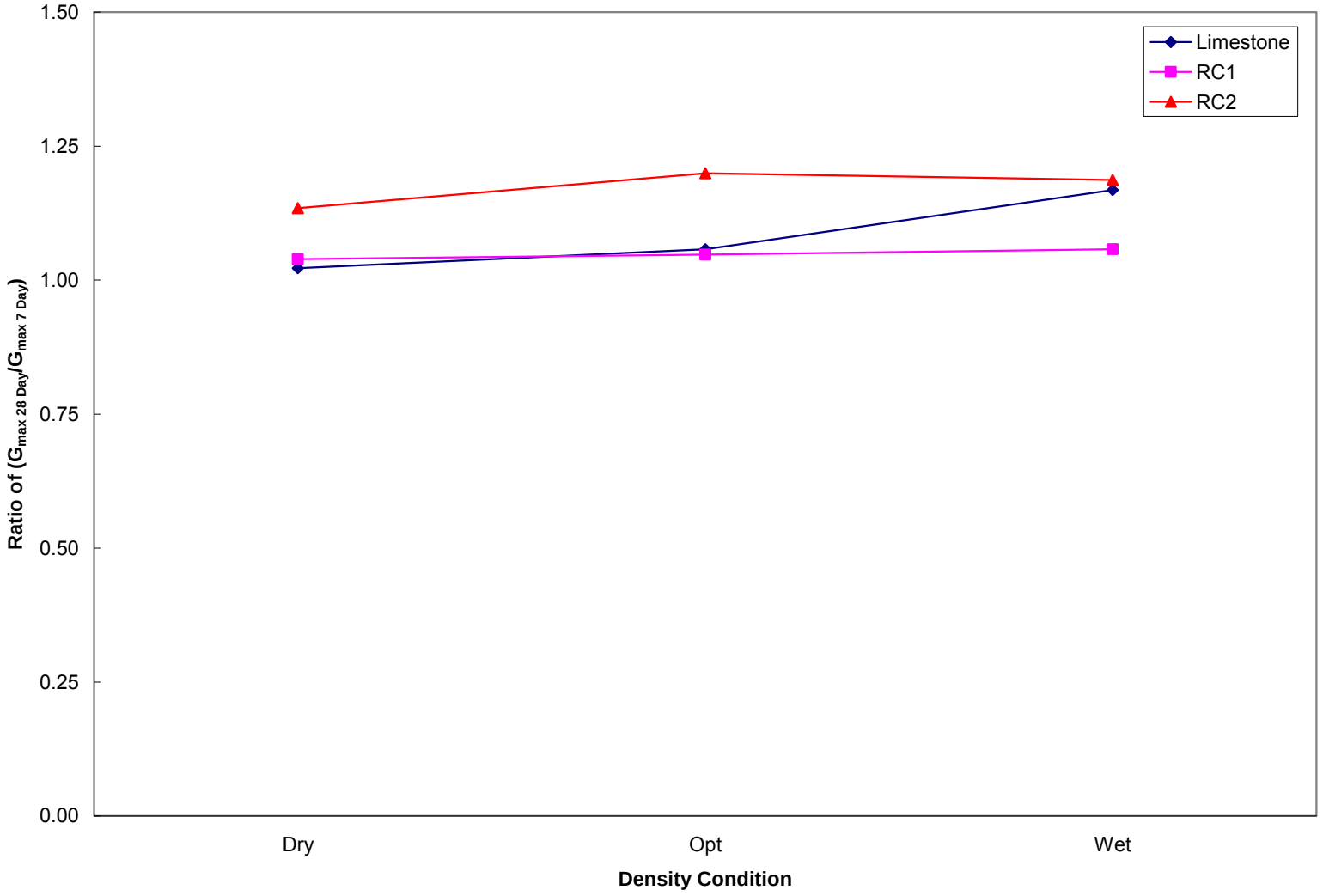


Figure 4.26 Ratio of 28-day to 7-day for average values of small strain $G_{max}$ for all three materials

*4.2.3 Determination of Coefficient of Permeability*

The specimens for all three materials tested were consistent with the three different percent moisture levels that represent each dry, optimum, and wet of optimum moisture content condition in each material. The results were determined from an average of four readings for each sample. All measurements for the coefficient of permeability, k, resulted in values above the recommended permeability of $1.4 \times 10^{-4}$ cm/s (Senior, 1992; MnDOT, 2007) for dense-graded materials. The results of the falling head permeability tests of all three materials are shown in figures 4.27, 4.28, and 4.29.

In order to evaluate the testing procedure for the measurement of permeability, the results were assessed for repeatability and reliability. The results of the analyses are presented in the tables 4.8, 4.9, and 4.10. The standard deviation for this property ranged from $0.01 \times 10^{-3}$ to $0.12 \times 10^{-3}$ cm/s. The coefficient of variation of the test results also remained low for all three materials tested.

Table 4.8 Results for Permeability of Recycled Concrete Aggregates RC1

| Material | Moisture Content | Permeability k | Permeability k | Permeability k | Permeability k | Mean | Variance | Standard Deviation | Coefficient of Variation |
|---|---|---|---|---|---|---|---|---|---|
| | % | cm/s | cm/s | cm/s | cm/s | cm/s | $(cm/s)^2$ | kPa | |
| RC1 | 12 | 1.75 | 1.70 | 1.66 | 1.68 | 1.70 | 0.00 | 0.04 | 2.54 |
| RC1 | 14 | 1.62 | 1.63 | 1.64 | 1.68 | 1.63 | 0.00 | 0.01 | 0.36 |
| RC1 | 18 | 1.45 | 1.27 | 1.50 | 1.43 | 1.41 | 0.01 | 0.12 | 8.50 |

Table 4.9 Results for Permeability of Recycled Concrete Aggregates RC2

| Material | Moisture Content | Permeability k | Permeability k | Permeability k | Permeability k | Mean | Variance | Standard Deviation | Coefficient of Variation |
|---|---|---|---|---|---|---|---|---|---|
| | % | cm/s | cm/s | cm/s | cm/s | cm/s | $(cm/s)^2$ | kPa | |
| RC2 | 10 | 1.70 | 1.75 | 1.74 | 1.71 | 1.73 | 0.00 | 0.03 | 1.54 |
| RC2 | 12 | 1.58 | 1.69 | 1.63 | 1.58 | 1.63 | 0.00 | 0.05 | 3.25 |
| RC2 | 17 | 1.49 | 1.50 | 1.47 | 1.48 | 1.49 | 0.00 | 0.02 | 1.15 |

Table 4.10 Results for Permeability of Limestone Aggregates

| Material | Moisture Content | Permeability k | Permeability k | Permeability k | Permeability k | Mean | Variance | Standard Deviation | Coefficient of Variation |
|---|---|---|---|---|---|---|---|---|---|
| | % | cm/s | cm/s | cm/s | cm/s | cm/s | $(cm/s)^2$ | kPa | |
| Limestone | 5 | 1.72 | 1.69 | 1.71 | 1.70 | 1.70 | 0.00 | 0.02 | 1.04 |
| Limestone | 6 | 1.62 | 1.62 | 1.63 | 1.64 | 1.62 | 0.00 | 0.01 | 0.47 |
| Limestone | 8 | 1.81 | 1.80 | 1.78 | 1.80 | 1.80 | 0.00 | 0.02 | 0.87 |

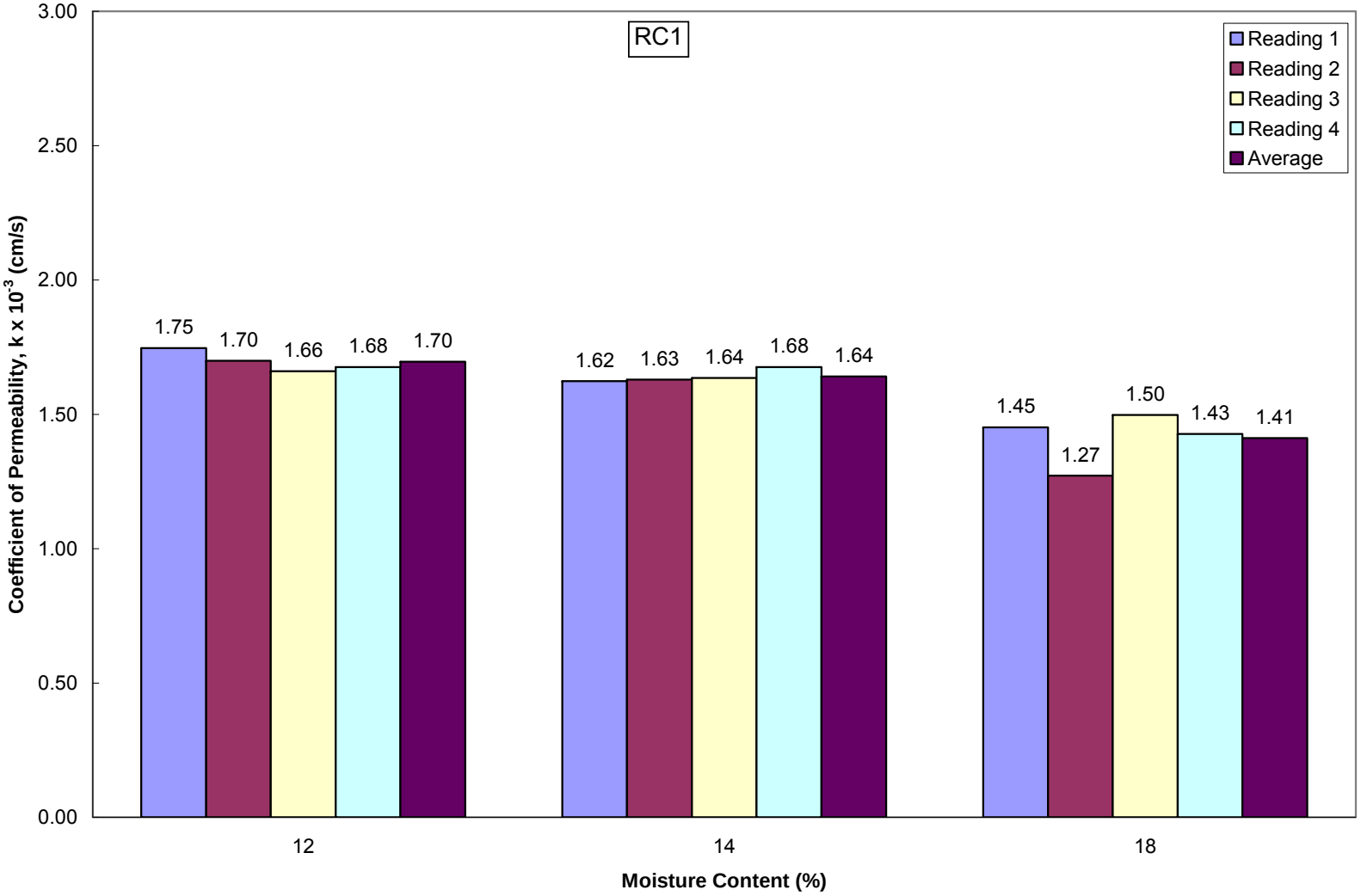


Figure 4.27 Coefficient of permeability of recycled concrete aggregate RC1 for varying moisture content

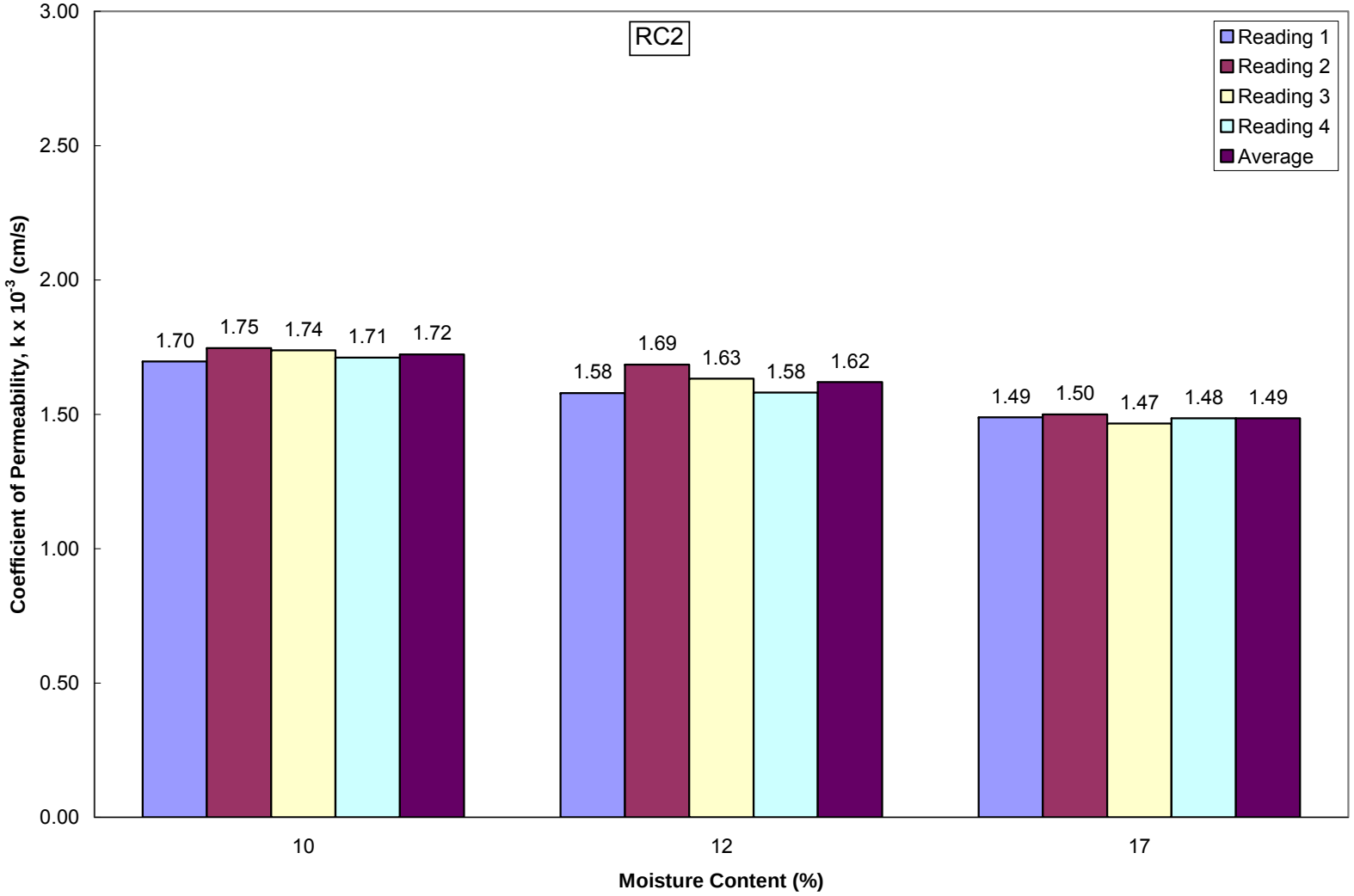


Figure 4.28 Coefficient of permeability of recycled concrete aggregate RC2 for varying moisture content

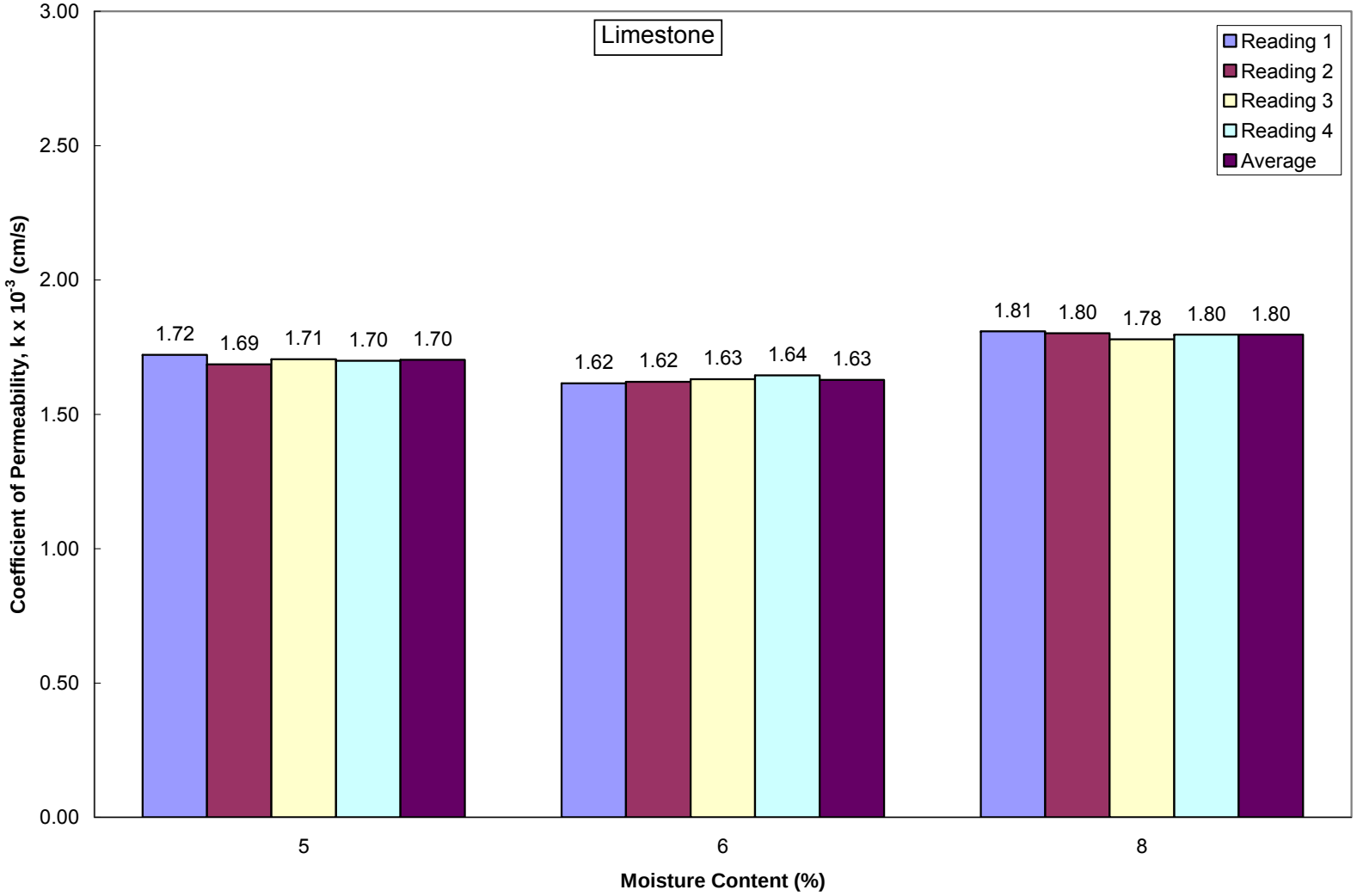


Figure 4.29 Coefficient of permeability of limestone aggregate for varying moisture content

#### 4.2.3.1 Effects of Moisture Content on Permeability

The average values for coefficient of permeability, k, in each material are presented in figure 4.30. The figure shows the average coefficient of permeability value at the different moisture content conditions for each material. The results for the recycled concrete aggregates show that permeability decreases with the increase in moisture content. For the crushed limestone, permeability increases at a higher moisture content as the density decreases. Figure 4.31 provides the coefficient of all three materials at the different moisture content conditions. The recycled concrete aggregates absorb more water than the natural limestone aggregates. The absorption of water is attributed to the cement paste found in the recycled concrete aggregates. This was noticed when the specimens were compacted. The recycled concrete aggregates at the higher water moisture contents behave similar to that of Portland cement concrete. The compaction of recycled concrete aggregate RC1 at a wet density condition is shown in figure 4.32 and figure 4.33.

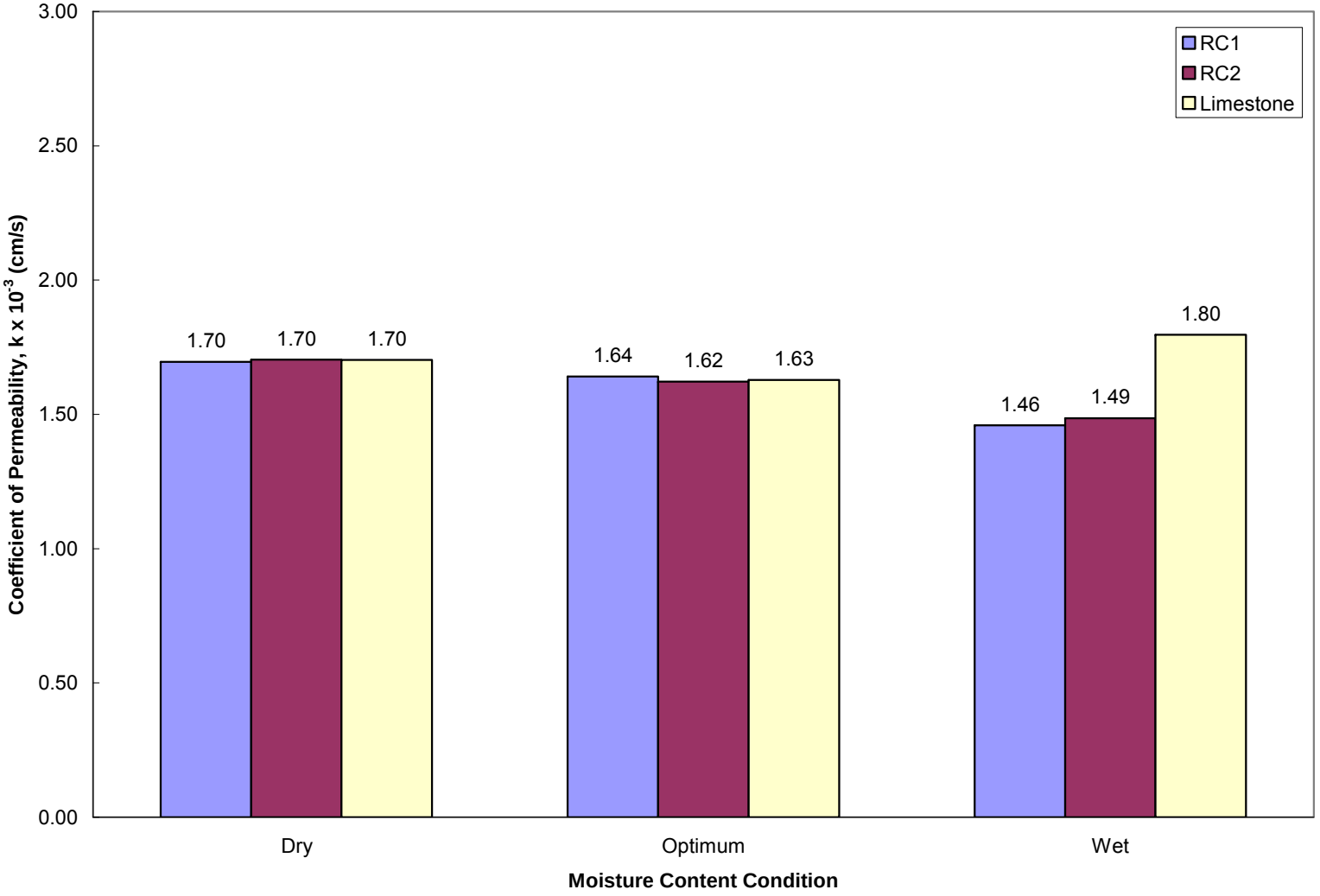


Figure 4.30 Average values for coefficient of permeability of all three materials at varying moisture content conditions

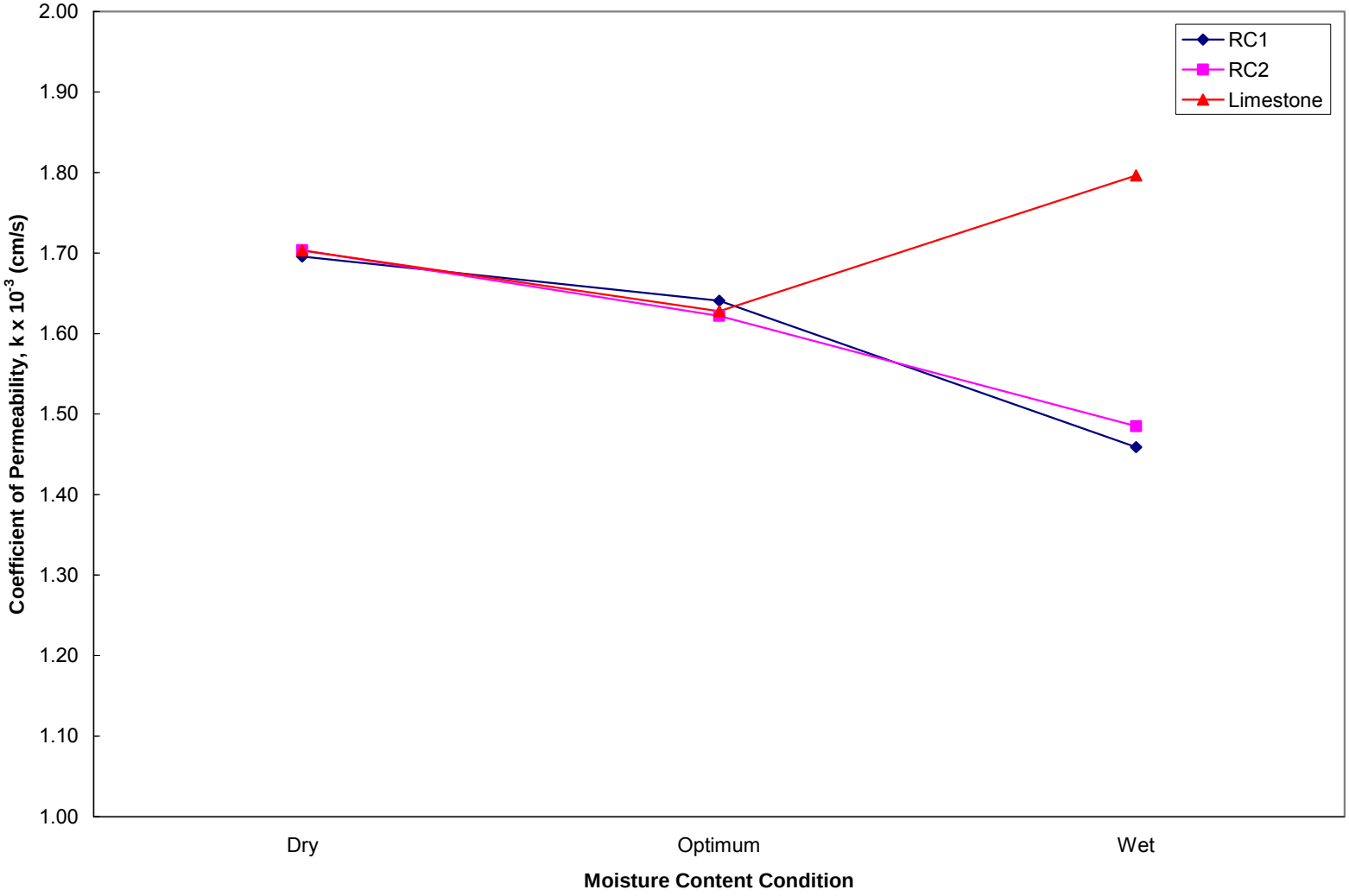


Figure 4.31 Comparison for coefficient of permeability for all three materials at varying moisture content conditions

Figure 4.32 Recycled concrete aggregate RC1 at wet density condition during compaction

Figure 4.33 Compacted recycled concrete aggregate RC1 at wet density condition

## 4.3 Statistical Analysis

The statistical analysis used here is a comparison type test, t-test. The analysis is used to evaluate the significant variances in the unconfined compression strength, small strain shear modulus $G_{max}$, and permeability within the material at different moisture contents and compacted density conditions. In addition, a comparison is also performed to evaluate the significant variances between the three materials at dry, optimum, and wet of optimum dry density conditions. A statistical program was used to perform all the analyses in this research.

### *4.3.1 Statistical Analysis Within Materials*

The data results for the unconfined compression strength, small strain shear modulus $G_{max}$, and permeability were analyzed using a two sample hypotheses testing procedure. Each material was evaluated at the different moisture contents and respective compacted density conditions. The analyses were performed at a 7-day and 28-day curing period. The analyses were performed on each material using $\alpha$=0.05, a null hypotheses assuming that the means between the moisture content and compacted density conditions were equal ($H_0$: $u_1=u_2$), and an alternate hypotheses in which the means are not equal ($H_1$: $u_1 \neq u_2$).

#### 4.3.1.1 Statistical Analysis of Unconfined Compression Strength

Significant differences in the unconfined compression strength due to the moisture content and compacted density condition are important in determining the materials' ability to provide the strength. The maximum shear strength of a material is normally considered to equal to one-half of the unconfined compression strength. When there are no significant differences between compacted density conditions of the material, it can be concluded that the moisture content of the material will have no affect on the shear strength of the material.

Tables 4.11 through 4.19 show the results of the t-test comparison within each material for the different moisture content and compacted density conditions. The results show that a significant increase in strength exists for the recycled concrete aggregates at the optimum moisture content – dry density condition when compared to the dry and wet of optimum density

condition. The recycled aggregate also show significant increases in strength at 28 days versus that of 7 days.

Table 4.11 UCS t-test Results for Recycled Concrete Aggregate RC1 at 7 days

| Material Comparison | UCS Mean RC1 | UCS Mean RC1 | Curing Days | t-value | 2 sided p-value | Means are Different |
|---|---|---|---|---|---|---|
| Dry to Optimum | 153.69 | 214.50 | 7 | -2.609 | 0.1209 | No |
| Dry to Wet | 153.69 | 127.14 | 7 | 2.296 | 0.1485 | No |
| Optimum to Wet | 214.50 | 127.14 | 7 | 4.048 | 0.0560 | No |

Table 4.12 UCS t-test Results for Recycled Concrete Aggregate RC1 at 28 days

| Material Comparison | UCS Mean RC1 | UCS Mean RC1 | Curing Days | t-value | 2 sided p-value | Means are Different |
|---|---|---|---|---|---|---|
| Dry to Optimum | 419.57 | 583.98 | 28 | -8.207 | 0.0145 | Yes |
| Dry to Wet | 419.57 | 354.52 | 28 | 3.199 | 0.0854 | No |
| Optimum to Wet | 583.98 | 354.52 | 28 | 26.423 | 0.0014 | Yes |

Table 4.13 UCS t-test Results for Recycled Concrete Aggregate RC1 for 7 day to 28 day Comparison

| Material Comparison | UCS Mean RC1 | UCS Mean RC1 | Moisture-Density Condition | t-value | 2 sided p-value | Means are Different |
|---|---|---|---|---|---|---|
| 7 Day to 28 Day | 153.69 | 419.57 | Dry | -12.195 | 0.0067 | Yes |
| 7 Day to 28 Day | 214.50 | 583.98 | Optimum | -17.056 | 0.0034 | Yes |
| 7 Day to 28 Day | 127.14 | 354.52 | Wet | -26.834 | 0.0014 | Yes |

Table 4.14 UCS t-test Results for Recycled Concrete Aggregate RC2 at 7 days

| Material Comparison | UCS Mean RC2 | UCS Mean RC2 | Curing Days | t-value | 2 sided p-value | Means are Different |
|---|---|---|---|---|---|---|
| Dry to Optimum | 104.71 | 158.83 | 7 | -10.033 | 0.0098 | Yes |
| Dry to Wet | 104.71 | 100.17 | 7 | 0.819 | 0.4991 | No |
| Optimum to Wet | 158.83 | 100.17 | 7 | 8.409 | 0.0138 | Yes |

Table 4.15 UCS t-test Results for Recycled Concrete Aggregate RC2 at 28 days

| Material Comparison | UCS Mean RC2 | UCS Mean RC2 | Curing Days | t-value | 2 sided p-value | Means are Different |
|---|---|---|---|---|---|---|
| Dry to Optimum | 462.76 | 538.27 | 28 | -8.111 | 0.0149 | Yes |
| Dry to Wet | 462.76 | 411.13 | 28 | 5.363 | 0.0331 | Yes |
| Optimum to Wet | 538.27 | 411.13 | 28 | 13.157 | 0.0057 | Yes |

Table 4.16 UCS t-test Results for Recycled Concrete Aggregate RC2 for 7 day to 28 day Comparison

| Material Comparison | UCS Mean RC2 | UCS Mean RC2 | Moisture-Density Condition | t-value | 2 sided p-value | Means are Different |
|---|---|---|---|---|---|---|
| 7 Day to 28 Day | 104.71 | 462.76 | Dry | -51.352 | 0.0004 | Yes |
| 7 Day to 28 Day | 158.83 | 538.27 | Optimum | -46.304 | 0.0005 | Yes |
| 7 Day to 28 Day | 100.17 | 411.13 | Wet | -35.934 | 0.0008 | Yes |

Table 4.17 UCS t-test Results for Limestone Aggregate at 7 days

| Material Comparison | UCS Mean Limestone | UCS Mean Limestone | Curing Days | t-value | 2 sided p-value | Means are Different |
|---|---|---|---|---|---|---|
| Dry to Optimum | 244.31 | 344.78 | 7 | -2.508 | 0.1290 | No |
| Dry to Wet | 244.31 | 290.50 | 7 | -0.827 | 0.4954 | No |
| Optimum to Wet | 344.78 | 290.50 | 7 | 1.337 | 0.3131 | No |

Table 4.18 UCS t-test Results for Limestone Aggregate at 28 days

| Material Comparison | UCS Mean Limestone | UCS Mean Limestone | Curing Days | t-value | 2 sided p-value | Means are Different |
|---|---|---|---|---|---|---|
| Dry to Optimum | 497.61 | 559.72 | 28 | -4.172 | 0.0529 | No |
| Dry to Wet | 497.61 | 443.51 | 28 | 3.616 | 0.0687 | No |
| Optimum to Wet | 559.72 | 443.51 | 28 | 6.545 | 0.0226 | Yes |

Table 4.19 UCS t-test Results for Limestone Aggregate for 7 day to 28 day Comparison

| Material Comparison | UCS Mean Limestone | UCS Mean Limestone | Moisture-Density Condition | t-value | 2 sided p-value | Means are Different |
|---|---|---|---|---|---|---|
| 7 Day to 28 Day | 244.31 | 497.61 | Dry | -6.323 | 0.0241 | Yes |
| 7 Day to 28 Day | 344.78 | 559.72 | Optimum | -14.426 | 0.0048 | Yes |
| 7 Day to 28 Day | 290.50 | 443.51 | Wet | -3.666 | 0.0670 | No |

4.3.1.2 Statistical Analysis of Small Strain Shear Modulus $G_{max}$

When significant differences in $G_{max}$ are found within the material, the required moisture content used for placement of the material affects the pavement structure. If the analysis does not show significant differences in $G_{max}$, then it can be concluded that the moisture content for placement of the material does not affect the pavement structure.

Tables 4.20 through 4.28 present the t-test results for the evaluation of $G_{max}$ at different moisture contents and compacted density conditions for the materials. At a 7-day curing period, there is no significant difference found between the moisture contents and compacted density of the recycled aggregates. The limestone aggregate did show a difference between the optimum and wet of optimum density condition. At a 28-day curing period, the recycled aggregates RC1 and RC2 did not show a significant decrease in $G_{max}$ between the optimum and dry of optimum compacted density condition while the limestone aggregate had a significant decrease in $G_{max}$ for results other than at the optimum moisture content density. The 7-day to 28-day

comparisons show an increase of $G_{max}$ for the recycled aggregates at the optimum moisture content density condition.

Table 4.20 $G_{max}$ t-test Results for Recycled Concrete Aggregate RC1 at 7 days

| Material Comparison | $G_{max}$ Mean RC2 | $G_{max}$ Mean RC2 | Curing Days | t-value | 2 sided p-value | Means are Different |
|---|---|---|---|---|---|---|
| Dry to Optimum | 103.69 | 95.59 | 7 | 1.443 | 0.2859 | No |
| Dry to Wet | 103.69 | 84.58 | 7 | 2.890 | 0.1018 | No |
| Optimum to Wet | 95.59 | 84.58 | 7 | 2.406 | 0.1379 | No |

Table 4.21 $G_{max}$ t-test Results for Recycled Concrete Aggregate RC1 at 28 days

| Material Comparison | $G_{max}$ Mean RC2 | $G_{max}$ Mean RC2 | Curing Days | t-value | 2 sided p-value | Means are Different |
|---|---|---|---|---|---|---|
| Dry to Optimum | 117.62 | 114.64 | 28 | 1.720 | 0.1605 | No |
| Dry to Wet | 117.62 | 107.30 | 28 | 1.715 | 0.0092 | Yes |
| Optimum to Wet | 114.64 | 107.30 | 28 | 3.132 | 0.0351 | Yes |

Table 4.22 $G_{max}$ t-test Results for Recycled Concrete Aggregate RC1 for 7 day to 28 day Comparison

| Material Comparison | $G_{max}$ Mean RC2 | $G_{max}$ Mean RC2 | Moisture-Density Condition | t-value | 2 sided p-value | Means are Different |
|---|---|---|---|---|---|---|
| 7 Day to 28 Day | 103.69 | 117.62 | Dry | -3.380 | 0.0431 | Yes |
| 7 Day to 28 Day | 95.59 | 114.64 | Optimum | -8.119 | 0.0039 | Yes |
| 7 Day to 28 Day | 84.58 | 107.30 | Wet | -5.808 | 0.0102 | Yes |

Table 4.23 $G_{max}$ t-test Results for Recycled Concrete Aggregate RC2 at 7 days

| Material Comparison | $G_{max}$ Mean RC1 | $G_{max}$ Mean RC1 | Curing Days | t-value | 2 sided p-value | Means are Different |
|---|---|---|---|---|---|---|
| Dry to Optimum | 103.08 | 99.82 | 7 | 0.323 | 0.7771 | No |
| Dry to Wet | 103.08 | 89.73 | 7 | 0.989 | 0.4269 | No |
| Optimum to Wet | 99.82 | 89.73 | 7 | 1.124 | 0.3779 | No |

Table 4.24 $G_{max}$ t-test Results for Recycled Concrete Aggregate RC2 at 28 days

| Material Comparison | $G_{max}$ Mean RC1 | $G_{max}$ Mean RC1 | Curing Days | t-value | 2 sided p-value | Means are Different |
|---|---|---|---|---|---|---|
| Dry to Optimum | 107.08 | 104.60 | 28 | 1.136 | 0.3193 | No |
| Dry to Wet | 107.08 | 94.89 | 28 | 4.734 | 0.0091 | Yes |
| Optimum to Wet | 104.60 | 94.89 | 28 | 6.166 | 0.0035 | Yes |

Table 4.25 $G_{max}$ t-test Results for Recycled Concrete Aggregate RC2 for 7 day to 28 day Comparison

| Material Comparison | $G_{max}$ Mean RC1 | $G_{max}$ Mean RC1 | Moisture-Density Condition | t-value | 2 sided p-value | Means are Different |
|---|---|---|---|---|---|---|
| 7 Day to 28 Day | 103.08 | 107.08 | Dry | -0.500 | 0.6514 | No |
| 7 Day to 28 Day | 99.82 | 104.60 | Optimum | -6.419 | 0.0077 | Yes |
| 7 Day to 28 Day | 89.73 | 94.89 | Wet | -0.741 | 0.5124 | No |

Table 4.26 $G_{max}$ t-test Results for Limestone Aggregate at 7 days

| Material Comparison | $G_{max}$ Mean Limestone | $G_{max}$ Mean Limestone | Curing Days | t-value | 2 sided p-value | Means are Different |
|---|---|---|---|---|---|---|
| Dry to Optimum | 126.24 | 146.37 | 7 | -1.520 | 0.2678 | No |
| Dry to Wet | 126.24 | 100.32 | 7 | 11.626 | 0.0073 | Yes |
| Optimum to Wet | 146.37 | 100.32 | 7 | 3.522 | 0.0720 | No |

Table 4.27 $G_{max}$ t-test Results for Limestone Aggregate at 28 days

| Material Comparison | $G_{max}$ Mean Limestone | $G_{max}$ Mean Limestone | Curing Days | t-value | 2 sided p-value | Means are Different |
|---|---|---|---|---|---|---|
| Dry to Optimum | 129.07 | 154.82 | 28 | -3.004 | 0.0398 | Yes |
| Dry to Wet | 129.07 | 117.22 | 28 | 2.718 | 0.0531 | No |
| Optimum to Wet | 154.82 | 117.20 | 28 | 4.825 | 0.0085 | Yes |

Table 4.28 $G_{max}$ t-test Results for Limestone Aggregate for 7 day to 28 day Comparison

| Material Comparison | $G_{max}$ Mean Limestone | $G_{max}$ Mean Limestone | Moisture-Density Condition | t-value | 2 sided p-value | Means are Different |
|---|---|---|---|---|---|---|
| 7 Day to 28 Day | 126.24 | 129.07 | Dry | -0.525 | 0.6360 | No |
| 7 Day to 28 Day | 146.37 | 154.82 | Optimum | -0.612 | 0.5840 | No |
| 7 Day to 28 Day | 100.32 | 117.20 | Wet | -7.254 | 0.0054 | Yes |

4.3.1.3 Statistical Analysis of Permeability

A minimum permeability must be maintained for a drainable material used as a base in a pavement structure. Any significant decreases in permeability can cause failure in the materials. Therefore, the permeability of the materials is analyzed for the different compacted density conditions.

Tables 4.29, 4.30, and 4.31 provide the t-test comparisons of permeability of the three materials. The analyses of the materials show that significant differences occur between compacted density conditions in all three materials. The dry of optimum compacted density for both recycled aggregates have increased permeability in comparison to the optimum and wet of optimum density conditions. Even though significant differences occur, all values of permeability surpass the minimum requirement of $1.4 \times 10^{-4}$ cm/s.

Table 4.29 Permeability t-test Results for Recycled Concrete Aggregate RC1

| Material Comparison | Permeability Mean x$10^{-3}$ RC1 | Permeability Mean x$10^{-3}$ Limestone | Material | t-value | 2-sided p-value | Means are Different |
|---|---|---|---|---|---|---|
| Dry to Optimum | 1.70 | 1.64 | RC1 | 2.462 | 0.0490 | Yes |
| Dry to Wet | 1.70 | 1.41 | RC1 | 5.400 | 0.0017 | Yes |
| Optimum to Wet | 1.64 | 1.41 | RC1 | 4.532 | 0.0040 | Yes |

Table 4.30 Permeability t-test Results for Recycled Concrete Aggregate RC2

| Material Comparison | Permeability Mean x$10^{-3}$ RC1 | Permeability Mean x$10^{-3}$ RC2 | Material | t-value | 2-sided p-value | Means are Different |
|---|---|---|---|---|---|---|
| Dry to Optimum | 1.72 | 1.62 | RC2 | 3.757 | 0.0094 | Yes |
| Dry to Wet | 1.72 | 1.49 | RC2 | 17.578 | <0.0001 | Yes |
| Optimum to Wet | 1.62 | 1.49 | RC2 | 5.153 | 0.0021 | Yes |

Table 4.31 Permeability t-test Results for Limestone Aggregate

| Material Comparison | Permeability Mean x$10^{-3}$ RC2 | Permeability Mean x$10^{-3}$ Limestone | Material | t-value | 2-sided p-value | Means are Different |
|---|---|---|---|---|---|---|
| Dry to Optimum | 1.70 | 1.63 | Limestone | 7.703 | 0.0003 | Yes |
| Dry to Wet | 1.70 | 1.80 | Limestone | -9.628 | <0.0001 | Yes |
| Optimum to Wet | 1.63 | 1.80 | Limestone | -18.582 | <0.0001 | Yes |

*4.3.2 Statistical Analysis Between Materials*

The data results for the unconfined compression strength, small strain shear modulus $G_{max}$, and permeability were analyzed using a two sample hypotheses testing procedure. Each material was compared to the other two materials and evaluated based on their compacted density conditions. The analyses were performed at 7-day and 28-day curing periods. The analyses were performed between the materials using $\alpha$=0.05, a null hypotheses assuming that

the means between the materials at each compacted density conditions are equal ($H_0$: $u_1=u_2$), and an alternate hypotheses in which the means between the materials are not equal ($H_1$: $u_1 \neq u_2$).

4.3.2.1 Statistical Analysis of Unconfined Compression Strength

Tables 4.32, 4.33, and 4.34 present the t-test comparison results between the materials for the unconfined compression strength. From these results, the unconfined compression strength is noted to have a more significant difference between the recycled concrete aggregates and the crushed limestone aggregate materials at a 7-day curing period for optimum and wet of optimum compacted density conditions. The limestone aggregate values are consistently higher than that of the recycled aggregates. Therefore, it is concluded that the limestone aggregate consistently exhibits higher maximum shear strength than the recycled concrete aggregates.

Table 4.32 t-test Comparison of Materials for Unconfined Compression Strength

| Material Comparison | UCS Mean RC1 | UCS Mean RC2 | Curing Days | Moisture-Density Condition | t-value | 2 sided p-value | Means are Different |
|---|---|---|---|---|---|---|---|
| RC1 to RC2 | 153.69 | 104.71 | 7 | Dry | 4.643 | 0.0434 | Yes |
| RC1 to RC2 | 214.5 | 158.83 | 7 | Optimum | 2.592 | 0.1221 | No |
| RC1 to RC2 | 127.14 | 100.17 | 7 | Wet | 3.696 | 0.0660 | No |
| RC1 to RC2 | 419.56 | 462.76 | 28 | Dry | -2.126 | 0.1673 | No |
| RC1 to RC2 | 583.98 | 538.27 | 28 | Optimum | 5.266 | 0.0342 | Yes |
| RC1 to RC2 | 354.52 | 411.13 | 28 | Wet | -5.856 | 0.0279 | Yes |

Table 4.33 t-test Comparison of Materials for Unconfined Compression Strength

| Material Comparison | UCS Mean RC1 | UCS Mean Limestone | Curing Days | Moisture-Density Condition | t-value | 2 sided p-value | Means are Different |
|---|---|---|---|---|---|---|---|
| RC1 to Limestone | 153.69 | 244.31 | 7 | Dry | -2.234 | 0.1550 | No |
| RC1 to Limestone | 214.5 | 344.78 | 7 | Optimum | -5.808 | 0.0284 | Yes |
| RC1 to Limestone | 127.13 | 290.5 | 7 | Wet | -4.070 | 0.0554 | No |
| RC1 to Limestone | 419.56 | 497.61 | 28 | Dry | -3.743 | 0.0646 | No |
| RC1 to Limestone | 583.98 | 559.72 | 28 | Optimum | 1.768 | 0.2190 | No |
| RC1 to Limestone | 354.52 | 443.51 | 28 | Wet | -6.253 | 0.0246 | Yes |

Table 4.34 t-test Comparison of Materials for Unconfined Compression Strength

| Material Comparison | UCS Mean RC2 | UCS Mean Limestone | Curing Days | Moisture-Density Condition | t-value | 2 sided p-value | Means are Different |
|---|---|---|---|---|---|---|---|
| RC2 to Limestone | 104.71 | 244.31 | 7 | Dry | -3.551 | 0.0710 | No |
| RC2 to Limestone | 158.83 | 344.78 | 7 | Optimum | -19.715 | 0.0026 | Yes |
| RC2 to Limestone | 100.17 | 290.5 | 7 | Wet | -4.746 | 0.0416 | Yes |
| RC2 to Limestone | 462.76 | 497.61 | 28 | Dry | -3.351 | 0.0787 | No |
| RC2 to Limestone | 538.27 | 559.72 | 28 | Optimum | -1.516 | 0.2688 | No |
| RC2 to Limestone | 411.13 | 443.51 | 28 | Wet | -2.243 | 0.1542 | No |

4.3.2.2 Statistical Analysis of Small Strain Shear Modulus $G_{max}$

Tables 4.35, 4.36, and 4.37 present the t-test comparison results for $G_{max}$ between the materials. The significant difference for small strain $G_{max}$ between the recycled aggregates and the crushed limestone aggregate occurs at a 28-day curing period at the optimum moisture content density conditions. Therefore, the affects on the pavement structure are significant due to the use of the recycled aggregates.

Table 4.35 t-test Comparison of Materials for Small Strain $G_{max}$

| Material Comparison | $G_{max}$ Mean RC1 | $G_{max}$ Mean RC2 | Curing Days | Moisture-Density Condition | t-value | 2 sided p-value | Means are Different |
|---|---|---|---|---|---|---|---|
| RC1 to RC2 | 103.08 | 103.69 | 7 | Dry | -0.054 | 0.9622 | No |
| RC1 to RC2 | 99.82 | 95.59 | 7 | Optimum | 2.013 | 0.1818 | No |
| RC1 to RC2 | 89.73 | 84.58 | 7 | Wet | 0.522 | 0.6534 | No |
| RC1 to RC2 | 107.08 | 117.62 | 28 | Dry | -4.446 | 0.0113 | Yes |
| RC1 to RC2 | 104.60 | 114.64 | 28 | Optimum | -6.829 | 0.0024 | Yes |
| RC1 to RC2 | 94.89 | 107.30 | 28 | Wet | -5.148 | 0.0068 | Yes |

Table 4.36 t-test Comparison of Materials for Small Strain $G_{max}$

| Material Comparison | $G_{max}$ Mean RC1 | $G_{max}$ Mean Limestone | Curing Days | Moisture-Density Condition | t-value | 2 sided p-value | Means are Different |
|---|---|---|---|---|---|---|---|
| RC1 to Limestone | 103.08 | 126.24 | 7 | Dry | -2.245 | 0.1539 | No |
| RC1 to Limestone | 99.82 | 146.37 | 7 | Optimum | -3.562 | 0.0706 | No |
| RC1 to Limestone | 89.73 | 100.32 | 7 | Wet | -1.177 | 0.3602 | No |
| RC1 to Limestone | 107.08 | 129.07 | 28 | Dry | -4.873 | 0.0082 | Yes |
| RC1 to Limestone | 104.60 | 154.82 | 28 | Optimum | -6.599 | 0.0027 | Yes |
| RC1 to Limestone | 94.89 | 117.20 | 28 | Wet | -9.678 | 0.0006 | Yes |

Table 4.37 t-test Comparison of Materials for Small Strain $G_{max}$

| Material Comparison | $G_{max}$ Mean RC2 | $G_{max}$ Mean Limestone | Curing Days | Moisture-Density Condition | t-value | 2 sided p-value | Means are Different |
|---|---|---|---|---|---|---|---|
| RC2 to Limestone | 103.69 | 126.24 | 7 | Dry | -3.998 | 0.0572 | No |
| RC2 to Limestone | 95.59 | 146.37 | 7 | Optimum | -3.837 | 0.0617 | No |
| RC2 to Limestone | 84.58 | 100.32 | 7 | Wet | -3.830 | 0.0619 | No |
| RC2 to Limestone | 117.62 | 129.07 | 28 | Dry | -2.775 | 0.0501 | Yes |
| RC2 to Limestone | 114.64 | 154.82 | 28 | Optimum | -5.211 | 0.0065 | Yes |
| RC2 to Limestone | 107.30 | 117.20 | 28 | Wet | -3.799 | 0.0191 | Yes |

4.3.2.3 Statistical Analysis of Permeability

Tables 4.38, 4.39, and 4.40 present the t-test comparison of the coefficient of permeability between the materials. The analyses show that a significant difference between the recycled concrete aggregates and the crushed limestone aggregate occurred only at wet of optimum density conditions. However, all values of permeability surpass the minimum value of $1.4 \times 10^{-4}$ cm/s to maintain a drainable base.

Table 4.38 t-test Comparison of Materials for Coefficient of Permeability

| Material Comparison | Permeability Mean $x10^{-3}$ RC1 | Permeability Mean $x10^{-3}$ RC2 | Moisture-Density Condition | t-value | 2-sided p-value | Means are Different |
|---|---|---|---|---|---|---|
| RC1 to RC2 | 1.696 | 1.723 | Dry | -1.254 | 0.2564 | No |
| RC1 to RC2 | 1.641 | 1.619 | Optimum | 0.770 | 0.4705 | No |
| RC1 to RC2 | 1.412 | 1.485 | Wet | -1.474 | 0.1909 | No |

Table 4.39 t-test Comparison of Materials for Coefficient of Permeability

| Material Comparison | Permeability Mean $x10^{-3}$ RC1 | Permeability Mean $x10^{-3}$ Limestone | Moisture-Density Condition | t-value | 2-sided p-value | Means are Different |
|---|---|---|---|---|---|---|
| RC1 to Limestone | 1.696 | 1.703 | Dry | -0.368 | 0.7258 | No |
| RC1 to Limestone | 1.641 | 1.628 | Optimum | 0.955 | 0.3764 | No |
| RC1 to Limestone | 1.412 | 1.796 | Wet | -7.769 | 0.0002 | Yes |

Table 4.40 t-test Comparison of Materials for Coefficient of Permeability

| Material Comparison | Permeability Mean $x10^{-3}$ RC2 | Permeability Mean $x10^{-3}$ Limestone | Moisture-Density Condition | t-value | 2-sided p-value | Means are Different |
|---|---|---|---|---|---|---|
| RC2 to Limestone | 1.723 | 1.703 | Dry | 1.479 | 0.1897 | No |
| RC2 to Limestone | 1.619 | 1.628 | Optimum | -0.325 | 0.7560 | No |
| RC2 to Limestone | 1.485 | 1.796 | Wet | -32.982 | <0.0001 | Yes |

## 4.4 Summary

The recycled concrete aggregates and crushed limestone aggregates have been studied and compared. The physical characteristics of the materials have been provided along with a comprehensive evaluation of the materials at dry, optimum, and wet conditions on the compaction moisture content – dry curve. The measured small strain shear modulus $G_{max}$ for the materials will be further evaluated in the next section as it is applied to rigid and flexible pavement designs as a Modulus of Elasticity for a base material. The statistical analysis has provided the necessary evaluation for the comparison of recycled concrete aggregates to the natural crushed limestone at varying moisture content density conditions and curing periods.

# CHAPTER 5

# FLEXIBLE AND RIGID PAVEMENT DESIGN

## 5.1 Introduction

This chapter presents the determination of the elastic modulus from the small strain shear modulus $G_{max}$ determined in the previous chapter. In turn, the elastic moduli of the materials are used as base course layers in the design of flexible and rigid pavements. The structural coefficients will be determined for each moduli and used in the determination of the design thickness of the base course in the flexible pavement structure. In rigid pavements, the moduli of the materials represent the base course of the pavement structure. Several scenarios are presented for both flexible and rigid pavement design under different ESAL traffic requirements and road use applications.

## 5.2 Modulus of Elasticity

The modulus of elasticity is determined as previously discussed in Chapter 2. The use of Equation 2.2 is employed to determine the modulus of elasticity from the measured small strain shear modulus $G_{max}$ of the previous chapter. The small strain shear modulus $G_{max}$ used is the average value determined for each material at each moisture content condition. Tables 5.1, 5.2, and 5.3 present the results for the modulus of elasticity of the three materials. The values for modulus of elasticity were determined using a poisson's ratio value of 0.14 for the aggregates as described by Terrell et al. (2003).

## 5.3 Flexible Pavement Design

Currently, the development of a mechanistic-empirical pavement design guide (MEPDG) is in progress. The MEPDG is currently being developed and analyzed in Texas by the Texas Department of Transportation. The current empirical methods employed will in the future include mechanistically based models. At this time, the calibration and validation of the mechanistic and empirical pavement performance models are not in place for flexible pavement design. Therefore, the flexible pavement design used for this is study is an empirical approach based on the 1993 AASHTO *Guide for Design of Pavement Structures*.

In using the AASHTO empirical approach, the flexible pavement design requires that the structural coefficients of the material comprising the pavement structure be known. In order to use test materials in the pavement structure as a granular base, the structural coefficient was determined with the use of the modulus of elasticity values calculated as mentioned in the previous section. In order to calculate the structural coefficient, Equation 5.1 is used as described by AASHTO (1993).

$$a_3 = 0.249 (\log_{10} E_{BS}) - 0.977 \qquad (5.1)$$

The $a_3$ represents the structural coefficient and $E_{BS}$ is the modulus of elasticity of granular base material in units of psi. The structural coefficients determined for the granular base of the flexible pavement structure are provided on Table 5.1, 5.2, and 5.3.

Table 5.1 Modulus of Elasticity and Structural Coefficients for Recycled Concrete Aggregate RC1

| Material Specimen | Curing Time Days | Percent Moisture % | $G_{max}$ MPa | Poisson's Ratio | Modulus of Elasticity MPa | Structural Coefficient $a_3$ |
|---|---|---|---|---|---|---|
| RC1 | 7 | 12 | 103.08 | 0.14 | 235 | 0.15 |
| RC1 | 7 | 14 | 99.82 | 0.14 | 228 | 0.15 |
| RC1 | 7 | 18 | 89.73 | 0.14 | 205 | 0.14 |
| RC1 | 28 | 12 | 107.08 | 0.14 | 244 | 0.16 |
| RC1 | 28 | 14 | 104.59 | 0.14 | 238 | 0.15 |
| RC1 | 28 | 18 | 94.89 | 0.14 | 216 | 0.14 |

Table 5.2 Modulus of Elasticity and Structural Coefficients for Recycled Concrete Aggregate RC2

| Material Specimen | Curing Time Days | Percent Moisture % | $G_{max}$ MPa | Poisson's Ratio | Modulus of Elasticity MPa | Structural Coefficient $a_3$ |
|---|---|---|---|---|---|---|
| RC2 | 7 | 12 | 103.69 | 0.14 | 236 | 0.15 |
| RC2 | 7 | 14 | 95.59 | 0.14 | 218 | 0.14 |
| RC2 | 7 | 18 | 84.58 | 0.14 | 193 | 0.13 |
| RC2 | 28 | 12 | 117.62 | 0.14 | 268 | 0.17 |
| RC2 | 28 | 14 | 114.64 | 0.14 | 261 | 0.16 |
| RC2 | 28 | 18 | 100.37 | 0.14 | 229 | 0.15 |

Table 5.3 Modulus of Elasticity and Structural Coefficients for Crushed Limestone Aggregate

| Material Specimen | Curing Time Days | Percent Moisture % | $G_{max}$ MPa | Poisson's Ratio | Modulus of Elasticity MPa | Structural Coefficient $a_3$ |
|---|---|---|---|---|---|---|
| Limestone | 7 | 12 | 126.24 | 0.14 | 288 | 0.17 |
| Limestone | 7 | 14 | 146.37 | 0.14 | 334 | 0.19 |
| Limestone | 7 | 18 | 100.32 | 0.14 | 229 | 0.15 |
| Limestone | 28 | 12 | 129.07 | 0.14 | 294 | 0.18 |
| Limestone | 28 | 14 | 154.82 | 0.14 | 353 | 0.20 |
| Limestone | 28 | 18 | 117.20 | 0.14 | 267 | 0.17 |

The average structural coefficient values for RC1, RC2, and limestone aggregates are 0.15, 0.15, and 0.18, respectively.

For the analysis of flexible pavement design, parameters were selected to maintain constant variables under varying traffic conditions between the designs of the pavement structures. In addition, material variables were used for the resilient modulus of the subgrade, and thickness of flexible pavement. Table 5.4 shows the selected traffic variables used for the analysis. Table 5.5 shows the material variables used for the analysis.

Table 5.4 Traffic Variables for Type of Highway System

| **Variable Type** | **Interstate Highway** | **State Highway** | **City Road** |
|---|---|---|---|
| ESAL's (in millions) | 1, 10, 20, and 40 | 1, 10 and 20 | 0.1, 1, and 10 |
| Reliability (%) | 95 | 95 | 95 |
| Standard Deviation | 0.45 | 0.45 | 0.45 |
| Initial Serviceability | 4.5 | 4.5 | 4.5 |
| Final Serviceability | 2.50 | 2.50 | 2.50 |

Table 5.5 Material Variables for Type of Highway System

| Variable Type | Interstate Highway | State Highway | City Road |
|---|---|---|---|
| Surface Asphalt | | | |
| Thickness (mm) | 50.8 | 50.8 | 50.8 |
| Structural Coefficient | 0.44 | 0.44 | 0.44 |
| Dense-Graded Asphalt | | | |
| Thickness (mm) | 203.2 | 152.4 | 101.6 |
| Structural Coefficient | 0.40 | 0.40 | 0.40 |
| Resilient Modulus of Subgrade (MPa) | 34.5, 68.9, and 137.9 | 34.5, 68.9, and 137.9 | 34.5, 68.9, and 137.9 |

In the design analysis, the selected asphalt thickness for each type of highway system is based on the thickness most commonly found in the Dallas-Fort Worth Area. The volume of traffic associated with each particular highway system coincides with expected volumes for interstates, state highways, and city roads. The volumes of traffic include a range from 0.1 million ESAL's to 40 million ESAL's for the three traffic systems. The factors of reliability, standard deviation, initial serviceability, and final serviceability remained constant to show the affects of the modulus of elasticity of the materials derived from this study. The resilient modulus of subgrade used represents three types of subgrade soil conditions.

From using the above conditions for traffic and material variables, the structural number was determined for each by using the nomograph shown in Figure 2.10 of Chapter 2. After determining the structural number, Equation 2.4 was used in conjunction with the structural coefficients determined for each material. By populating Equation 2.4, the base layer thickness was determined for each condition of each material used in the study. The results of the base layer thickness of each material for interstates, state highways, and city roads are provided in tables 5.6 through 5.14. The results from the tables are used to develop design charts for

determining the thickness of a base layer using the recycled concrete aggregates and limestone aggregates.

The design charts for flexible pavement are presented in figures 5.1 through 5.27. From the observation of the design charts, it can be seen that the recycled aggregates thickness requirement as a base layer is comparable to that of limestone aggregates for all subgrade conditions and all traffic loading conditions. All three materials exhibit sharp decreases in thickness requirements of base layer at particular locations with increases of the base layer modulus. The decreases are in line with the increase of the structural coefficient of the base layer. The required thickness for all three materials decreased with the increase of the subgrade modulus or with a decrease in traffic volume. Therefore, the base course improves the design of a flexible pavement structure for poor subgrade conditions. In some cases, the minimum required base layer thickness of 152.4 mm (6 inches) is noted due to recommendations by AASHTO (1993).

Table 5.6 Design Table for Interstate Traffic Conditions with Recycled Concrete Aggregate RC1 as Base Material

| Base Moduli MPa | Structural Coefficient $a_3$ | Base Layer Thickness (mm) | | | | Base Layer Thickness (mm) | | | | Base Layer Thickness (mm) | | | |
|---|---|---|---|---|---|---|---|---|---|---|---|---|---|
| | | Subgrade Modulus, 34.5 MPa | | | | Subgrade Modulus, 68.9 MPa | | | | Subgrade Modulus, 137.9 MPa | | | |
| | | I | II | III | IV | I | II | III | IV | I | II | III | IV |
| 205 | 0.14 | 152* | 305 | 406 | 508 | 152* | 152* | 178 | 279 | 152* | 152* | 152* | 152* |
| 216 | 0.14 | 152* | 305 | 406 | 508 | 152* | 152* | 178 | 279 | 152* | 152* | 152* | 152* |
| 228 | 0.15 | 152* | 279 | 381 | 457 | 152* | 152* | 178 | 254 | 152* | 152* | 152* | 152* |
| 235 | 0.15 | 152* | 279 | 381 | 457 | 152* | 152* | 178 | 254 | 152* | 152* | 152* | 152* |
| 238 | 0.15 | 152* | 279 | 381 | 457 | 152* | 152* | 178 | 254 | 152* | 152* | 152* | 152* |
| 244 | 0.16 | 152* | 254 | 356 | 432 | 152* | 152* | 152 | 229 | 152* | 152* | 152* | 152* |

Note: I = ESAL of 1 E+06; II = ESAL of 10 E+06; III = ESAL of 20 E+06; IV = ESAL of 40 E+06; Reliability = 95%; Standard Deviation = 0.45; Initial Serviceability = 4.5; Terminal Serviceability = 2.5; Asphalt Thickness (Surface) = 51 mm with $a_1$ = 0.44; Asphalt Thickness (Dense-Graded) = 203 mm with $a_2$ = 0.40; Base Thickness is rounded to nearest millimeter; * = Minimum Base Layer Thickness



Table 5.7 Design Table for State Highway Traffic Conditions with Recycled Concrete Aggregate RC1 as Base Material

| Base Moduli MPa | Structural Coefficient $a_3$ | Base Layer Thickness (mm) | | | Base Layer Thickness (mm) | | | Base Layer Thickness (mm) | | |
|---|---|---|---|---|---|---|---|---|---|---|
| | | Subgrade Modulus, 34.5 MPa | | | Subgrade Modulus, 68.9 MPa | | | Subgrade Modulus, 137.9 MPa | | |
| | | I | II | III | I | II | III | I | II | III |
| 205 | 0.14 | 203 | 508 | 610 | 152 | 279 | 381 | 152* | 152* | 178 |
| 216 | 0.14 | 203 | 508 | 610 | 152 | 279 | 381 | 152* | 152* | 178 |
| 228 | 0.15 | 178 | 457 | 559 | 152 | 254 | 356 | 152* | 152* | 152 |
| 235 | 0.15 | 178 | 457 | 559 | 152 | 254 | 356 | 152* | 152* | 152 |
| 238 | 0.15 | 178 | 457 | 559 | 152 | 254 | 356 | 152* | 152* | 152 |
| 244 | 0.16 | 178 | 432 | 533 | 152 | 254 | 330 | 152* | 152* | 152 |

Note: I = ESAL of 1 E+06; II = ESAL of 10 E+06; III = ESAL of 20 E+06; Reliability = 95%; Standard Deviation = 0.45; Initial Serviceability = 4.5; Terminal Serviceability = 2.5; Asphalt Thickness (Surface) = 51 mm with $a_1$ = 0.44; Asphalt Thickness (Dense-Graded) = 203 mm with $a_2$ = 0.40; Base Thickness is rounded to nearest millimeter; * = Minimum Base Layer Thickness

Table 5.8 Design Table for City Road Traffic Conditions with Recycled Concrete Aggregate RC1 as Base Material

| Base Moduli MPa | Structural Coefficient $a_3$ | Base Layer Thickness (mm) | | | Base Layer Thickness (mm) | | | Base Layer Thickness (mm) | | |
|---|---|---|---|---|---|---|---|---|---|---|
| | | Subgrade Modulus, 34.5 MPa | | | Subgrade Modulus, 68.9 MPa | | | Subgrade Modulus, 137.9 MPa | | |
| | | I | II | III | I | II | III | I | II | III |
| 205 | 0.14 | 152* | 330 | 610 | 152* | 152* | 406 | 152* | 152* | 229 |
| 216 | 0.14 | 152* | 330 | 610 | 152* | 152* | 406 | 152* | 152* | 229 |
| 228 | 0.15 | 152* | 330 | 610 | 152* | 152* | 406 | 152* | 152* | 229 |
| 235 | 0.15 | 152* | 330 | 610 | 152* | 152* | 406 | 152* | 152* | 229 |
| 238 | 0.15 | 152* | 330 | 610 | 152* | 152* | 406 | 152* | 152* | 229 |
| 244 | 0.16 | 152* | 305 | 559 | 152* | 152* | 381 | 152* | 152* | 203 |

Note: I = ESAL of 1 E+05; II = ESAL of 1 E+06; III = ESAL of 10 E+06; Reliability = 95%; Standard Deviation = 0.45; Initial Serviceability = 4.5; Terminal Serviceability = 2.5; Asphalt Thickness (Surface) = 51 mm with $a_1$ = 0.44; Asphalt Thickness (Dense-Graded) = 203 mm with $a_2$ = 0.40; Base Thickness is rounded to nearest millimeter; * = Minimum Base Layer Thickness



Table 5.9 Design Table for Interstate Traffic Conditions with Recycled Concrete Aggregate RC2 as Base Material

| Base Moduli MPa | Structural Coefficient $a_3$ | Base Layer Thickness (mm) | | | | Base Layer Thickness (mm) | | | | Base Layer Thickness (mm) | | | |
|---|---|---|---|---|---|---|---|---|---|---|---|---|---|
| | | Subgrade Modulus, 34.5 MPa | | | | Subgrade Modulus, 68.9 MPa | | | | Subgrade Modulus, 137.9 MPa | | | |
| | | I | II | III | IV | I | II | III | IV | I | II | III | IV |
| 193 | 0.13 | 152* | 330 | 432 | 533 | 152* | 152* | 203 | 279 | 152* | 152* | 152* | 152* |
| 218 | 0.14 | 152* | 305 | 406 | 508 | 152* | 152* | 178 | 279 | 152* | 152* | 152* | 152* |
| 229 | 0.15 | 152* | 279 | 381 | 457 | 152* | 152* | 178 | 254 | 152* | 152* | 152* | 152* |
| 236 | 0.15 | 152* | 279 | 381 | 457 | 152* | 152* | 178 | 254 | 152* | 152* | 152* | 152* |
| 261 | 0.16 | 152* | 254 | 356 | 432 | 152* | 152* | 152 | 229 | 152* | 152* | 152* | 152* |
| 268 | 0.17 | 152* | 254 | 330 | 406 | 152* | 152* | 152 | 229 | 152* | 152* | 152* | 152* |

Note: I = ESAL of 1 E+06; II = ESAL of 10 E+06; III = ESAL of 20 E+06; IV = ESAL of 40 E+06; Reliability = 95%; Standard Deviation = 0.45; Initial Serviceability = 4.5; Terminal Serviceability = 2.5; Asphalt Thickness (Surface) = 51 mm with $a_1$ = 0.44; Asphalt Thickness (Dense-Graded) = 203 mm with $a_2$ = 0.40; Base Thickness is rounded to nearest millimeter; * = Minimum Base Layer Thickness

Table 5.10 Design Table for State Highway Traffic Conditions with Recycled Concrete Aggregate RC2 as Base Material

| Base Moduli MPa | Structural Coefficient $a_3$ | Base Layer Thickness (mm) | | | Base Layer Thickness (mm) | | | Base Layer Thickness (mm) | | |
|---|---|---|---|---|---|---|---|---|---|---|
| | | Subgrade Modulus, 34.5 MPa | | | Subgrade Modulus, 68.9 MPa | | | Subgrade Modulus, 137.9 MPa | | |
| | | I | II | III | I | II | III | I | II | III |
| 193 | 0.13 | 178 | 483 | 584 | 152* | 254 | 356 | 152* | 152* | 152* |
| 218 | 0.14 | 152* | 457 | 533 | 152* | 254 | 330 | 152* | 152* | 152* |
| 229 | 0.15 | 152* | 406 | 508 | 152* | 229 | 305 | 152* | 152* | 152* |
| 236 | 0.15 | 152* | 406 | 508 | 152* | 229 | 305 | 152* | 152* | 152* |
| 261 | 0.16 | 152* | 381 | 483 | 152* | 203 | 279 | 152* | 152* | 152* |
| 268 | 0.17 | 152* | 381 | 457 | 152* | 203 | 279 | 152* | 152* | 152* |

Note: I = ESAL of 1 E+06; II = ESAL of 10 E+06; III = ESAL of 20 E+06; Reliability = 95%; Standard Deviation = 0.45; Initial Serviceability = 4.5; Terminal Serviceability = 2.5; Asphalt Thickness (Surface) = 51 mm with $a_1$ = 0.44; Asphalt Thickness (Dense-Graded) = 203 mm with $a_2$ = 0.40; Base Thickness is rounded to nearest millimeter; * = Minimum Base Layer Thickness



Table 5.11 Design Table for City Road Traffic Conditions with Recycled Concrete Aggregate RC2 as Base Material

| Base Moduli MPa | Structural Coefficient $a_3$ | Base Layer Thickness (mm) | | | Base Layer Thickness (mm) | | | Base Layer Thickness (mm) | | |
|---|---|---|---|---|---|---|---|---|---|---|
| | | Subgrade Modulus, 34.5 MPa | | | Subgrade Modulus, 68.9 MPa | | | Subgrade Modulus, 137.9 MPa | | |
| | | I | II | III | I | II | III | I | II | III |
| 193 | 0.13 | 152* | 330 | 635 | 152* | 152* | 406 | 152* | 152* | 229 |
| 218 | 0.14 | 152* | 305 | 584 | 152* | 152* | 381 | 152* | 152* | 203 |
| 229 | 0.15 | 152* | 279 | 559 | 152* | 152* | 356 | 152* | 152* | 203 |
| 236 | 0.15 | 152* | 279 | 559 | 152* | 152* | 356 | 152* | 152* | 203 |
| 261 | 0.16 | 152* | 279 | 508 | 152* | 152* | 330 | 152* | 152* | 178 |
| 268 | 0.17 | 152* | 254 | 483 | 152* | 152* | 330 | 152* | 152* | 178 |

Note: I = ESAL of 1 E+05; II = ESAL of 1 E+06; III = ESAL of 10 E+06; Reliability = 95%; Standard Deviation = 0.45; Initial Serviceability = 4.5; Terminal Serviceability = 2.5; Asphalt Thickness (Surface) = 51 mm with $a_1$ = 0.44; Asphalt Thickness (Dense-Graded) = 203 mm with $a_2$ = 0.40; Base Thickness is rounded to nearest millimeter; * = Minimum Base Layer Thickness

Table 5.12 Design Table for Interstate Traffic Conditions with Limestone Aggregate as Base Material

| Base Moduli MPa | Structural Coefficient $a_3$ | Base Layer Thickness (mm) | | | | Base Layer Thickness (mm) | | | | Base Layer Thickness (mm) | | | |
|---|---|---|---|---|---|---|---|---|---|---|---|---|---|
| | | Subgrade Modulus, 34.5 MPa | | | | Subgrade Modulus, 68.9 MPa | | | | Subgrade Modulus, 137.9 MPa | | | |
| | | I | II | III | IV | I | II | III | IV | I | II | III | IV |
| 229 | 0.15 | 152* | 279 | 381 | 457 | 152* | 152* | 203 | 254 | 152* | 152* | 152* | 152* |
| 267 | 0.17 | 152* | 254 | 330 | 406 | 152* | 152* | 152* | 229 | 152* | 152* | 152* | 152* |
| 288 | 0.17 | 152* | 254 | 330 | 406 | 152* | 152* | 152* | 229 | 152* | 152* | 152* | 152* |
| 295 | 0.18 | 152* | 229 | 305 | 381 | 152* | 152* | 152* | 203 | 152* | 152* | 152* | 152* |
| 334 | 0.19 | 152* | 229 | 305 | 381 | 152* | 152* | 152* | 203 | 152* | 152* | 152* | 152* |
| 353 | 0.20 | 152* | 203 | 279 | 356 | 152* | 152* | 152* | 203 | 152* | 152* | 152* | 152* |

Note: I = ESAL of 1 E+06; II = ESAL of 10 E+06; III = ESAL of 20 E+06; IV = ESAL of 40 E+06; Reliability = 95%; Standard Deviation = 0.45; Initial Serviceability = 4.5; Terminal Serviceability = 2.5; Asphalt Thickness (Surface) = 51 mm with $a_1$ = 0.44; Asphalt Thickness (Dense-Graded) = 203 mm with $a_2$ = 0.40; Base Thickness is rounded to nearest millimeter; * = Minimum Base Layer Thickness



Table 5.13 Design Table for State Highway Traffic Conditions with Limestone Aggregate as Base Material

| Base Moduli MPa | Structural Coefficient $a_3$ | Base Layer Thickness (mm) | | | Base Layer Thickness (mm) | | | Base Layer Thickness (mm) | | |
|---|---|---|---|---|---|---|---|---|---|---|
| | | Subgrade Modulus, 34.5 MPa | | | Subgrade Modulus, 68.9 MPa | | | Subgrade Modulus, 137.9 MPa | | |
| | | I | II | III | I | II | III | I | II | III |
| 229 | 0.15 | 152* | 406 | 508 | 152* | 229 | 305 | 152* | 152* | 152* |
| 267 | 0.17 | 152* | 381 | 457 | 152* | 203 | 279 | 152* | 152* | 152* |
| 288 | 0.17 | 152* | 381 | 457 | 152* | 203 | 279 | 152* | 152* | 152* |
| 295 | 0.18 | 152* | 356 | 432 | 152* | 203 | 254 | 152* | 152* | 152* |
| 334 | 0.19 | 152* | 330 | 406 | 152* | 178 | 254 | 152* | 152* | 152* |
| 353 | 0.20 | 152* | 305 | 381 | 152* | 152* | 229 | 152* | 152* | 152* |

Note: I = ESAL of 1 E+06; II = ESAL of 10 E+06; III = ESAL of 20 E+06; Reliability = 95%; Standard Deviation = 0.45; Initial Serviceability = 4.5; Terminal Serviceability = 2.5; Asphalt Thickness (Surface) = 51 mm with $a_1$ = 0.44; Asphalt Thickness (Dense-Graded) = 203 mm with $a_2$ = 0.40; Base Thickness is rounded to nearest millimeter; * = Minimum Base Layer Thickness

Table 5.14 Design Table for City Road Traffic Conditions with Limestone Aggregate as Base Material

| Base Moduli MPa | Structural Coefficient $a_3$ | Base Layer Thickness (mm) | | | Base Layer Thickness (mm) | | | Base Layer Thickness (mm) | | |
|---|---|---|---|---|---|---|---|---|---|---|
| | | Subgrade Modulus, 34.5 MPa | | | Subgrade Modulus, 68.9 MPa | | | Subgrade Modulus, 137.9 MPa | | |
| | | I | II | III | I | II | III | I | II | III |
| 229 | 0.15 | 152* | 279 | 559 | 152* | 152* | 356 | 152* | 152* | 203 |
| 267 | 0.17 | 152* | 254 | 483 | 152* | 152* | 330 | 152* | 152* | 178 |
| 288 | 0.17 | 152* | 254 | 483 | 152* | 152* | 330 | 152* | 152* | 178 |
| 295 | 0.18 | 152* | 254 | 457 | 152* | 152* | 305 | 152* | 152* | 178 |
| 334 | 0.19 | 152* | 229 | 432 | 152* | 152* | 279 | 152* | 152* | 152* |
| 353 | 0.20 | 152* | 229 | 406 | 152* | 152* | 279 | 152* | 152* | 152* |

Note: I = ESAL of 1 E+05; II = ESAL of 1 E+06; III = ESAL of 10 E+06; Reliability = 95%; Standard Deviation = 0.45; Initial Serviceability = 4.5; Terminal Serviceability = 2.5; Asphalt Thickness (Surface) = 51 mm with $a_1$ = 0.44; Asphalt Thickness (Dense-Graded) = 203 mm with $a_2$ = 0.40; Base Thickness is rounded to nearest millimeter; * = Minimum Base Layer Thickness

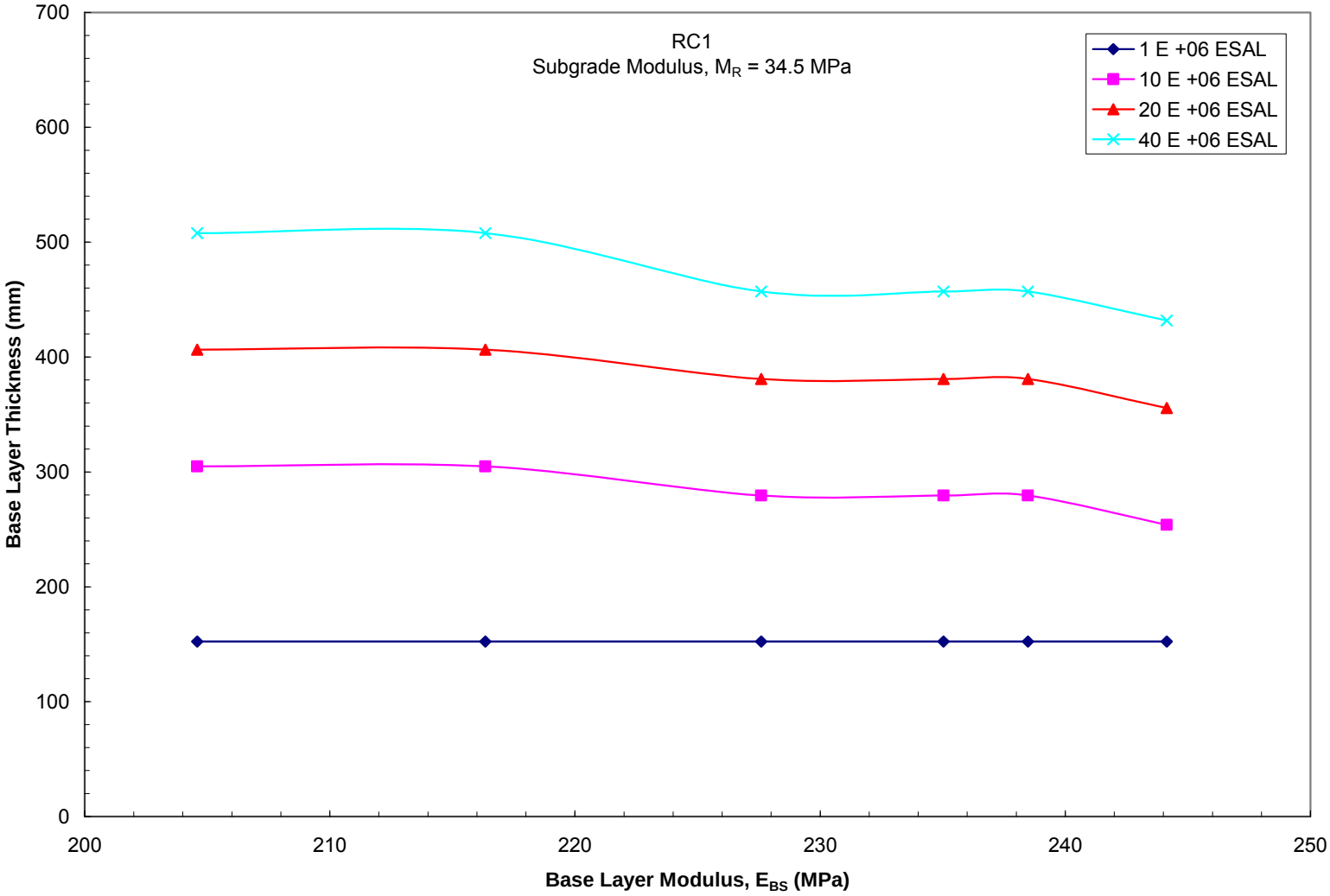


Figure 5.1 Design chart for determining thickness of base layer for interstates using recycled concrete aggregate RC1

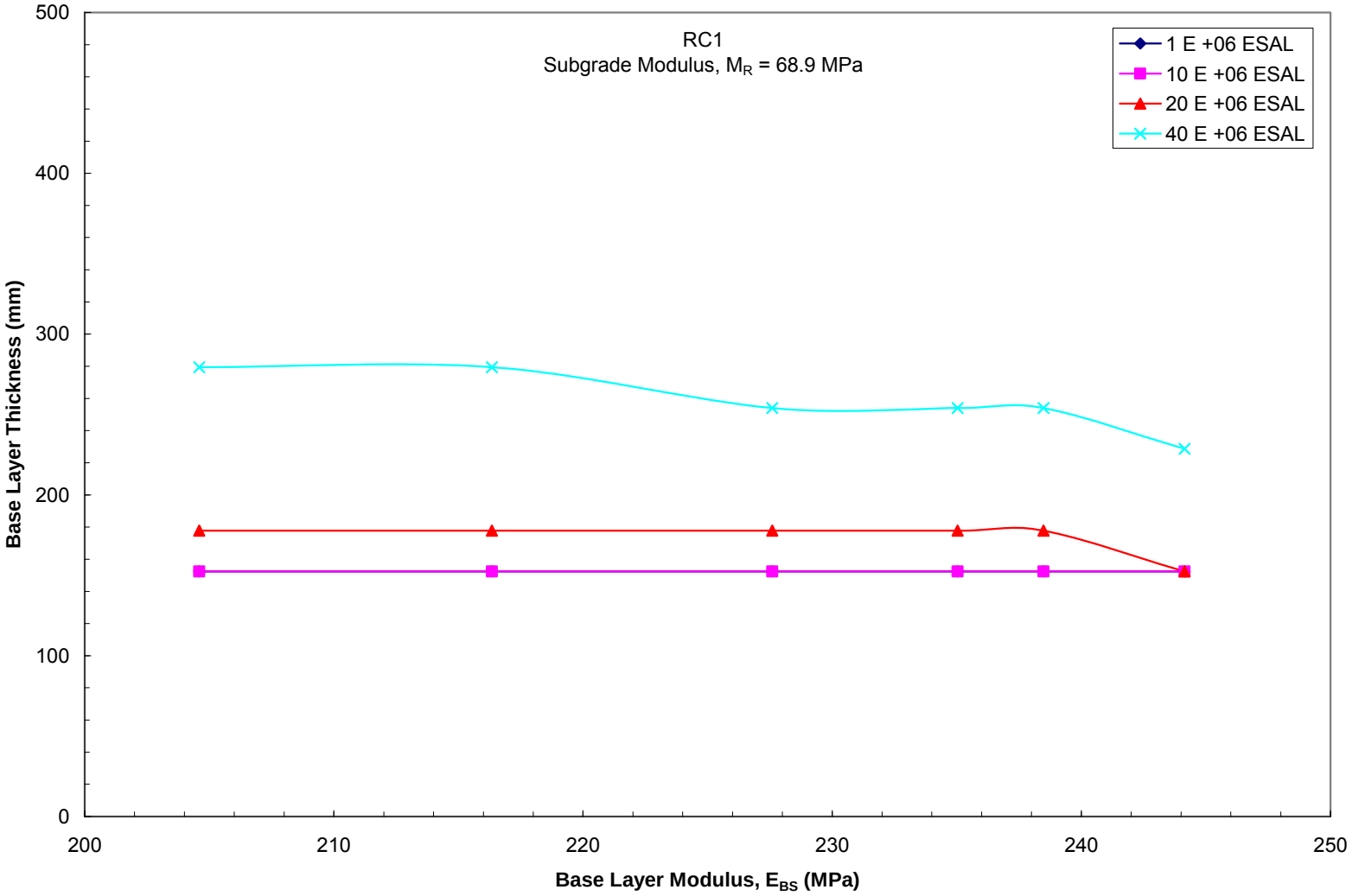


Figure 5.2 Design chart for determining thickness of base layer for interstates using recycled concrete aggregate RC1

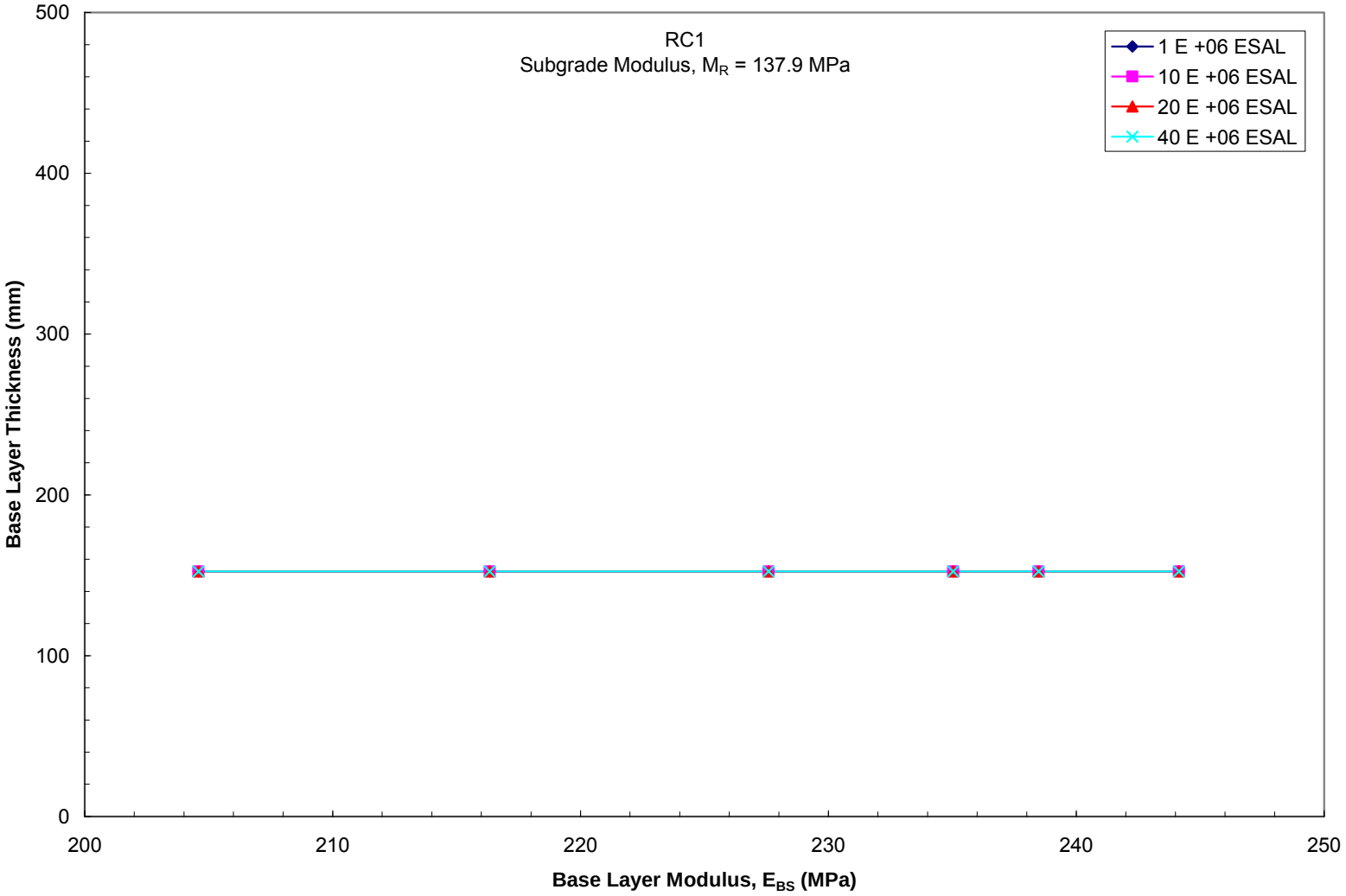


Figure 5.3 Design chart for determining thickness of base layer for interstates using recycled concrete aggregate RC1

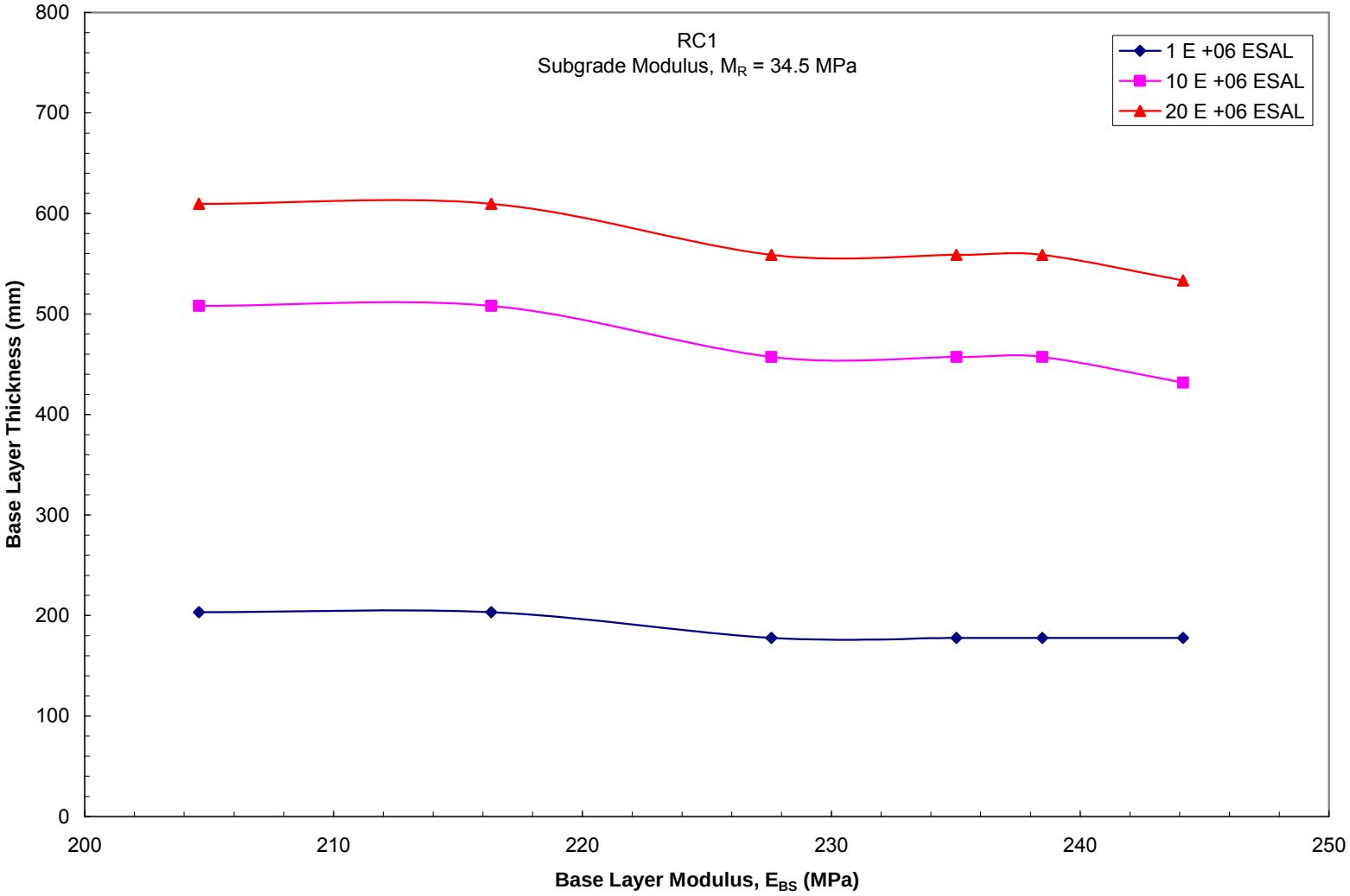


Figure 5.4 Design chart for determining thickness of base layer for state highways using recycled concrete aggregate RC1

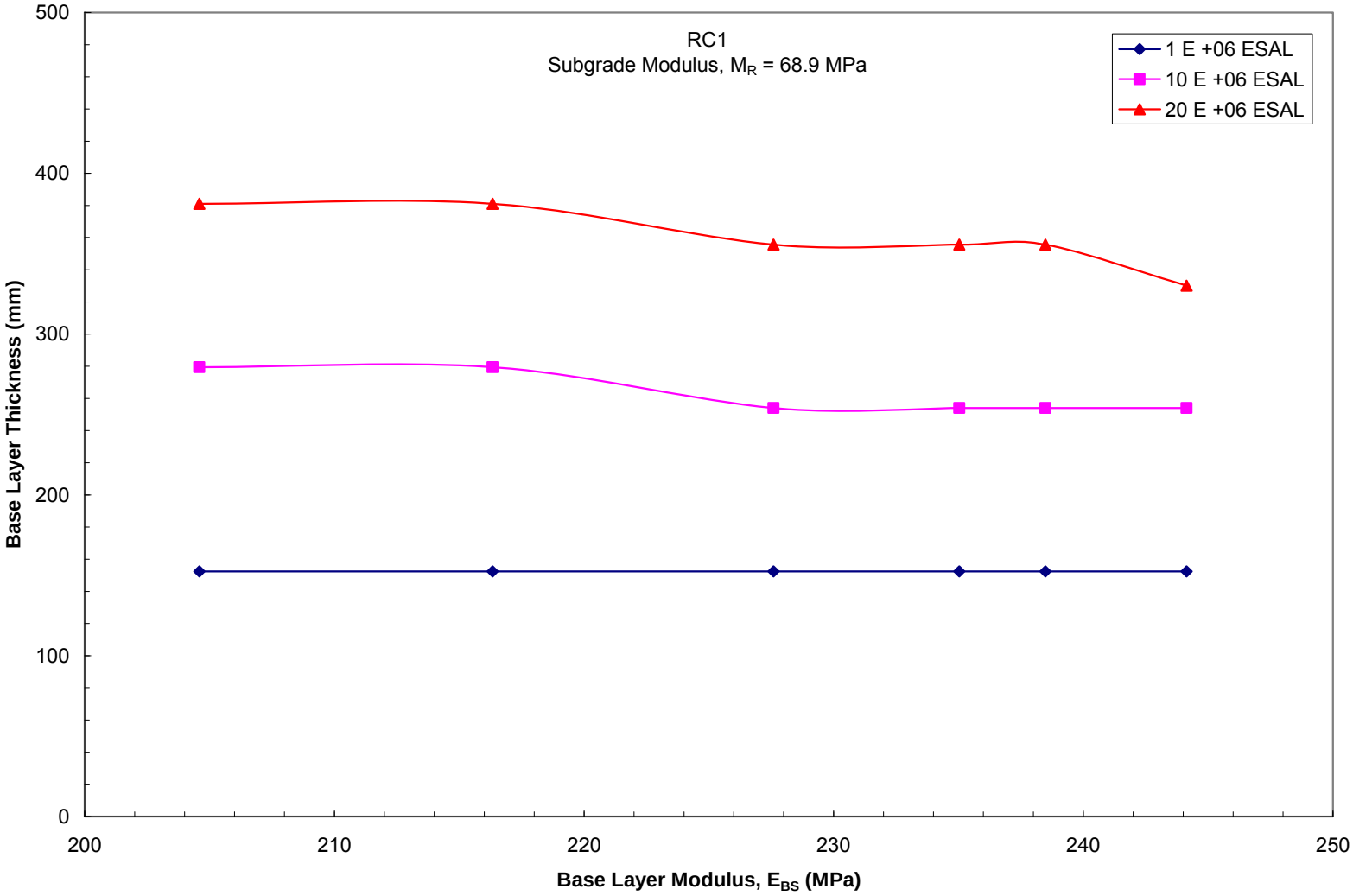


Figure 5.5 Design chart for determining thickness of base layer for state highways using recycled concrete aggregate RC1

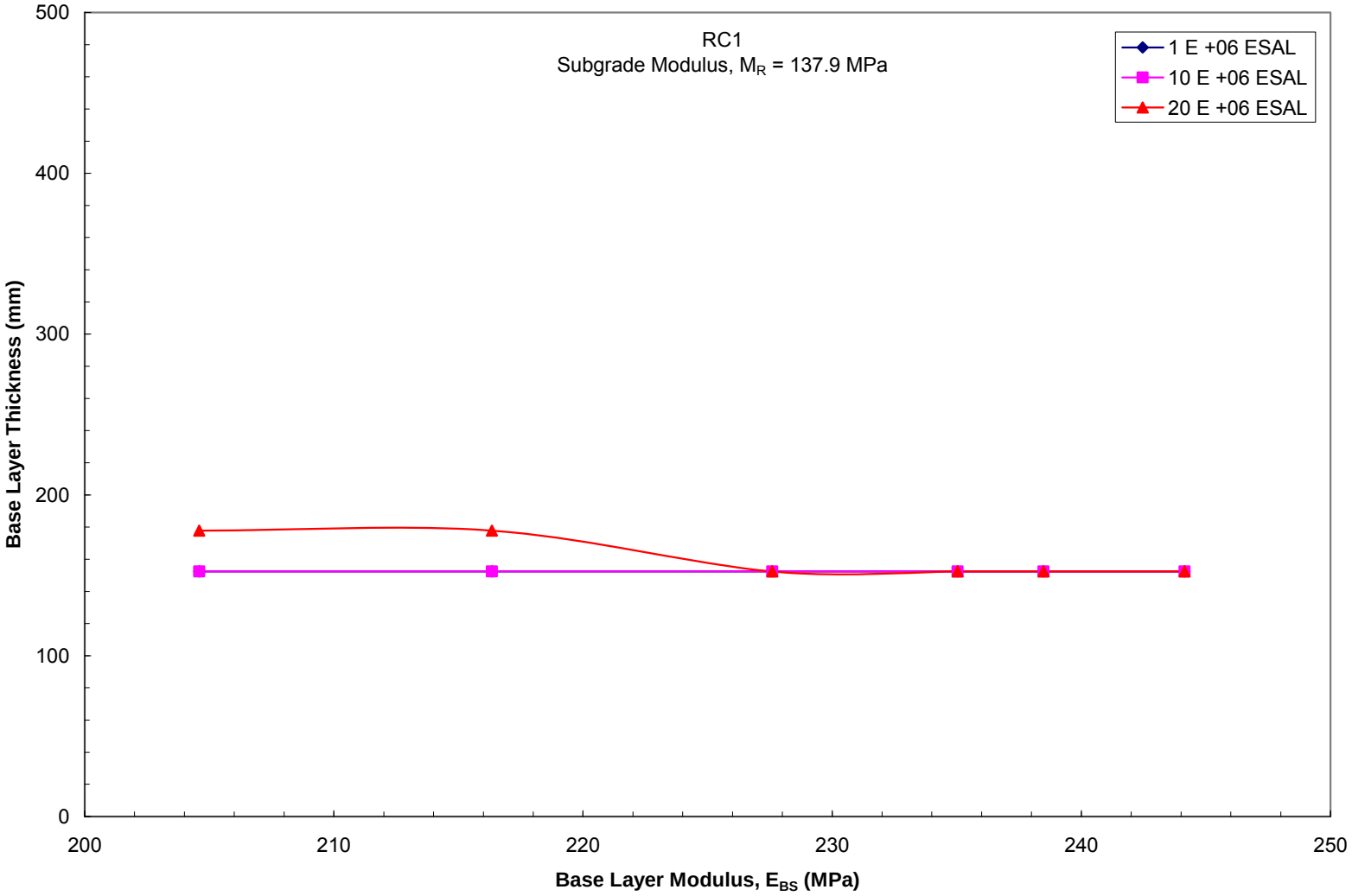


Figure 5.6 Design chart for determining thickness of base layer for state highways using recycled concrete aggregate RC1

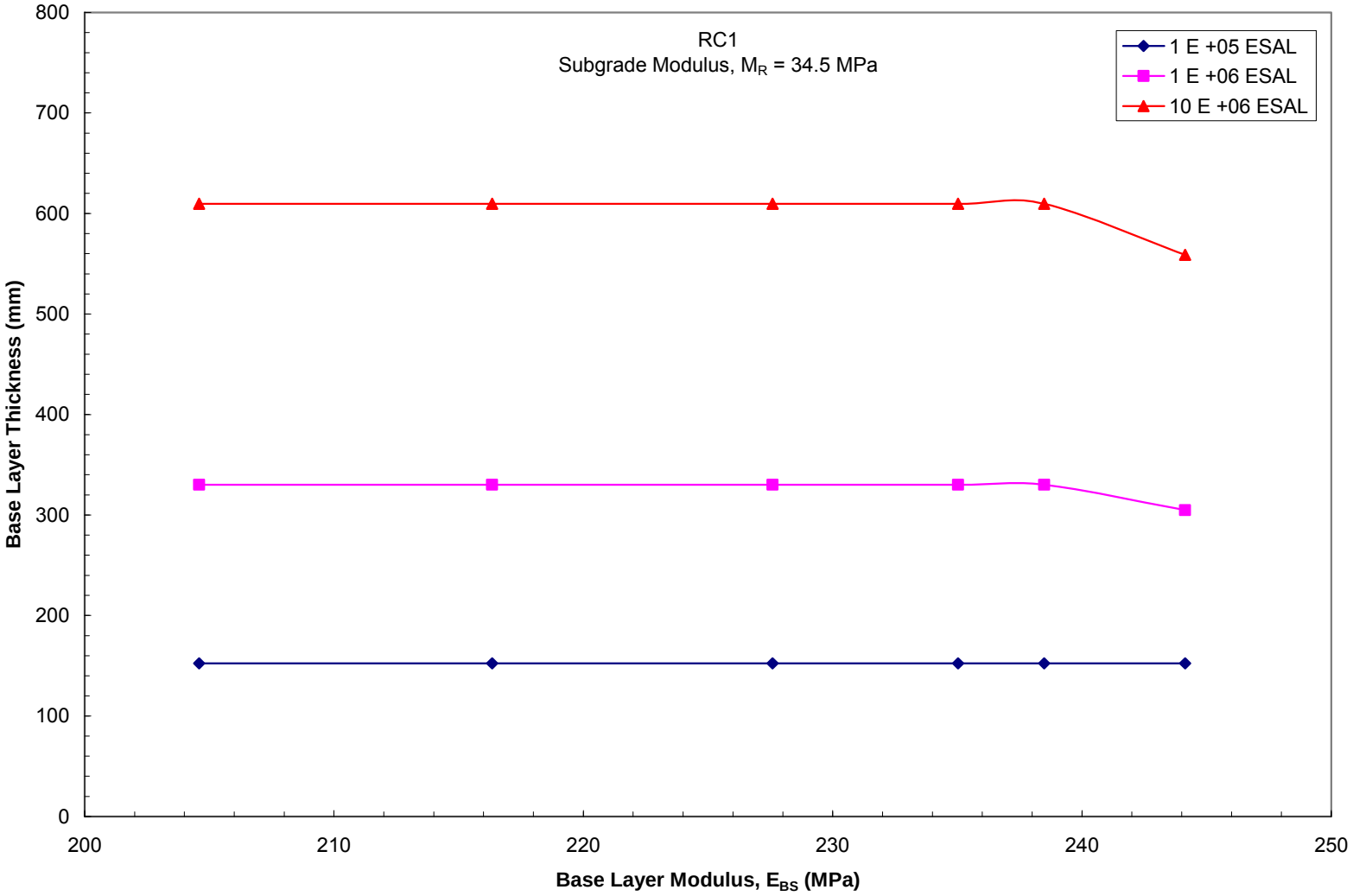


Figure 5.7 Design chart for determining thickness of base layer for city roads using recycled concrete aggregate RC1

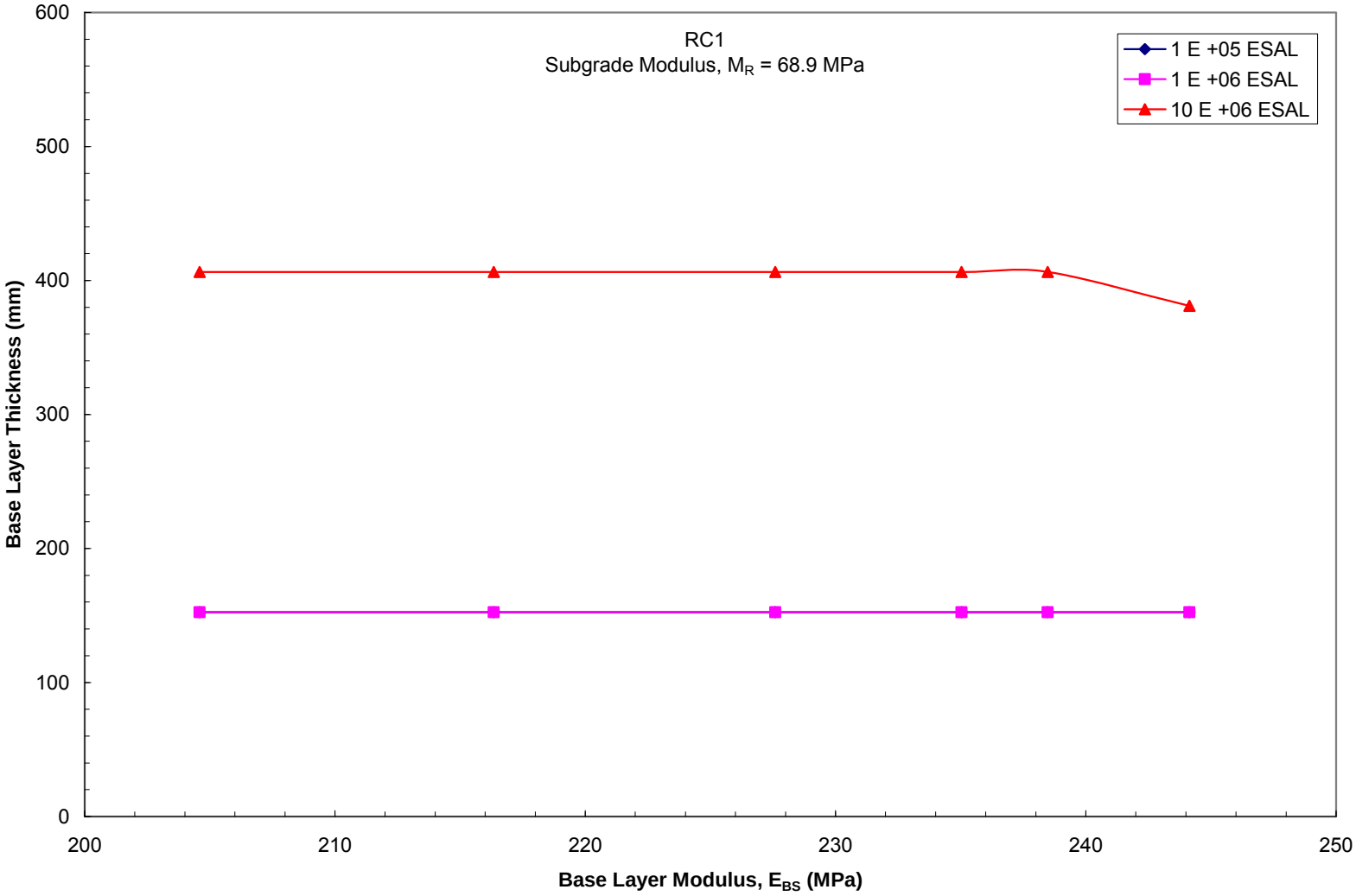


Figure 5.8 Design chart for determining thickness of base layer for city roads using recycled concrete aggregate RC1

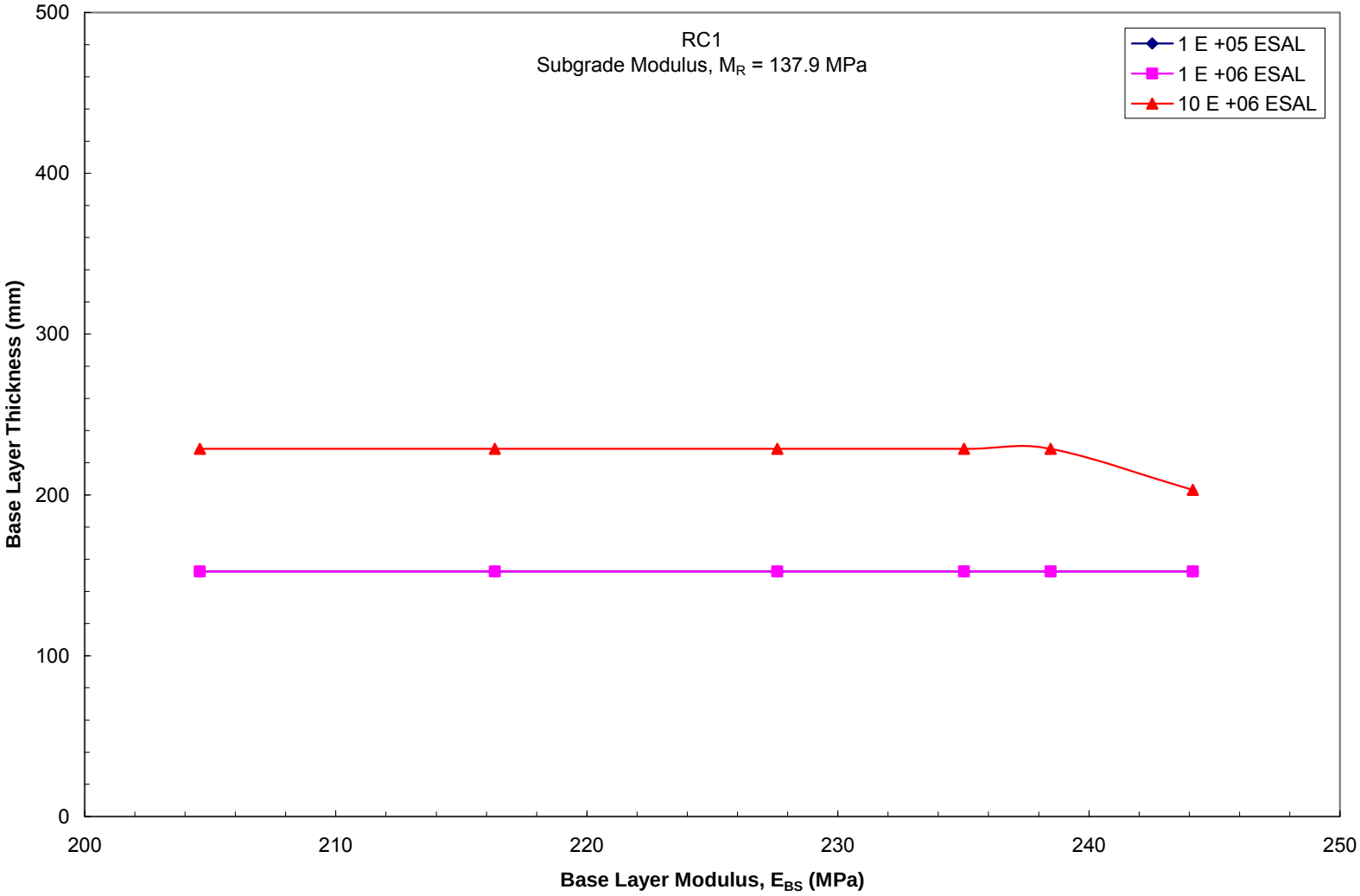


Figure 5.9 Design chart for determining thickness of base layer for city roads using recycled concrete aggregate RC1

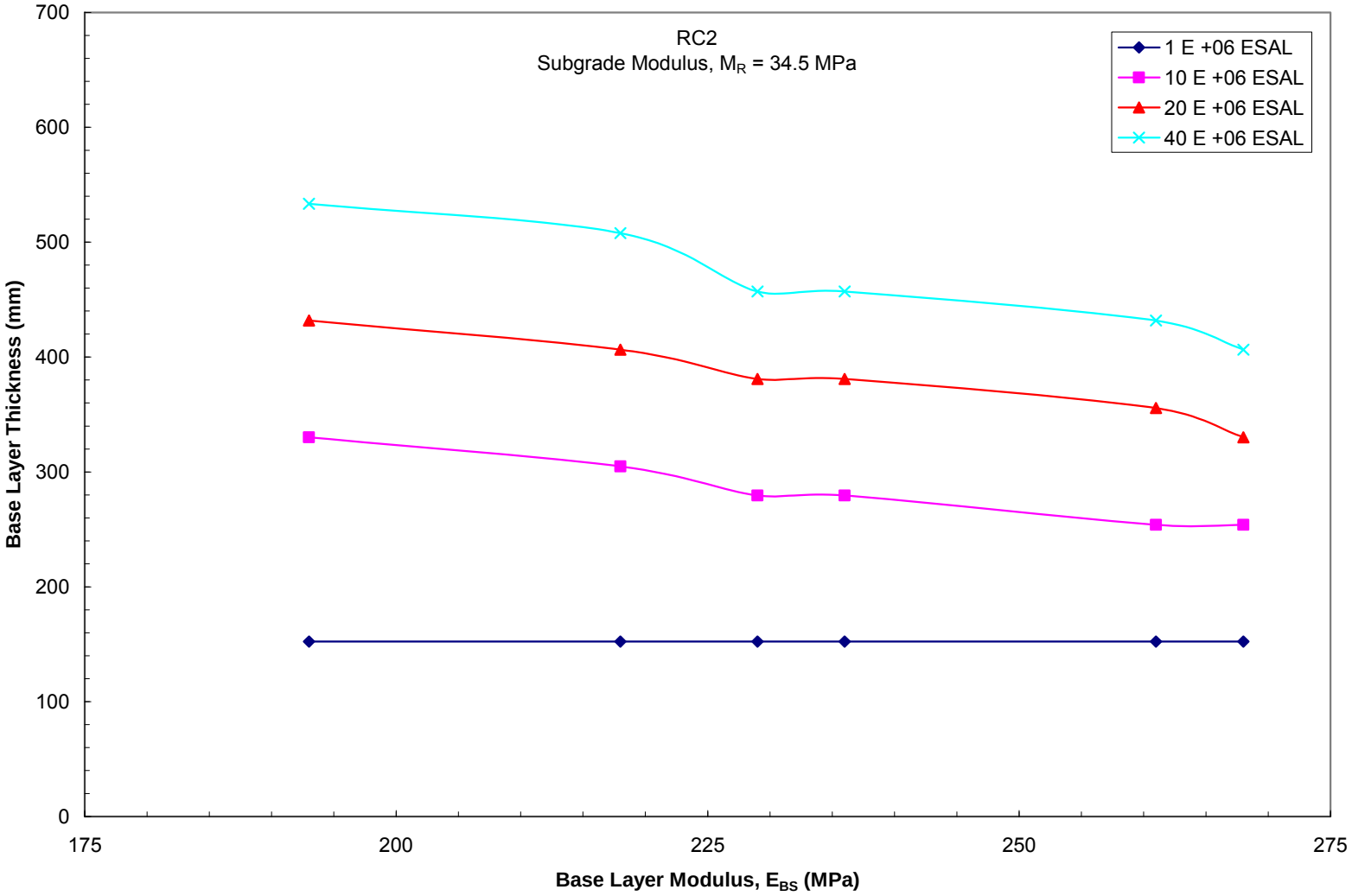


Figure 5.10 Design chart for determining thickness of base layer for interstates using recycled concrete aggregate RC2

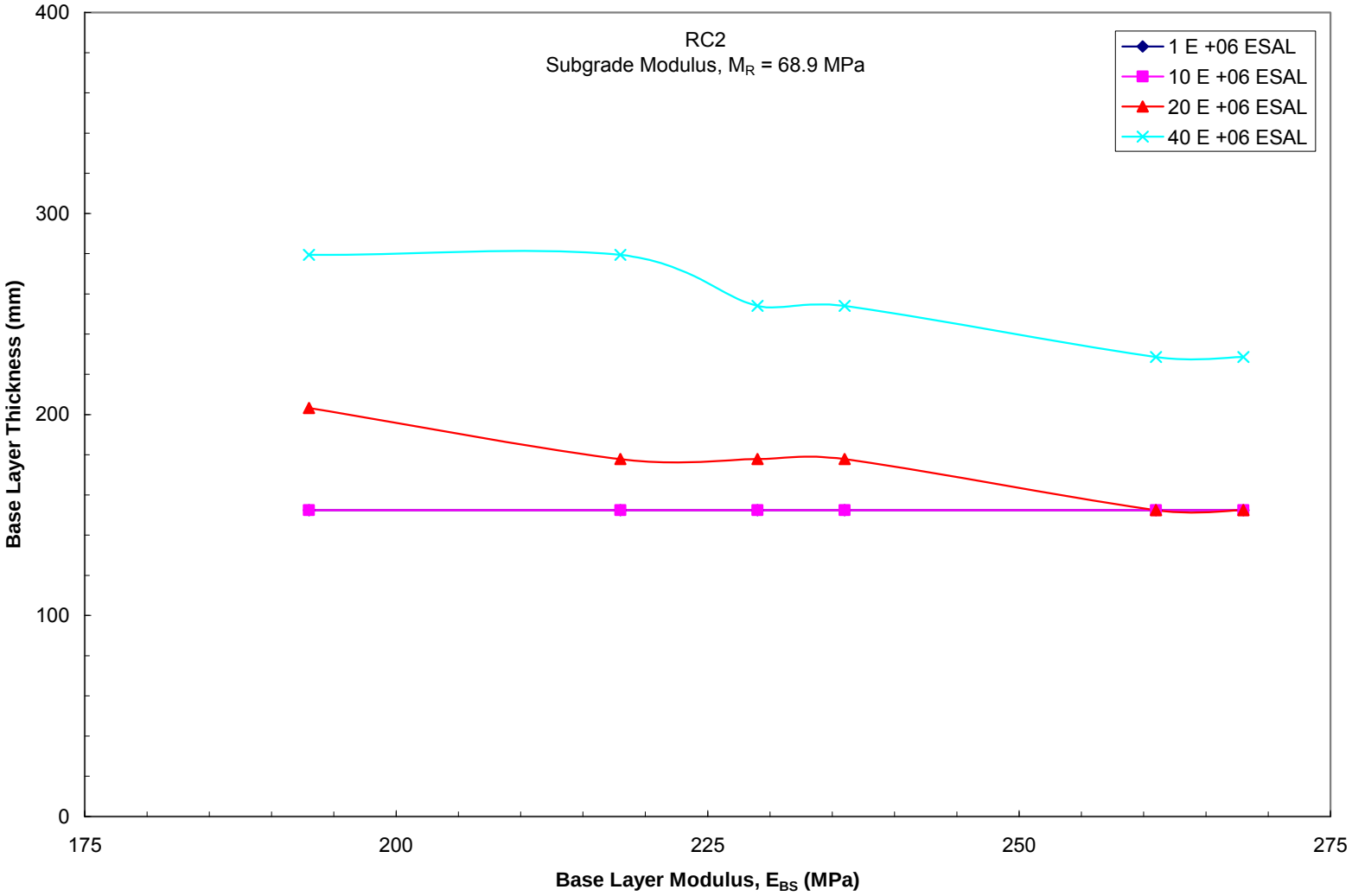


Figure 5.11 Design chart for determining thickness of base layer for interstates using recycled concrete aggregate RC2

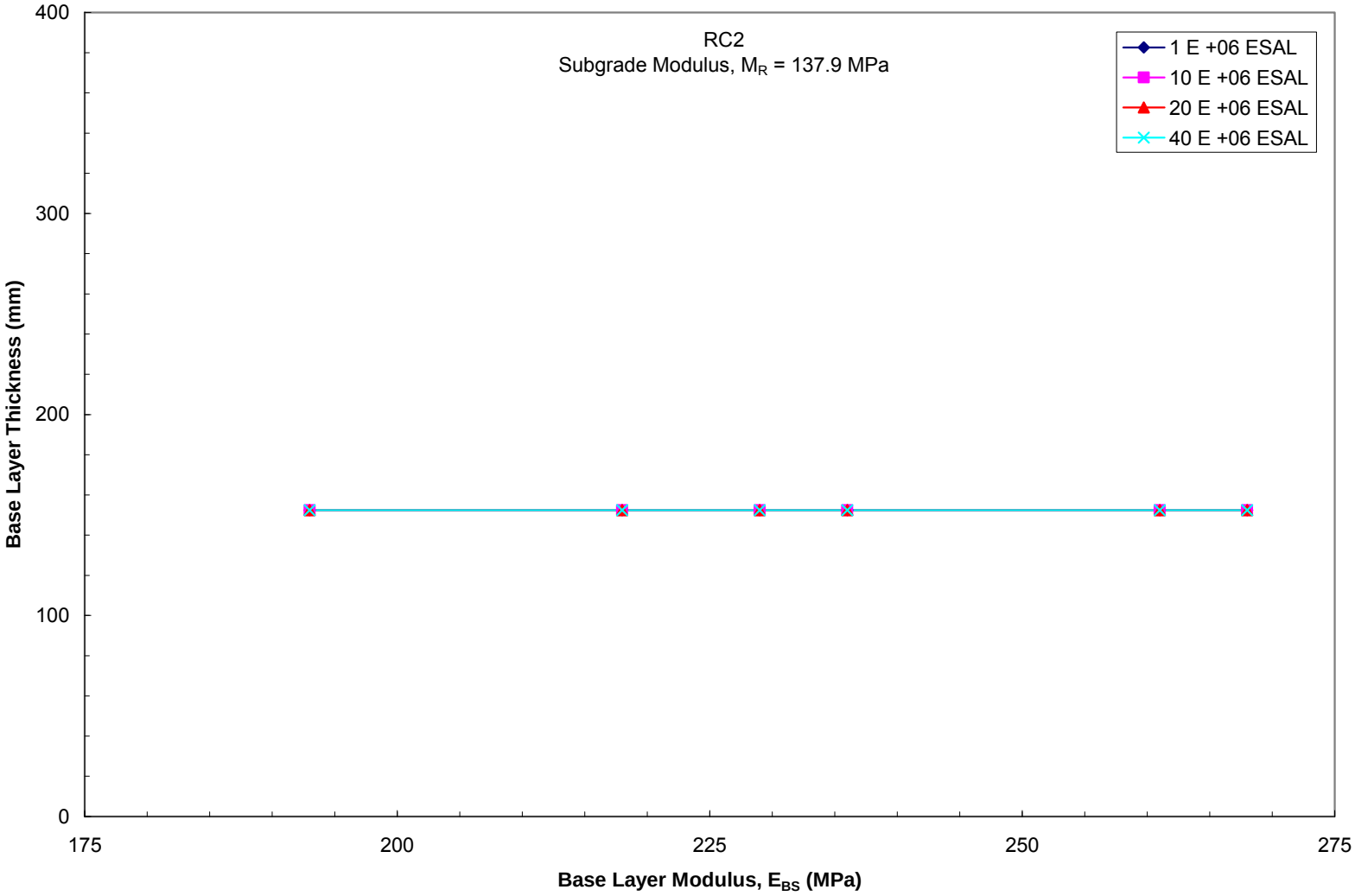


Figure 5.12 Design chart for determining thickness of base layer for interstates using recycled concrete aggregate RC2

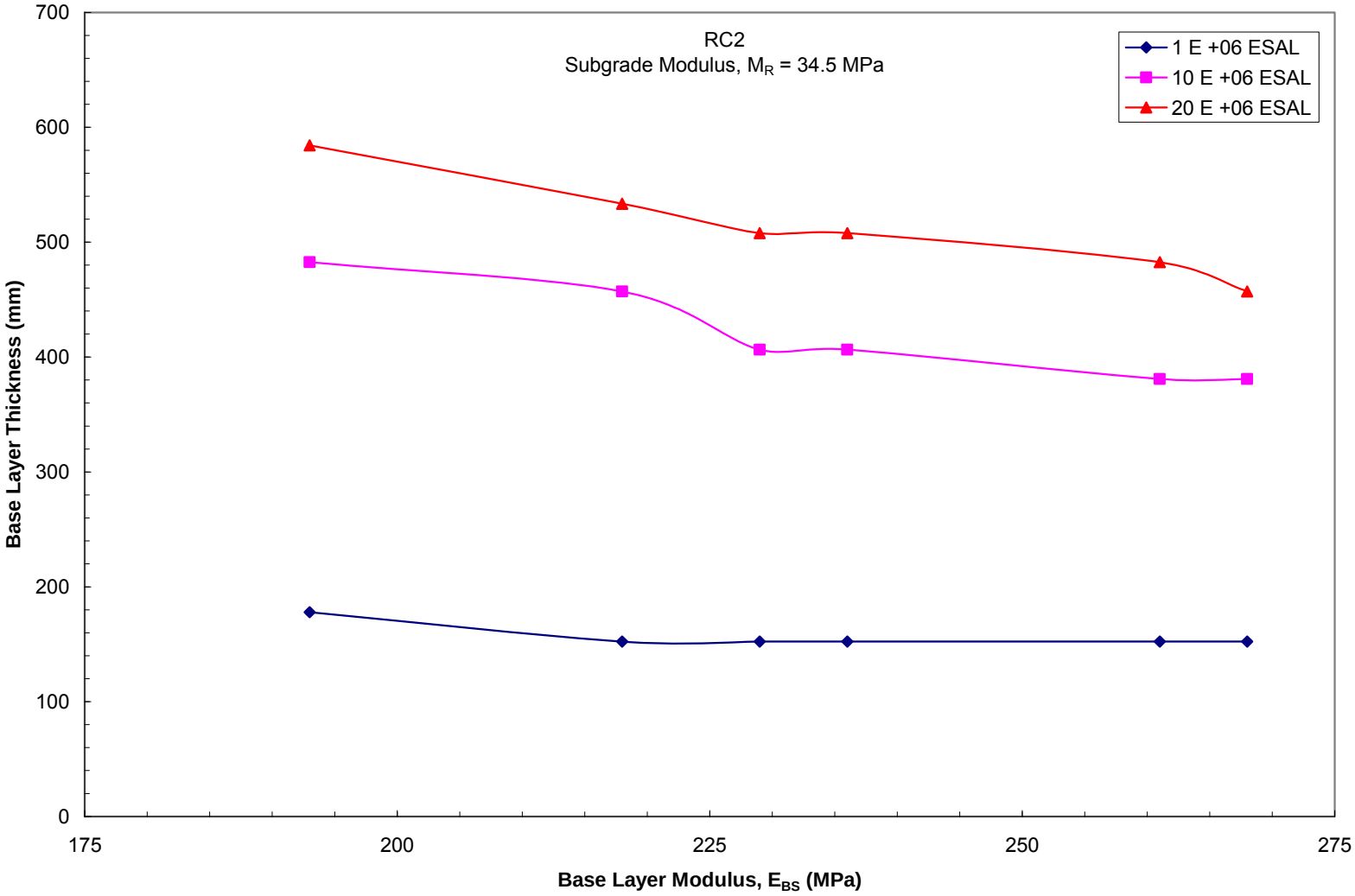


Figure 5.13 Design chart for determining thickness of base layer for state highways using recycled concrete aggregate RC2

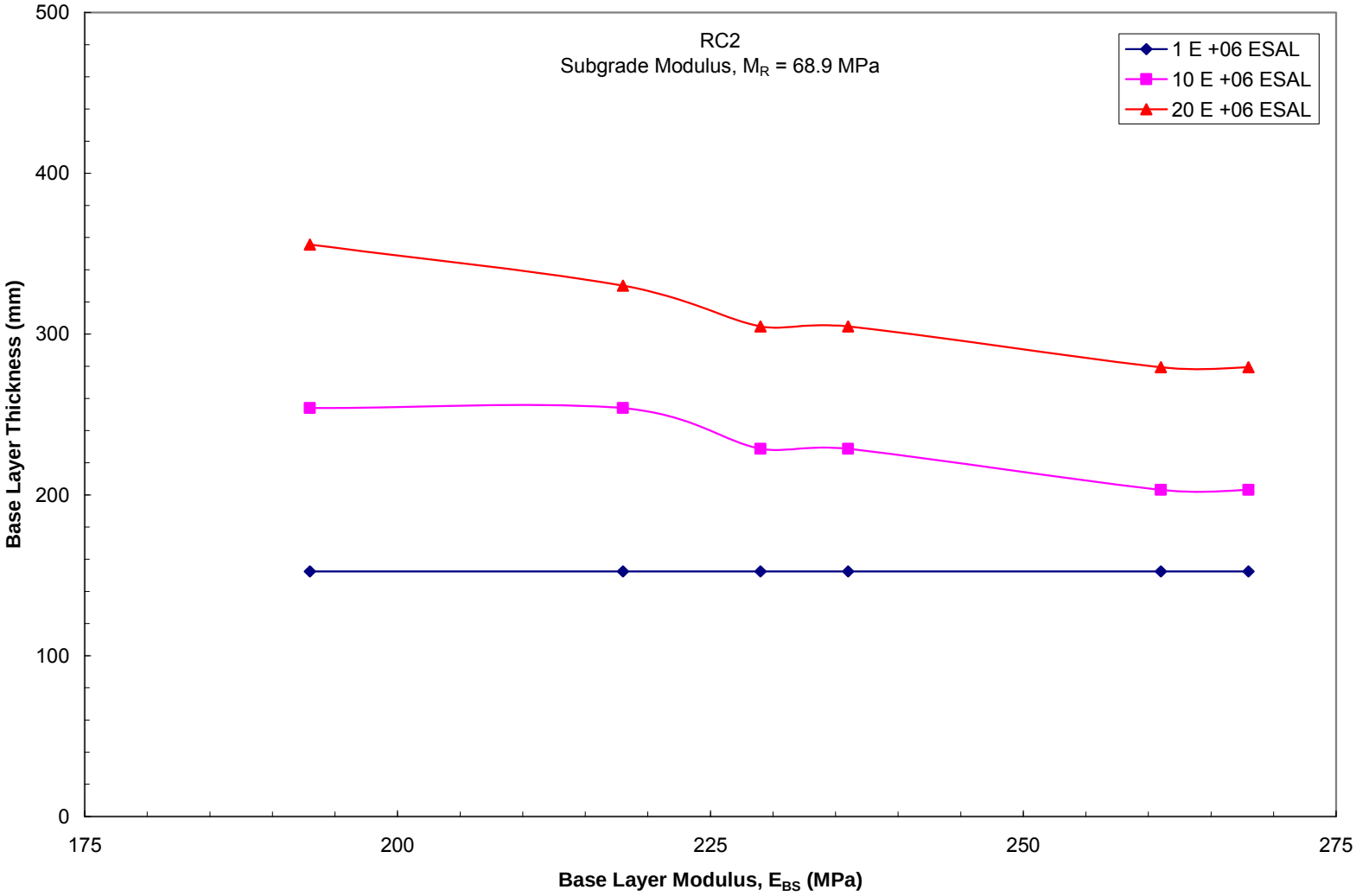


Figure 5.14 Design chart for determining thickness of base layer for state highways using recycled concrete aggregate RC2

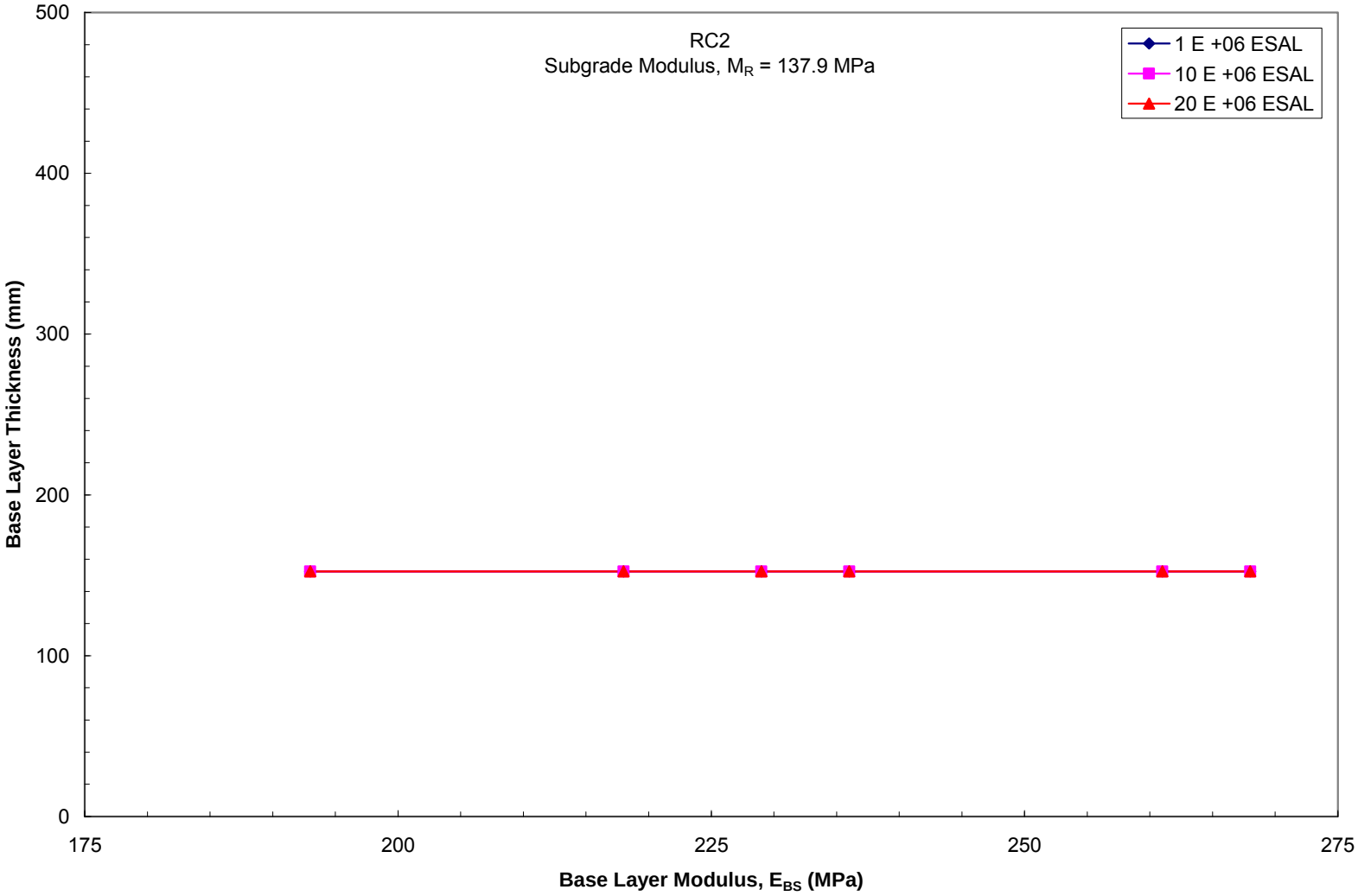


Figure 5.15 Design chart for determining thickness of base layer for state highways using recycled concrete aggregate RC2

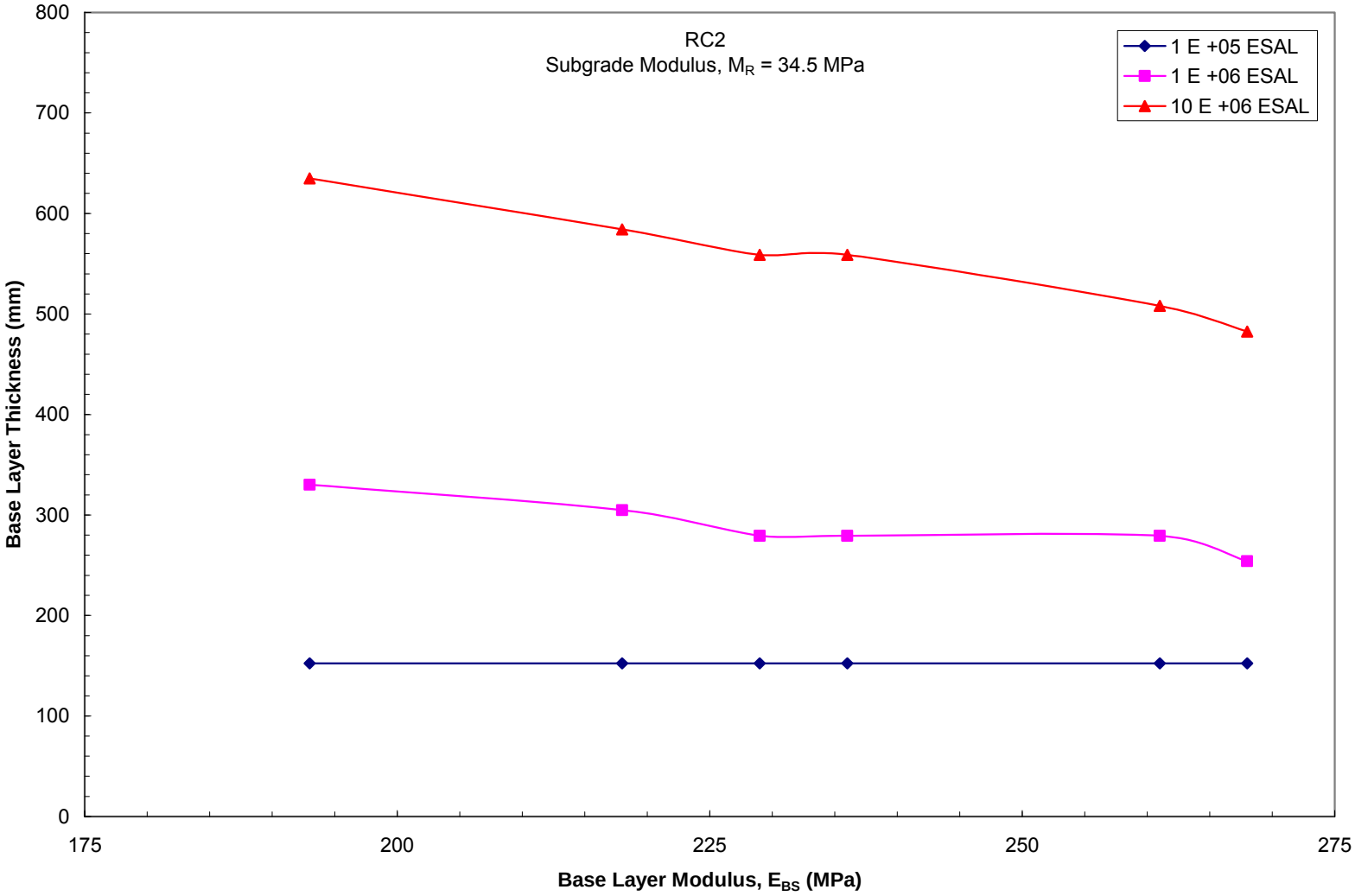


Figure 5.16 Design chart for determining thickness of base layer for city roads using recycled concrete aggregate RC2

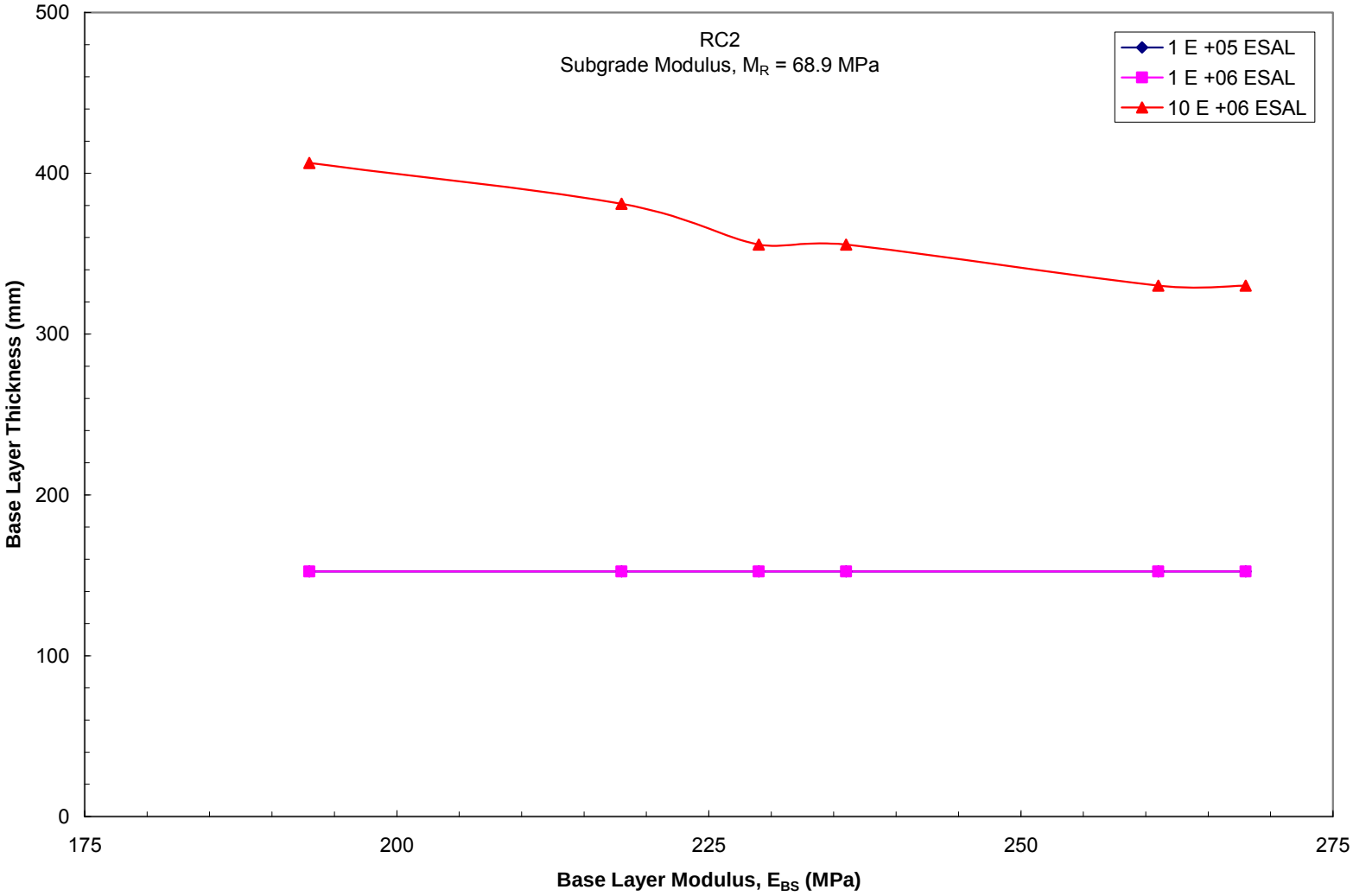


Figure 5.17 Design chart for determining thickness of base layer for city roads using recycled concrete aggregate RC2

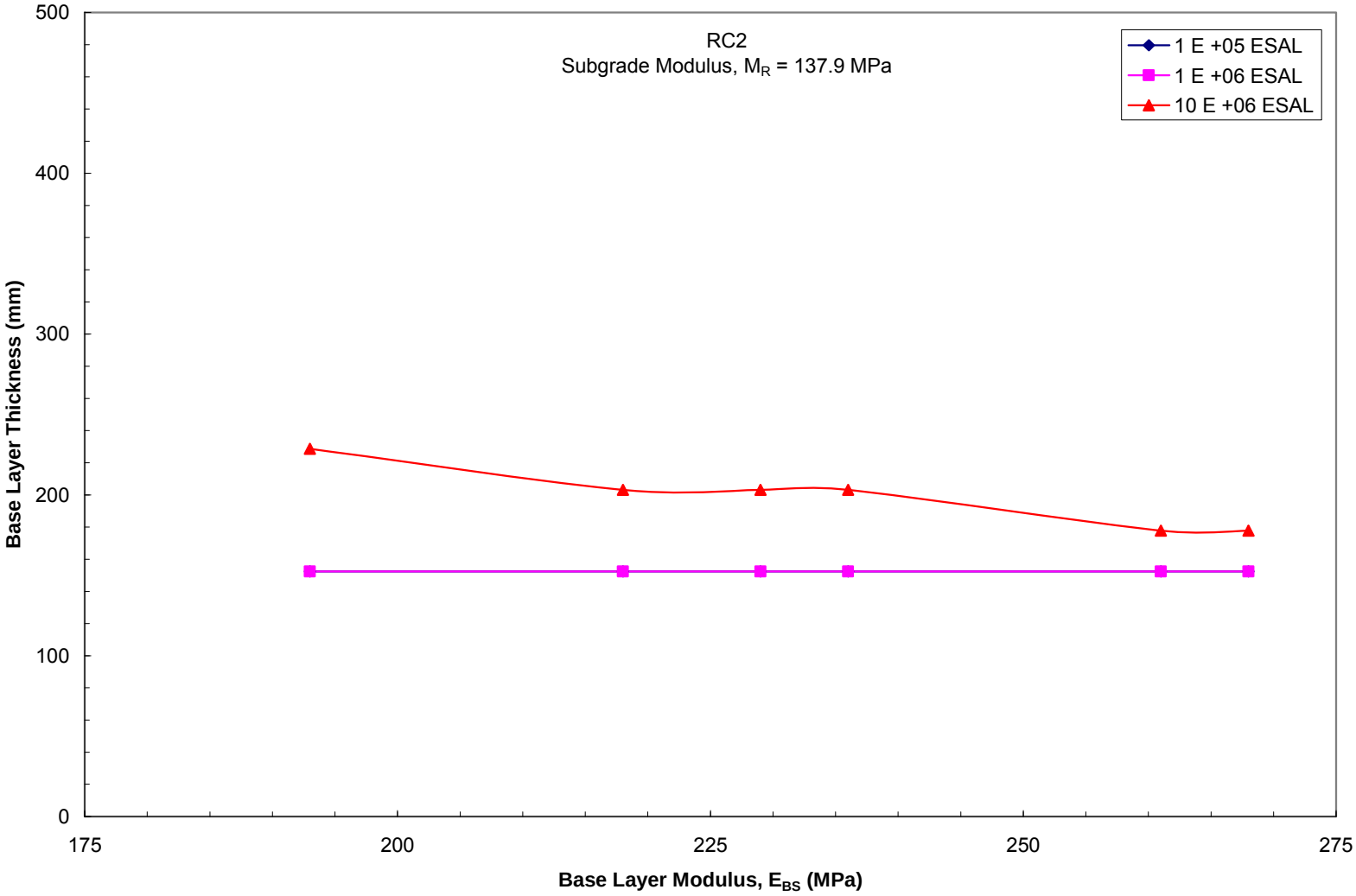


Figure 5.18 Design chart for determining thickness of base layer for city roads using recycled concrete aggregate RC2

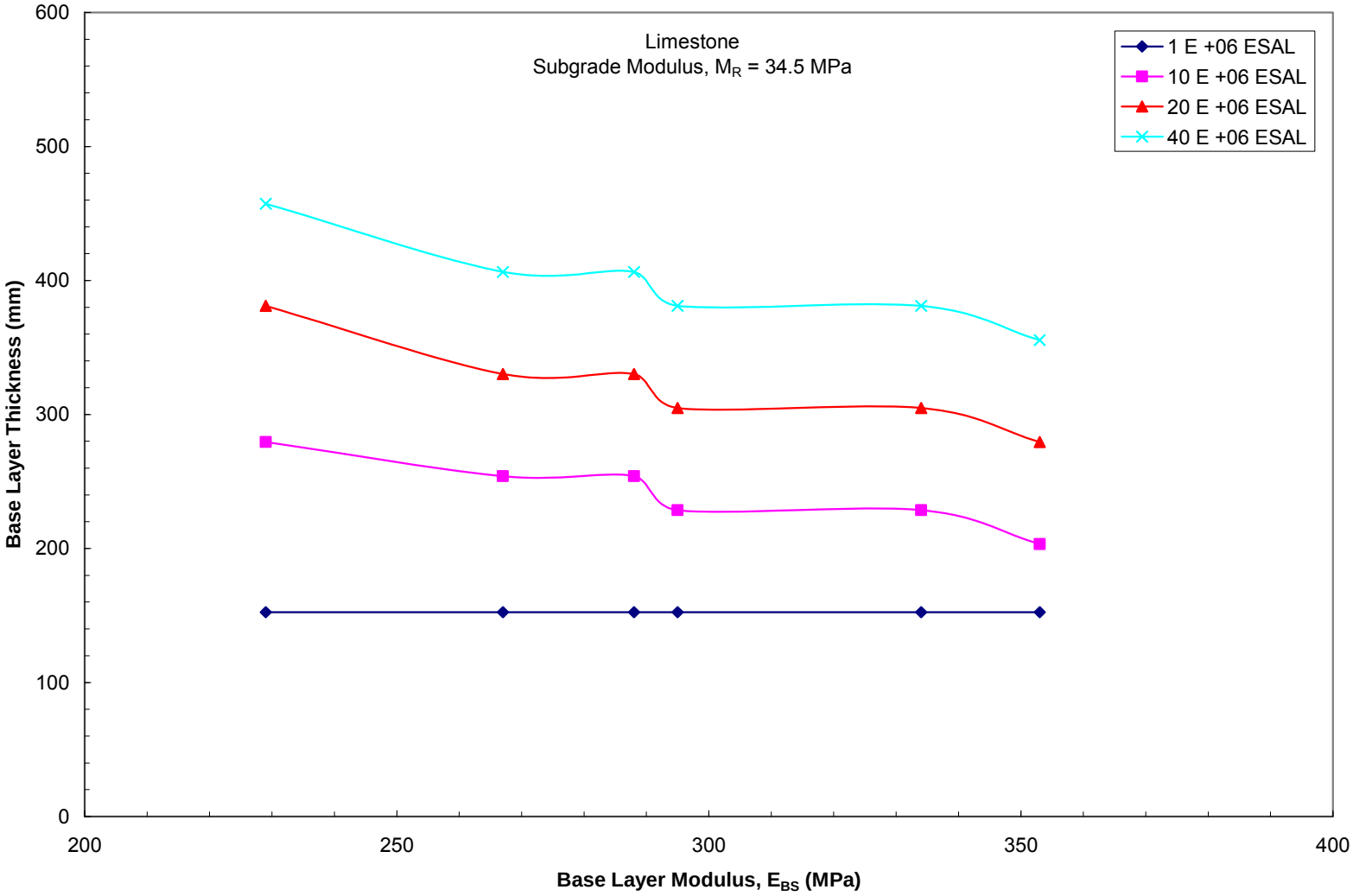


Figure 5.19 Design chart for determining thickness of base layer for interstates using limestone aggregate

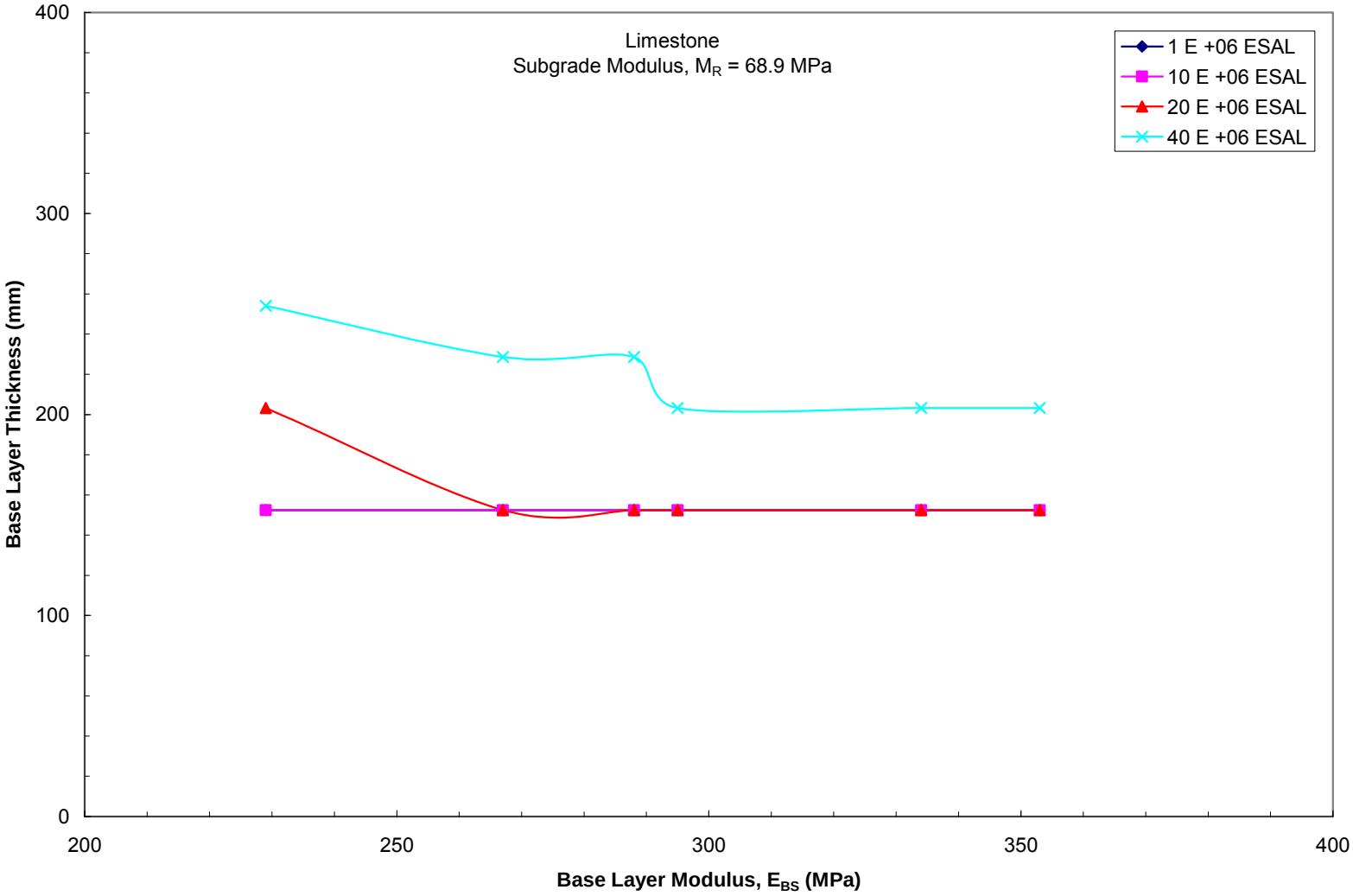


Figure 5.20 Design chart for determining thickness of base layer for interstates using limestone aggregate

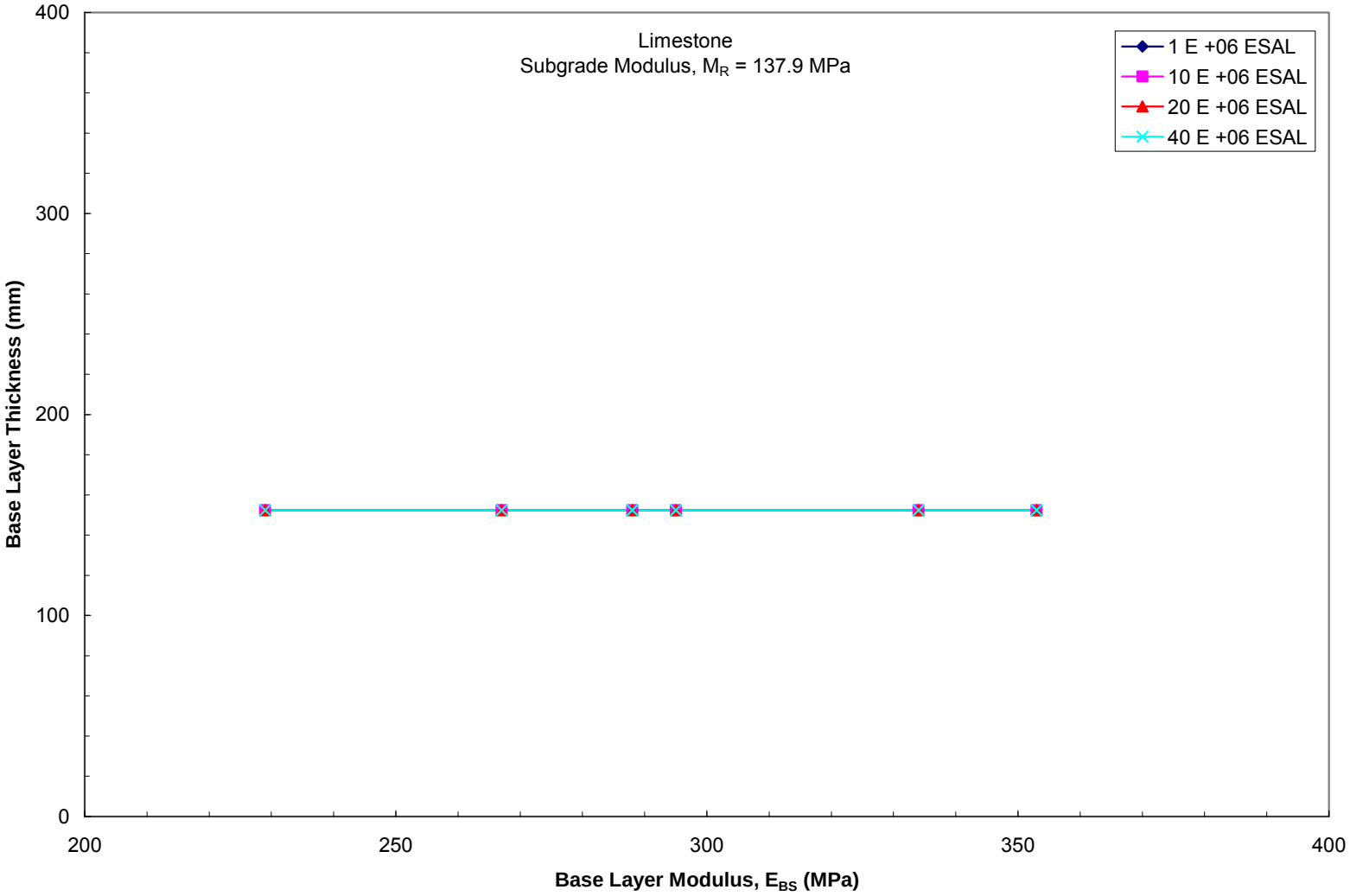


Figure 5.21 Design chart for determining thickness of base layer for interstates using limestone aggregate

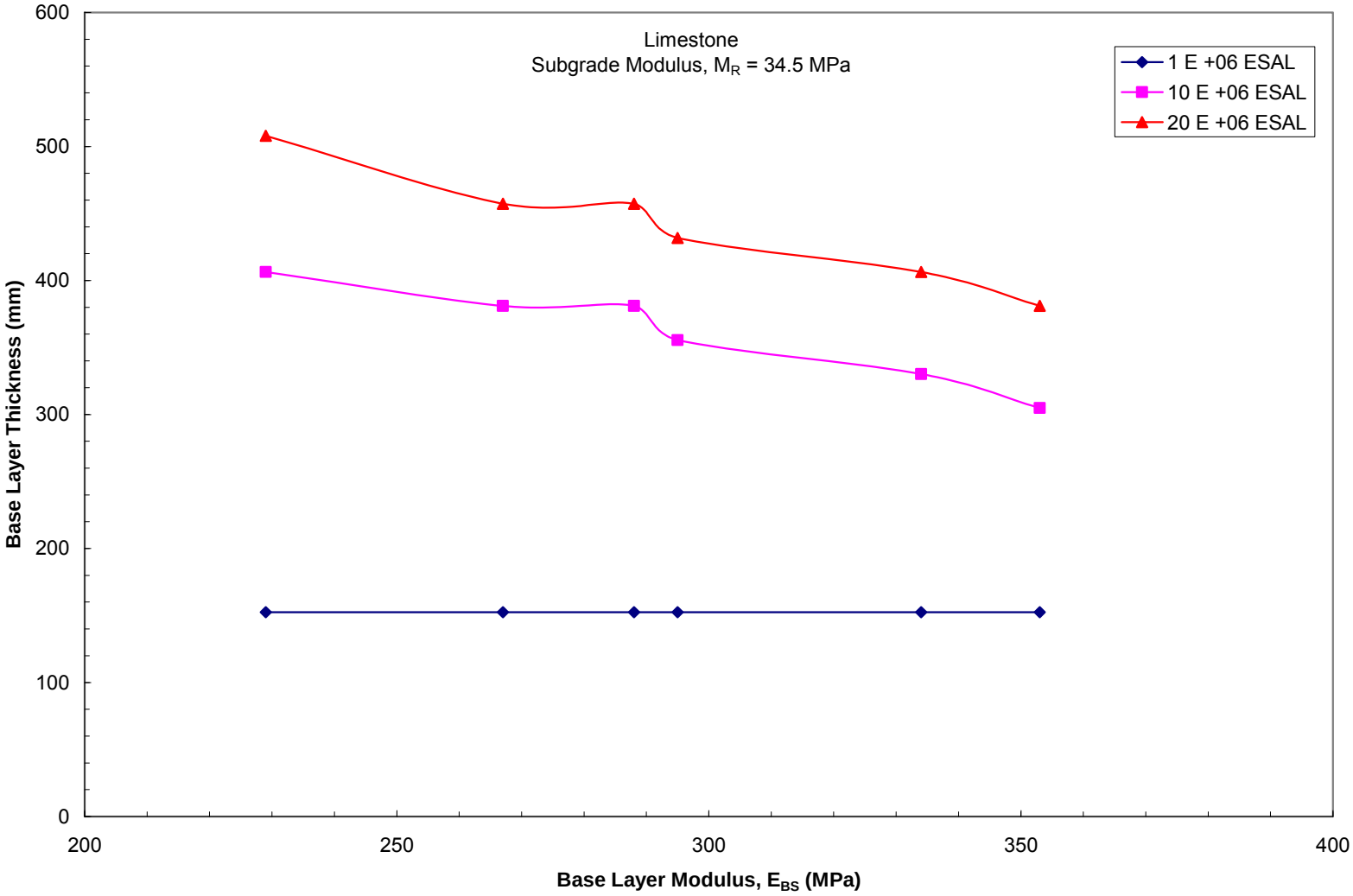


Figure 5.22 Design chart for determining thickness of base layer for state highways using limestone aggregate

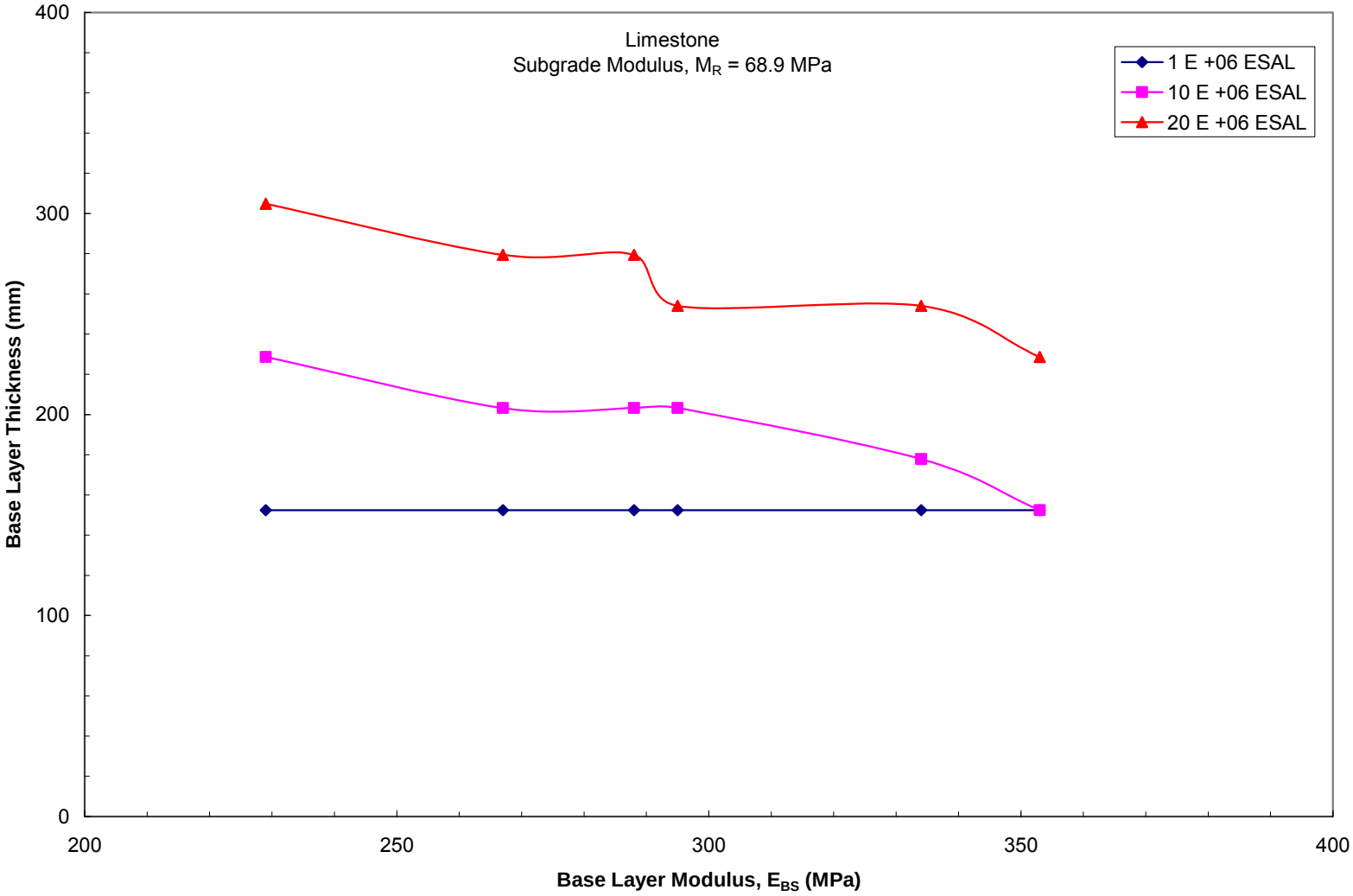


Figure 5.23 Design chart for determining thickness of base layer for state highways using limestone aggregate

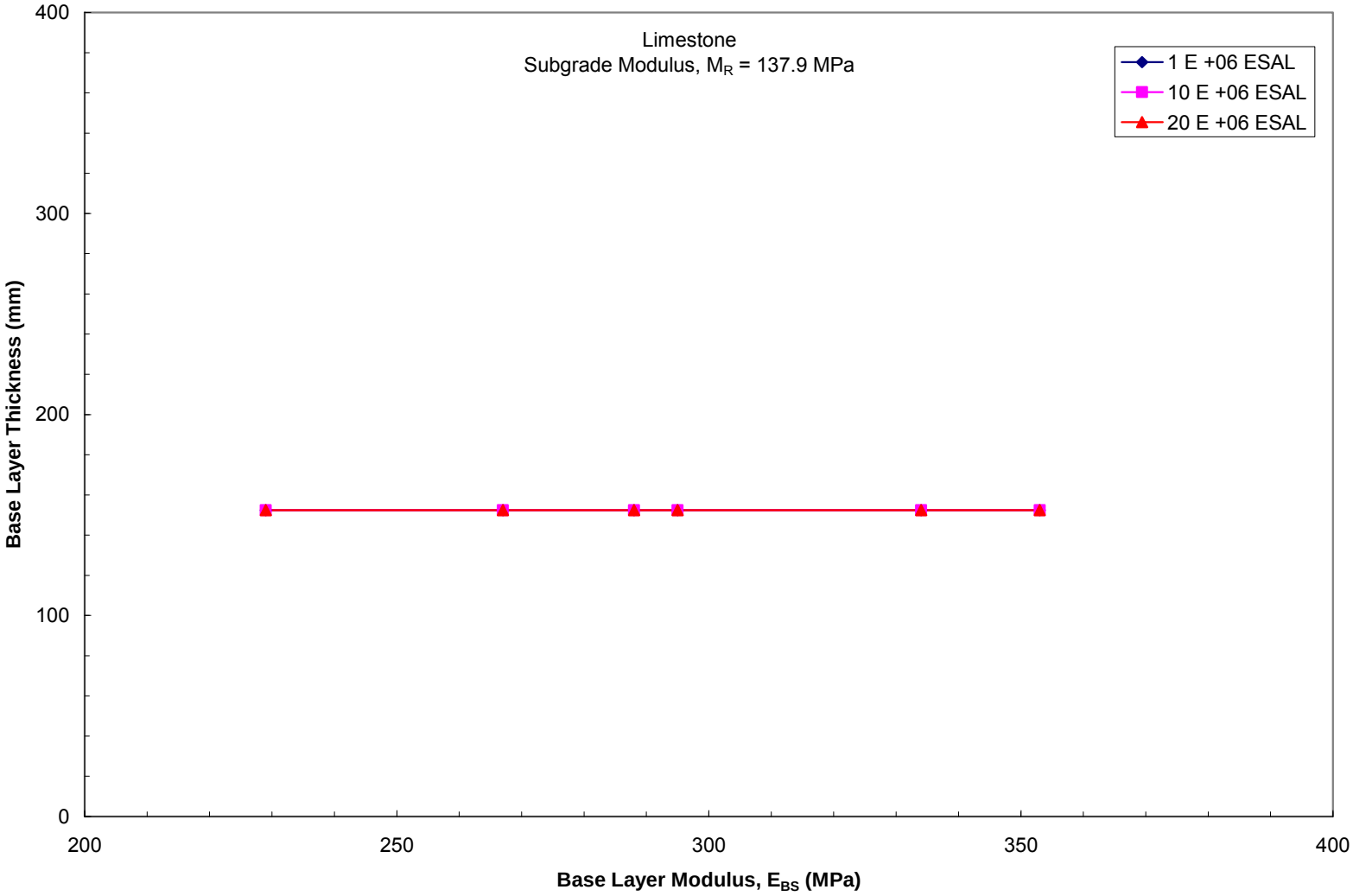


Figure 5.24 Design chart for determining thickness of base layer for state highways using limestone aggregate

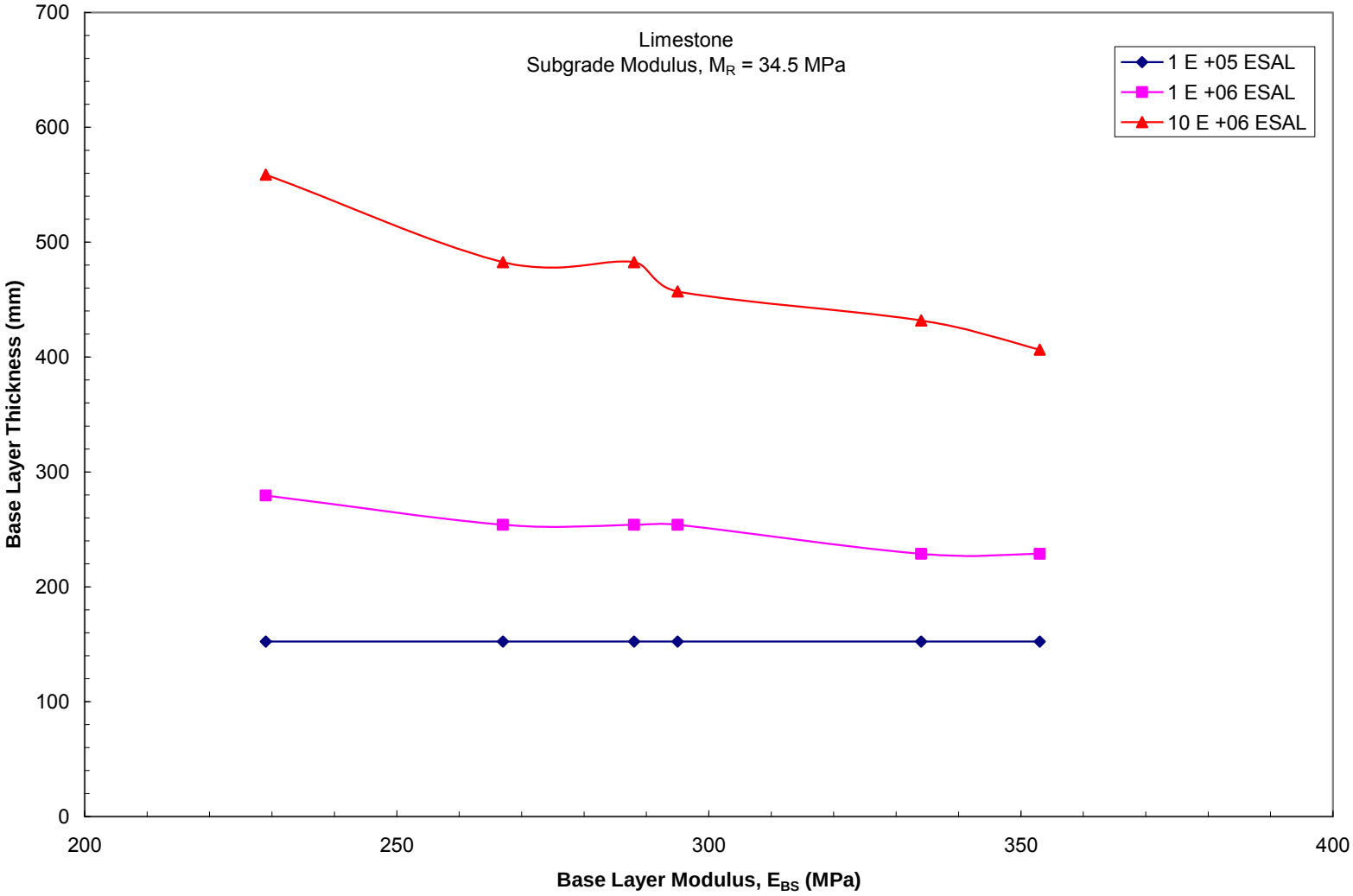


Figure 5.25 Design chart for determining thickness of base layer for city roads using limestone aggregate

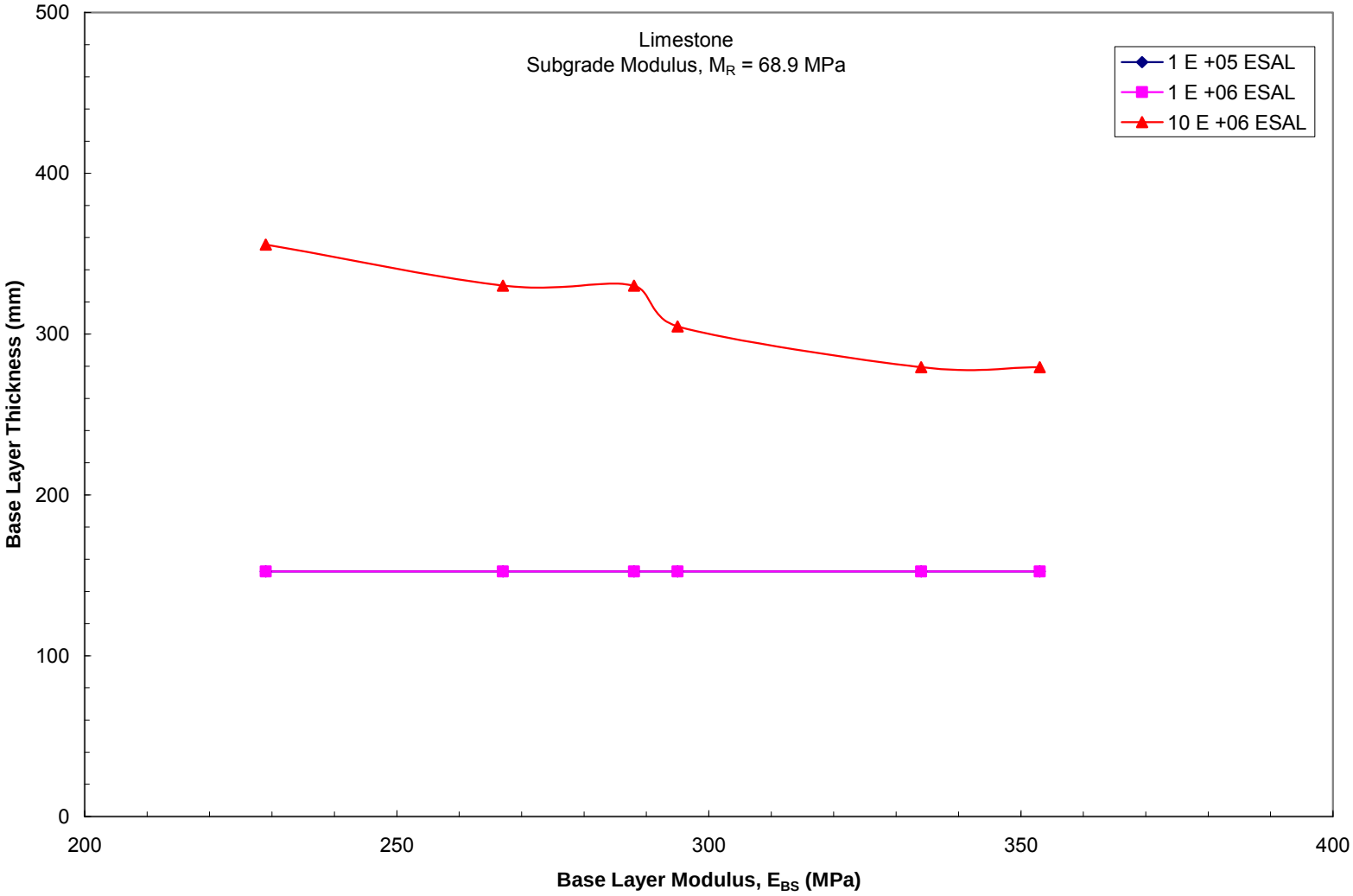


Figure 5.26 Design chart for determining thickness of base layer for city roads using limestone aggregate

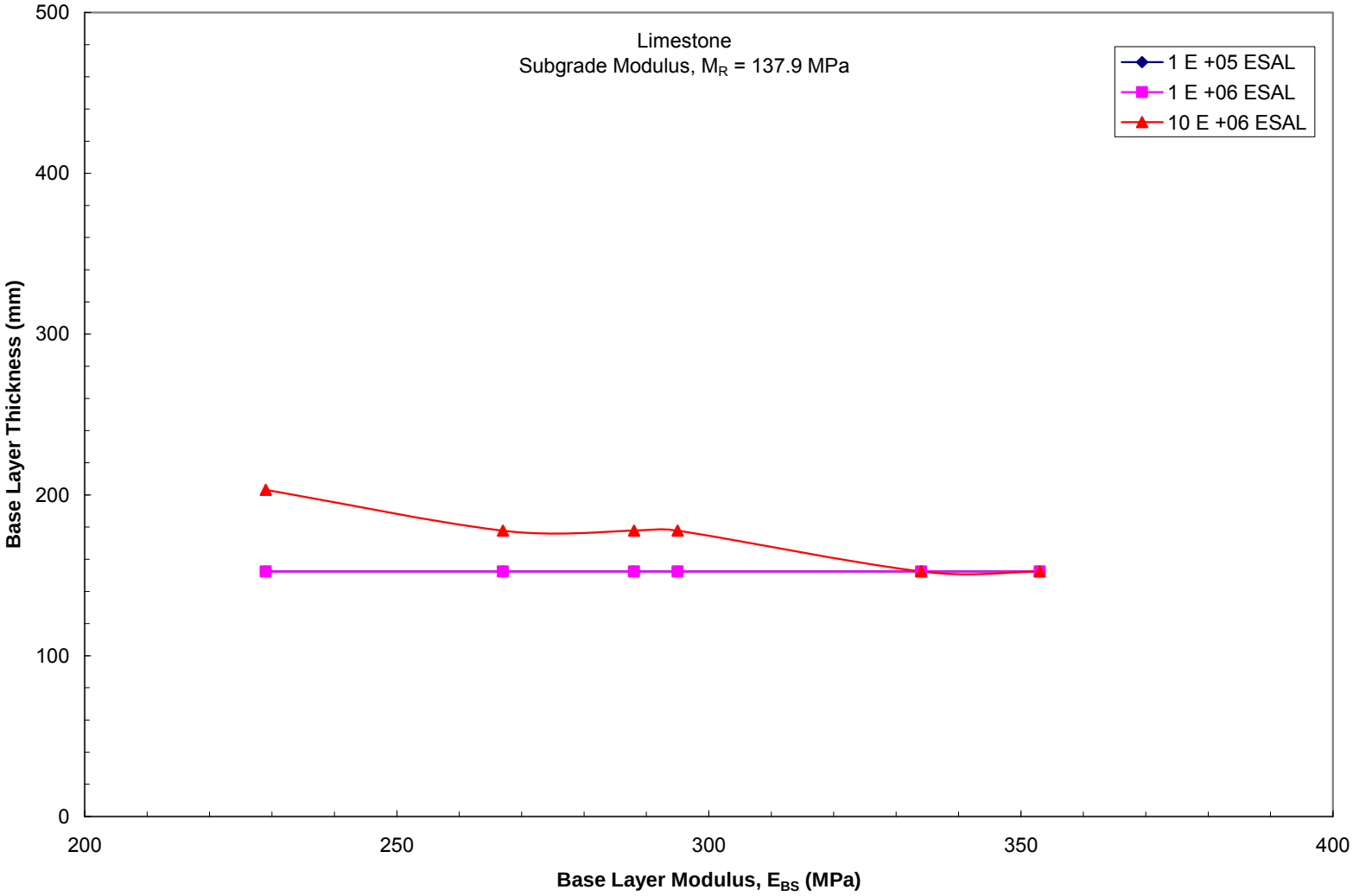


Figure 5.27 Design chart for determining thickness of base layer for city roads using limestone aggregate

The flexible pavement tables and charts developed correspond to the traffic and materials conditions provided on Tables 5.4 and 5.5. Further design analysis can be conducted by varying the design condition for the traffic conditions and material properties. For use of the recycled aggregates and limestone aggregates used in this research, the provided moduli should be used for the base layer materials.

## 5.4 Flexible Pavement Design Comparisons

A comparison of the flexible design was conducted to determine the effects of the base moduli on the base layer thickness. The comparison was based on the average structural coefficients determined for the materials provided on Table 5.1, 5.2, and 5.3. As previously mentioned, the average structural coefficients for the aggregates were 0.15, 0.15, and 0.18 for RC1, RC2, and limestone, respectively.

The comparisons show that the required base layer thickness for recycled aggregates is larger when compared to the limestone aggregate in poor subgrade conditions and in high traffic volume conditions. However, the interstate conditions show a smaller difference in required thickness between the recycled aggregates and the limestone aggregates. This is mainly due to the larger thickness of the overlaying asphalt course.

This comparison provides significant information for a pavement designer. It shows that certain design criteria must be reviewed to provide adequate comparison on the use of recycled aggregates. A flexible pavement designer must consider subgrade conditions, traffic volumes, asphalt thickness, and aggregate costs to determine the most efficient aggregate to use in the pavement structure. Figures 5.28 through 5.36 show the comparison of the required base layer thickness for recycled aggregates and limestone aggregates for varying subgrade conditions under interstate, highway, and city traffic conditions.

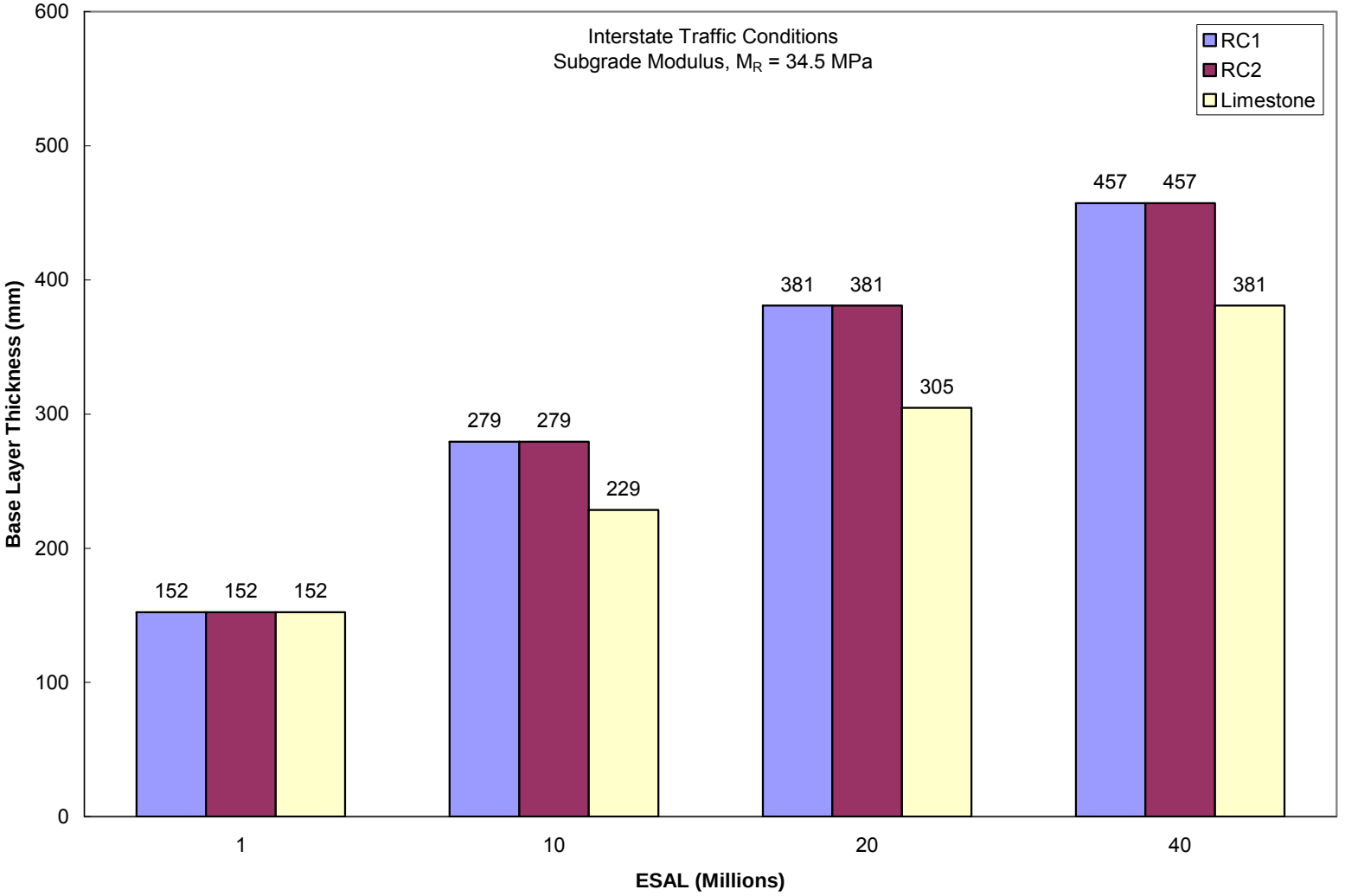


Figure 5.28 Comparison of base layer between recycled aggregates and limestone aggregates for interstate traffic conditions

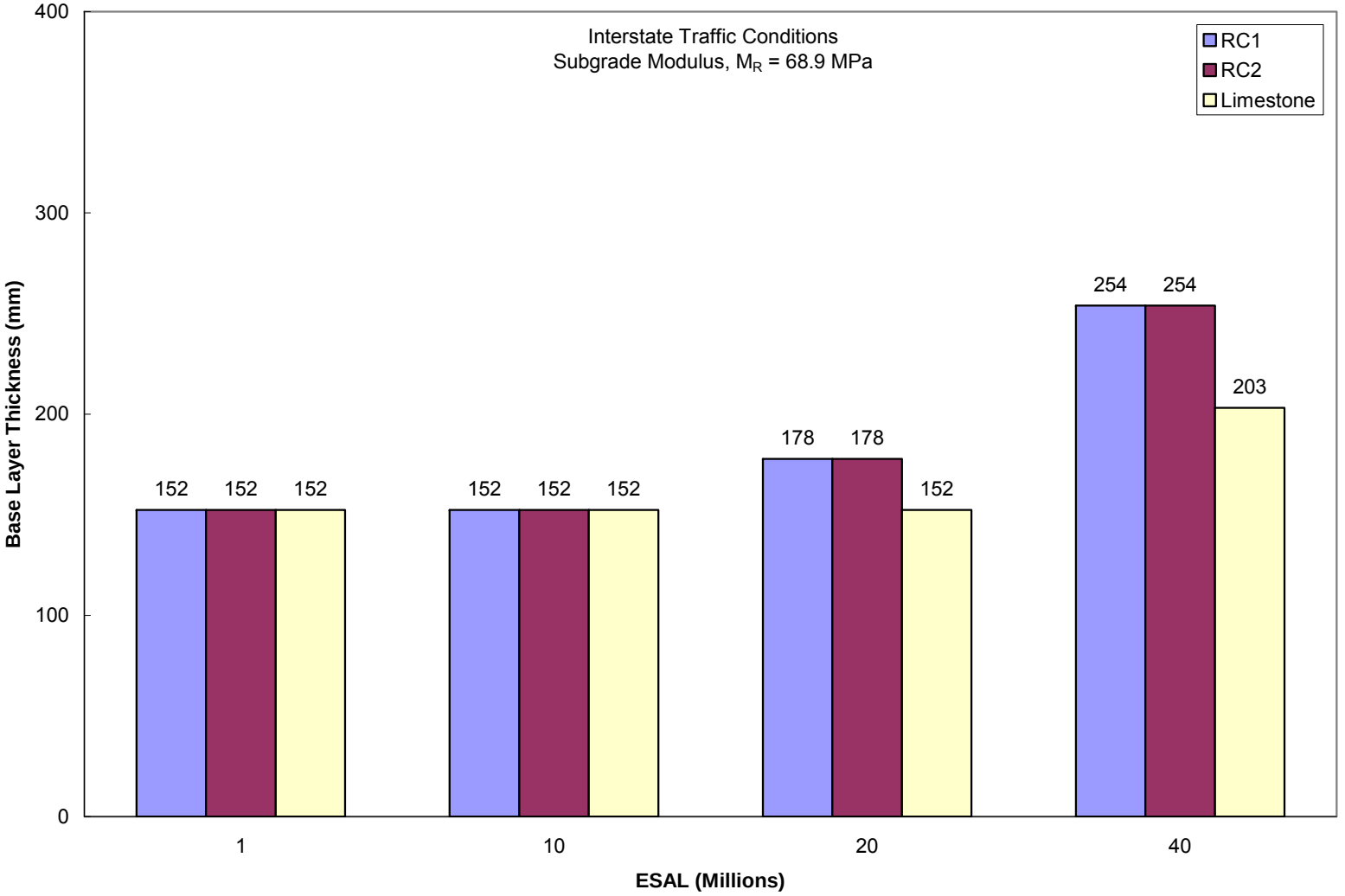


Figure 5.29 Comparison of base layer thickness between recycled aggregates and limestone aggregates for interstate traffic conditions

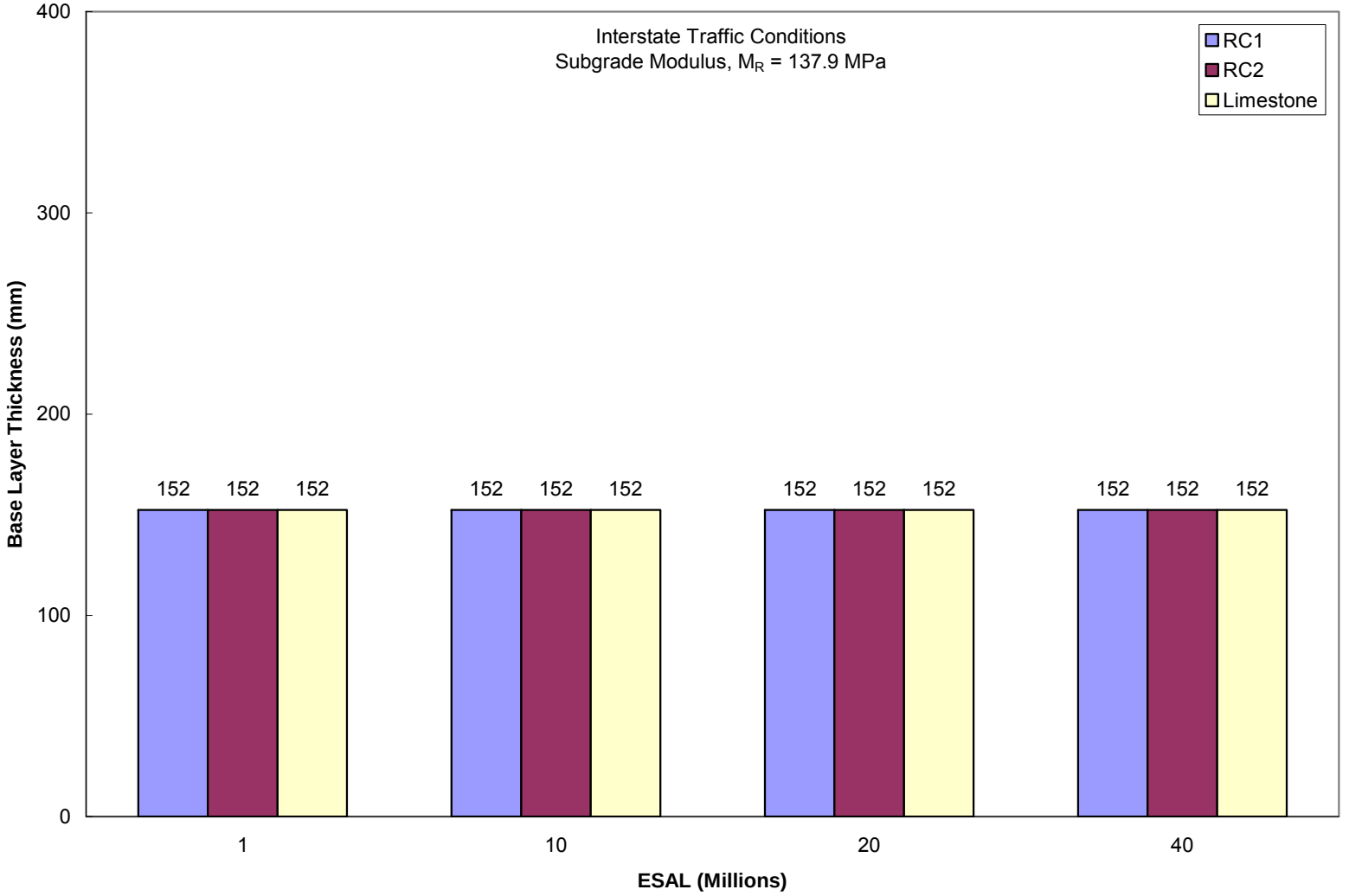


Figure 5.30 Comparison of base layer thickness between recycled aggregates and limestone aggregates for interstate traffic conditions

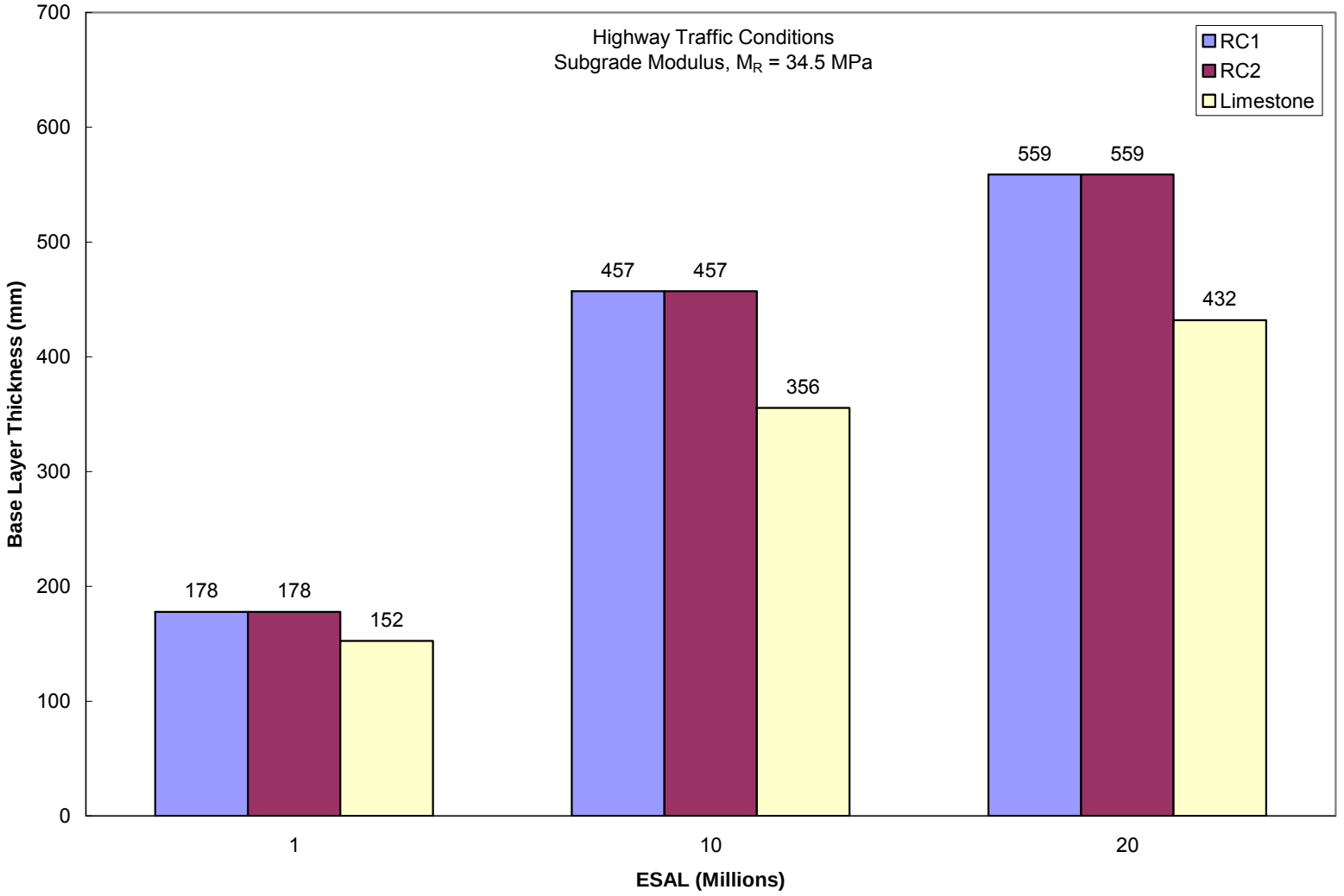


Figure 5.31 Comparison of base layer thickness between recycled aggregates and limestone aggregates for highway traffic conditions

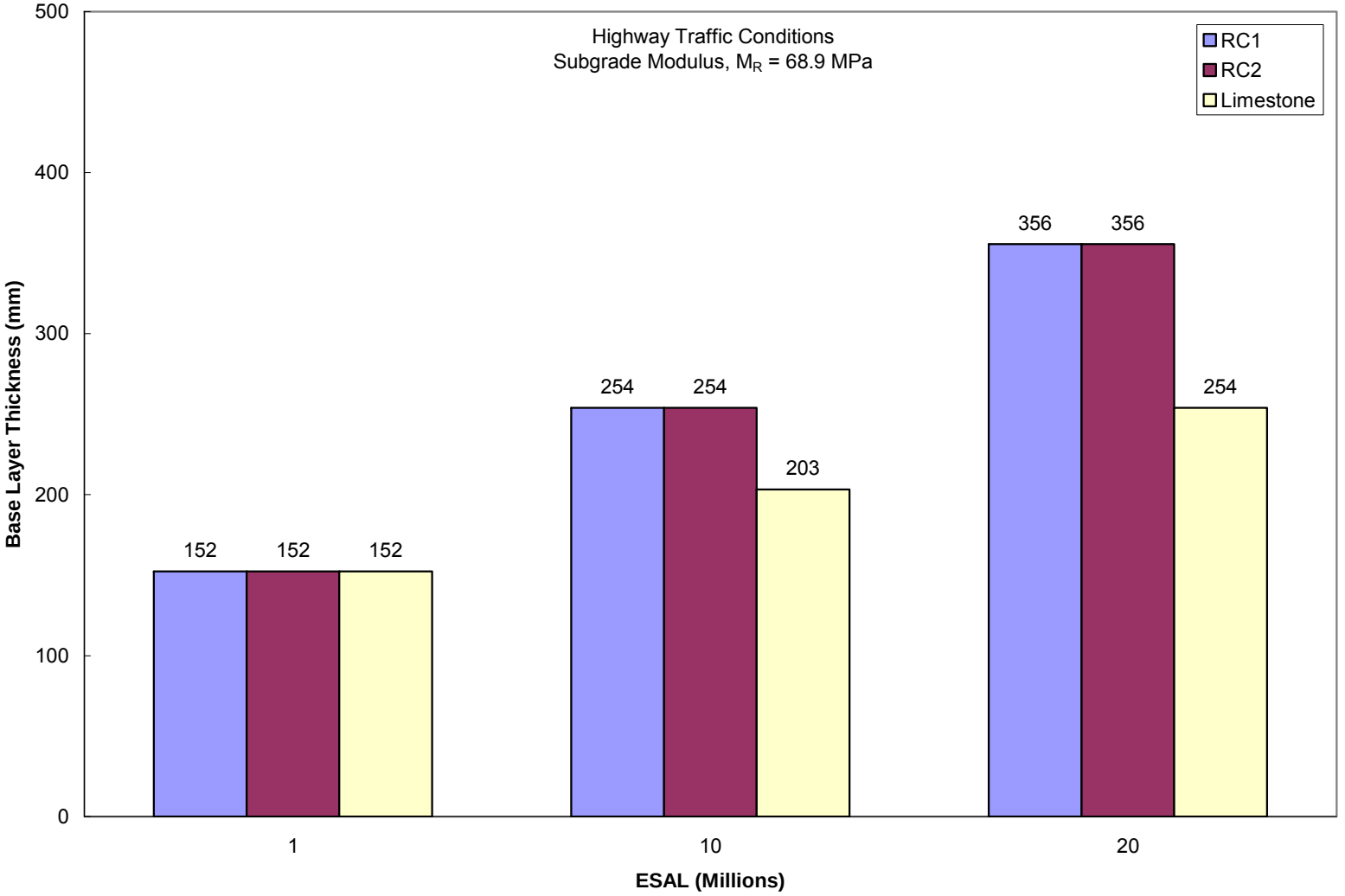


Figure 5.32 Comparison of base layer thickness between recycled aggregates and limestone aggregates for highway traffic conditions

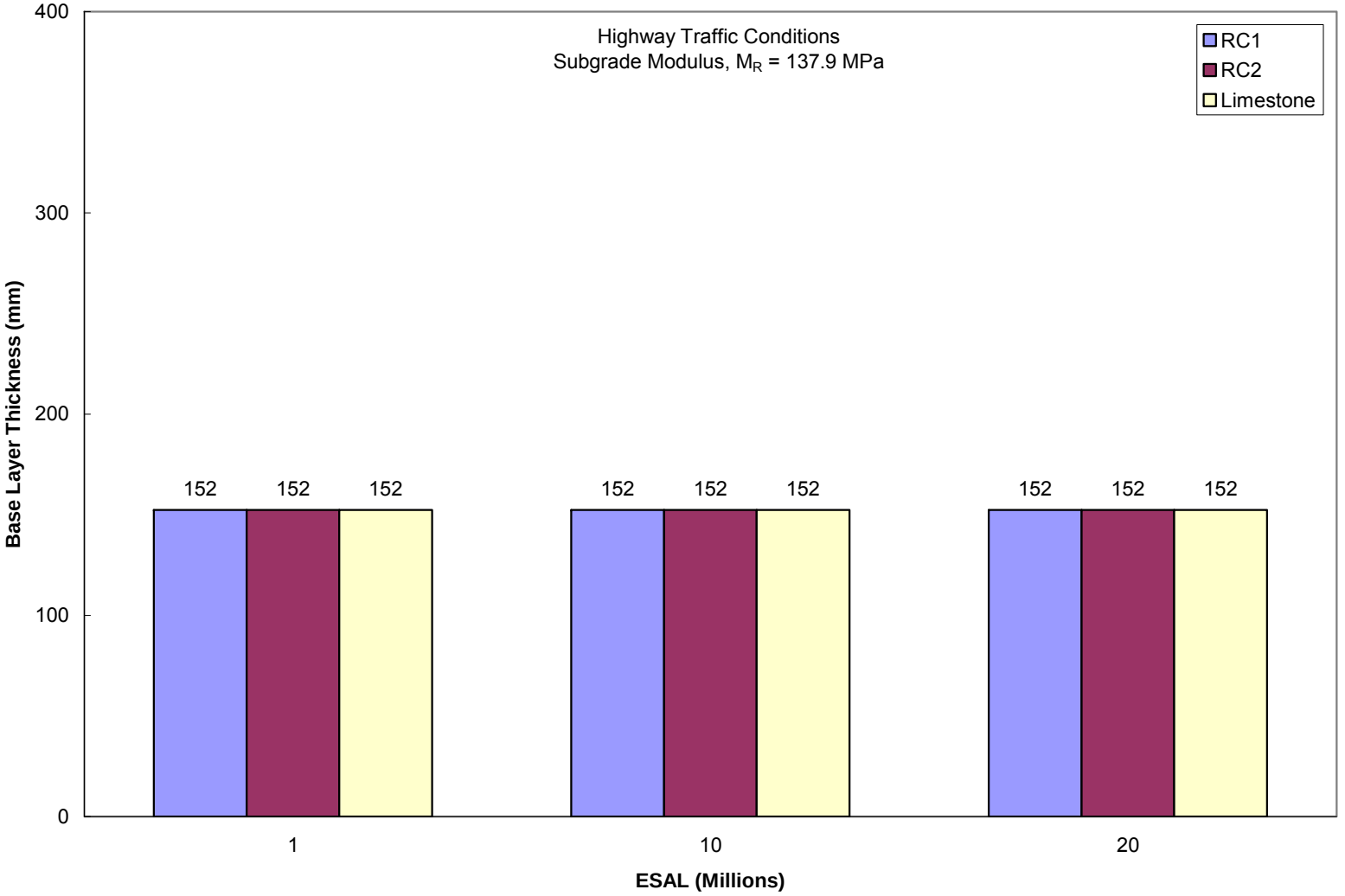


Figure 5.33 Comparison of base layer thickness between recycled aggregates and limestone aggregates for highway traffic conditions

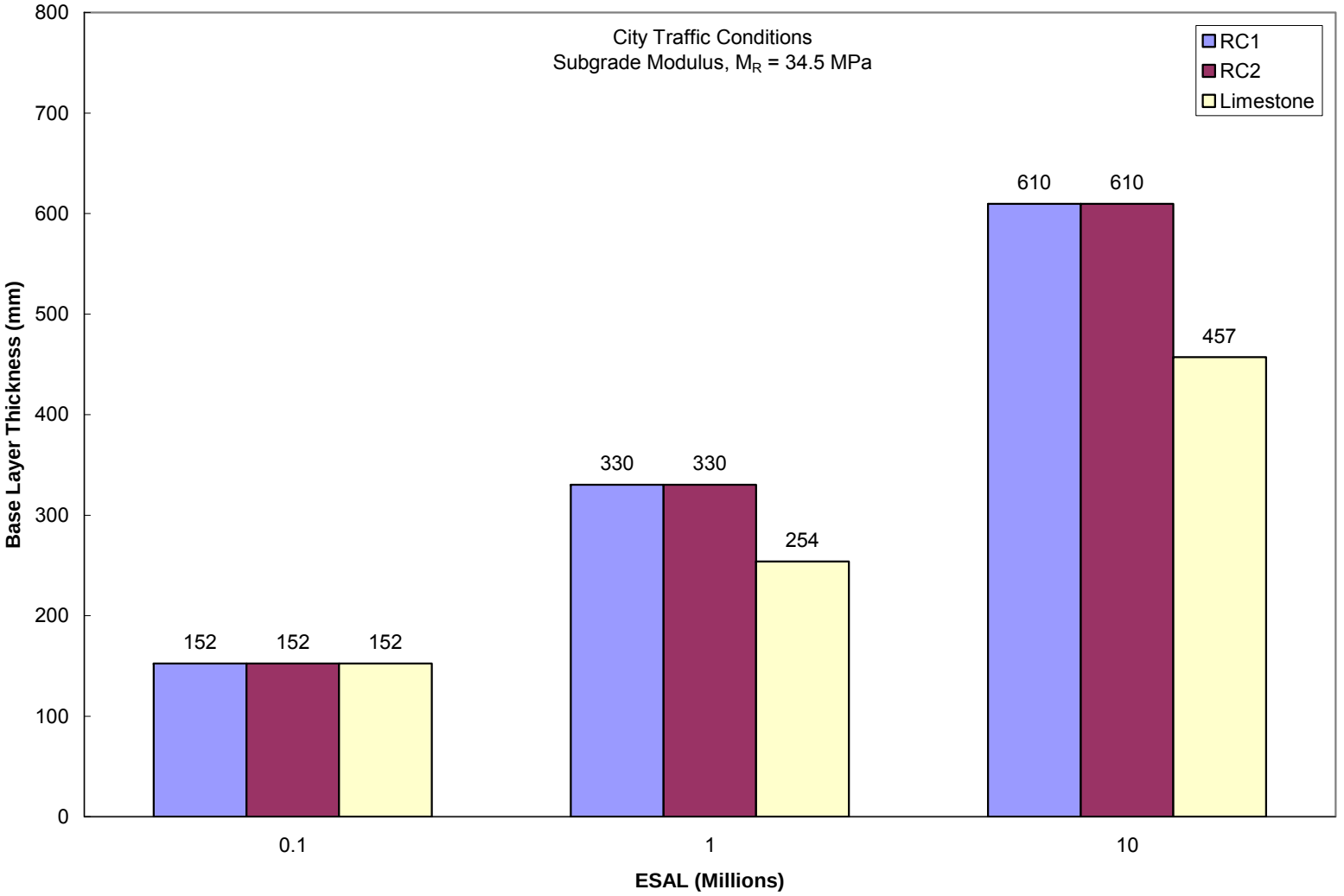


Figure 5.34 Comparison of base layer thickness between recycled aggregates and limestone aggregates for city traffic conditions

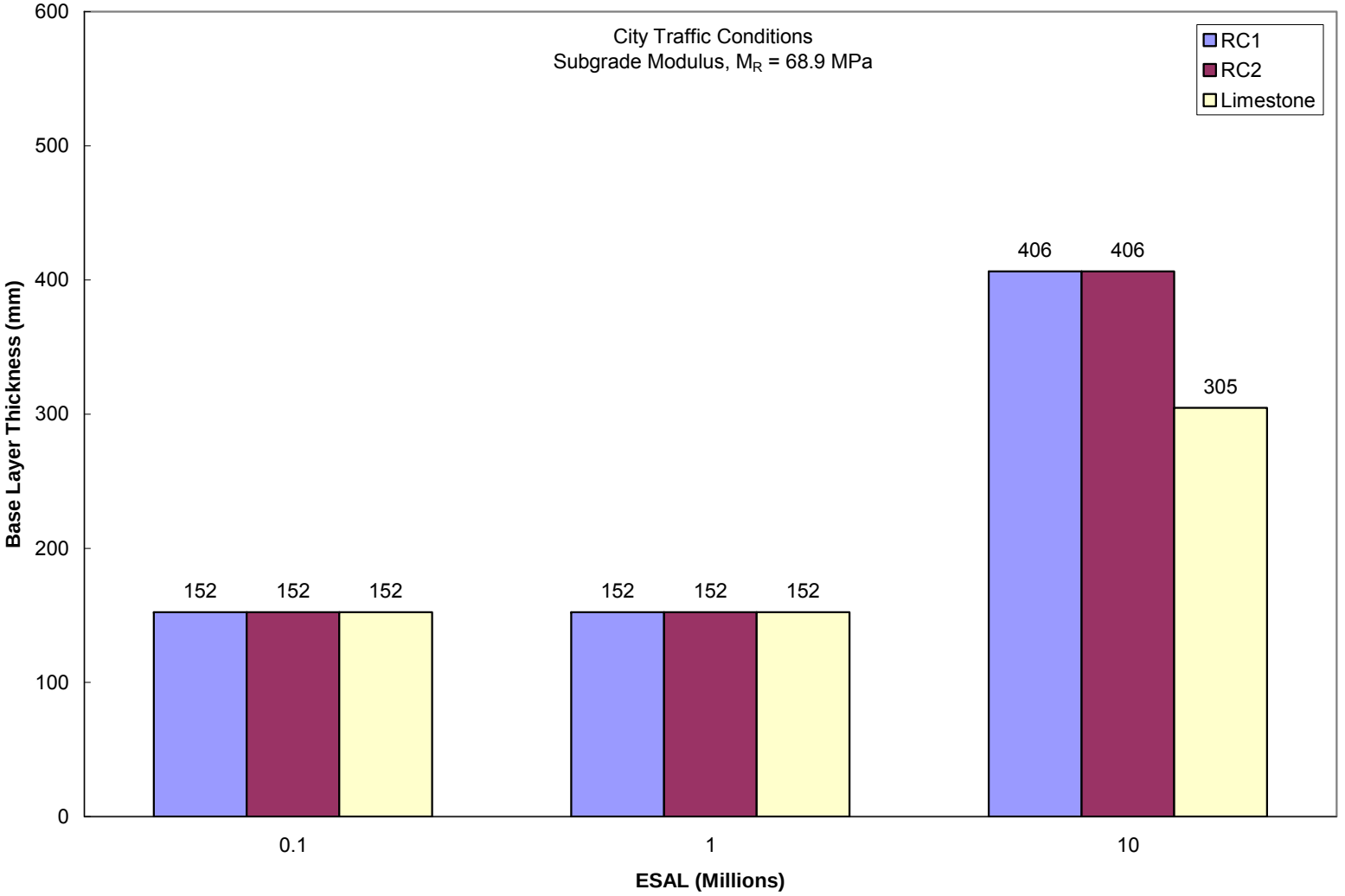


Figure 5.35 Comparison of base layer thickness between recycled aggregates and limestone aggregates for city traffic conditions

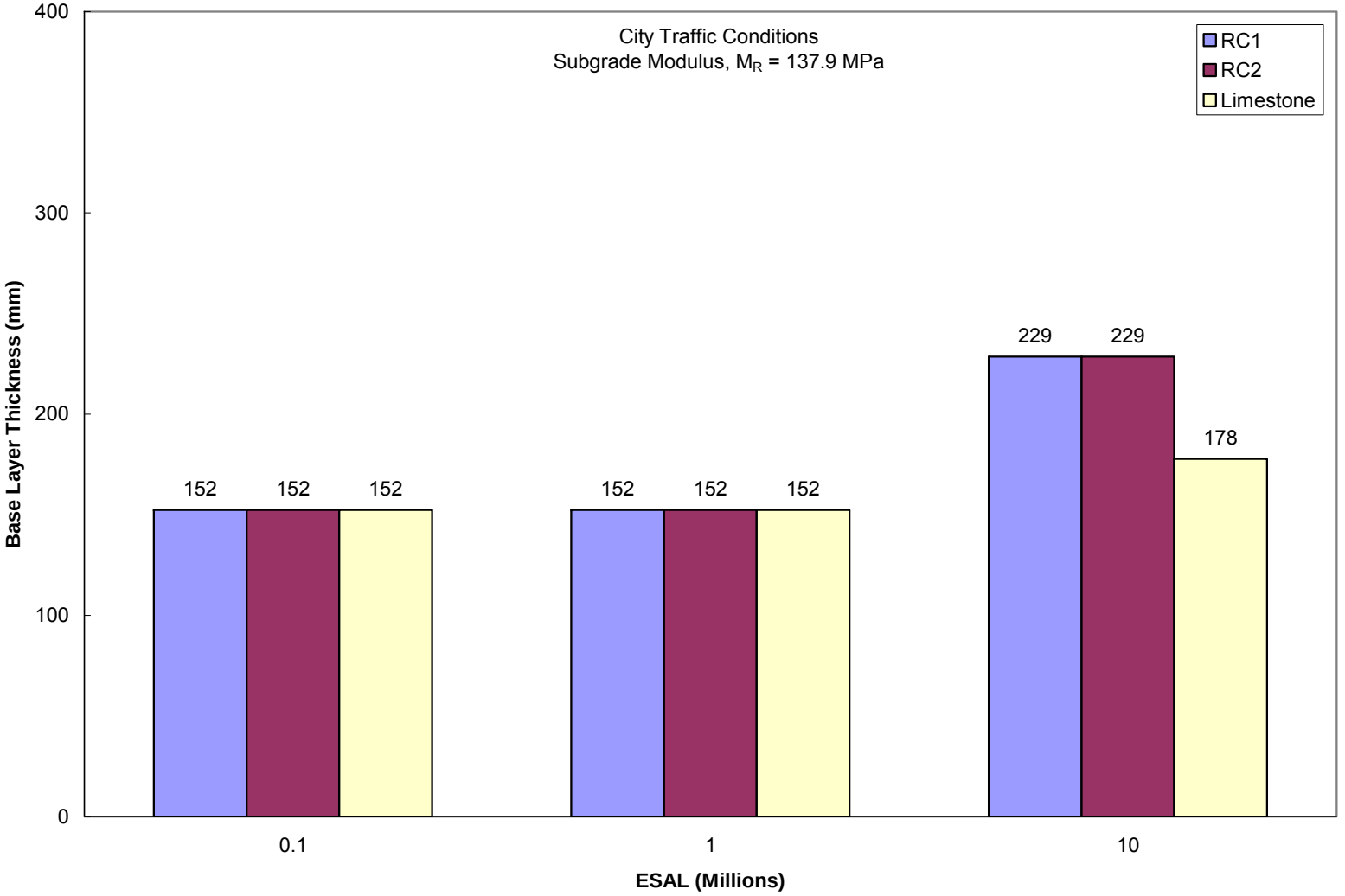


Figure 5.36 Comparison of base layer thickness between recycled aggregates and limestone aggregates for city traffic conditions

## 5.5 Rigid Pavement Design

The rigid pavement design requires that an effective modulus of subgrade reaction ($k_{eff}$) is determined for the support of the rigid pavement. The effective modulus of subgrade is affected by the material conditions of the subgrade and base or subbase layers. AASHTO (1993) describes the determination of the effective modulus of subgrade due to the affects of the material types, material layer thickness, and loss of support.

In the design analysis of rigid pavement, the continuously reinforced concrete pavement (CRCP) was assumed to have tied concrete shoulders. The modulus of subgrade reaction (k) used was varied from 50 to 200 psi/in. The modulus of elasticity determined for the recycled aggregates and limestone aggregate in the study were used as values for the base material. The climatic properties used are those provided in the Rigid Pavement Design Software for the Dallas, Texas area. The modulus of rupture for the slab, elastic modulus for concrete, and poisson's ratio for concrete were constant values used in the determination of the rigid pavement thickness. The slab-base friction factor was chosen to be high for all base materials. The reliability, standard deviation, initial serviceability, and terminal serviceability were also kept constant in the determination of the rigid pavement thickness. The loadings for volume of traffic used are for the interstate, state highways, and city roads conditions. These loads are 1, 5, 10, 20, and 40 million ESAL's. The traffic and material variables used in the analysis are summarized in tables 5.15 and 5.16.

Table 5.15 Traffic Variables for Type of Highway System

| Variable Type | Interstate Highway | State Highway | City Road |
|---|---|---|---|
| ESAL's (in millions) | 1, 5,10, 20, and 40 | 1, 5, 10, 20, and 40 | 1, 5, 10, 20, and 40 |
| Reliability (%) | 95 | 95 | 95 |
| Standard Deviation | 0.35 | 0.35 | 0.35 |
| Initial Serviceability | 4.5 | 4.5 | 4.5 |
| Final Serviceability | 2.50 | 2.50 | 2.50 |

Table 5.16 Material Variables for Type of Highway System

| Variable Type | Interstate Highway | State Highway | City Road |
|---|---|---|---|
| Concrete | | | |
| Modulus of Rupture (MPa) | 4.14 | 4.14 | 4.14 |
| Elastic Modulus (GPa) | 34.47 | 34.47 | 34.47 |
| Poisson's Ratio | 0.15 | 0.15 | 0.15 |
| Slab-Base Friction Factor | 2.0 | 2.0 | 2.0 |
| Resilient Modulus of Subgrade (MPa/m) | 13.5, 27.1, and 54.3 | 13.5, 27.1, and 54.3 | 13.5, 27.1, and 54.3 |

For this study, Rigid Pavement Design Software obtained from FHWA was used to determine the thickness of the continuously reinforced concrete pavement (CRCP). The thickness of the concrete pavement was determined using each of the three test materials as a base course. Each base material was analyzed under each subgrade condition with varying traffic loading conditions. The results for the rigid pavement designs are provided in tables 5.17 through 5.25. The results from the analysis are used to develop design charts for determining the concrete pavement thickness using the recycled aggregates and limestone aggregates as

base course layers. The rigid pavement design charts are presented in figures 5.37 through 5.63.

From the results of the tables and design graphs, it can be seen that the use of the recycled aggregates produces similar results as those from the limestone aggregate. However, the use of aggregates as a base course in rigid pavement design does not produced significant changes to the required concrete pavement thickness. This is seen when the pavement thickness does not vary as the different thickness of base course is varied under similar traffic loading conditions. The base course affects only the effective modulus of subgrade. The modulus of subgrade is known to not have significant affects on the required thickness of concrete pavement.

Table 5.17 Design Table for Interstate Traffic Conditions with Recycled Concrete Aggregate RC1 as Base Material
CRCP Layer Thickness

| Base Moduli MPa | Base Layer Thickness (457 mm) | | | | | Base Layer Thickness (457 mm) | | | | | Base Layer Thickness (457 mm) | | | | |
|---|---|---|---|---|---|---|---|---|---|---|---|---|---|---|---|
| | Subgrade k-value, 13.5 MPa/m | | | | | Subgrade k-value, 27.1 MPa/m | | | | | Subgrade k-value, 54.3 MPa/m | | | | |
| | I | II | III | IV | V | I | II | III | IV | V | I | II | III | IV | V |
| 205 | 229 | 279 | 305 | 330 | 381 | 229 | 305 | 330 | 356 | 381 | 254 | 305 | 356 | 381 | 406 |
| 216 | 229 | 279 | 305 | 330 | 381 | 229 | 305 | 330 | 356 | 381 | 254 | 305 | 356 | 381 | 406 |
| 228 | 229 | 279 | 305 | 330 | 381 | 229 | 305 | 330 | 356 | 381 | 254 | 305 | 356 | 381 | 406 |
| 235 | 229 | 279 | 305 | 330 | 381 | 229 | 305 | 330 | 356 | 381 | 254 | 305 | 356 | 381 | 406 |
| 238 | 229 | 279 | 305 | 330 | 381 | 229 | 305 | 330 | 356 | 381 | 254 | 305 | 356 | 381 | 406 |
| 244 | 229 | 279 | 305 | 330 | 381 | 229 | 305 | 330 | 356 | 381 | 254 | 305 | 356 | 381 | 406 |

Note: I = ESAL of 1 E+06; II = ESAL of 5 E+06; III = ESAL of 10 E+06; IV = ESAL of 20 E+06; V = ESAL of 40 E+06; Reliability = 95%; Standard Deviation = 0.35; Initial Serviceability = 4.5; Terminal Serviceability = 2.5; Modulus of Rupture (Slab) = 4.14 MPa; Modulus of Elasticity (Concrete) = 34.47 GPa; Poisson's Ratio (Concrete) = 0.15



Table 5.18 Design Table for State Highway Traffic Conditions with Recycled Concrete Aggregate RC1 as Base Material
CRCP Layer Thickness

| Base Moduli MPa | Base Layer Thickness (305 mm) | | | | | Base Layer Thickness (305 mm) | | | | | Base Layer Thickness (305 mm) | | | | |
|---|---|---|---|---|---|---|---|---|---|---|---|---|---|---|---|
| | Subgrade k-value, 13.5 MPa/m | | | | | Subgrade k-value, 27.1 MPa/m | | | | | Subgrade k-value, 54.3 MPa/m | | | | |
| | I | II | III | IV | V | I | II | III | IV | V | I | II | III | IV | V |
| 205 | 229 | 279 | 305 | 356 | 381 | 229 | 305 | 330 | 356 | 406 | 254 | 305 | 356 | 381 | 406 |
| 216 | 229 | 279 | 305 | 356 | 381 | 229 | 305 | 330 | 356 | 406 | 254 | 305 | 356 | 381 | 406 |
| 228 | 229 | 279 | 305 | 356 | 381 | 229 | 305 | 330 | 356 | 406 | 254 | 305 | 356 | 381 | 406 |
| 235 | 229 | 279 | 305 | 356 | 381 | 229 | 305 | 330 | 356 | 381 | 254 | 305 | 356 | 381 | 406 |
| 238 | 229 | 279 | 305 | 356 | 381 | 229 | 305 | 330 | 356 | 381 | 254 | 305 | 356 | 381 | 406 |
| 244 | 229 | 279 | 305 | 356 | 381 | 229 | 305 | 330 | 356 | 381 | 254 | 305 | 356 | 381 | 406 |

Note: I = ESAL of 1 E+06; II = ESAL of 5 E+06; III = ESAL of 10 E+06; IV = ESAL of 20 E+06; V = ESAL of 40 E+06; Reliability = 95%; Standard Deviation = 0.35; Initial Serviceability = 4.5; Terminal Serviceability = 2.5; Modulus of Rupture (Slab) = 4.14 MPa; Modulus of Elasticity (Concrete) = 34.47 GPa; Poisson's Ratio (Concrete) = 0.15

Table 5.19 Design Table for City Road Traffic Conditions with Recycled Concrete Aggregate RC1 as Base Material
CRCP Layer Thickness

| Base Moduli MPa | Base Layer Thickness (152 mm) | | | | | Base Layer Thickness (152 mm) | | | | | Base Layer Thickness (152 mm) | | | | |
|---|---|---|---|---|---|---|---|---|---|---|---|---|---|---|---|
| | Subgrade k-value, 13.5 MPa/m | | | | | Subgrade k-value, 27.1 MPa/m | | | | | Subgrade k-value, 54.3 MPa/m | | | | |
| | I | II | III | IV | V | I | II | III | IV | V | I | II | III | IV | V |
| 205 | 229 | 305 | 330 | 356 | 381 | 229 | 305 | 330 | 356 | 406 | 254 | 305 | 356 | 381 | 406 |
| 216 | 229 | 305 | 330 | 356 | 381 | 229 | 305 | 330 | 356 | 406 | 254 | 305 | 356 | 381 | 406 |
| 228 | 229 | 305 | 330 | 356 | 381 | 229 | 305 | 330 | 356 | 406 | 254 | 305 | 356 | 381 | 406 |
| 235 | 229 | 305 | 330 | 356 | 381 | 229 | 305 | 330 | 356 | 406 | 254 | 305 | 356 | 381 | 406 |
| 238 | 229 | 305 | 330 | 356 | 381 | 229 | 305 | 330 | 356 | 406 | 254 | 305 | 356 | 381 | 406 |
| 244 | 229 | 305 | 330 | 356 | 381 | 229 | 305 | 330 | 356 | 406 | 254 | 305 | 356 | 381 | 406 |

Note: I = ESAL of 1 E+06; II = ESAL of 5 E+06; III = ESAL of 10 E+06; IV = ESAL of 20 E+06; V = ESAL of 40 E+06; Reliability = 95%; Standard Deviation = 0.35; Initial Serviceability = 4.5; Terminal Serviceability = 2.5; Modulus of Rupture (Slab) = 4.14 MPa; Modulus of Elasticity (Concrete) = 34.47 GPa; Poisson's Ratio (Concrete) = 0.15



Table 5.20 Design Table for Interstate Traffic Conditions with Recycled Concrete Aggregate RC2 as Base Material
CRCP Layer Thickness

| Base Moduli MPa | Base Layer Thickness (457 mm) | | | | | Base Layer Thickness (457 mm) | | | | | Base Layer Thickness (457 mm) | | | | |
|---|---|---|---|---|---|---|---|---|---|---|---|---|---|---|---|
| | Subgrade k-value, 13.5 MPa/m | | | | | Subgrade k-value, 27.1 MPa/m | | | | | Subgrade k-value, 54.3 MPa/m | | | | |
| | I | II | III | IV | V | I | II | III | IV | V | I | II | III | IV | V |
| 193 | 229 | 279 | 305 | 330 | 381 | 229 | 305 | 330 | 356 | 381 | 254 | 305 | 356 | 381 | 406 |
| 218 | 229 | 279 | 305 | 330 | 381 | 229 | 305 | 330 | 356 | 381 | 254 | 305 | 356 | 381 | 406 |
| 229 | 229 | 279 | 305 | 330 | 381 | 229 | 305 | 330 | 356 | 381 | 254 | 305 | 356 | 381 | 406 |
| 236 | 229 | 279 | 305 | 330 | 381 | 229 | 305 | 330 | 356 | 381 | 254 | 305 | 356 | 381 | 406 |
| 261 | 229 | 279 | 305 | 330 | 381 | 229 | 305 | 330 | 356 | 381 | 254 | 305 | 330 | 381 | 406 |
| 268 | 229 | 279 | 305 | 330 | 381 | 229 | 305 | 330 | 356 | 381 | 254 | 305 | 330 | 381 | 406 |

Note: I = ESAL of 1 E+06; II = ESAL of 5 E+06; III = ESAL of 10 E+06; IV = ESAL of 20 E+06; V = ESAL of 40 E+06; Reliability = 95%; Standard Deviation = 0.35; Initial Serviceability = 4.5; Terminal Serviceability = 2.5; Modulus of Rupture (Slab) = 4.14 MPa; Modulus of Elasticity (Concrete) = 34.47 GPa; Poisson's Ratio (Concrete) = 0.15

Table 5.21 Design Table for State Highway Traffic Conditions with Recycled Concrete Aggregate RC2 as Base Material
CRCP Layer Thickness

| Base Moduli MPa | Base Layer Thickness (305 mm) | | | | | Base Layer Thickness (305 mm) | | | | | Base Layer Thickness (305 mm) | | | | |
|---|---|---|---|---|---|---|---|---|---|---|---|---|---|---|---|
| | Subgrade k-value, 13.5 MPa/m | | | | | Subgrade k-value, 27.1 MPa/m | | | | | Subgrade k-value, 54.3 MPa/m | | | | |
| | I | II | III | IV | V | I | II | III | IV | V | I | II | III | IV | V |
| 193 | 229 | 279 | 305 | 356 | 381 | 229 | 305 | 330 | 356 | 406 | 254 | 305 | 356 | 381 | 406 |
| 218 | 229 | 279 | 305 | 356 | 381 | 229 | 305 | 330 | 356 | 406 | 254 | 305 | 356 | 381 | 406 |
| 229 | 229 | 279 | 305 | 356 | 381 | 229 | 305 | 330 | 356 | 406 | 254 | 305 | 356 | 381 | 406 |
| 236 | 229 | 279 | 305 | 356 | 381 | 229 | 305 | 330 | 356 | 381 | 254 | 305 | 356 | 381 | 406 |
| 261 | 229 | 279 | 305 | 330 | 381 | 229 | 305 | 330 | 356 | 381 | 254 | 305 | 356 | 381 | 406 |
| 268 | 229 | 279 | 305 | 330 | 381 | 229 | 305 | 330 | 356 | 381 | 254 | 305 | 356 | 381 | 406 |

Note: I = ESAL of 1 E+06; II = ESAL of 5 E+06; III = ESAL of 10 E+06; IV = ESAL of 20 E+06; V = ESAL of 40 E+06; Reliability = 95%; Standard Deviation = 0.35; Initial Serviceability = 4.5; Terminal Serviceability = 2.5; Modulus of Rupture (Slab) = 4.14 MPa; Modulus of Elasticity (Concrete) = 34.47 GPa; Poisson's Ratio (Concrete) = 0.15



Table 5.22 Design Table for City Road Traffic Conditions with Recycled Concrete Aggregate RC2 as Base Material
CRCP Layer Thickness

| Base Moduli MPa | Base Layer Thickness (152 mm) | | | | | Base Layer Thickness (152 mm) | | | | | Base Layer Thickness (152 mm) | | | | |
|---|---|---|---|---|---|---|---|---|---|---|---|---|---|---|---|
| | Subgrade k-value, 13.5 MPa/m | | | | | Subgrade k-value, 27.1 MPa/m | | | | | Subgrade k-value, 54.3 MPa/m | | | | |
| | I | II | III | IV | V | I | II | III | IV | V | I | II | III | IV | V |
| 193 | 229 | 305 | 330 | 356 | 381 | 229 | 305 | 330 | 356 | 406 | 254 | 305 | 356 | 381 | 406 |
| 218 | 229 | 305 | 330 | 356 | 381 | 229 | 305 | 330 | 356 | 406 | 254 | 305 | 356 | 381 | 406 |
| 229 | 229 | 305 | 330 | 356 | 381 | 229 | 305 | 330 | 356 | 406 | 254 | 305 | 356 | 381 | 406 |
| 236 | 229 | 305 | 330 | 356 | 381 | 229 | 305 | 330 | 356 | 406 | 254 | 305 | 356 | 381 | 406 |
| 261 | 229 | 279 | 330 | 356 | 381 | 229 | 305 | 330 | 356 | 406 | 254 | 305 | 356 | 381 | 406 |
| 268 | 229 | 279 | 330 | 356 | 381 | 229 | 305 | 330 | 356 | 406 | 254 | 305 | 356 | 381 | 406 |

Note: I = ESAL of 1 E+06; II = ESAL of 5 E+06; III = ESAL of 10 E+06; IV = ESAL of 20 E+06; V = ESAL of 40 E+06; Reliability = 95%; Standard Deviation = 0.35; Initial Serviceability = 4.5; Terminal Serviceability = 2.5; Modulus of Rupture (Slab) = 4.14 MPa; Modulus of Elasticity (Concrete) = 34.47 GPa; Poisson's Ratio (Concrete) = 0.15

Table 5.23 Design Table for Interstate Traffic Conditions with Limestone Aggregate as Base Material
CRCP Layer Thickness

| Base Moduli MPa | Base Layer Thickness (457 mm) | | | | | Base Layer Thickness (457 mm) | | | | | Base Layer Thickness (457 mm) | | | | |
|---|---|---|---|---|---|---|---|---|---|---|---|---|---|---|---|
| | Subgrade k-value, 13.5 MPa/m | | | | | Subgrade k-value, 27.1 MPa/m | | | | | Subgrade k-value, 54.3 MPa/m | | | | |
| | I | II | III | IV | V | I | II | III | IV | V | I | II | III | IV | V |
| 229 | 229 | 279 | 305 | 330 | 381 | 229 | 305 | 330 | 356 | 381 | 254 | 305 | 356 | 381 | 406 |
| 267 | 229 | 279 | 305 | 330 | 381 | 229 | 305 | 330 | 356 | 381 | 254 | 305 | 356 | 381 | 406 |
| 288 | 229 | 279 | 305 | 330 | 381 | 229 | 305 | 330 | 356 | 381 | 254 | 305 | 356 | 381 | 406 |
| 295 | 229 | 279 | 305 | 330 | 381 | 229 | 305 | 330 | 356 | 381 | 254 | 305 | 356 | 381 | 406 |
| 334 | 229 | 279 | 305 | 330 | 356 | 229 | 305 | 330 | 356 | 381 | 254 | 305 | 356 | 381 | 406 |
| 353 | 229 | 279 | 305 | 330 | 356 | 229 | 305 | 330 | 356 | 381 | 254 | 305 | 356 | 381 | 406 |

Note: I = ESAL of 1 E+06; II = ESAL of 5 E+06; III = ESAL of 10 E+06; IV = ESAL of 20 E+06; V = ESAL of 40 E+06; Reliability = 95%; Standard Deviation = 0.35; Initial Serviceability = 4.5; Terminal Serviceability = 2.5; Modulus of Rupture (Slab) = 4.14 MPa; Modulus of Elasticity (Concrete) = 34.47 GPa; Poisson's Ratio (Concrete) = 0.15



Table 5.24 Design Table for State Highway Traffic Conditions with Limestone Aggregate as Base Material
CRCP Layer Thickness

| Base Moduli MPa | Base Layer Thickness (305 mm) | | | | | Base Layer Thickness (305 mm) | | | | | Base Layer Thickness (305 mm) | | | | |
|---|---|---|---|---|---|---|---|---|---|---|---|---|---|---|---|
| | Subgrade k-value, 13.5 MPa/m | | | | | Subgrade k-value, 27.1 MPa/m | | | | | Subgrade k-value, 54.3 MPa/m | | | | |
| | I | II | III | IV | V | I | II | III | IV | V | I | II | III | IV | V |
| 229 | 229 | 279 | 305 | 356 | 381 | 229 | 305 | 330 | 356 | 406 | 254 | 305 | 356 | 381 | 406 |
| 267 | 229 | 279 | 305 | 330 | 381 | 229 | 305 | 330 | 356 | 381 | 254 | 305 | 356 | 381 | 406 |
| 288 | 229 | 279 | 305 | 330 | 381 | 229 | 305 | 330 | 356 | 381 | 254 | 305 | 356 | 381 | 406 |
| 295 | 229 | 279 | 305 | 330 | 381 | 229 | 305 | 330 | 356 | 381 | 254 | 305 | 356 | 381 | 406 |
| 334 | 229 | 279 | 305 | 330 | 381 | 229 | 305 | 330 | 356 | 381 | 254 | 305 | 356 | 381 | 406 |
| 353 | 229 | 279 | 305 | 330 | 381 | 229 | 305 | 330 | 356 | 381 | 254 | 305 | 356 | 381 | 406 |

Note: I = ESAL of 1 E+06; II = ESAL of 5 E+06; III = ESAL of 10 E+06; IV = ESAL of 20 E+06; V = ESAL of 40 E+06; Reliability = 95%; Standard Deviation = 0.35; Initial Serviceability = 4.5; Terminal Serviceability = 2.5; Modulus of Rupture (Slab) = 4.14 MPa; Modulus of Elasticity (Concrete) = 34.47 GPa; Poisson's Ratio (Concrete) = 0.15

Table 5.25 Design Table for City Road Traffic Conditions with Limestone Aggregate as Base Material
CRCP Layer Thickness

| Base Moduli MPa | Base Layer Thickness (152 mm) | | | | | Base Layer Thickness (152 mm) | | | | | Base Layer Thickness (152 mm) | | | | |
|---|---|---|---|---|---|---|---|---|---|---|---|---|---|---|---|
| | Subgrade k-value, 13.5 MPa/m | | | | | Subgrade k-value, 27.1 MPa/m | | | | | Subgrade k-value, 54.3 MPa/m | | | | |
| | I | II | III | IV | V | I | II | III | IV | V | I | II | III | IV | V |
| 229 | 229 | 305 | 330 | 356 | 381 | 229 | 305 | 330 | 356 | 406 | 254 | 305 | 356 | 381 | 406 |
| 267 | 229 | 279 | 330 | 356 | 381 | 229 | 305 | 330 | 356 | 406 | 254 | 305 | 356 | 381 | 406 |
| 288 | 229 | 279 | 330 | 356 | 381 | 229 | 305 | 330 | 356 | 406 | 254 | 305 | 356 | 381 | 406 |
| 295 | 229 | 279 | 330 | 356 | 381 | 229 | 305 | 330 | 356 | 406 | 254 | 305 | 356 | 381 | 406 |
| 334 | 229 | 279 | 305 | 356 | 381 | 229 | 305 | 330 | 356 | 406 | 254 | 305 | 356 | 381 | 406 |
| 353 | 229 | 279 | 305 | 356 | 381 | 229 | 305 | 330 | 356 | 381 | 254 | 305 | 356 | 381 | 406 |

Note: I = ESAL of 1 E+06; II = ESAL of 5 E+06; III = ESAL of 10 E+06; IV = ESAL of 20 E+06; V = ESAL of 40 E+06; Reliability = 95%; Standard Deviation = 0.35; Initial Serviceability = 4.5; Terminal Serviceability = 2.5; Modulus of Rupture (Slab) = 4.14 MPa; Modulus of Elasticity (Concrete) = 34.47 GPa; Poisson's Ratio (Concrete) = 0.15

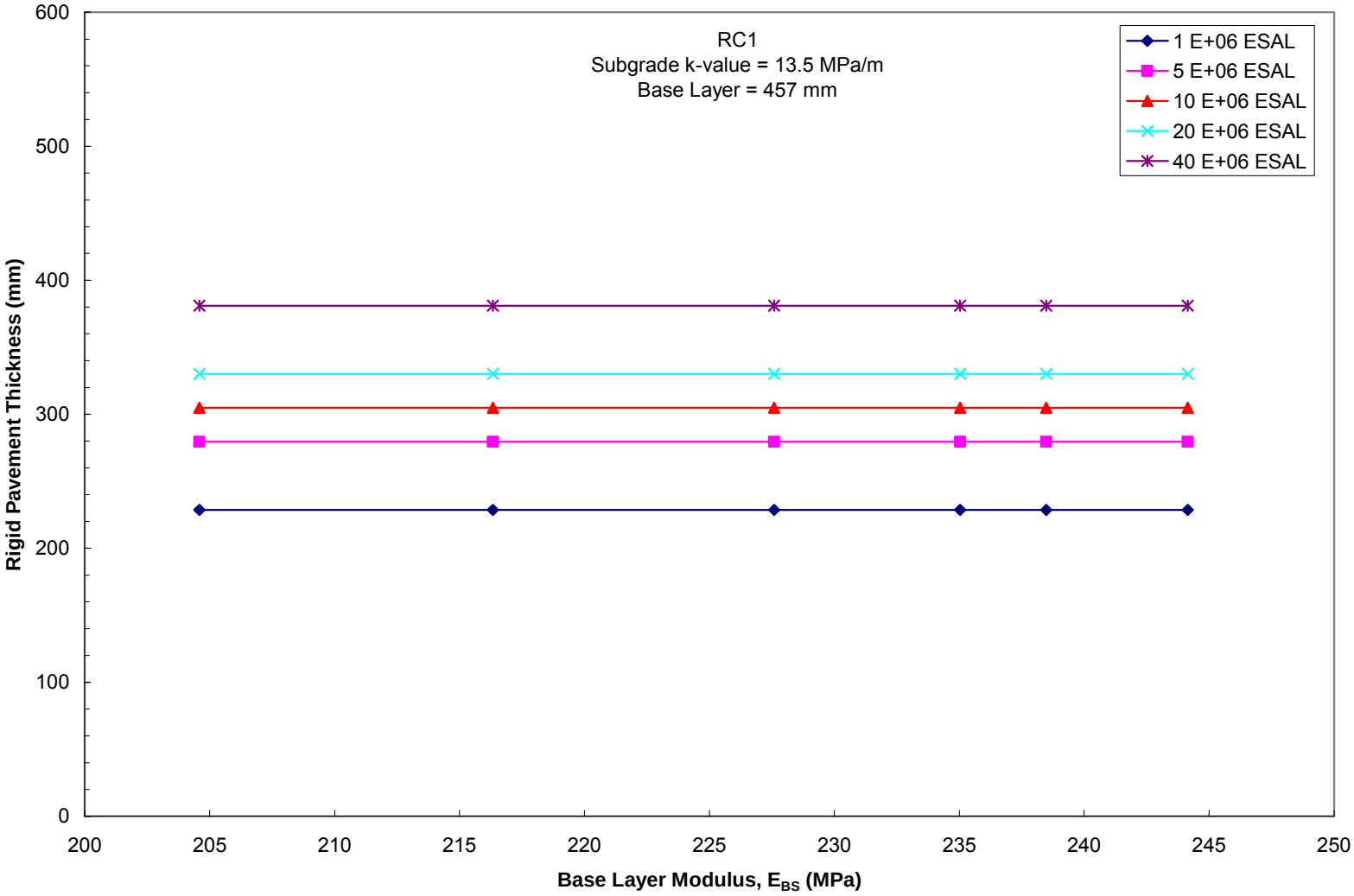


Figure 5.37 Design chart for determining rigid pavement thickness for interstates using recycled concrete aggregate RC1

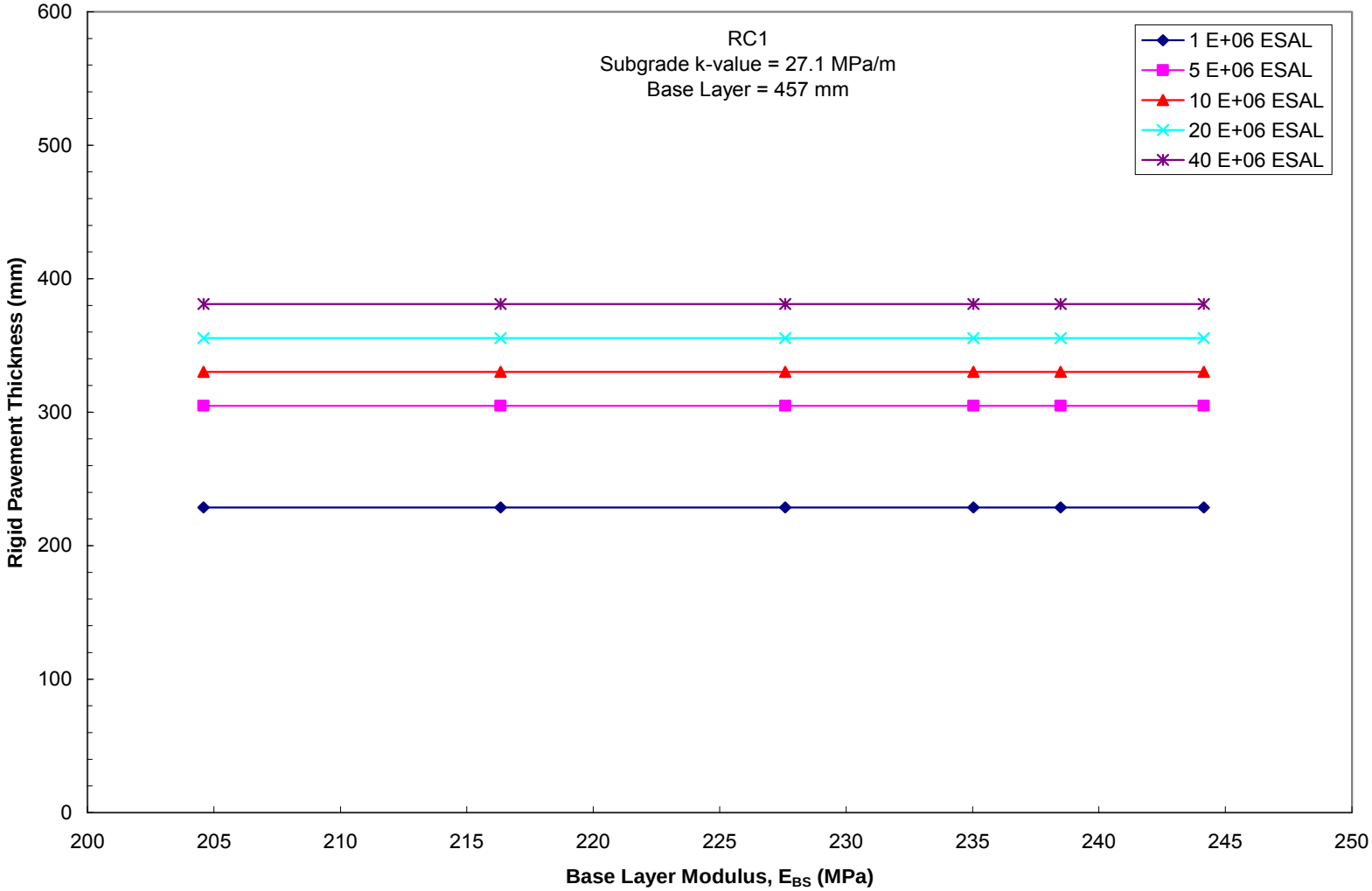


Figure 5.38 Design chart for determining rigid pavement thickness for interstates using recycled concrete aggregate RC1

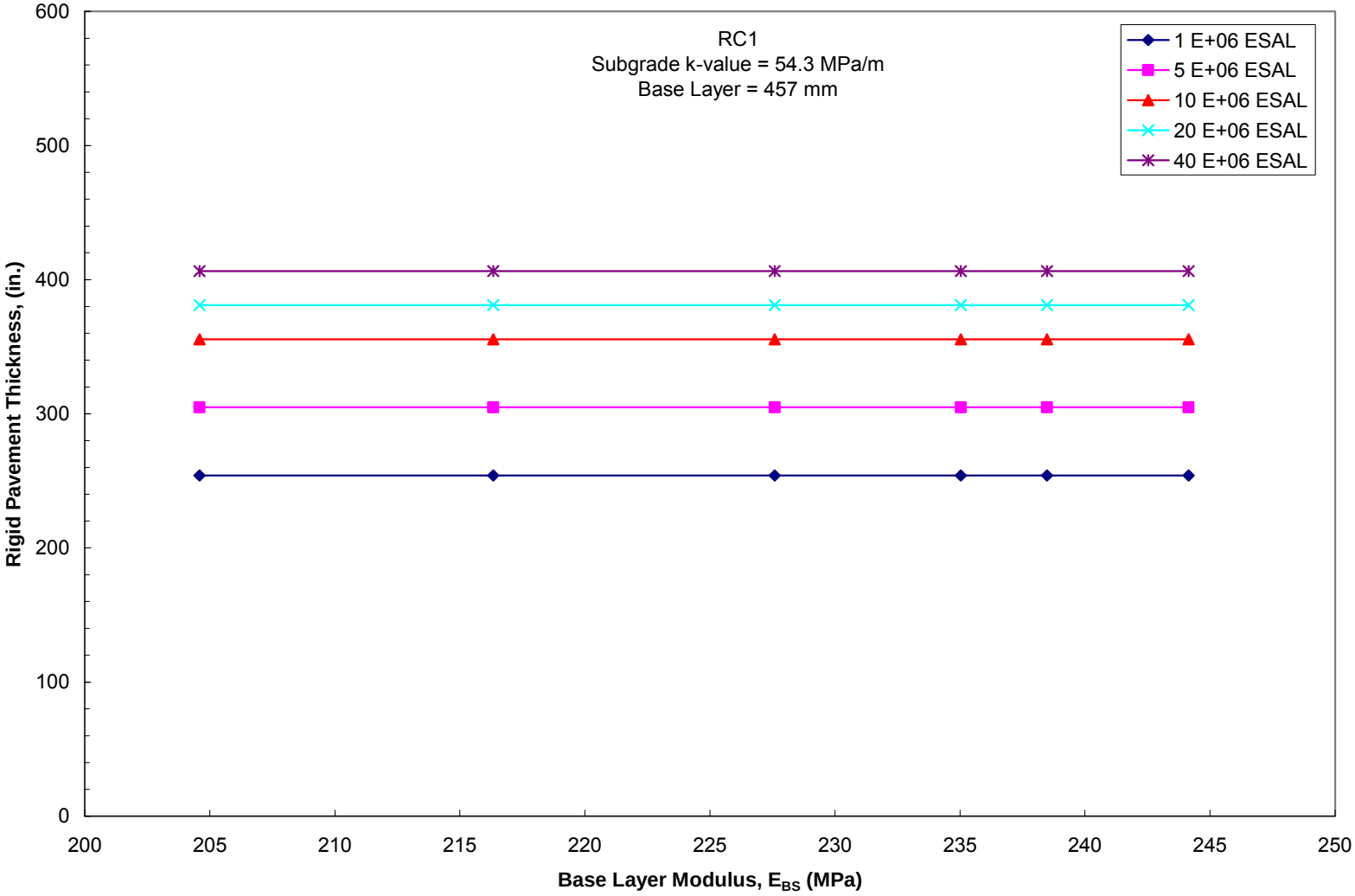


Figure 5.39 Design chart for determining rigid pavement thickness for interstates using recycled concrete aggregate RC1

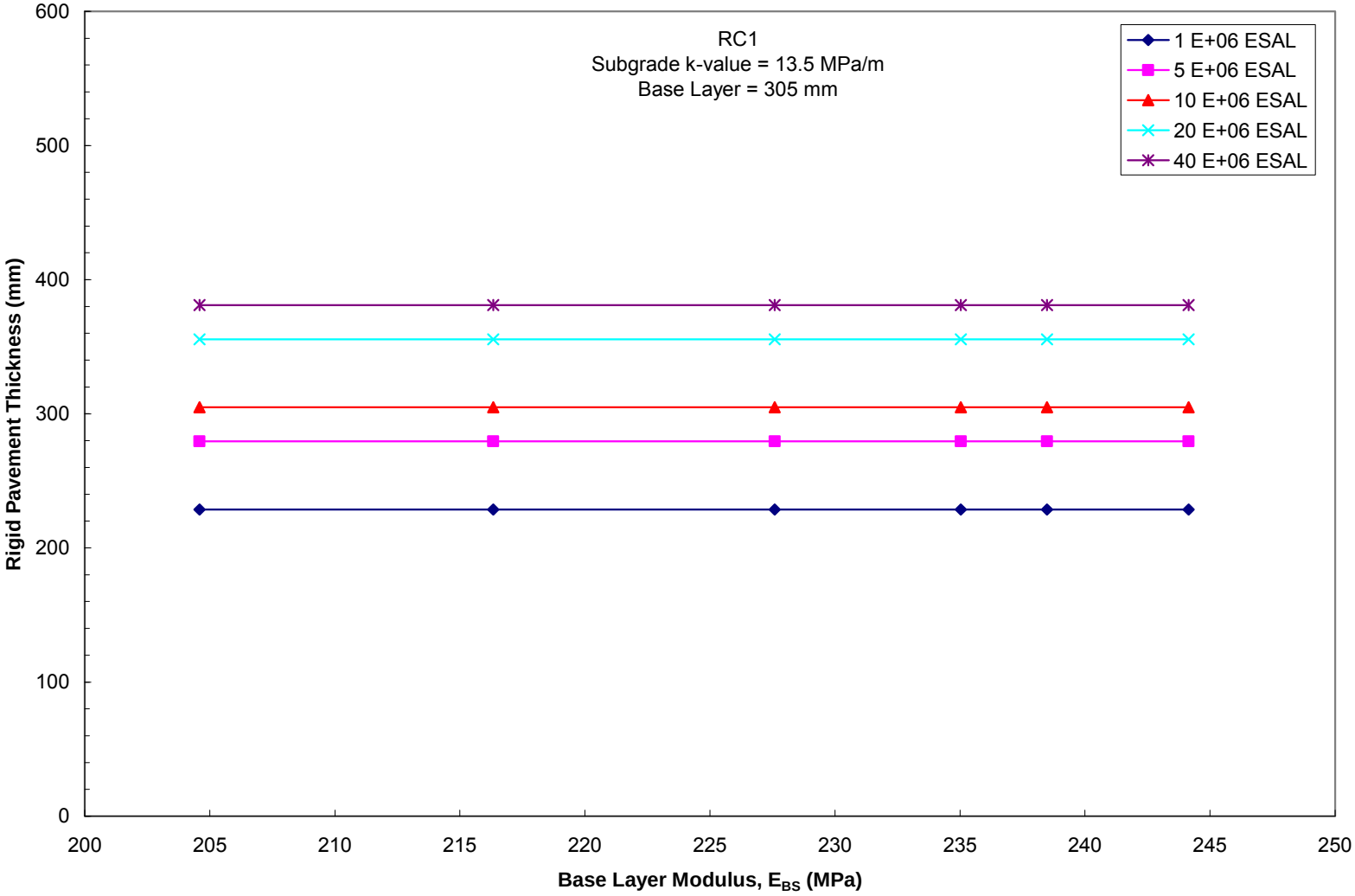


Figure 5.40 Design chart for determining rigid pavement thickness for state highways using recycled concrete aggregate RC1

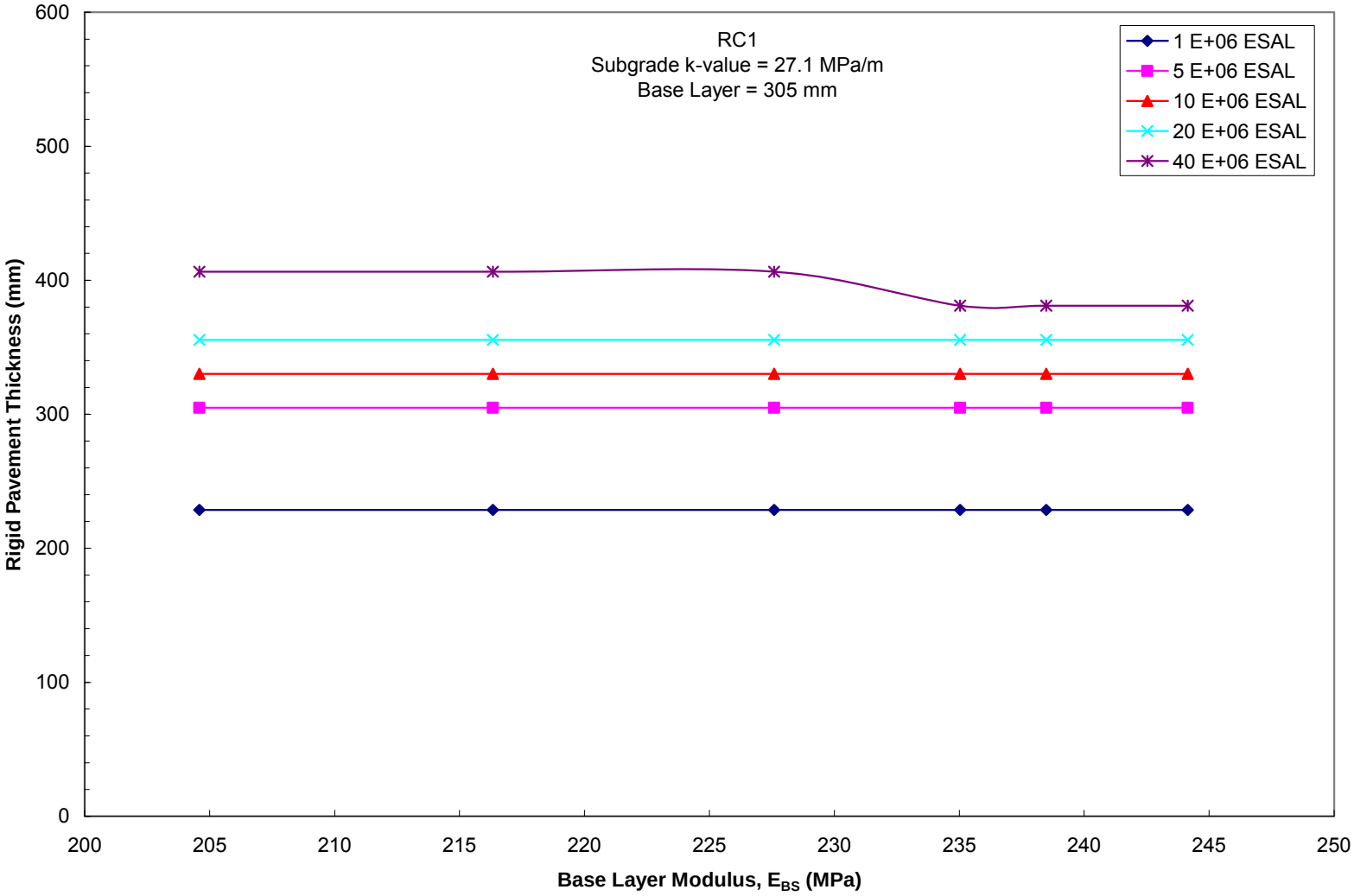


Figure 5.41 Design chart for determining rigid pavement thickness for state highways using recycled concrete aggregate RC1

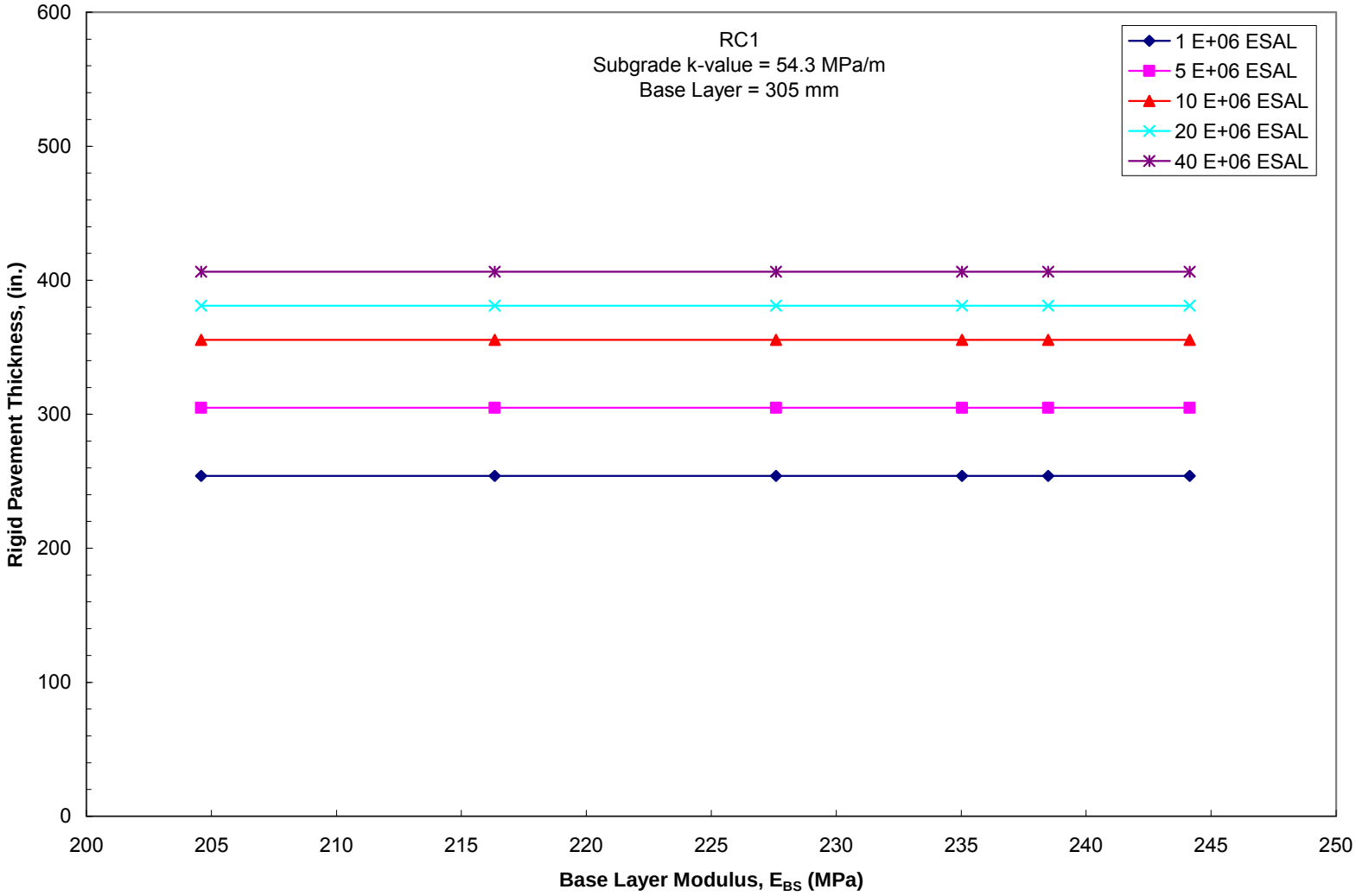


Figure 5.42 Design chart for determining rigid pavement thickness for state highways using recycled concrete aggregate RC1

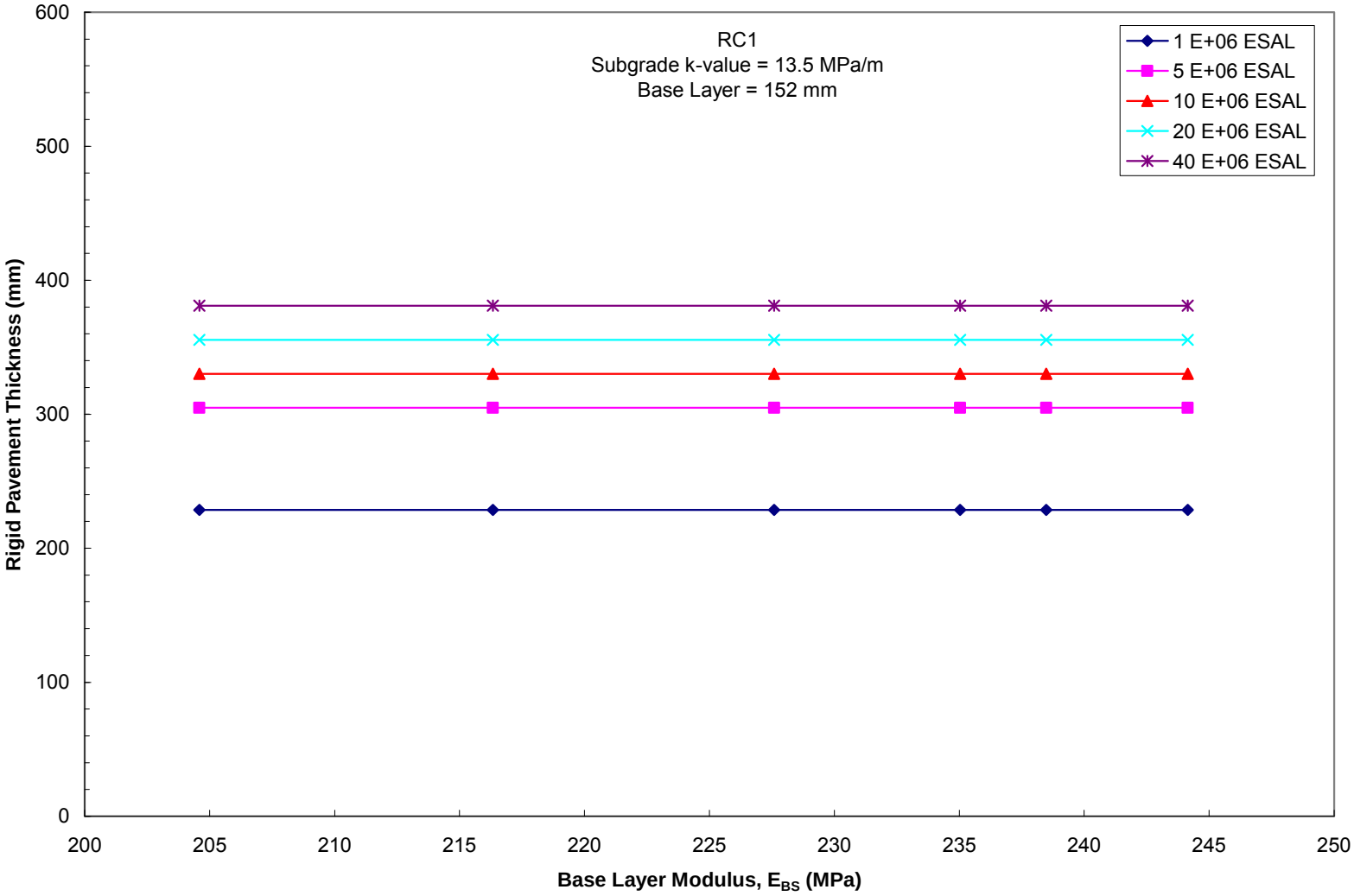


Figure 5.43 Design chart for determining rigid pavement thickness for city roads using recycled concrete aggregate RC1

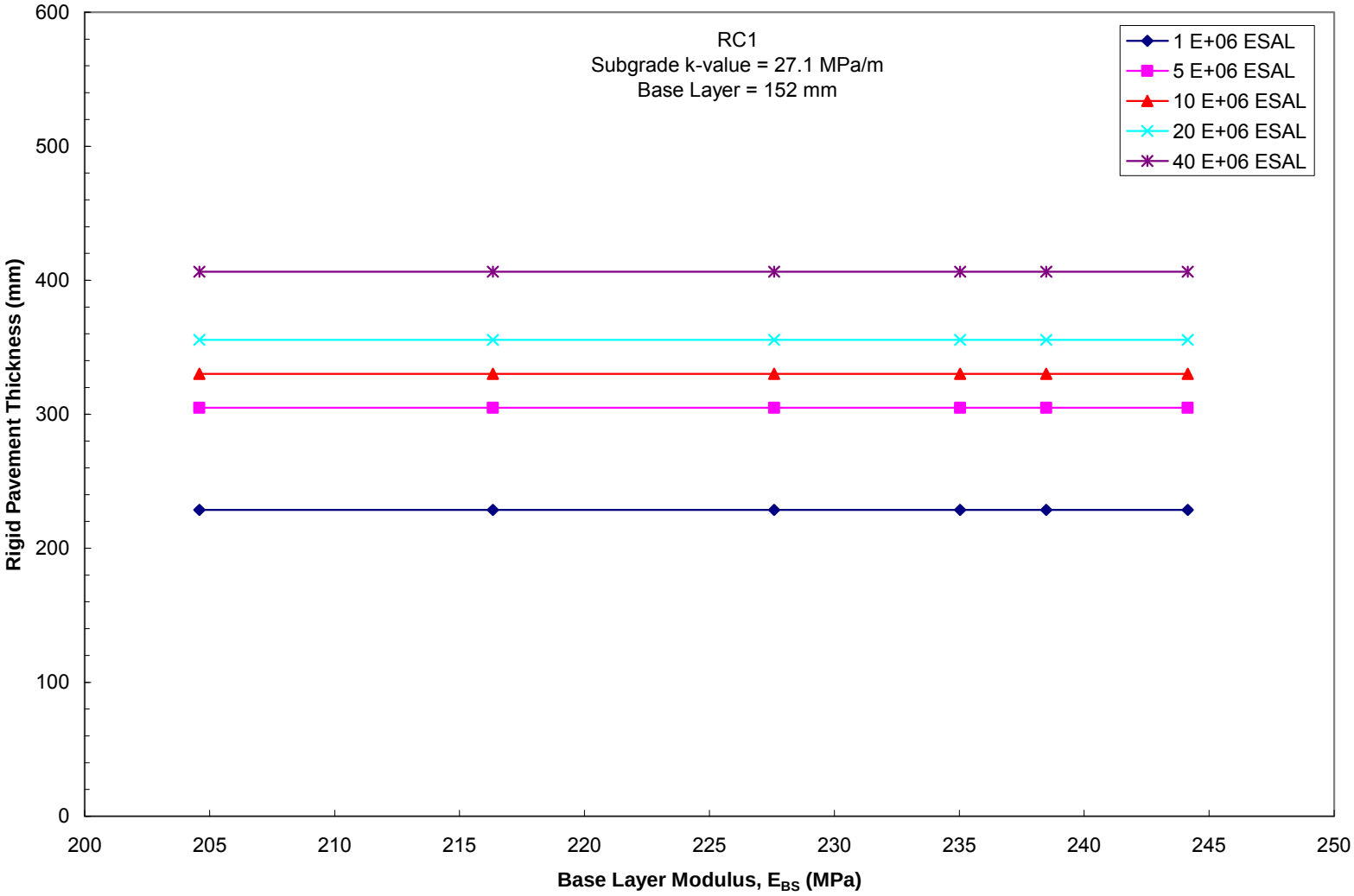


Figure 5.44 Design chart for determining rigid pavement thickness for city roads using recycled concrete aggregate RC1

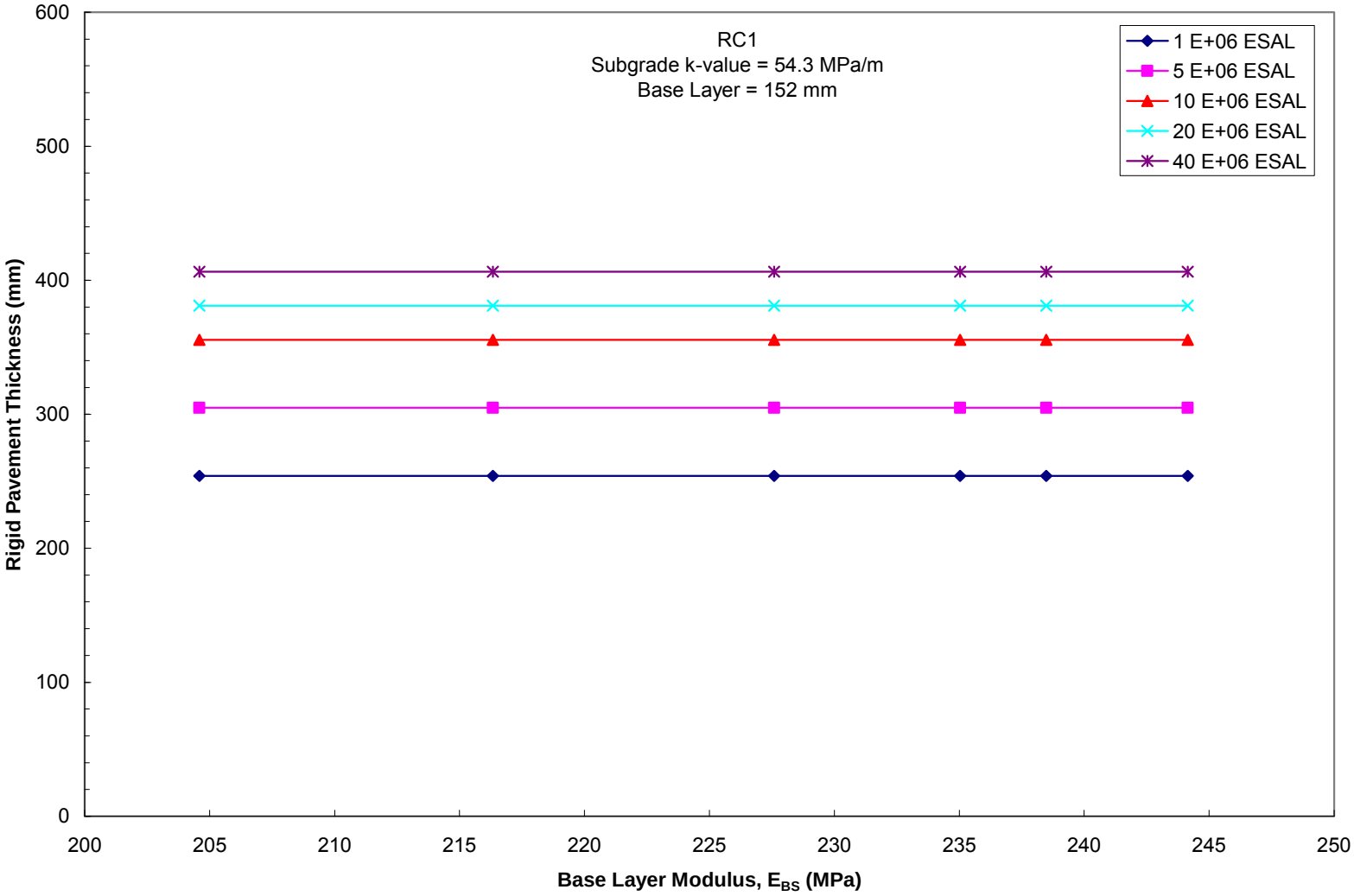


Figure 5.45 Design chart for determining rigid pavement thickness for city roads using recycled concrete aggregate RC1

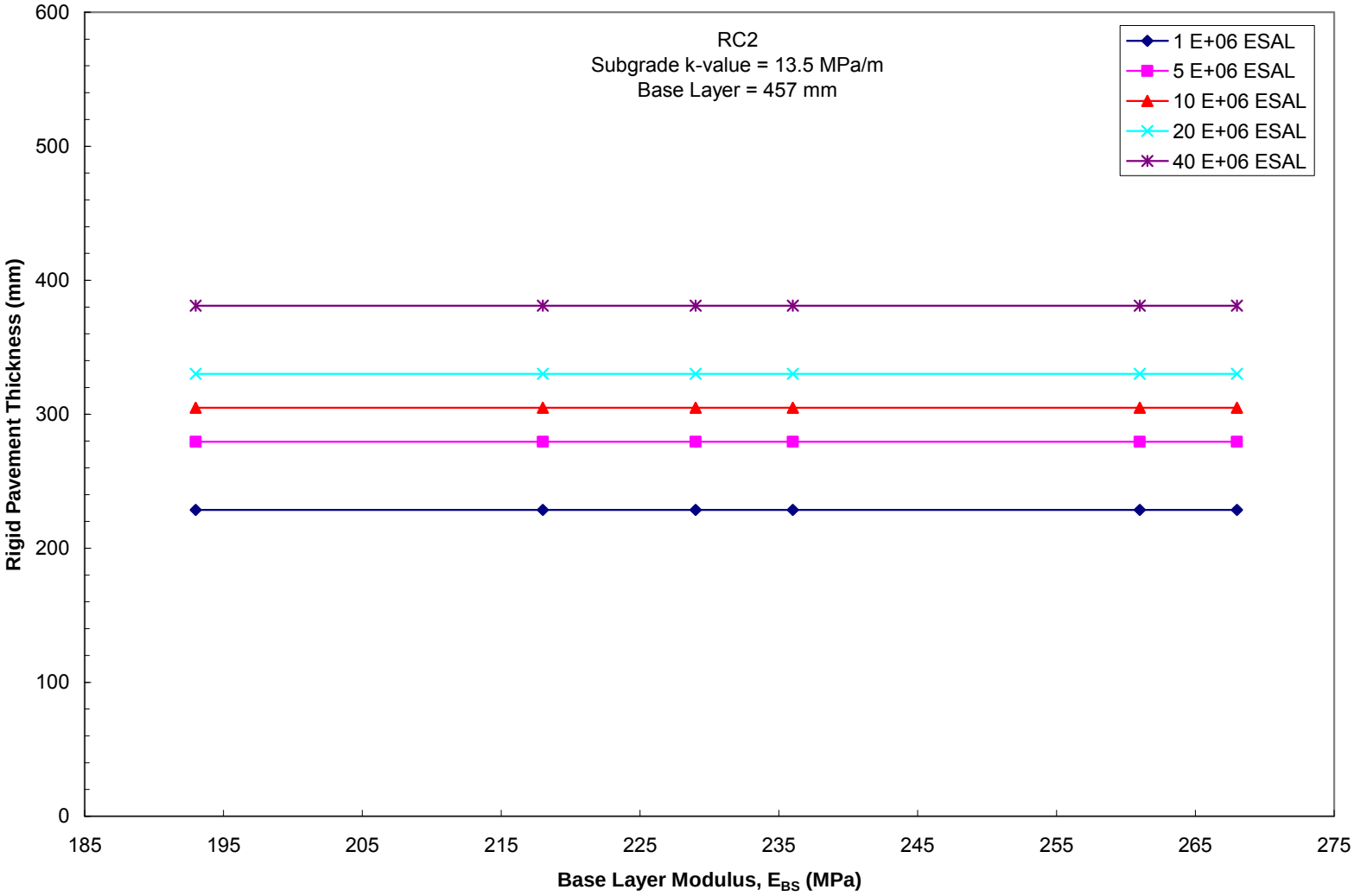


Figure 5.46 Design chart for determining rigid pavement thickness for interstates using recycled concrete aggregate RC2

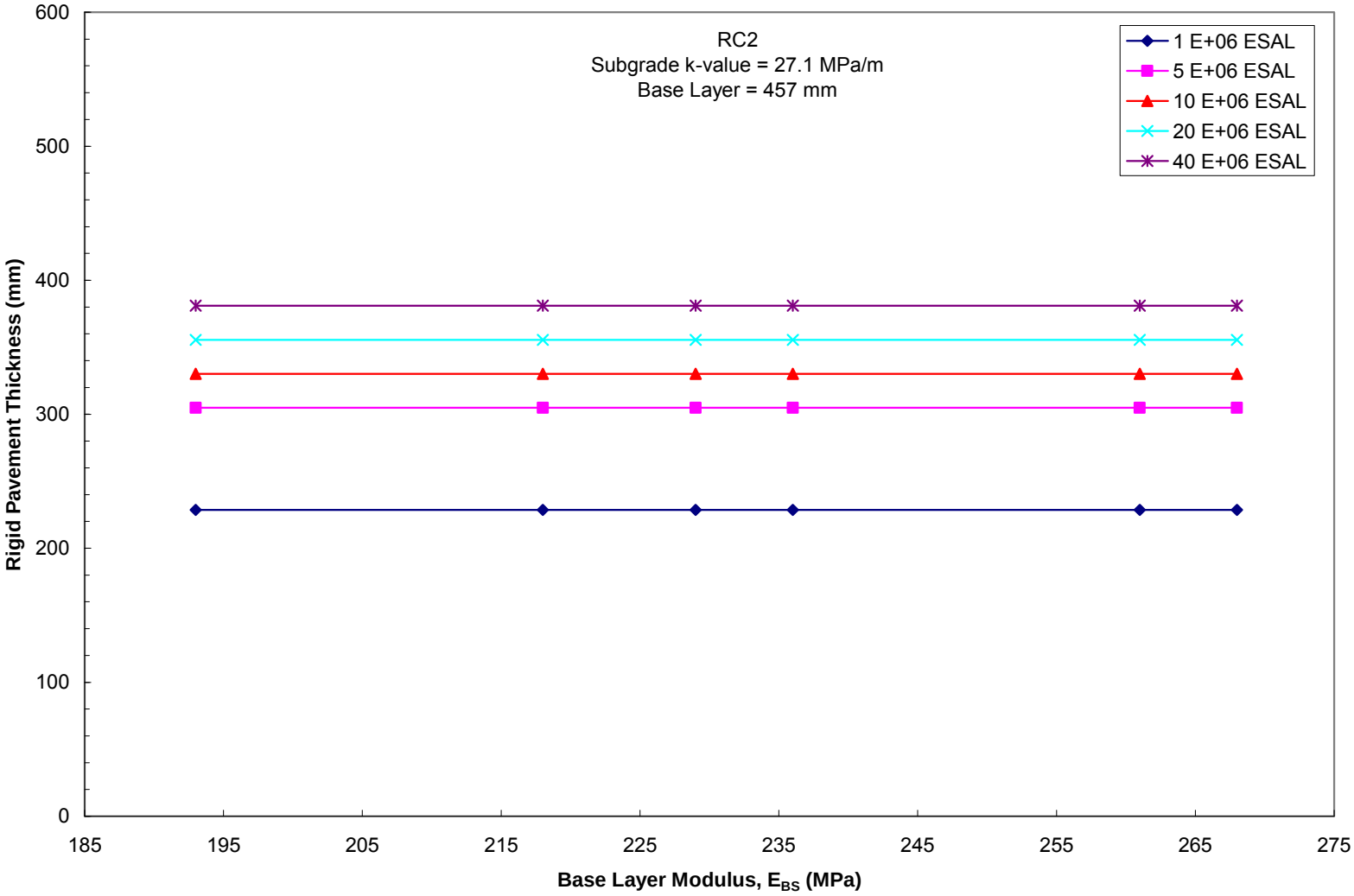


Figure 5.47 Design chart for determining rigid pavement thickness for interstates using recycled concrete aggregate RC2

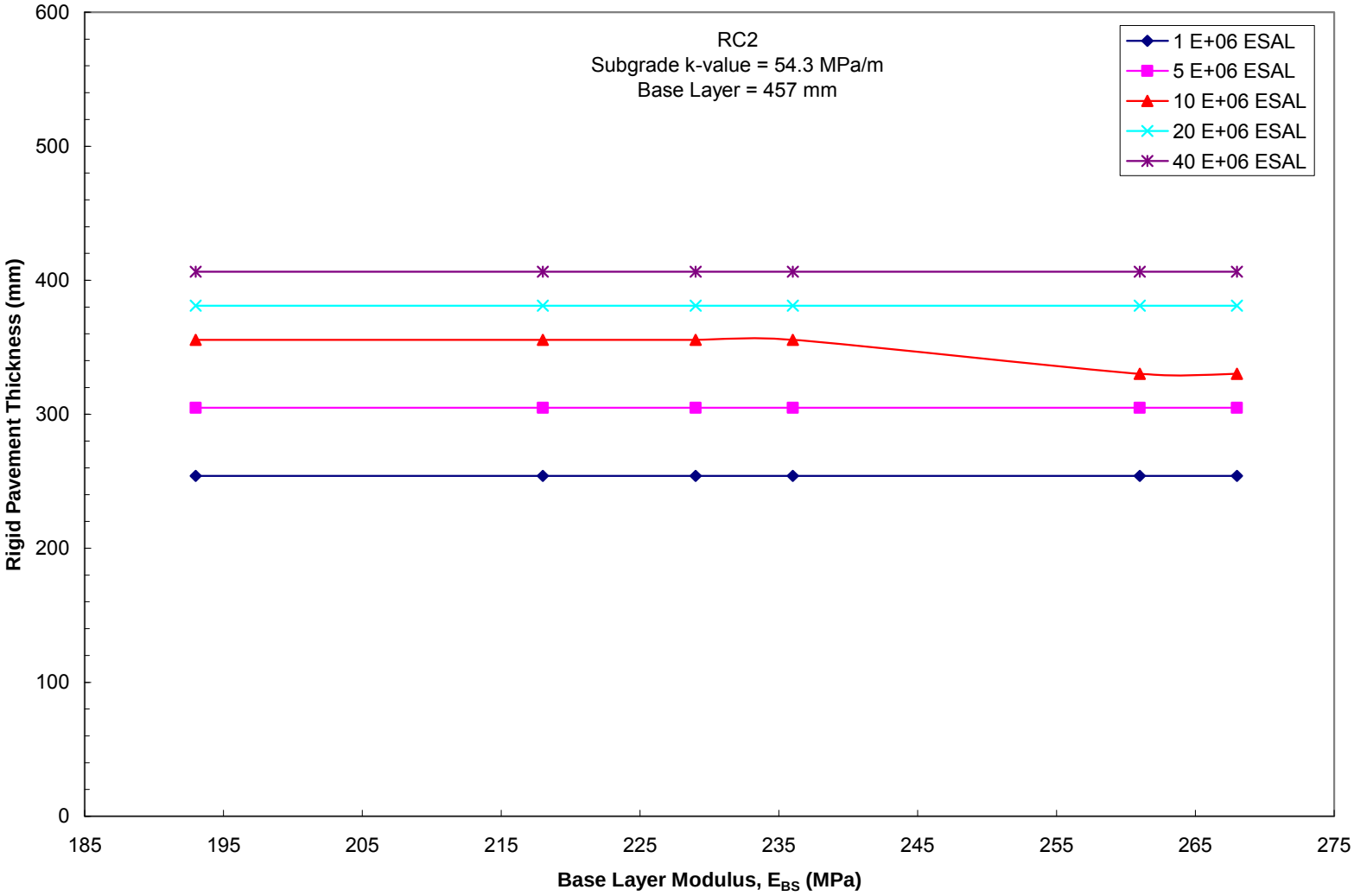


Figure 5.48 Design chart for determining rigid pavement thickness for interstates using recycled concrete aggregate RC2

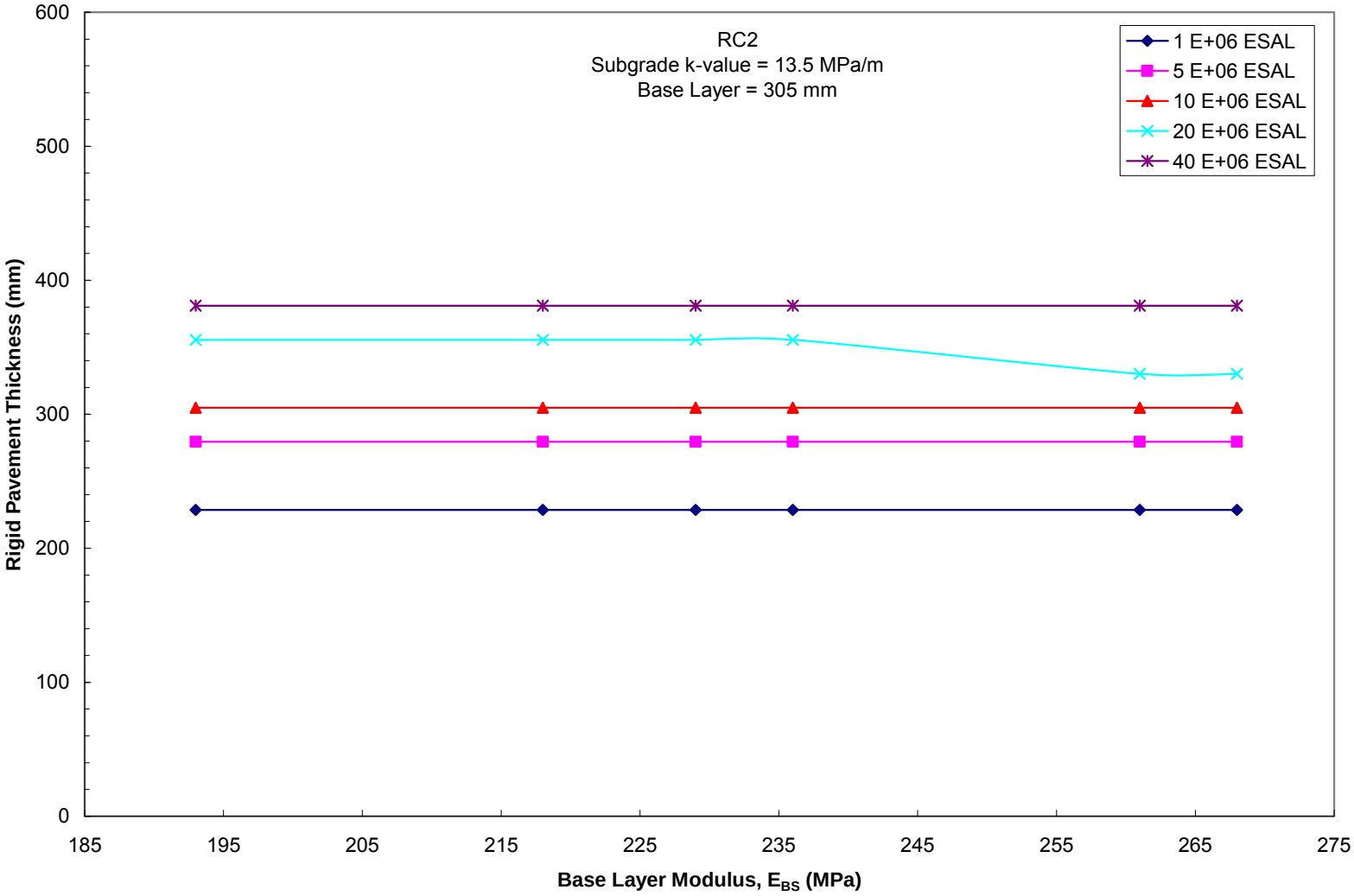


Figure 5.49 Design chart for determining rigid pavement thickness for state highways using recycled concrete aggregate RC2

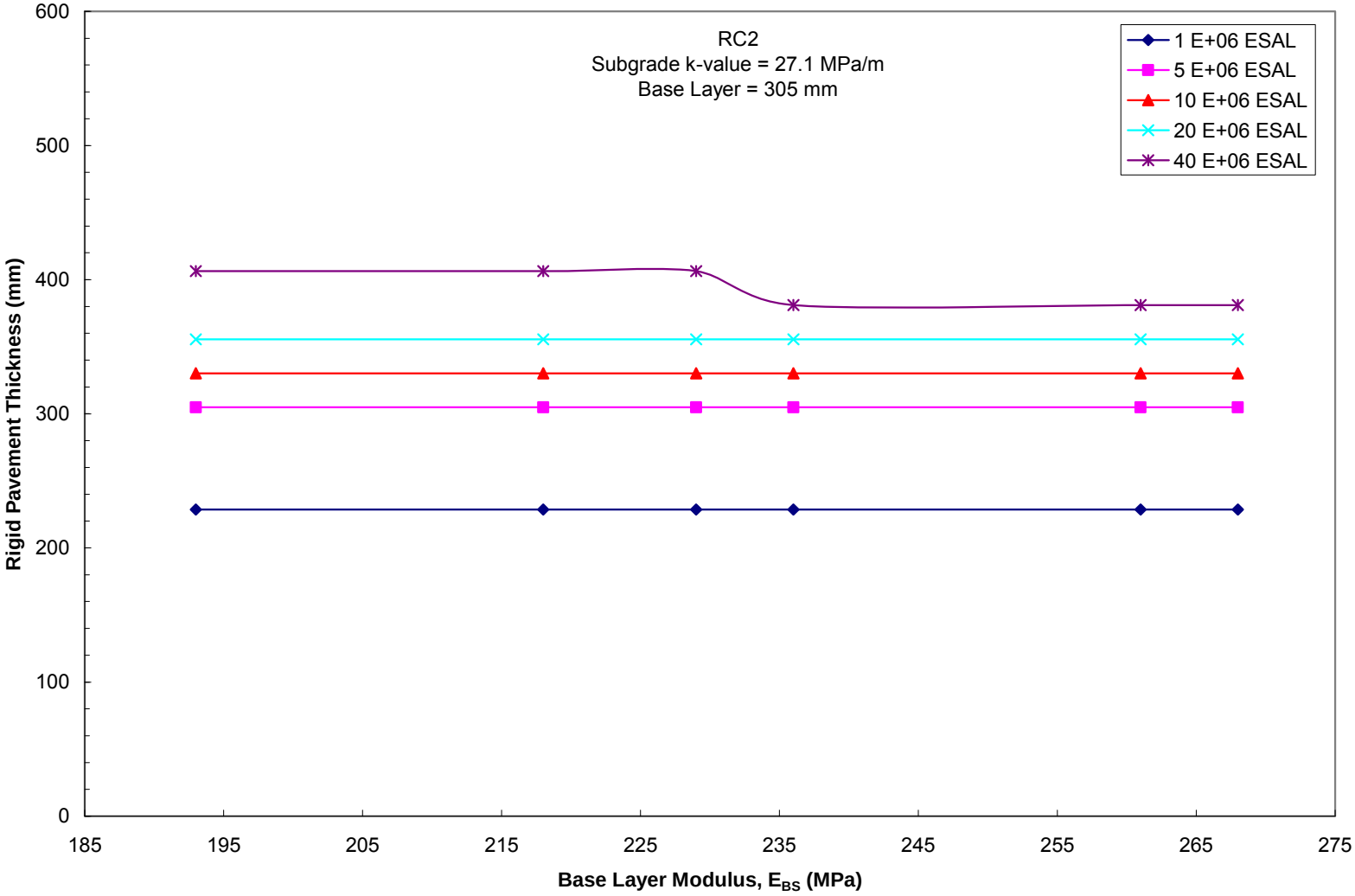


Figure 5.50 Design chart for determining rigid pavement thickness for state highways using recycled concrete aggregate RC2

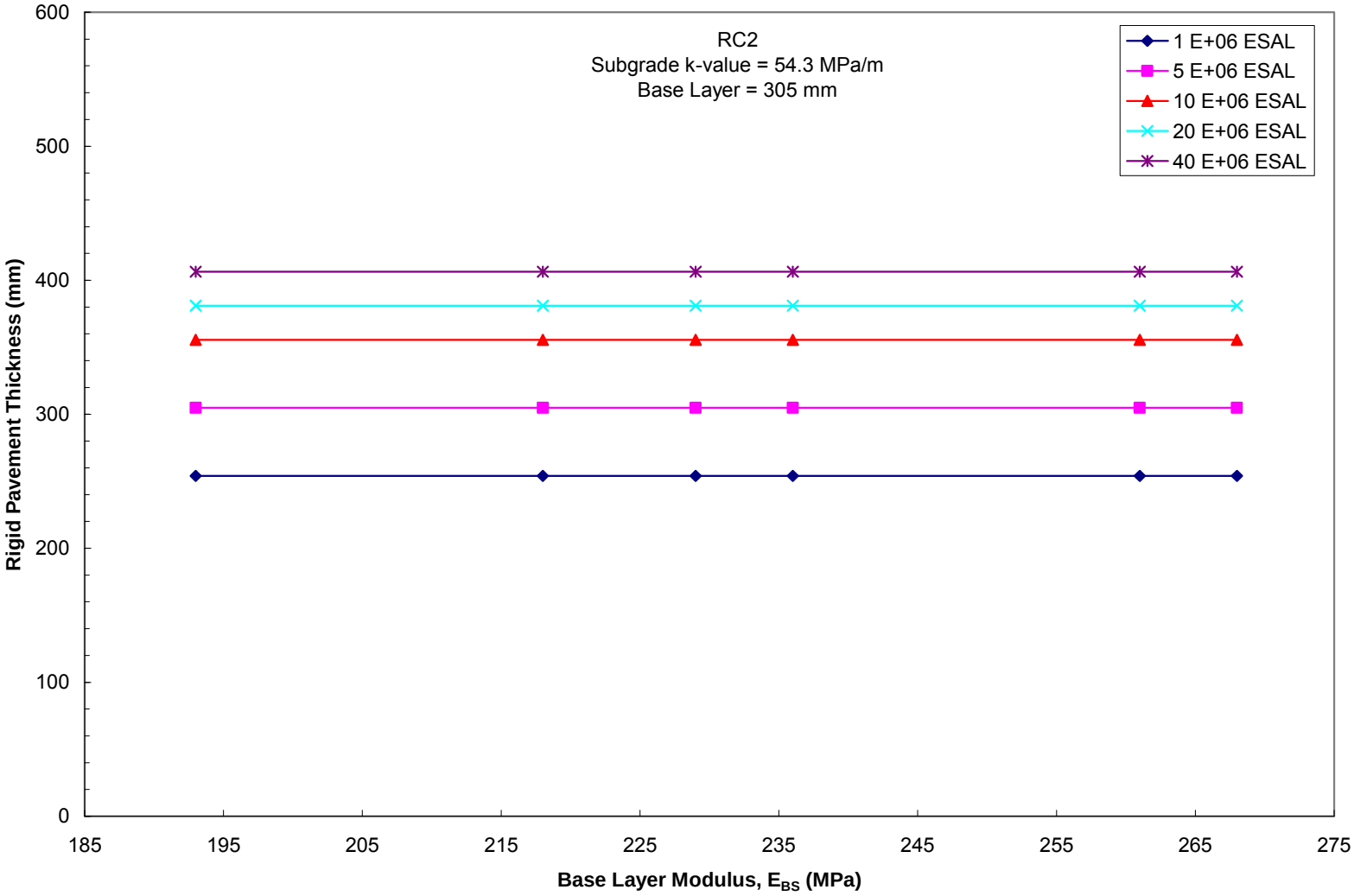


Figure 5.51 Design chart for determining rigid pavement thickness for state highways using recycled concrete aggregate RC2

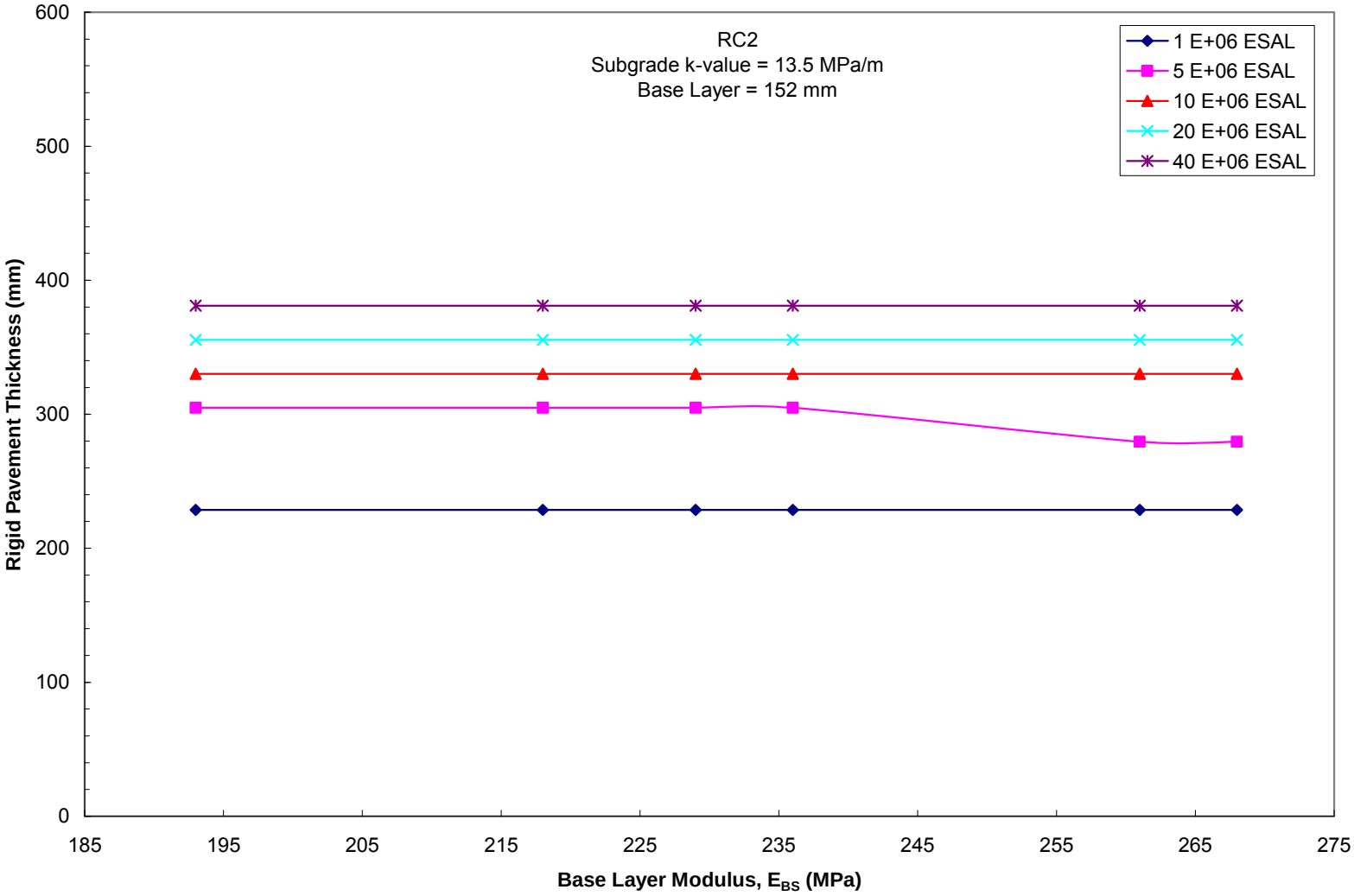


Figure 5.52 Design chart for determining rigid pavement thickness for city roads using recycled concrete aggregate RC2

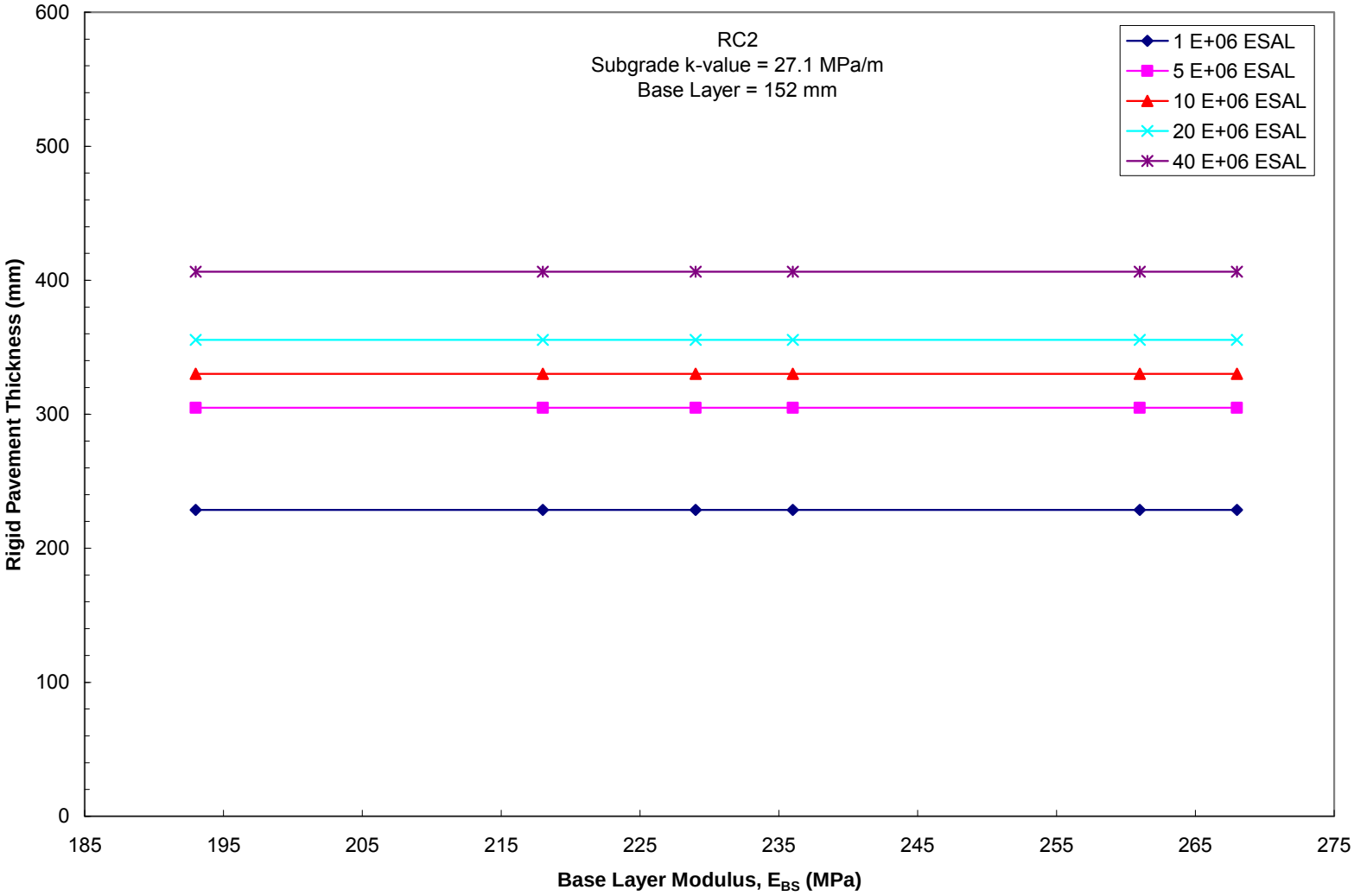


Figure 5.53 Design chart for determining rigid pavement thickness for city roads using recycled concrete aggregate RC2

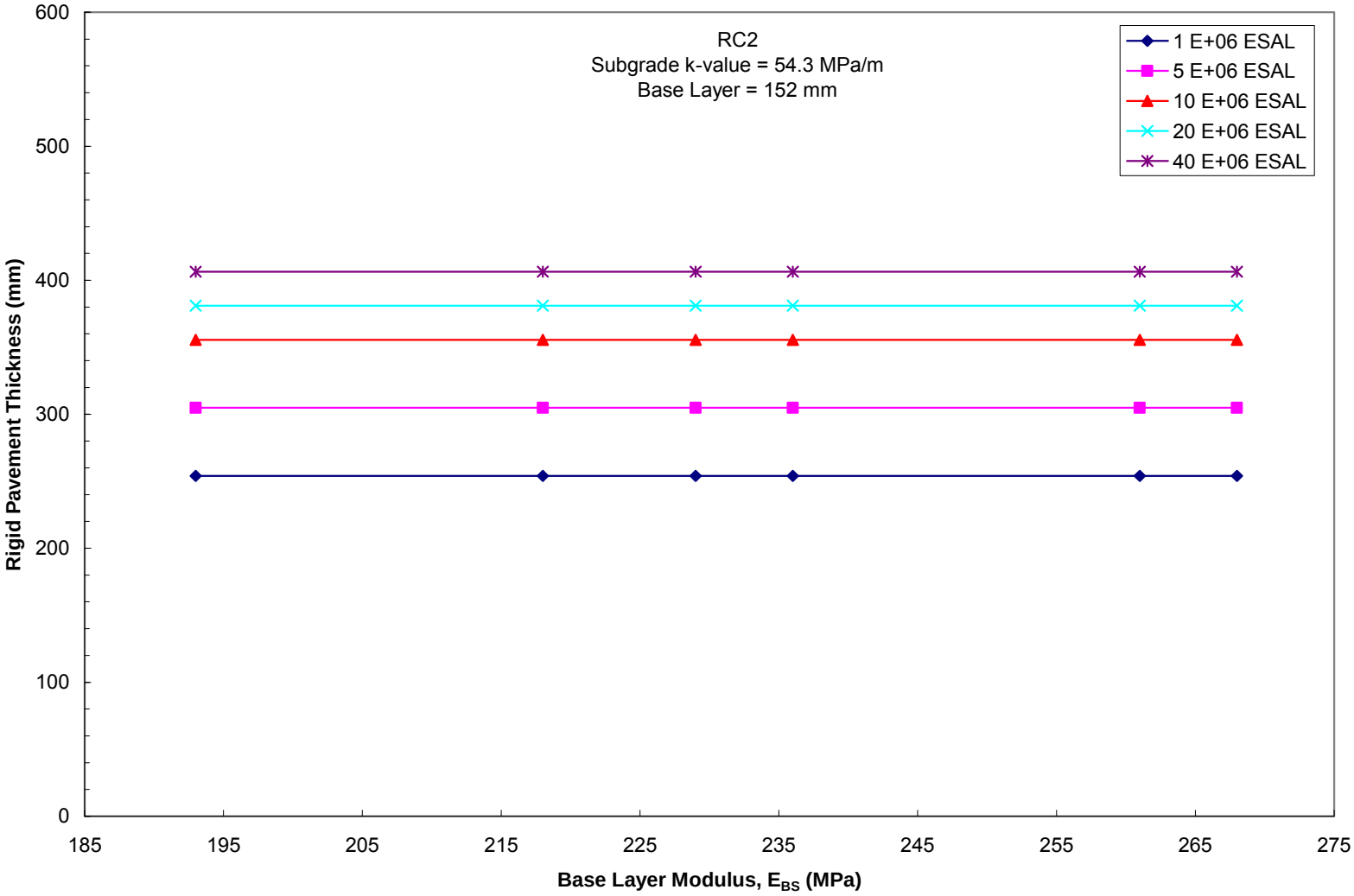


Figure 5.54 Design chart for determining rigid pavement thickness for city roads using recycled concrete aggregate RC2

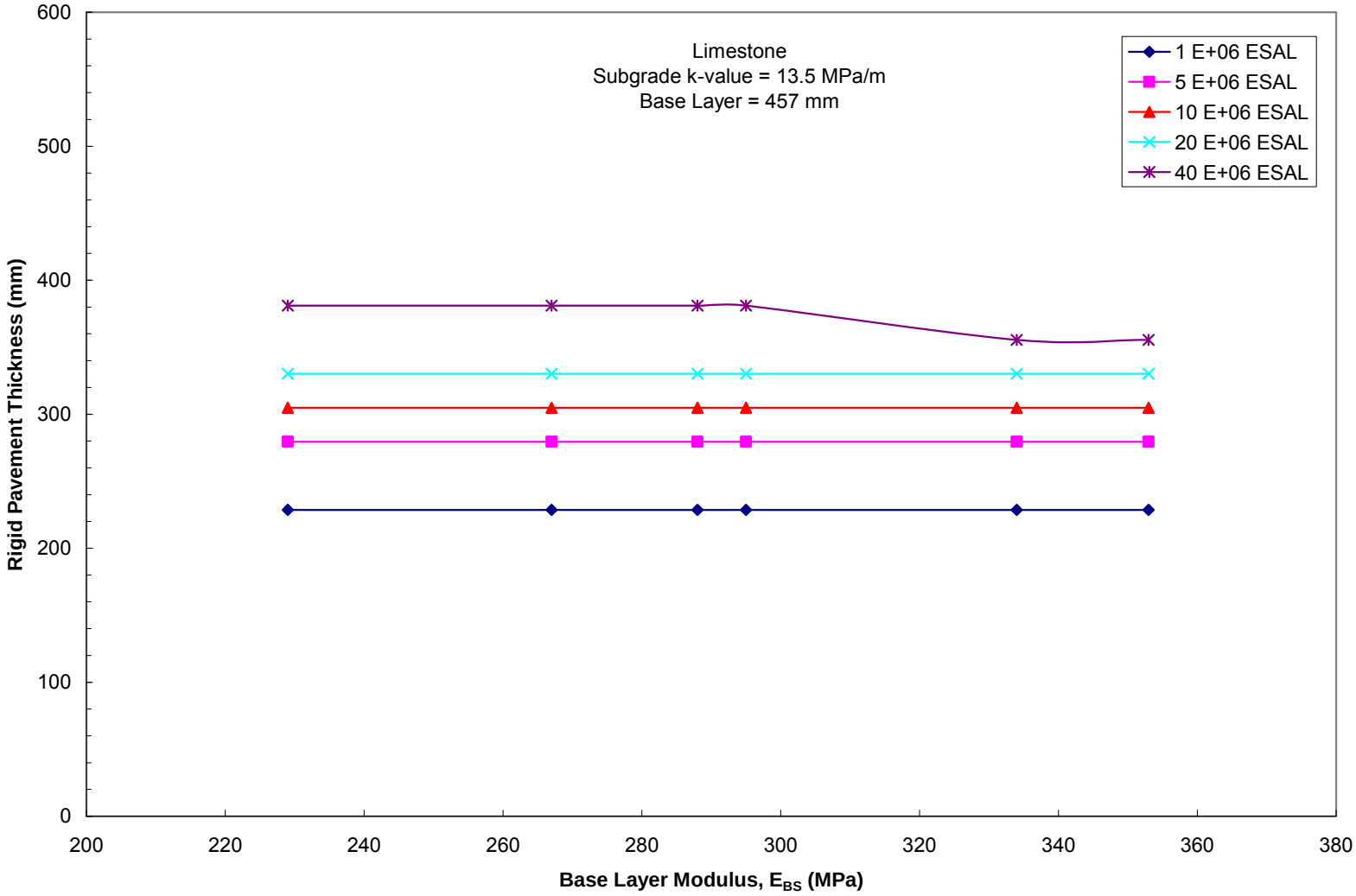


Figure 5.55 Design chart for determining rigid pavement thickness for interstates using limestone aggregate

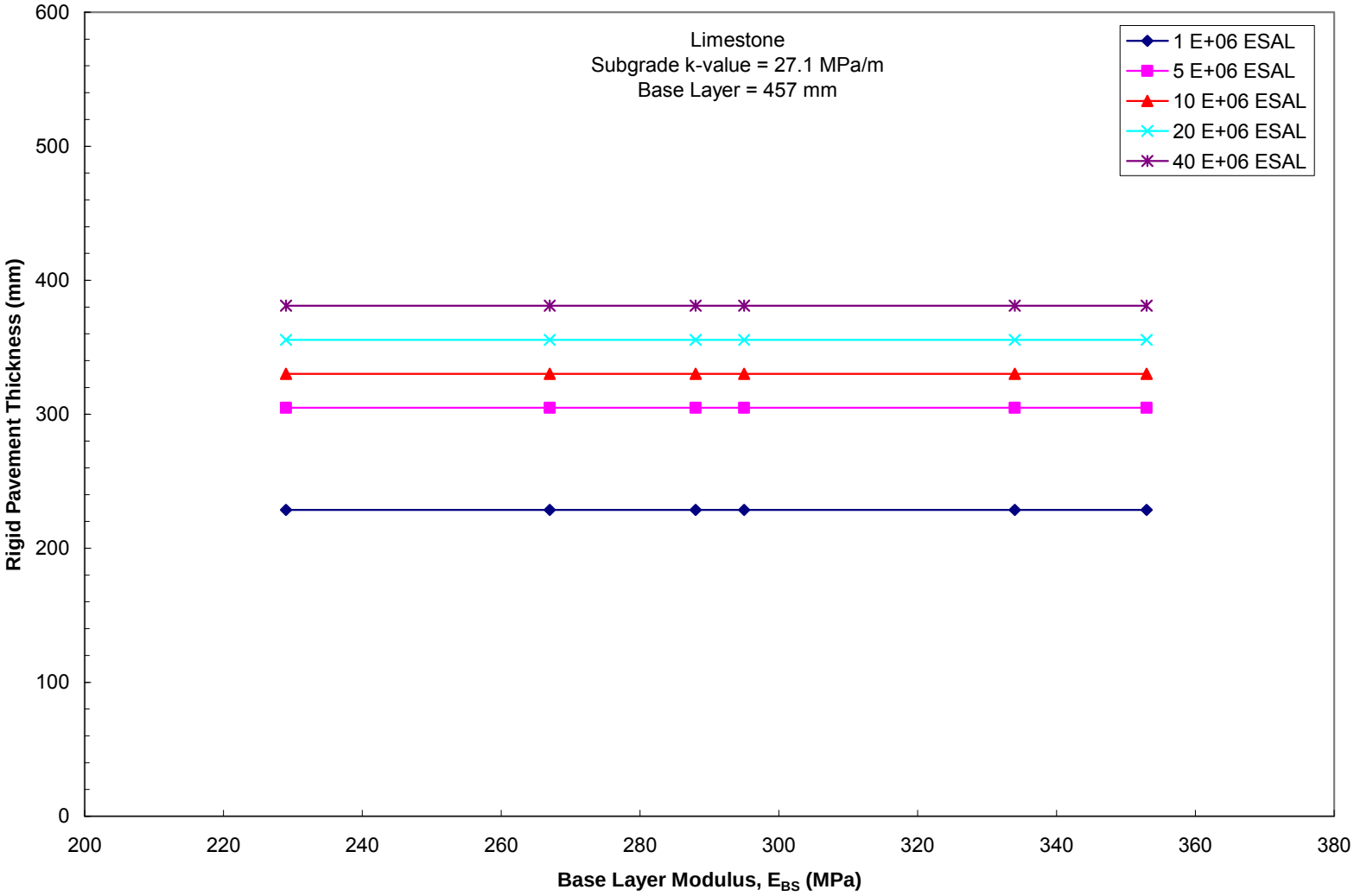


Figure 5.56 Design chart for determining rigid pavement thickness for interstates using limestone aggregate

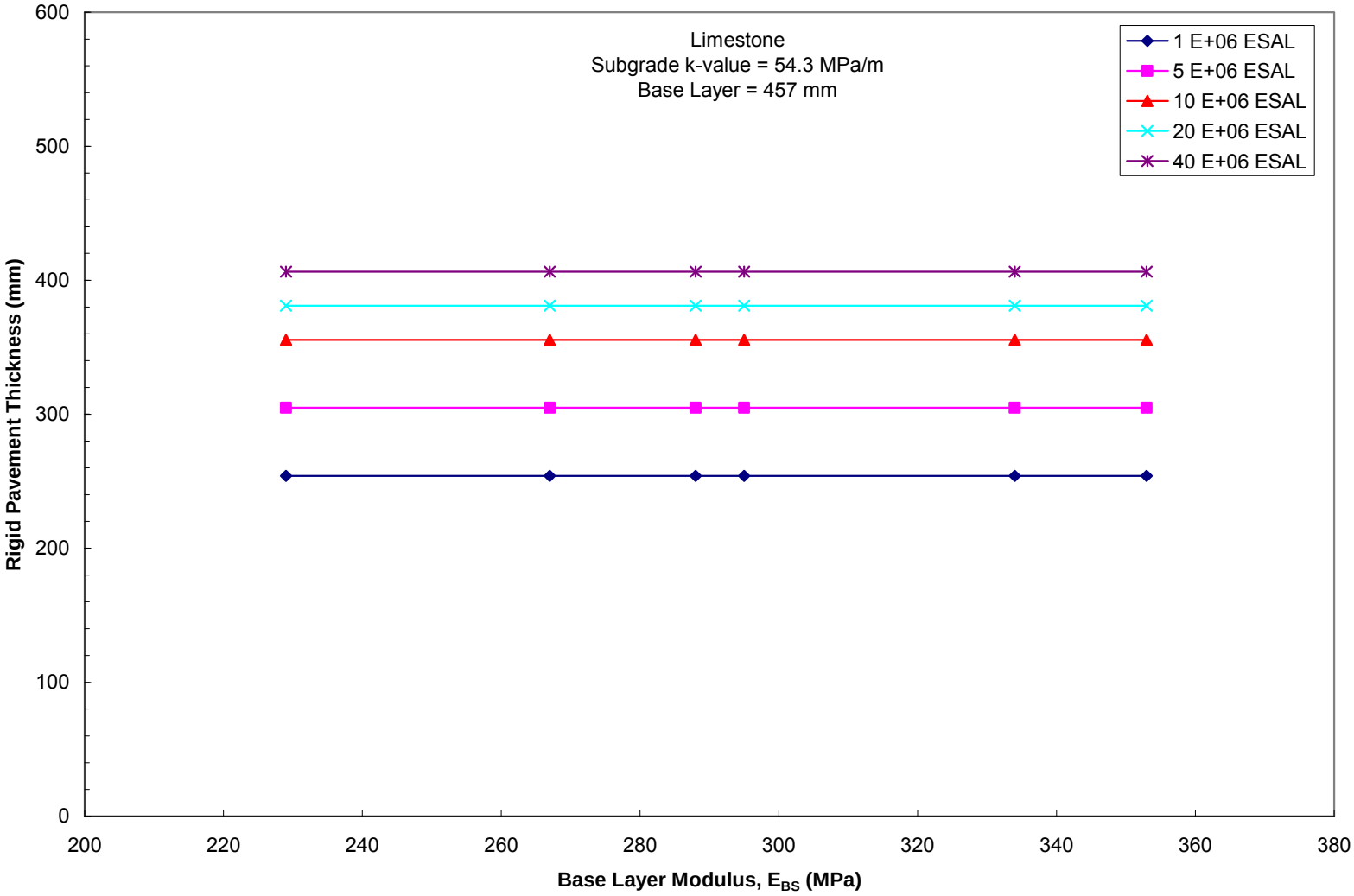


Figure 5.57 Design chart for determining rigid pavement thickness for interstates using limestone aggregate

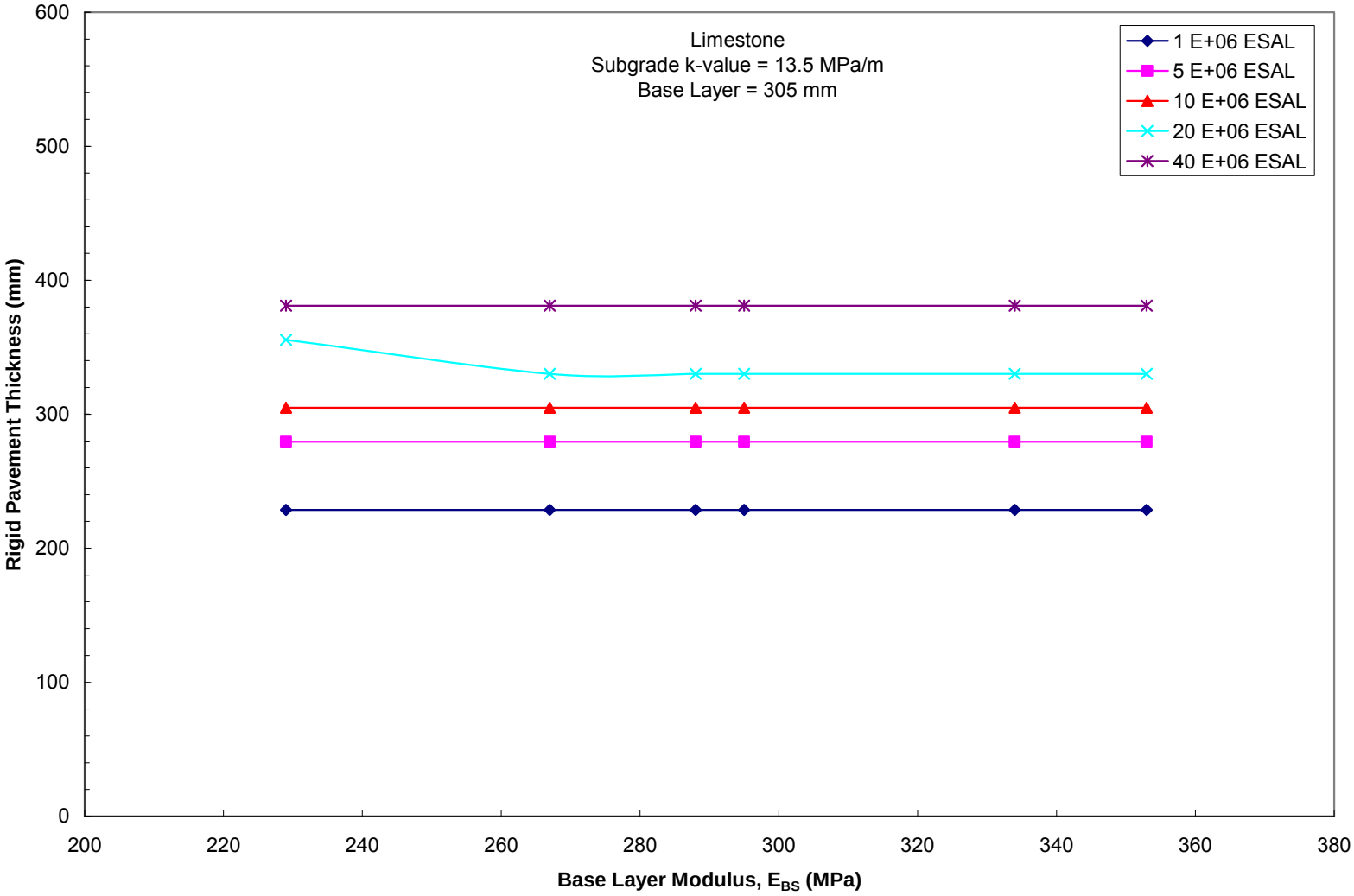


Figure 5.58 Design chart for determining rigid pavement thickness for state highways using limestone aggregate

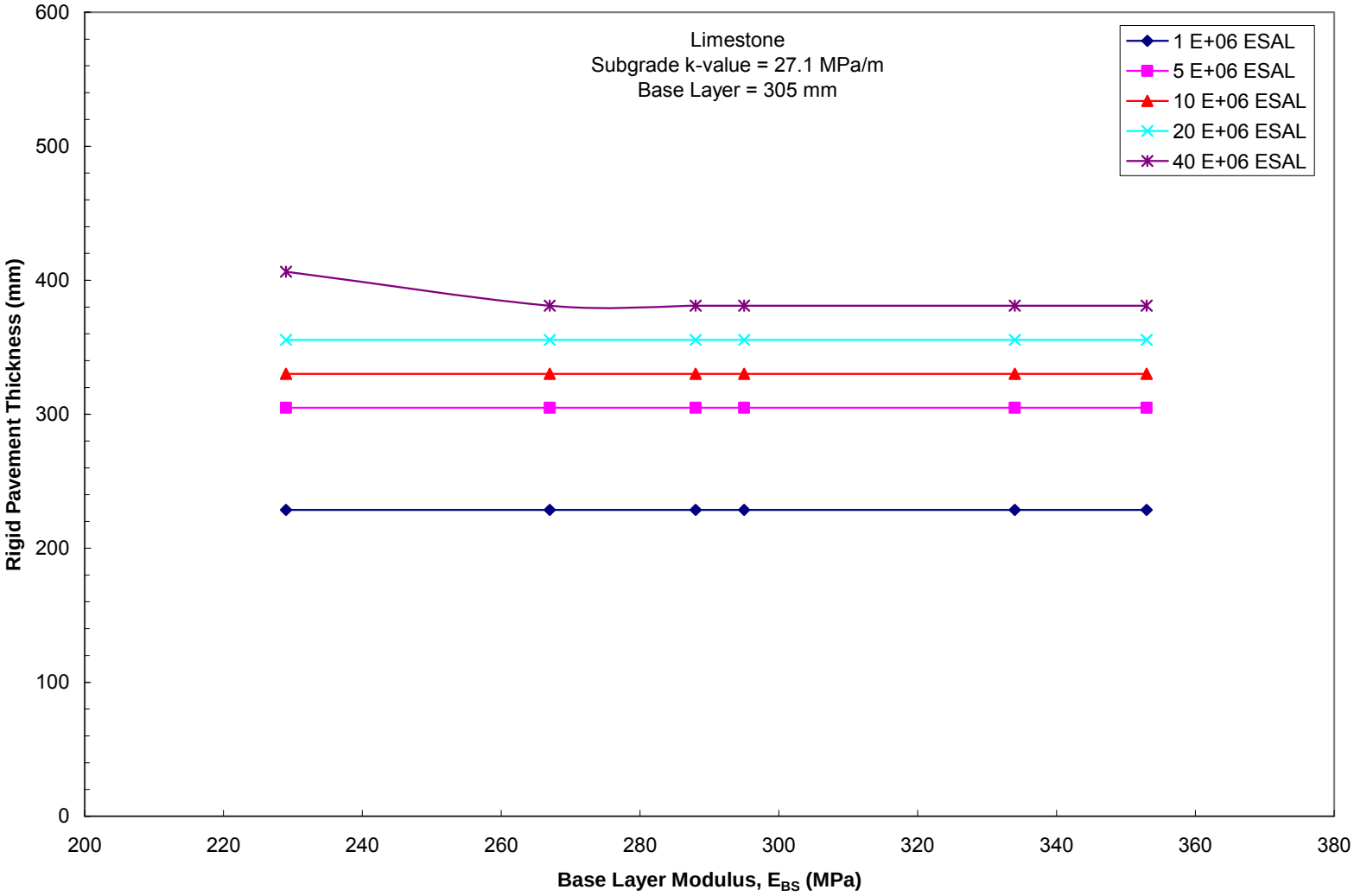


Figure 5.59 Design chart for determining rigid pavement thickness for state highways using limestone aggregate

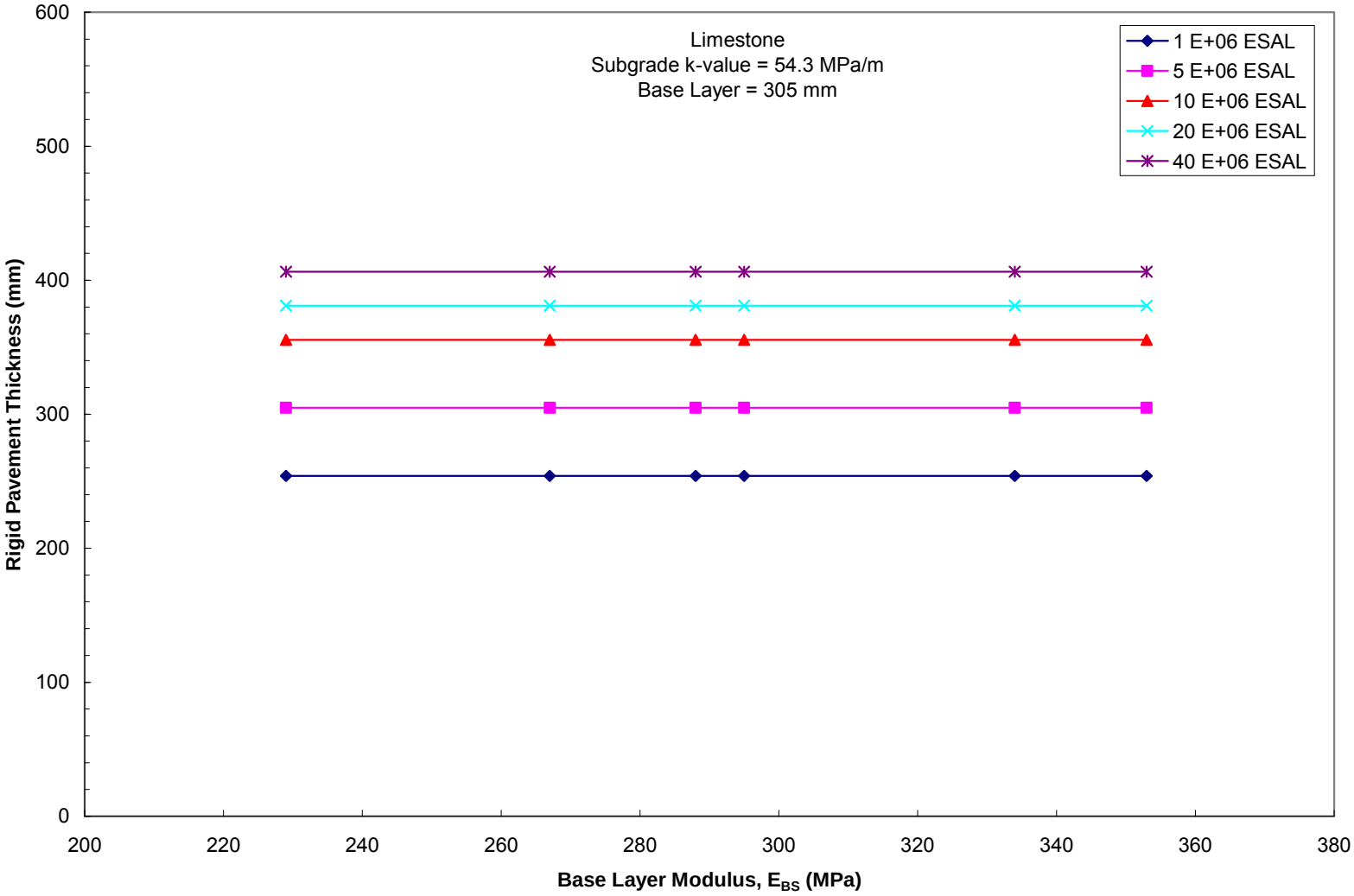


Figure 5.60 Design chart for determining rigid pavement thickness for state highways using limestone aggregate

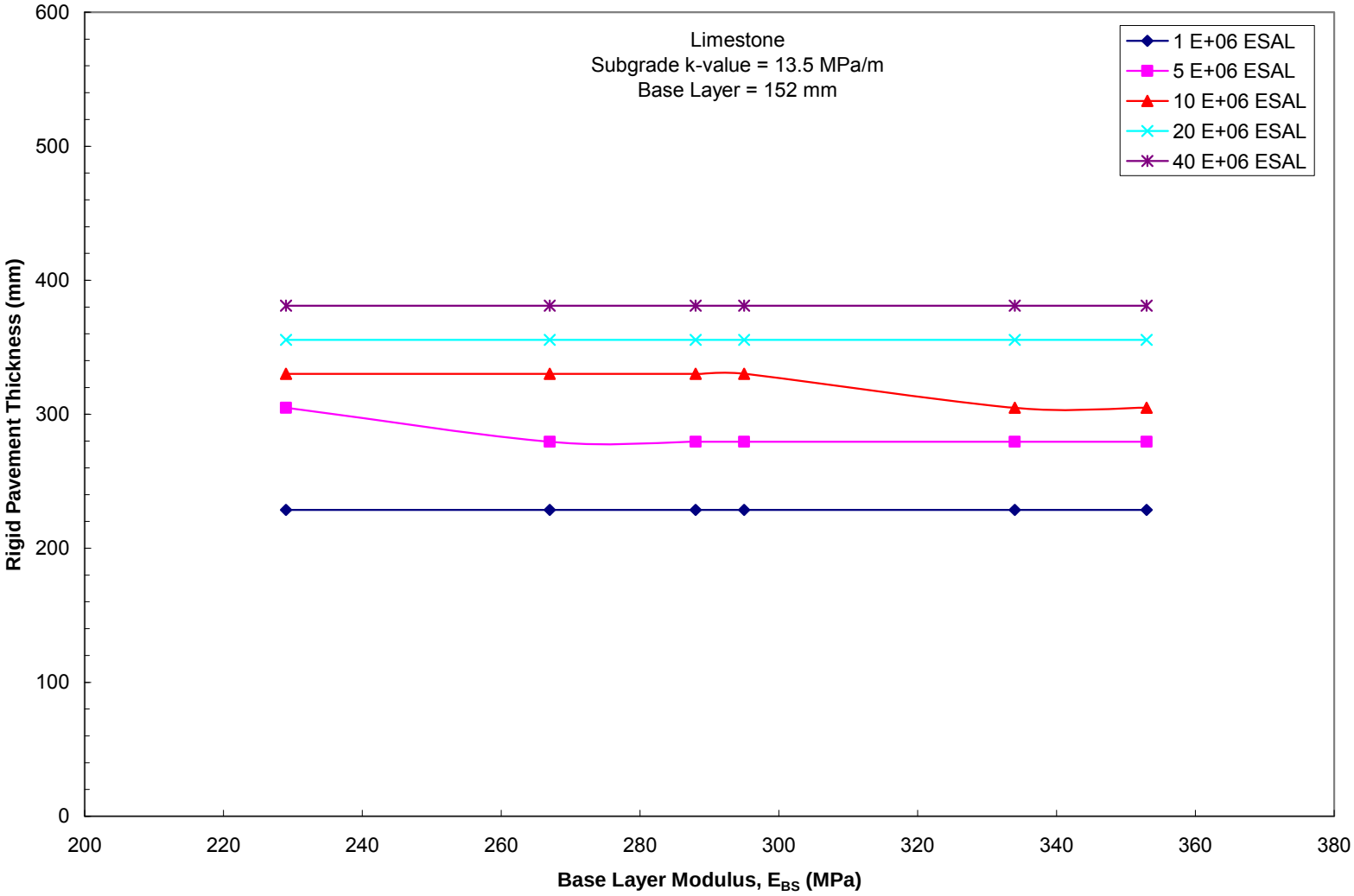


Figure 5.61 Design chart for determining rigid pavement thickness for city roads using limestone aggregate

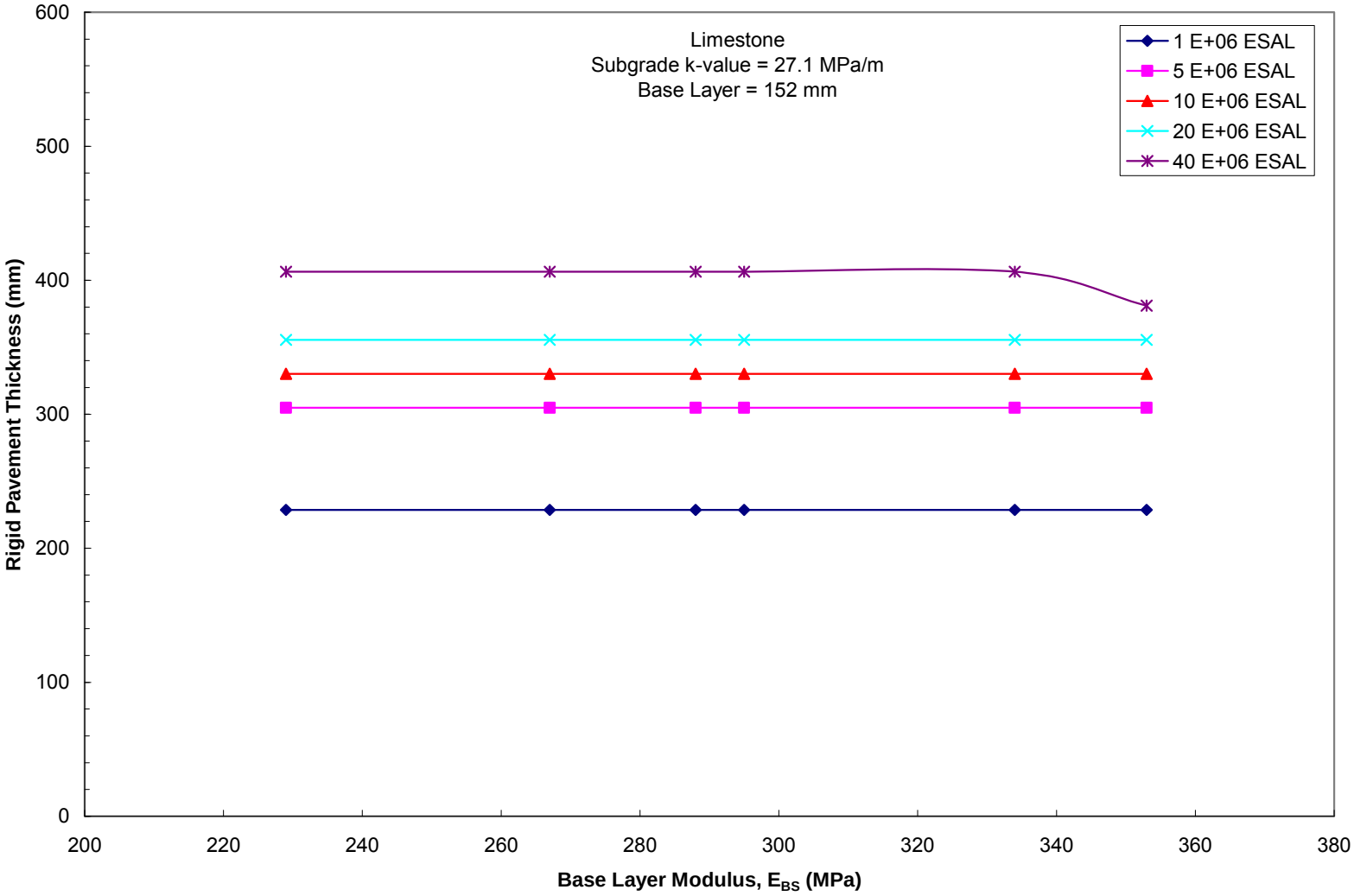


Figure 5.62 Design chart for determining rigid pavement thickness for city roads using limestone aggregate

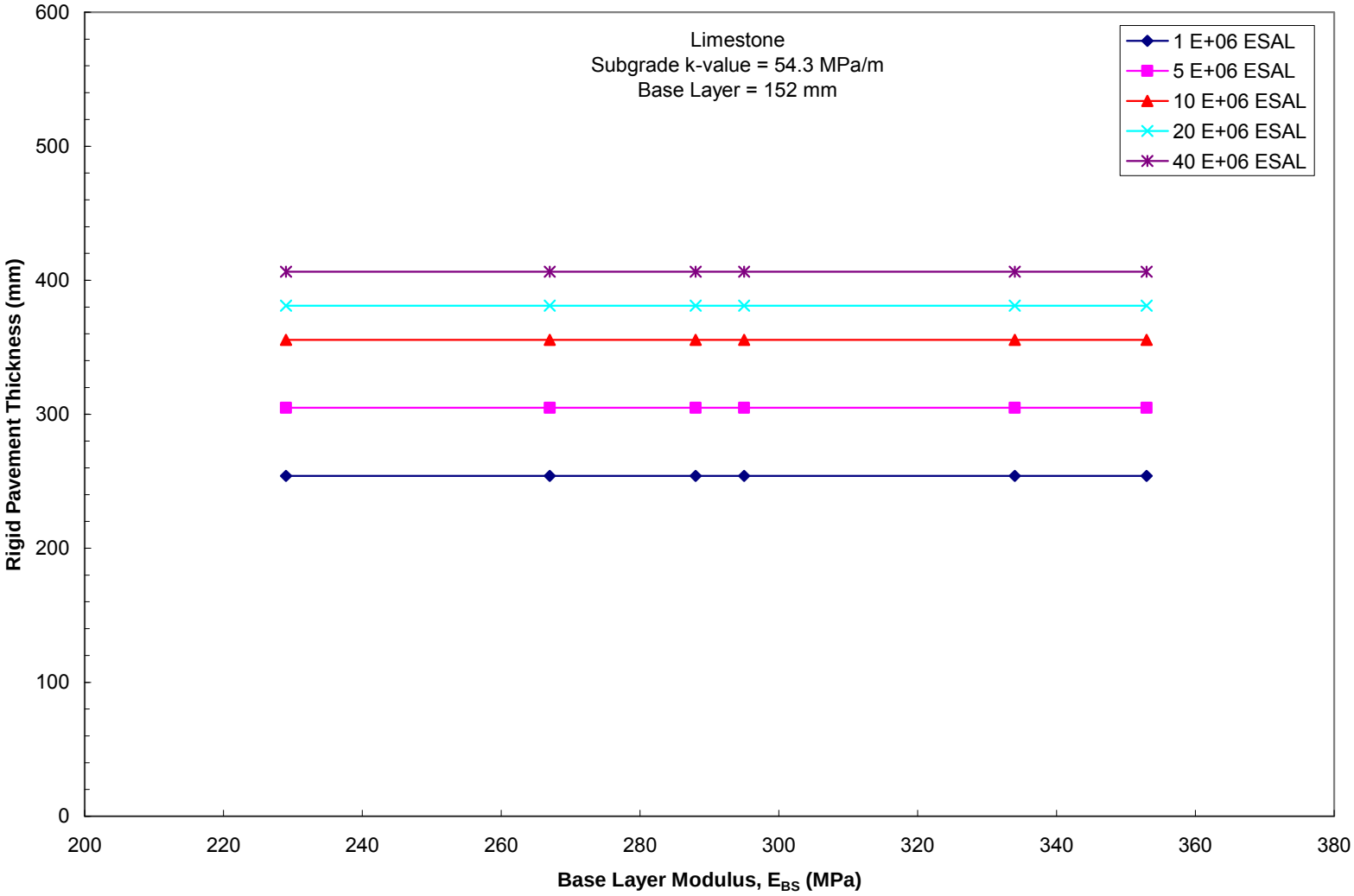


Figure 5.63 Design chart for determining rigid pavement thickness for city roads using limestone aggregate

## 5.6 Rigid Pavement Design Comparisons

A comparison of the rigid pavement design was conducted to determine the effects of the base layer thickness on the thickness of continuously reinforced concrete pavement. The average base moduli of 228 MPa (33,000 psi), 235 MPa (34,100 psi), and 294 MPa (42,800 psi) were used in the comparison of the rigid pavement design for RC1, RC2, and limestone, respectively. The average moduli were determined by averaging the six values of modulus of elasticity for each material provided on Table 5.1, 5.2, and 5.3. The rigid pavement design layer thickness was evaluated on the varying base layer thickness, traffic and subgrade conditions.

Figures 5.64 through 5.72 show the comparisons in continuously reinforced concrete pavement thickness required for the different base layer materials. The comparisons show that the base layer thickness had no effect on the thickness of CRCP pavement. The subgrade k-value also had no effect on the thickness of the pavement. The only notable effects on the thickness of the continuously reinforced concrete pavement occurred with the increase in traffic loading conditions.

The comparison shows that in rigid pavement design, the use of a granular base layer does not provide added benefits to the thickness of the CRCP pavement. The use of aggregates can be useful to improve subgrade conditions that will provide a better working subgrade for the construction of rigid pavement structures. The following figures demonstrate the results from the rigid pavement design comparisons of the recycled aggregates and limestone aggregates used in this study.

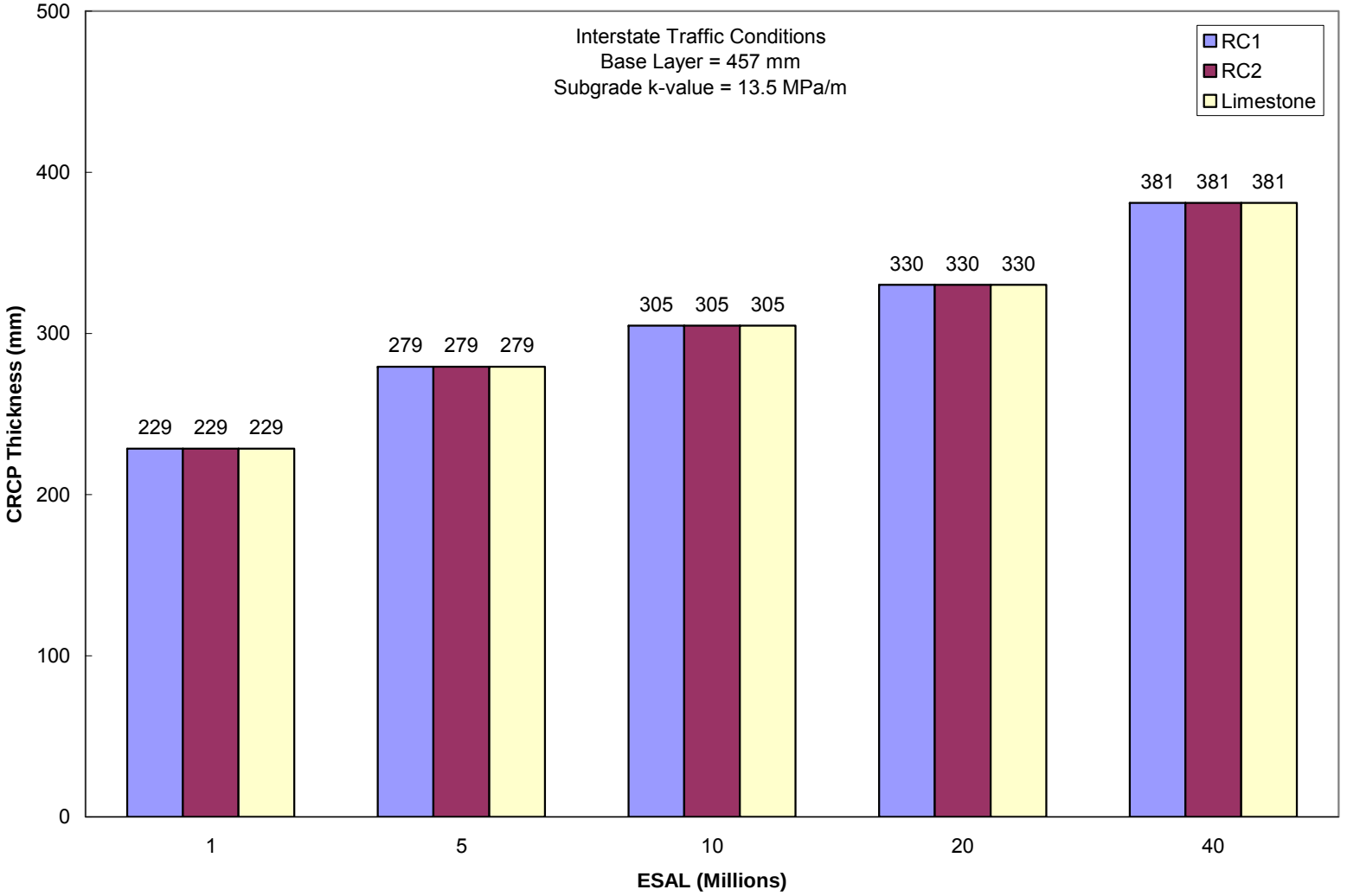


Figure 5.64 Comparison of CRCP pavement thickness with aggregate base layer for interstate traffic conditions

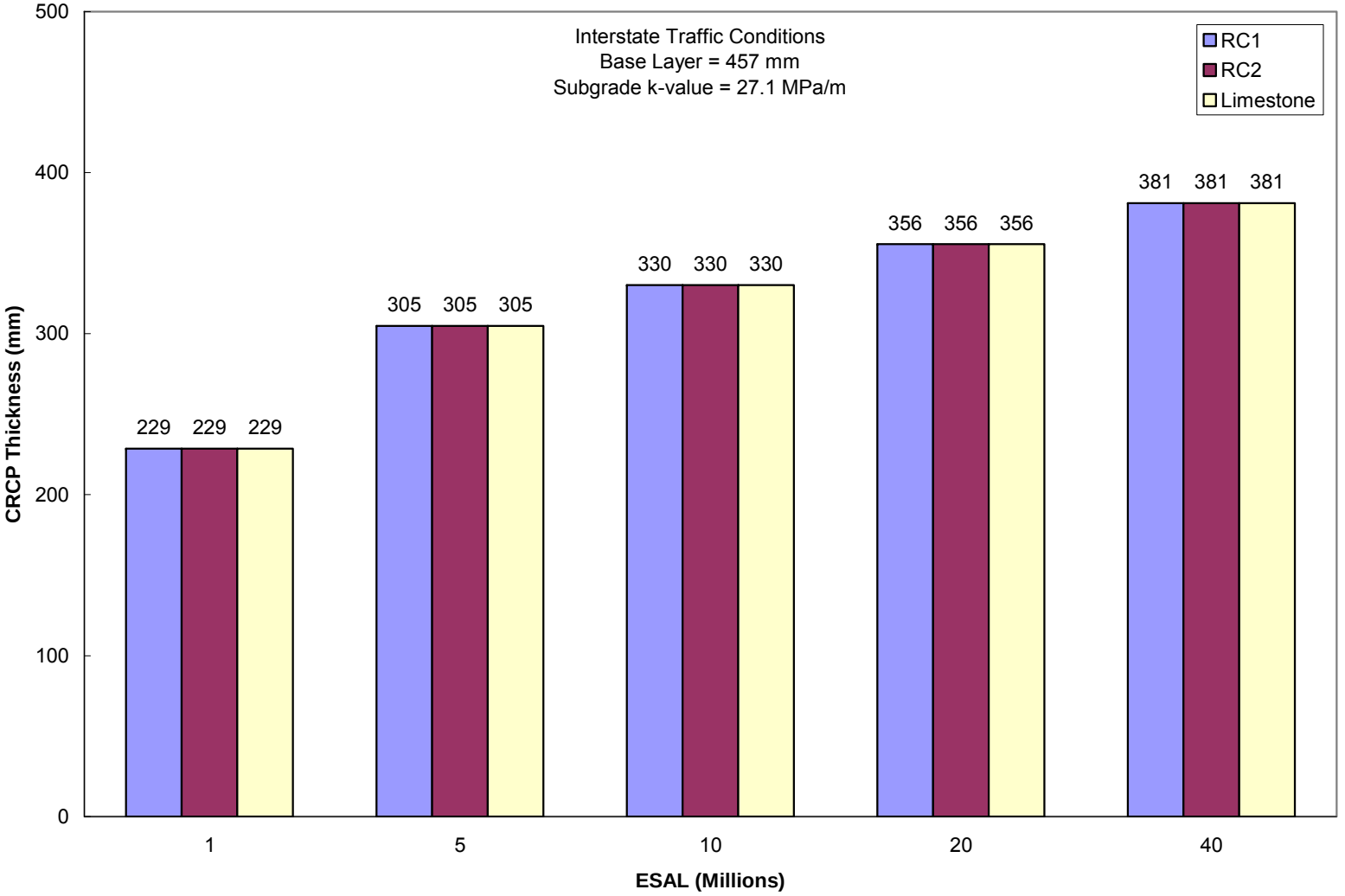


Figure 5.65 Comparison of CRCP pavement thickness with aggregate base layer for interstate traffic conditions

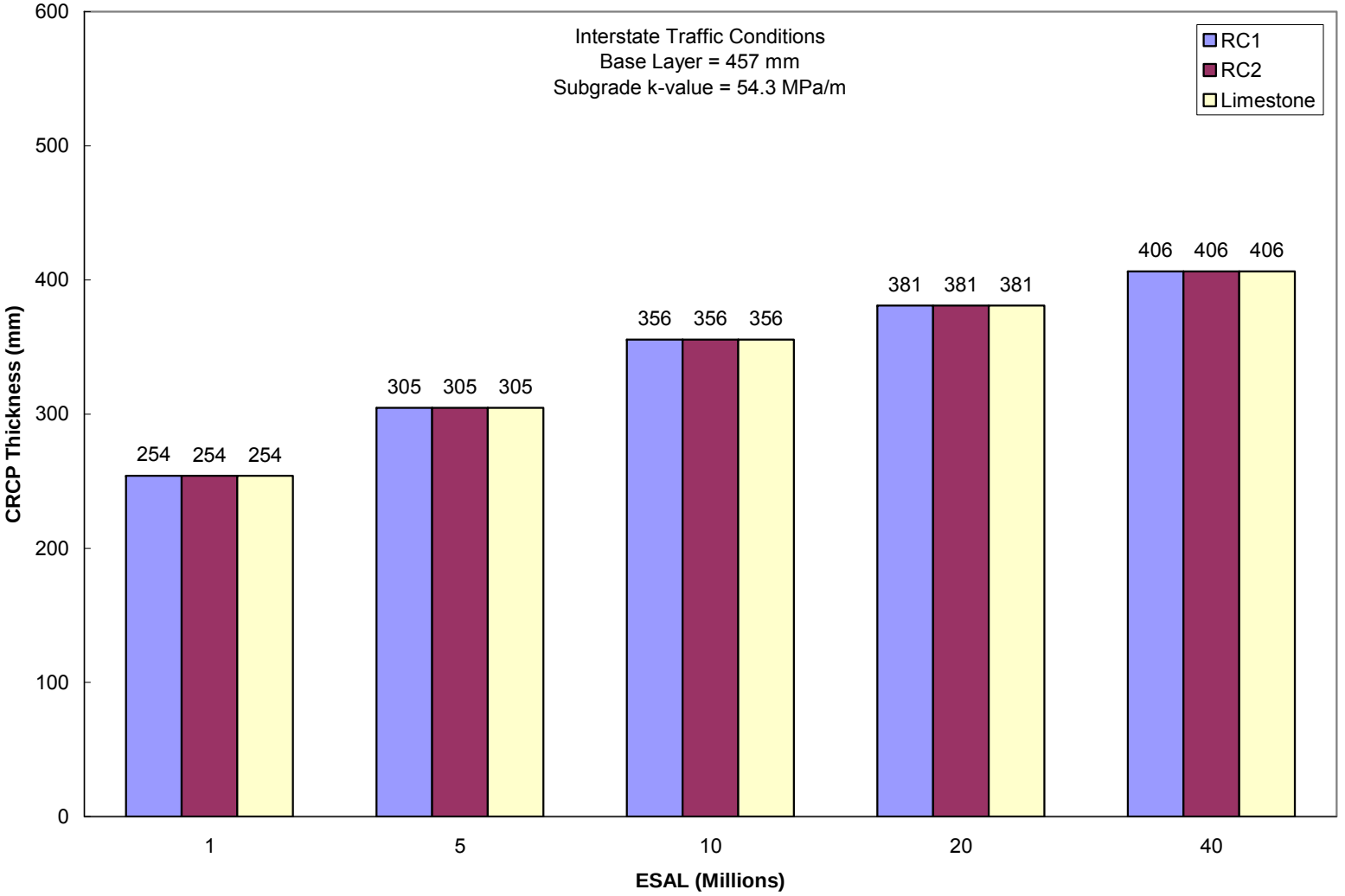


Figure 5.66 Comparison of CRCP pavement thickness with aggregate base layer for interstate traffic conditions

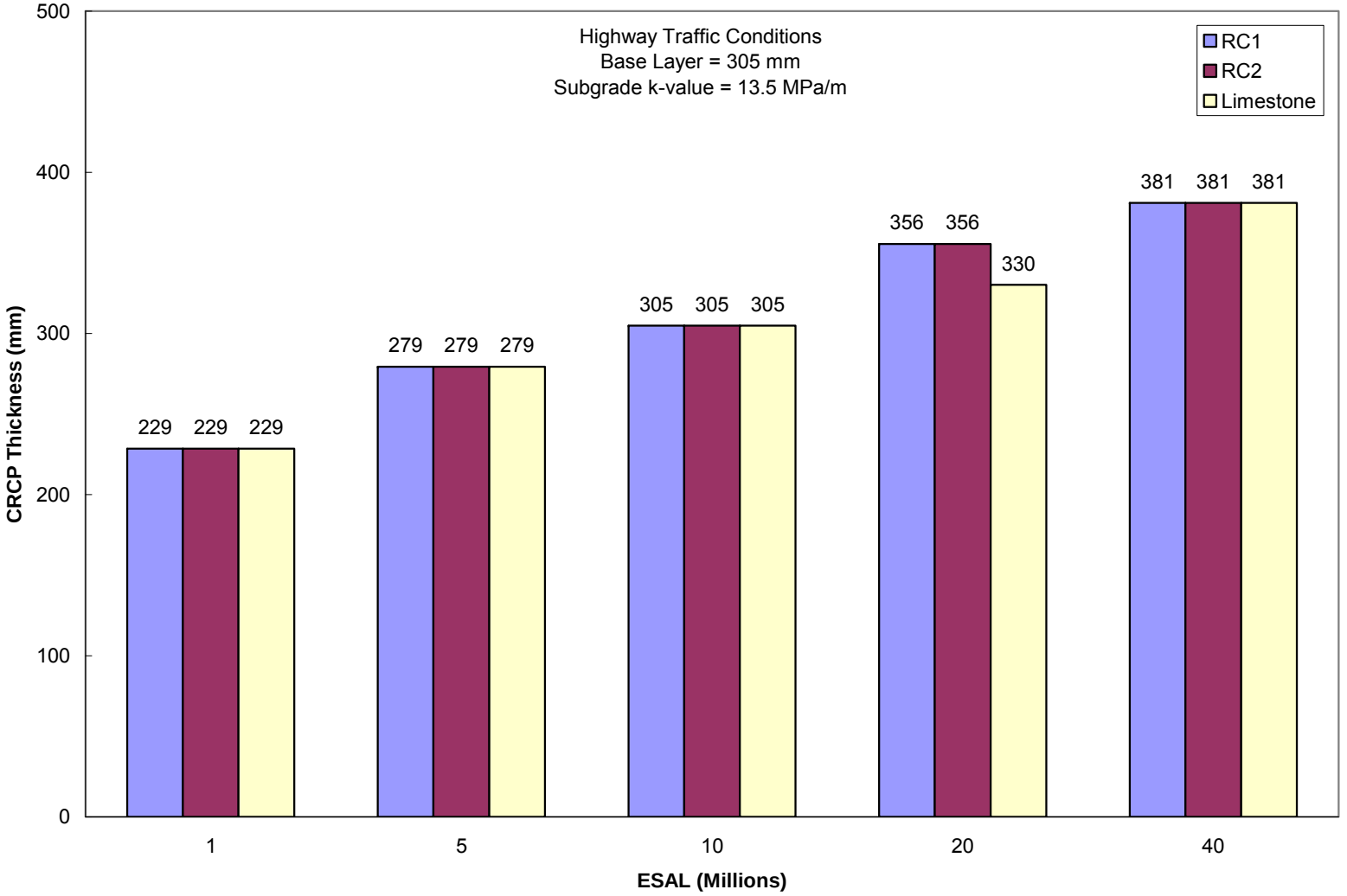


Figure 5.67 Comparison of CRCP pavement thickness with aggregate base layer for highway traffic conditions

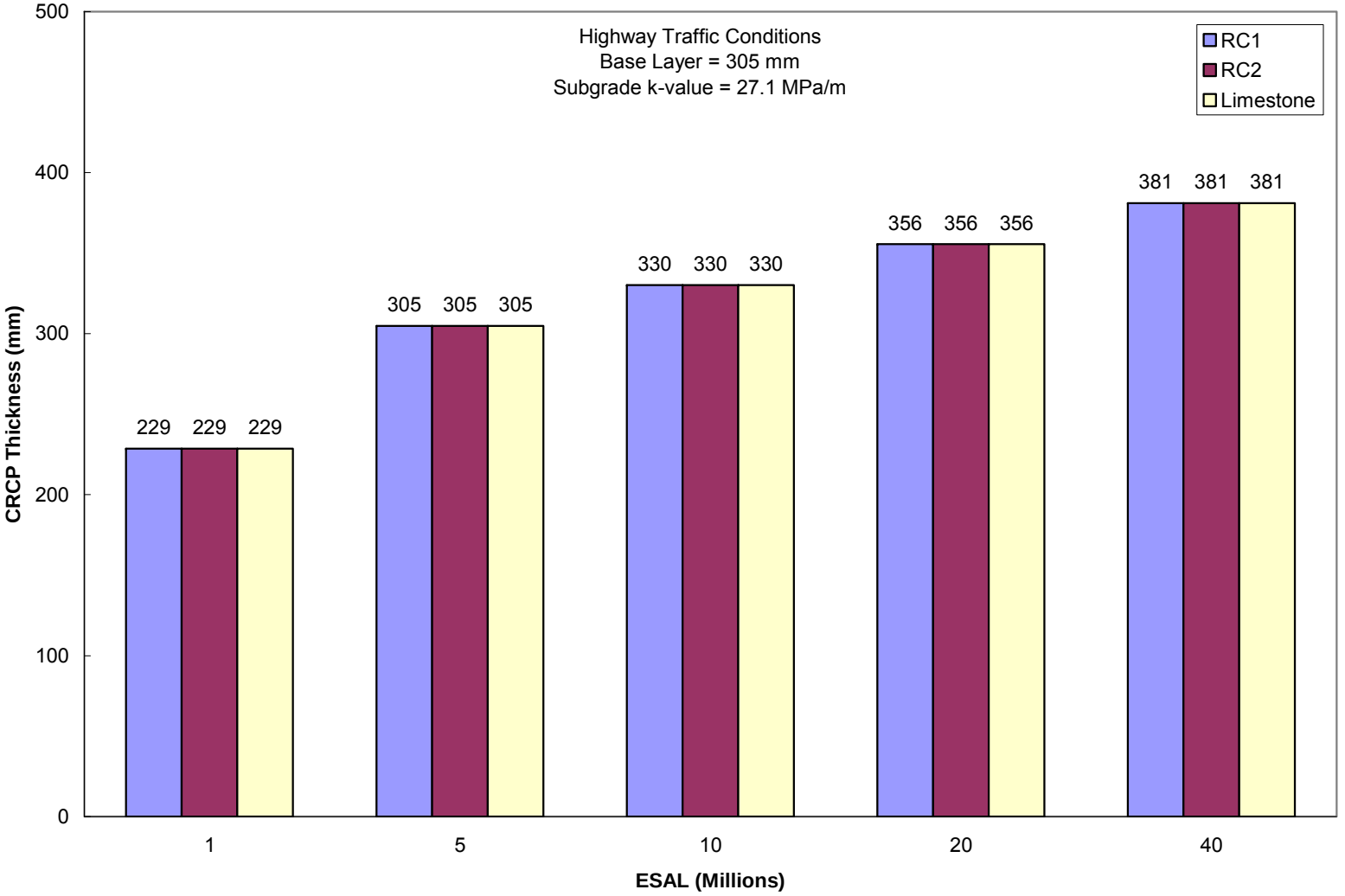


Figure 5.68 Comparison of CRCP pavement thickness with aggregate base layer for highway traffic conditions

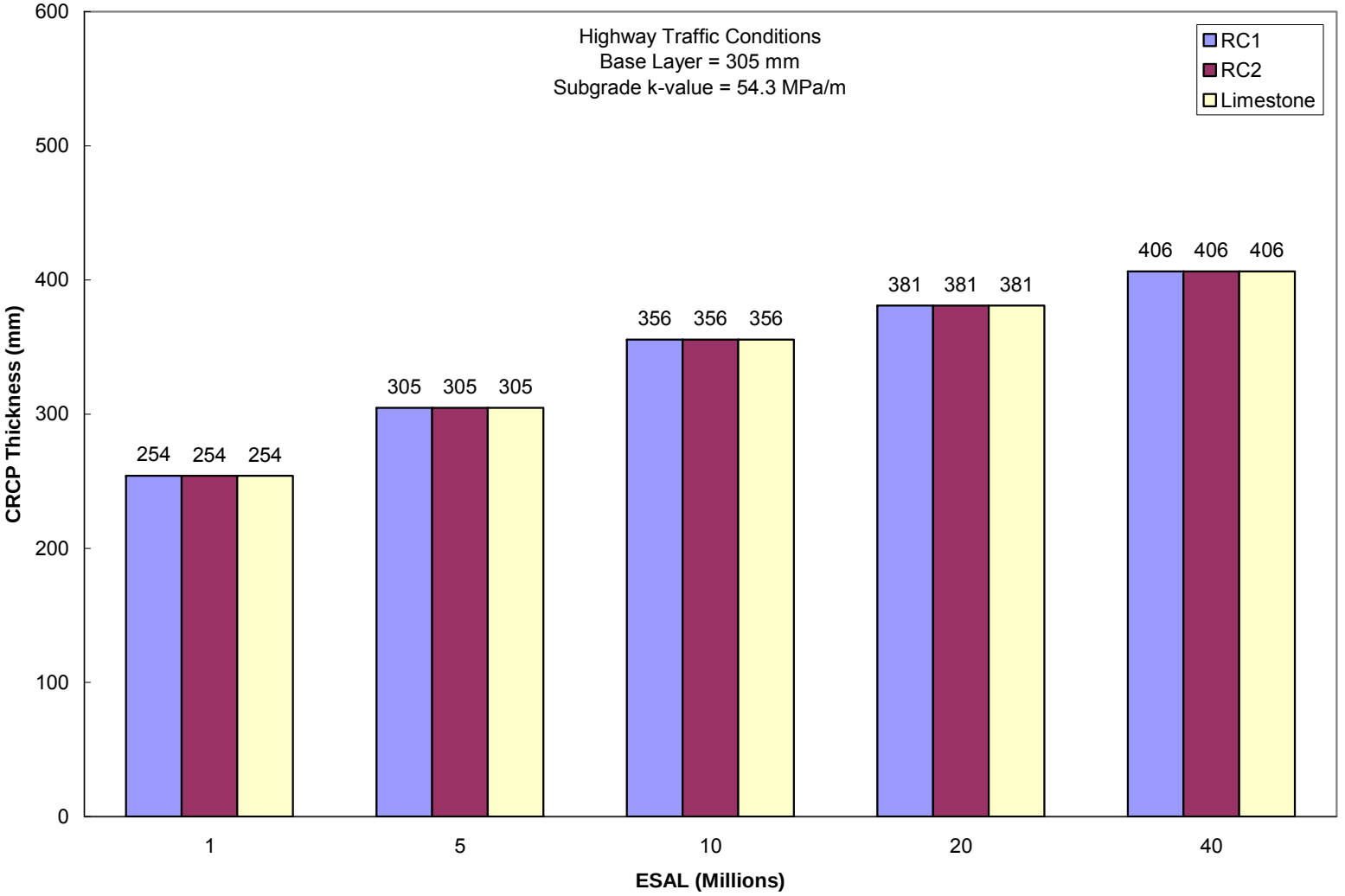


Figure 5.69 Comparison of CRCP pavement thickness with aggregate base layer for highway traffic conditions

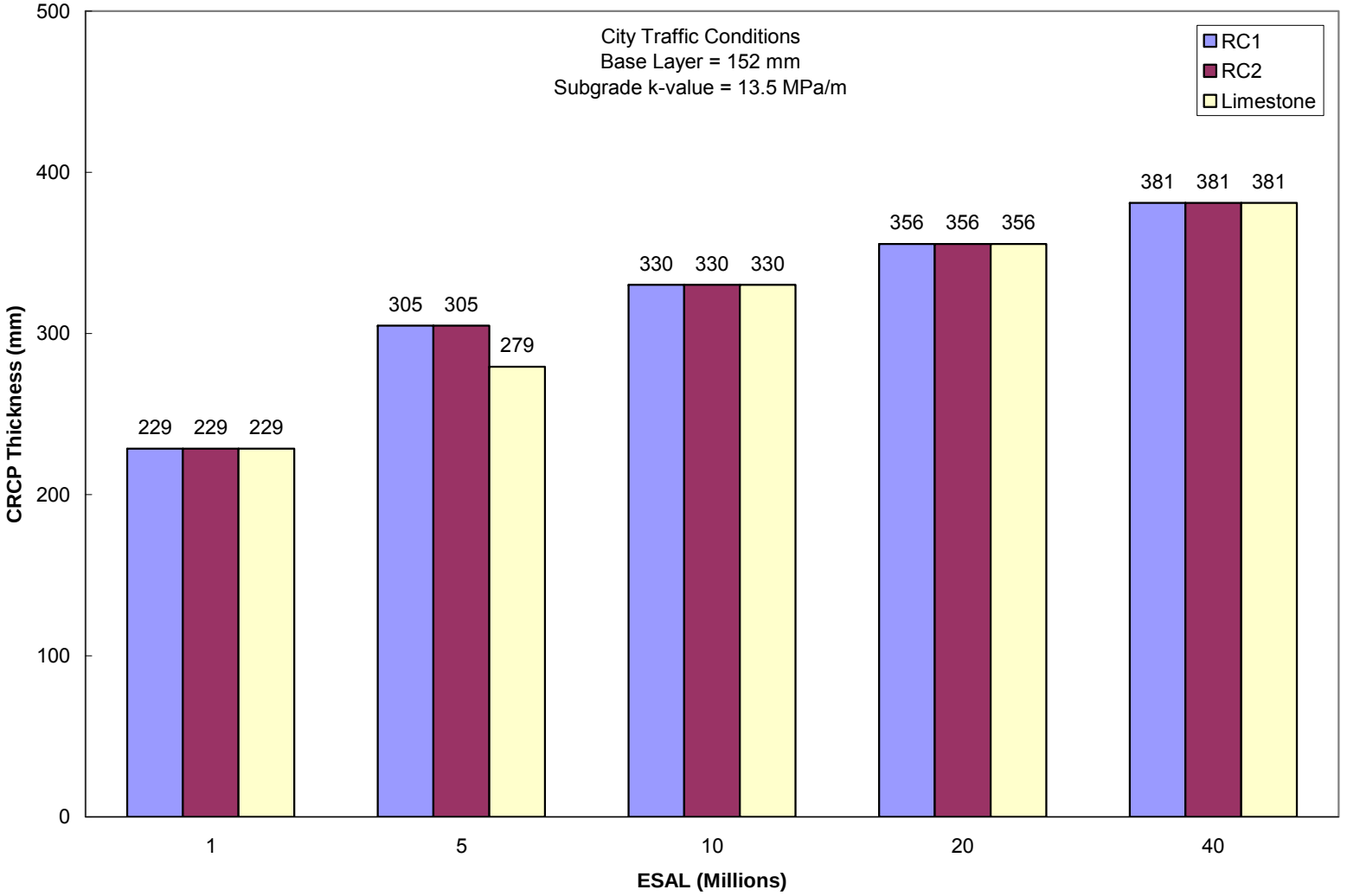


Figure 5.70 Comparison of CRCP pavement thickness with aggregate base layer for city traffic conditions

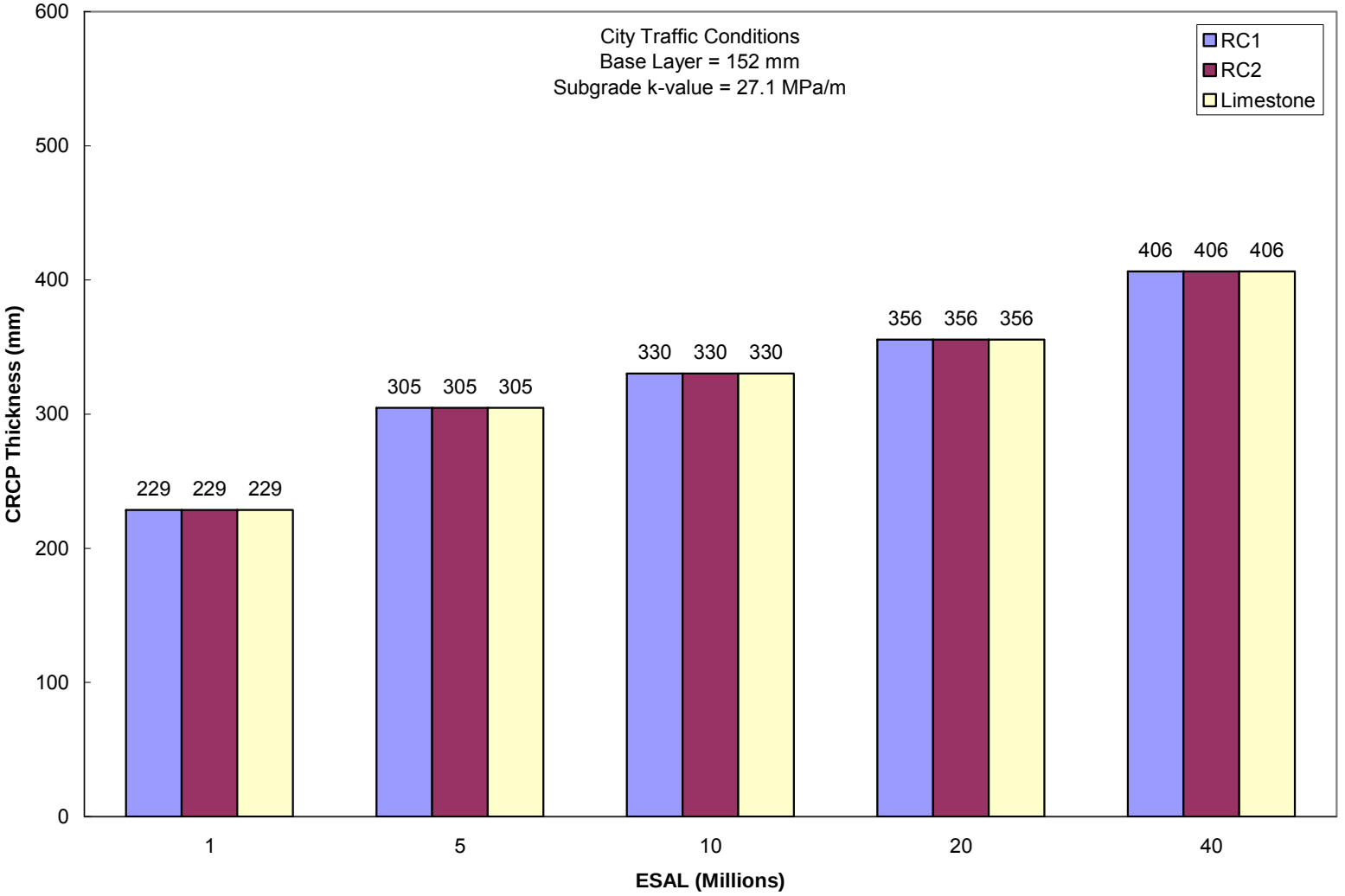


Figure 5.71 Comparison of CRCP pavement thickness with aggregate base layer for city traffic conditions

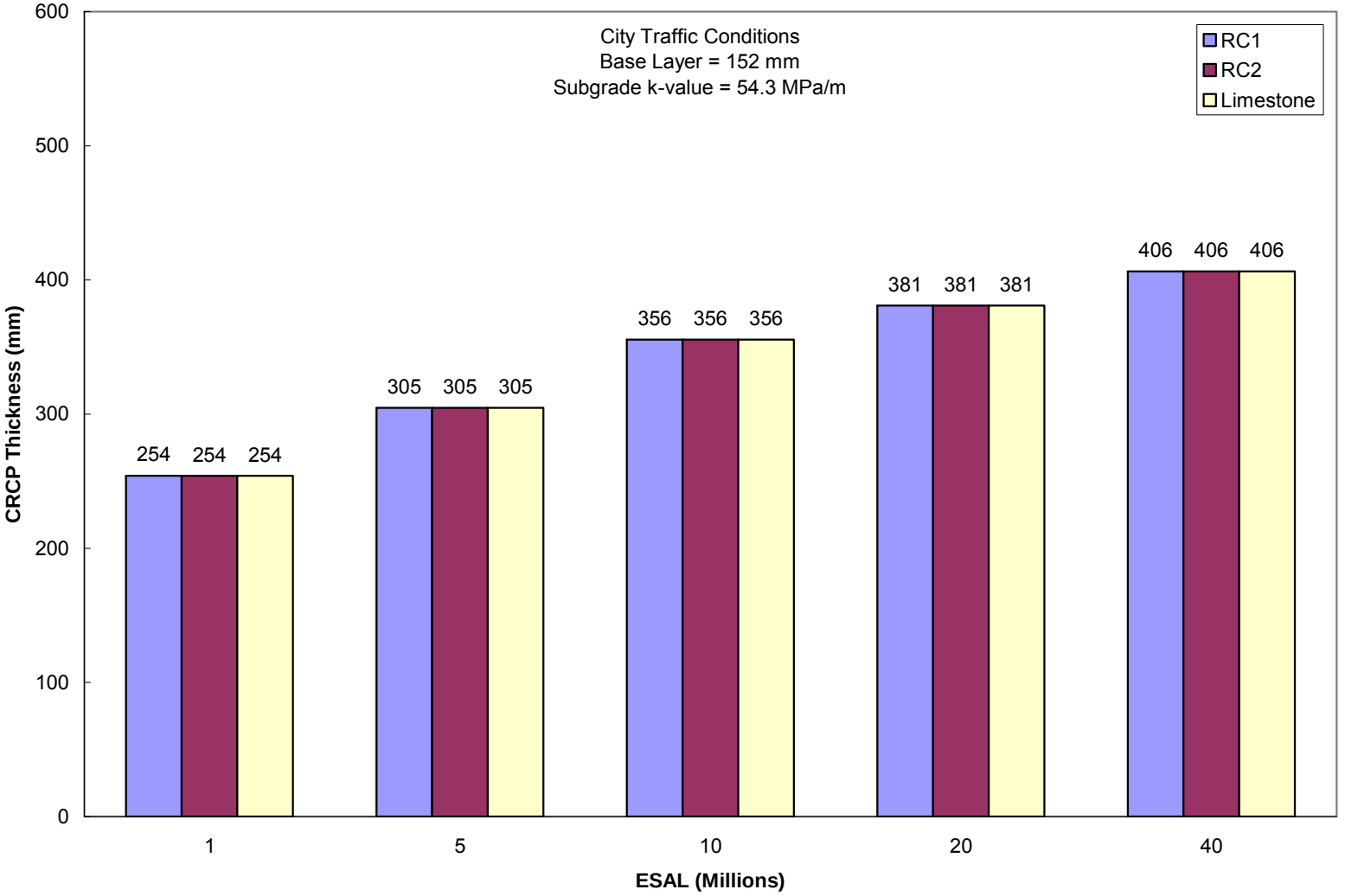


Figure 5.72 Comparison of CRCP pavement thickness with aggregate base layer for city traffic conditions

## 5.7 Benefits of Using Recycled Aggregates

The use of recycled aggregates in lieu of limestone aggregates shows to be a viable application of recycled materials. From the flexible and rigid design analyses performed, it is apparent that the use of recycled concrete aggregates can be substituted for natural limestone aggregates as a base layer without comprising the pavement structure. By incorporating recycled aggregates into the pavement structure, the demand on the natural aggregate supply is reduced. The reduction on the demand of natural aggregates has many indirect benefits. These benefits include a reduction of landfill space occupied by demolished concrete, the lessening of environmental impacts associated with the operation of a quarry, and the effects of transportation on costs and reduction of carbon dioxide emissions.

## 5.8 Summary

The flexible and rigid pavement structures have been developed using the test materials as base course layers. It is noted that the effects of the base course layers had a more significant affect on the flexible pavement structure. The thickness of the base layer was influenced by both the traffic loading and the subgrade condition. Both the recycled aggregates and limestone aggregates produced comparable results for flexible and rigid pavement. However, the rigid pavement structure was not affected by the base course layer thickness when using the procedure from the 1993 AASHTO *Guide for Design of Pavement Structures*.

# CHAPTER 6

# COST ANALYSIS

## 6.1 Introduction

This chapter presents an analysis to evaluate the construction costs involved with life cycle costs for the recycled concrete aggregates and natural limestone aggregates used as base materials for flexible and rigid pavements. The majority of the analysis focuses on the material and hauling costs. Since the means and methods for placement of the materials are similar, the overall material costs and delivery of materials is of major concern. The use of recycled aggregates on highway construction projects can reduce costs of construction and provide sustainability benefits. It is more advantageous to recycled materials on reconstruction projects that allow the necessary phasing. However, the use of recycled aggregates can only be considered sustainable if they perform at the same level as the primary aggregates.

## 6.2 Life Cycle Cost Analysis (LCCA)

In engineering, a life cycle cost analysis serves the purpose for performing an economic analysis on multiple or alternative designs. In this study, the materials used as base course in flexible and rigid pavements structures are the main focus. An approach is taken to demonstrate the cost savings that are achieved during construction by using recycled concrete aggregates over limestone aggregates. The necessary components for the cost analysis require an evaluation of labor and equipment costs, and of material and delivery costs for construction. These costs are combined and evaluated under the basis of a unit price.

The construction costs are estimated from historical data used in the Dallas/Fort Worth Area. The information provided includes production rates, labor and equipment costs, and

material costs. By using this information, a unit price can be established for the cost associated with the construction of the flexible base used in flexible and rigid pavements.

## 6.3 Construction Costs

In the construction of pavement structures, a flexible base is normally utilized to provide foundation support for flexible and rigid pavements. The flexible base materials are traditionally derived from natural aggregates. In the Dallas/Fort Worth area, these materials are of natural limestone. Like most quarries, the sources of the limestone are located outside the immediate Dallas/Fort Worth metro area. With this as a basis, an evaluation is performed to compare the use of natural limestone aggregates to that of recycled concrete aggregates.

The costs for the construction of a flexible base include the purchase of the materials from local suppliers, haul costs to the job site, and labor and equipment costs for processing the materials in accordance with Texas Department of Transportation Specifications (2004). The following table presents the comparison in cost of the delivered materials to jobsites within the city limits of Fort Worth and Dallas. The quarries in the Dallas-Ft Worth Area are located in Bridgeport, Texas. The material haul distance for the limestone aggregate is based from the quarry location from which the material originated to the city destination chosen. The recycled concrete aggregates source locations are assumed to be at a haul distance of thirty minutes from the project location. The assumption for the haul distance for recycled aggregate is based on the various locations of crushers in the Dallas-Fort Worth Area that process demolished concrete. The processing of the material is included and shown as two separate work activities: (1) Spread and Compact and (2) Finish Material. The spread and compact activity consists of labor and equipment costs involved in the placement of the material into its final compacted density. This is normally accomplished in lifts as directed by plans and specifications. The finish material activity consists of the labor and equipment costs associated with grading the final lift of compacted material. The production for the work is estimated for the processing of a

152.4 mm (6-inch) lift of material per square yard and 228.6 mm (9-inch) lift of material per square yard.

The following tables provide the total costs for the use of limestone aggregates and crushed concrete aggregates as flexible base. Table 6.1 provides the cost estimate of a 152.4mm (6-inch) layer of base aggregate and table 6.2 provides the cost estimate of a 228.6mm (9-inch) layer of base aggregate. The production of the Spread and Compact activity is estimated to be at 382.3 $m^3$ (500 CY) per Crew Shift. The production of the Finish Material activity is estimated to be at 1252.2 $m^2$ (1500 SY) per Crew Shift. The materials cost are based as per the average compacted maximum dry density determined in this study. Thus, the recycled concrete aggregates are based on an average of 18.86 $kN/m^3$ (120.0 $lb/ft^3$) and the limestone at an average of 22.24 $kN/m^3$ (141.5 $lb/ft^3$). Figure 6.1 presents the results of the cost comparisons for the materials.

Table 6.1 Cost for Use of Flexible Base per Square Meter

| Aggregate Type | Quarry Location | Project Location | Material Cost (Material & Haul) | (1) Spread and Compact (Labor & Equipment) | (2) Finish Material (Labor & Equipment) | Total Cost |
|---|---|---|---|---|---|---|
| | | | $/m$^2$ | $/m$^2$ | $/m$^2$ | $/m$^2$ |
| Limestone | Bridgeport, Texas | Dallas, Texas | $5.67 | $0.90 | $0.67 | $7.24 |
| Limestone | Bridgeport, Texas | Fort Worth, Texas | $5.13 | $0.90 | $0.67 | $6.70 |
| Crushed Concrete | Off-Site (30 Minutes) | Project Site | $3.55 | $0.90 | $0.67 | $5.12 |

Note: The costs provided are for a 152.4 mm (6-inch) lift of aggregate material.



Table 6.2 Cost for Use of Flexible Base per Square Meter

| Aggregate Type | Quarry Location | Project Location | Material Cost (Material & Haul) | (1) Spread and Compact (Labor & Equipment) | (2) Finish Material (Labor & Equipment) | Total Cost |
|---|---|---|---|---|---|---|
| | | | $/m$^2$ | $/m$^2$ | $/m$^2$ | $/m$^2$ |
| Limestone | Bridgeport, Texas | Dallas, Texas | $8.50 | $1.35 | $0.67 | $10.52 |
| Limestone | Bridgeport, Texas | Fort Worth, Texas | $7.70 | $1.35 | $0.67 | $9.72 |
| Crushed Concrete | Off-Site (30 Minutes) | Project Site | $5.37 | $1.35 | $0.67 | $7.39 |

Note: The costs provided are for a 228.6 mm (9-inch) lift of aggregate material.

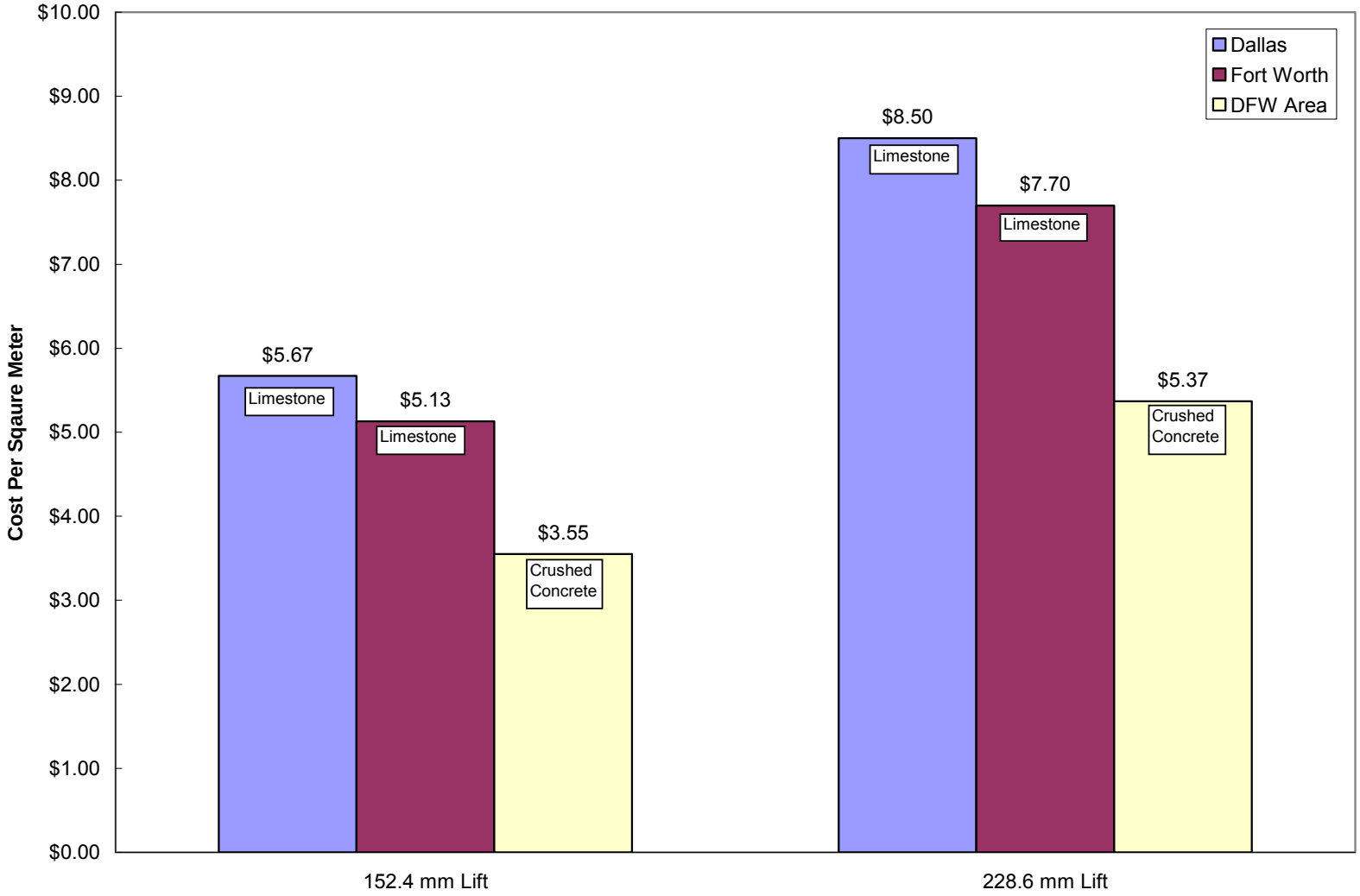


Figure 6.1 Comparison in cost of limestone and recycled aggregates as flexible base material

The determination of the cost for material, hauling, labor, and equipment were determined based on using historical data and current rates for the Dallas-Fort Worth Area. The costs provided for the 152.4mm (6-inch) and 228.6 mm (9-inch) lifts can be combined or used in multiples for determining the costs of thicker sections of flexible base. The finishing of the materials is not affected by thickness of the flexible base required. The final finish is only applied to the top layer for grading purposes and is contingent on surface area.

The following provides an example for determining and evaluating the construction costs for the use of limestone and crushed concrete aggregates as a flexible base. The assumptions are provided below for this example.

Flexible Pavement Design (Example)

Length of Project = 1609.34 m (5280 ft)

Width of Pavement = 7.32 m (24 ft)

Base Material Width 7.92 m (26 ft) (Base material is 1 ft wider on each side of pavement)

ESAL = 20,000,000 (Interstate Traffic Condition)

Subgrade Modulus = 34.47 MPa (5,000 psi)

Reliability = 95%

Standard Deviation = 0.45

Initial Serviceability = 4.5

Terminal Serviceability = 2.5

Asphalt Thickness (Surface) = 50.8 mm (2.0 inches) and structural coefficient of 0.44

Asphalt Thickness (Dense-Graded) = 203.2 mm (8.0 Inches) and structural coefficient of 0.40

A base modulus of 229 MPA (33,200 psi), yields a structural coefficient of 0.15 is used.

From the design tables provided in Chapter 5, a base thickness of 381 mm (15 inches) is required.

Table 6.3 Example Cost Analysis for Flexible Base Requirement

| Project Location | Base Material | Area of Base Material $m^2$ | Material Cost $/m^2$ | Total Material Cost $ | Spread & Compact Labor & Equipment $/m^2$ | Spread & Compact Total Cost $ | Finish Material Labor & Equipment $/m^2$ | Finish Material Total Cost $ | Total Cost $ |
|---|---|---|---|---|---|---|---|---|---|
| Dallas | Limestone | 12,753.73 | $14.17 | $180,720.35 | $2.25 | $28,695.89 | $0.67 | $8,545.00 | $217,961.24 |
| Ft Worth | Limestone | 12,753.73 | $12.83 | $163,630.36 | $2.25 | $28,695.89 | $0.67 | $8,545.00 | $200,871.25 |
| DFW Area | Crushed Concrete | 12,753.73 | $8.92 | $113,763.27 | $2.25 | $28,695.89 | $0.67 | $8,545.00 | $151,004.16 |

Note: The rates are for a 381.0 mm (15-inch) layer of flexible base. The rates were determined by combining the provided rates for a 152.4 mm (6-inch) and 228.6 mm (9-inch) layer. Project locations are considered to be at central location in the cities Fort Worth and Dallas for haul distances. Crushed concrete aggregate is considered to be a 30-minute haul distance.

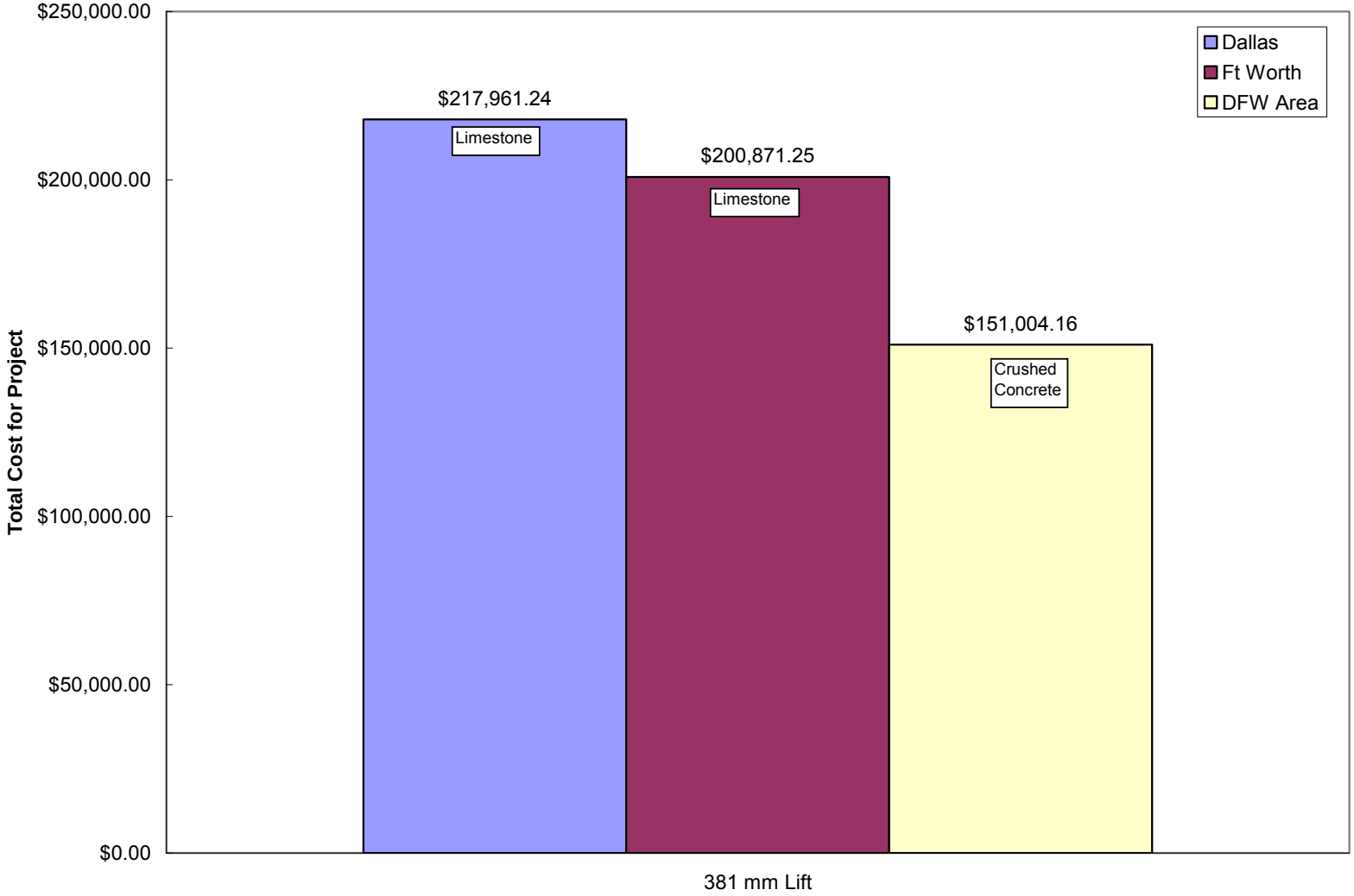


Figure 6.2 Total cost for flexible base construction of a 381.0 mm (15-inch) lift

The table provided models the costs for the construction of the flexible base in three scenarios. The first scenario presents the construction of the flexible base foundation in the City of Fort Worth with limestone aggregate. The second scenario presents the construction of the flexible base foundation in the City of Dallas with limestone aggregate. The third scenario presents the construction of the flexible base foundation at any location with a crushing plant producing recycling concrete aggregate within a thirty minutes haul distance. From the cost comparison of the materials, it can be seen that the use of recycled aggregates can yield substantial savings in construction. The substantial savings are mainly due to the higher cost of hauling from quarries that are located outside the city limits of the Dallas/Fort Worth metro area. The hauling distance from the quarries to the city of Fort Worth are normally one hour in each direction. The haul distance to the city of Dallas is normally a one and one-half hour from the same quarries. Currently, trucking costs average at $70/hr, therefore a haul cost of $140 per load of limestone aggregate is expected for the Fort Worth area and a $210 cost per load of limestone aggregate for the Dallas area. By using recycled aggregates from existing crushing plants or by setting a crushing plant up on site, the haul cost for recycled aggregates is maintained lower than that of limestone aggregates. A thirty minute haul distance will result in a one hour turnaround and a haul cost of $70 per load of recycled aggregates. It is clearly seen that the use of recycled aggregates that are locally produced can yield substantial savings. The savings presented in the sample project within the city of Fort Worth amounts to $49,867.09 or $10.26 per cubic meter. The savings presented in the sample project within the city of Dallas amounts to $66,957.08 or $13.78 per cubic meter. These savings can become more significant when they are applied to larger projects. This sample project consists only of 4,859 cubic meters of flexible base. In respect to many current projects, the sample project used in the cost analysis is considered to be a very small project. A larger project can easily produce more substantial and notable savings by using larger quantities of flexible base.

Typically, the life cycle cost studies include maintenance and rehabilitation costs over the design life period. Such analysis could not be conducted here as it was assumed that those

costs will be similar as material characterizations of this research showed similar properties between recycled and conventional aggregates. In addition, field trial sections are needed to further understand the behavior of these recycled aggregate bases to assess any distress patterns on these materials. Hence, the analysis did not account for maintenance and rehabilitation costs in the cost analysis.

## 6.4 Sustainability of Recycled Aggregates

In the past few years, changes in the environment have led to more effective management of environmental impacts. The World Commission on Environment and Development defines sustainable development as “Development that meets the needs of the present without comprising the ability of future generations to meet their own needs”. With this in mind, designers, engineers, owners, contractors, and manufacturers are encouraged to create a more sustainable built environment.

In construction, Life Cycle Analysis includes environmental impacts for use of raw material, and disposal of waste materials. In order to lessen the impacts of mining raw materials, the use of recycled and secondary aggregates make an important contribution in achieving sustainable construction by reducing and possibly, in some cases, eliminating the use of raw materials. This study has concentrated on the use of recycled materials derived from the crushing of Portland cement concrete that has reached its end of life.

The use of recycled aggregates from demolished concrete pavements and structures can reduce the vast quantities of limestone aggregate used for base materials of concrete pavements. As shown in this study, recycled aggregates can meet the requirements specified for flexible base in the State of Texas. By substituting recycled aggregates in place of limestone aggregates, a reduction in quarrying for raw materials can be achieved. With a reduction in quarrying of raw materials, the environmental concerns that surround existing quarries can be reduced or eliminated. In addition, the landfill space is increased due to less waste material from the demolition of concrete. This in turn, provides social benefits for the communities that

are affected by mining operations and landfill sites. The social benefits include the reduction in noise, less traffic congestion, and reduction of dust.

Similarly, there are many economic benefits in the use of recycled aggregates. Construction project costs can be lowered with the use of recycled aggregates as shown previously in this study. The costs can be lowered further by using mobile crushing plants that can be set on project sites that have an opportunity to reuse demolished concrete materials. By having on-site crushing plants, the haul truck traffic is reduced significantly to and from the quarry and landfill locations. By reducing the hauling traffic, the longevity of roads used by the trucks is improved and the maintenance is reduced. The lesser trucking will also reduce congestion of traffic and $CO_2$ emissions produced due to transporting distances.

## 6.5 Summary

The cost analysis conducted to compare the use of recycled concrete aggregates and limestone aggregates as a flexible has concurred that savings can be expected with the use of recycled aggregates. Maintenance and rehabilitation costs were not included in the analysis since both materials showed similar properties. Both materials used as a base course will provide similar performance in the field. Hence, costs of repairs are expected to be the same for both materials. The recycled aggregates produced from the crushing of demolished concrete provide sustainable construction benefits. These benefits produce positive impacts on engineering, economic, and social environments that help alleviate many of the challenges that are currently being encountered.

# CHAPTER 7

# SUMMARY OF FINDINGS AND FUTURE RESEARCH DIRECTIONS

## 7.1 Introduction

This chapter provides a comprehensive summary of laboratory data analyses of recycled crushed concrete aggregates and natural limestone aggregates found in the Dallas/Fort Worth Area. The aggregates were tested to determine their engineering properties and modeled for the use as base course in flexible and rigid pavement structures. With the information derived from the pavement design modeling, a cost analysis was conducted to compare the costs of recycled aggregates and natural limestone aggregates.

## 7.2 Summary of Findings

From the laboratory test results presented in Chapter 3, the crushed concrete aggregates were determined to have physical properties that are similar to those of the natural limestone aggregates. The sieve analysis showed that the gradation of crushed concrete can be provided to meet the specifications of flexible base requirements. The compacted optimum dry density achieved by using a modified proctor compaction effort showed that the recycled concrete aggregates are lighter than the limestone aggregates. The specific gravity also shows that the values of the crushed concrete aggregates are lower than the limestone aggregates. The liquid limit and plastic limit were close to zero for the crushed concrete aggregates. The pH test results show that the crushed concrete aggregates have a slightly higher pH value than the limestone. The pH value is considered to be alkaline. The linear bar shrinkage method results showed that the crushed concrete aggregates exhibit close to zero shrinkage strains, possibly due to low fine content.

The mechanical and flow properties of the crushed concrete aggregates and limestone aggregates were presented in Chapter 4. These properties included the unconfined compression strength, small strain shear modulus $G_{max}$, and hydraulic conductivity or permeability of the aggregates. The compacted specimens were tested at three compaction moisture contents that represent a dry, optimum, and wet of optimum moisture condition related to 95% and optimum dry conditions. The tests were conducted at 7-day and 28-day curing periods to monitor significant changes due to curing conditions.

The unconfined compression strengths were evaluated for the effects due to moisture content. The results for all three materials showed similar results. The results of the unconfined compression strengths show that the lowest strengths occur at the wet side of optimum moisture content condition. The low strengths are due to moderate softening of the bonds between particles. The highest strengths occurred at the optimum moisture content condition. The high strength at optimum moisture content was attributed to closer and compacted structures of the aggregate specimens.

The unconfined compression strengths evaluated at different curing periods show that the unconfined compression strength increases from 7 days to 28 days for the crushed concrete. The largest increase occurred in recycled concrete aggregate RC2. The increase of the unconfined compression strength in the crushed concrete was expected due to the activation of cementitious material that resulted from the crushing of Portland cement concrete. The unconfined compression strength of all three materials at a 28 day curing period yielded similar values. However, the increase of the unconfined compression strength of limestone aggregate was unexpected and requires further evaluation.

The small shear modulus strain $G_{max}$ was measured for all three materials at the different moisture contents. The evaluation of the results shows the crushed concrete aggregates values of $G_{max}$ to decrease with an increase in moisture while the highest value occurs at the dry of optimum moisture content condition. On the other hand, the limestone aggregates show an increase with the increase in moisture content from the dry of optimum to

optimum moisture content condition. On the wet side of optimum moisture content condition, the limestone aggregates decrease as the moisture content increases. In all materials, the lowest values of $G_{max}$ were measured at the wet of optimum moisture content condition. It was also noted that the $G_{max}$ values of the limestone aggregates were higher that those of the crushed concrete aggregates.

The small strain shear modulus $G_{max}$ was evaluated at 7-day and at 28-day curing periods. In all three materials, an increase in $G_{max}$ occurred from the 7-day to the 28-day curing period. An increase in $G_{max}$ values was expected for the recycled concrete aggregates but not in the limestone aggregates. As seen in the unconfined compression strength, the largest increases occurred for the recycled concrete aggregate RC2. The magnitude of the increase of $G_{max}$ that occurred from the 7-day to the 28-day curing period increased with moisture content. The higher increases in recycled concrete aggregate RC2 may be attributed to the cement content available in the material. Further, evaluation is required to evaluate the affects of cement content on the measured $G_{max}$ values. In relation to the increases, further evaluation is also required to explain the increase occurring in limestone aggregates.

The evaluation of the results of the hydraulic conductivity show that the recycled concrete aggregate materials decrease in permeability with an increase in moisture content. The decrease is seen in both recycled aggregates. Both recycled aggregates also yield similar values for the coefficient of permeability, k. The recycled concrete aggregates absorb more water than the natural limestone aggregates. The higher absorption of water is attributed to the cement paste found in the recycled concrete aggregates. In the limestone aggregate, the permeability increases with an increase in moisture content. The increase in permeability of the limestone aggregate at higher moisture coincides with the decrease in density.

The development of pavement models for flexible and rigid pavement structures required for the Modulus of Elasticity to be calculated from the measured small strain shear modulus $G_{max}$. The calculated Modulus of Elasticity for the base materials was used to determine the structural coefficient representing the granular base as required in flexible

pavement structures. The structural coefficients for the recycled concrete aggregates ranged from 0.14 to 0.17. The structural coefficients for the limestone aggregates ranged from 0.15 to 0.20. The smaller structural coefficients were found in the wet of optimum moisture content conditions while the larger structural coefficients were found at the optimum of moisture content condition. From the developed flexible pavement structures, the recycled concrete aggregates produce comparable thickness requirements for base layers as to that of the limestone aggregate. It was noted that all three materials had a decrease in base layer thickness with an increase of the subgrade modulus or with a decrease in traffic volume. The base course materials improve the design of a flexible pavement structure in poor subgrade conditions.

For the design of rigid pavement structures, the recycled concrete aggregates and limestone aggregates were modeled as base course layers. From the developed rigid pavement design for varying traffic and materials conditions, it was concluded that the base course of recycled concrete aggregates and limestone aggregates produced similar results. However, the use of all three as base course layers in rigid pavement had no significant effect on the thickness of concrete pavement. The base course affects only the effective modulus of subgrade. The modulus of subgrade is known to not have significant influence on the required on the thickness of concrete pavement.

In order to provide a practical application of the influence of using these materials as base course layers on flexible pavements, a construction cost analysis was performed on the use of recycled concrete aggregates versus that of natural limestone aggregates. The costs for the placement of the materials were found to be identical for each material. The most significant difference was found to be in the cost of the materials to be used as base course in the pavement structure. The reason for the difference in costs of the materials is mainly due to the transportation involved in delivery of materials to project sites. The Dallas/Fort Worth area has one particular location in which most granular aggregates are produced. The quarries from this location are at a minimum of one hour haul distance from the cities of Fort Worth and Dallas. Unlike the quarry locations, there are several concrete crushing plants throughout the

Dallas/Fort Worth area. The locations of these plants allow for transportation costs to be at least 50% less than that from the quarries. The results from much lower transportation costs can have a significant impact on the cost of construction. With the proven tests results, the durability of the recycled concrete aggregates are expected to perform comparably to the limestone aggregates. The use of recycled concrete aggregates from demolished concrete pavements and structures in turn can lessen the environmental impacts and improves the chances of achieving sustainable construction.

## 7.3 Future Recommendations

The following recommendations will further the development and understanding of the use of recycled concrete aggregates as base courses in pavement structure.

1. Field studies for test pavement sections are recommended for the validation of laboratory findings and development of database for pavement modeling.
2. Test pavements sections should be developed to allow a performance comparison between natural aggregates and recycled concrete aggregates as base courses.
3. Resilient moduli and structural coefficients should be evaluated by performing Falling Weight Deflectometer (FWD) studies on pavement test sections using recycled aggregates as base courses in pavement structure.
4. Investigations should be conducted to determine the effects of reactivated cement on the unconfined compression strength and small strain shear modulus of recycled concrete aggregates.

# APPENDIX A

## PHOTOS OF LABORATORY SAMPLES AND TESTING

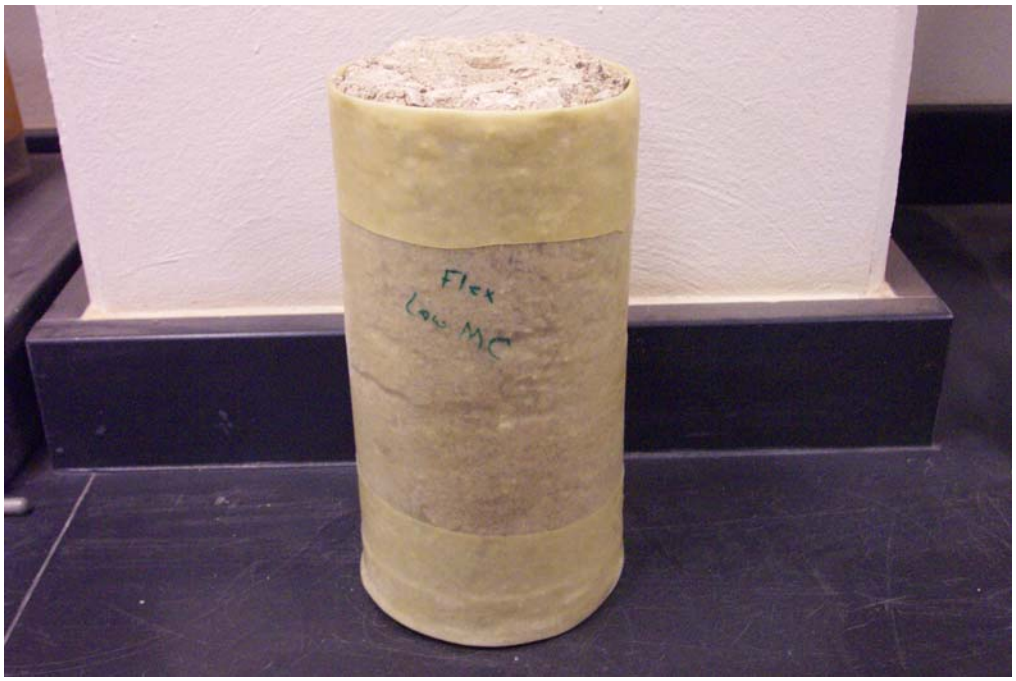

Figure A1 Original sample size chosen (152.4 mm diameter x 304.8 mm length)


Figure A2 Secondary sample size chosen (101.6 mm diameter x 231.8 mm)

Figure A3 Samples size used for testing (101.6 mm diameter x 120.7 mm length)


Figure A4 Recycled concrete aggregate RC1 after unconfined compression strength test


Figure A5 Recycled concrete aggregate RC2 after unconfined compression strength test


Figure A6 Limestone aggregate test sample after unconfined compression strength test

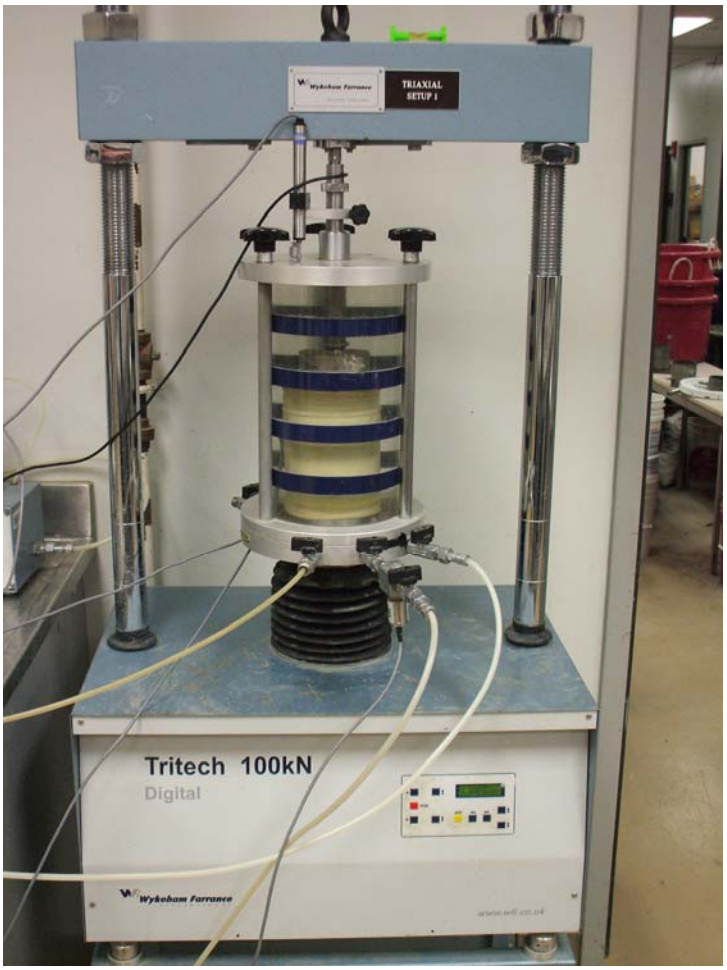

Figure A7 Bender element testing in confined triaxial setup

# APPENDIX B

## PHOTOS OF CONCRETE RECYCLING EQUIPMENT


Figure B1 Portable and mobile crushing plant (www.txlsm.com)

Figure B2 Portable and mobile crushing equipment (www.concreterecycling.org)

# REFERENCES


Abou-Zied, M.N. and McCabe, S.L. (2002). Feasibility of waste concrete as recycled aggregates in construction. Waste Management and the Environment, September, pp 537-546.

American Association of State Highway Transportation Official. (1993). *AASHTO Guide for Design of Pavement Structures*, American Association of State Highway and Transportation Officials, Washington, D.C.

Arm, M. (2001). Self-cementing properties of crushed demolished concrete in unbound layers: results from triaxial tests and field tests. Waste Management, Vol. 21, No. 3, pp 235-239.

Arulnathan, R., Boulanger, R.W., and Riemer, M.F. (1998). Analysis of bender element tests. Geotechnical Testing Journal, Vol. 21, No. 2, pp 120-131.

Aqil, U., Tatsuoka, F., and Uchimura, T. (2005). Strength and deformation characteristics of recycled concrete aggregate in triaxial compression. Geotechnical Special Publication, No. 130-142, pp 2231-2240.

Baghdadi, Z.A., Fatani, M.N., and Sabban, N.A. (1995). Soil modification by cement kiln dust. Journal of Materials in Civil Engineering, Vol. 7, No. 4, pp 218-222.

Baig, S. and Nazarian, S. (1995). Determination of resilient modulus of subgrades using bender elements. Transportation Research Record, No. 1504, pp 79-86.

Benson, C.H. and Khire, M.V. (1994). Reinforcing sand with strips of reclaimed high-density polyethylene. Journal of Geotechnical Engineering, Vol. 120, No. 5, pp 838-855.

Cervantes, V. and Roesler, J. (2007). Ground granulated blast furnace slag. Center of Excellence for Airport Technology. Technical Note No. 35.

Chini, A.R. and Monteiro, F.M.B.R. (1999). Use of recycled concrete aggregate as a base course. ASC Proceedings of the 35th Annual Conference, April, pp 307-318.

Dyvik, R. and Madshus, C. (1986). Laboratory measurements of $G_{max}$ using bender elements. Publication – Norges Geotechnical Institute, No. 161, pp 1-7.

Eldin, N.N., and Senouci, A.B. (1992). Use of scrap tires in road construction. Journal of Construction Engineering and Management, Vol. 118, No. 3, pp 561-576.

Federal Highway Administration (FHWA). Transportation Applications of Recycled Concrete Aggregate. State of the Practice National Review, September 2004.

Hansen, K.R., McGennis, R.B., Prowell, B.D., and Stonex, A. (2000). Current and future uses of non-bituminous components of bituminous paving mixtures. Transportation in the New Millennium TRB A2D02, Washington, DC, USA.

Hossein, G., Poorebrahim, G., and Gray, D.H. (2004). Soil reinforcement with recycled carpet wastes. Waste Management and Research, Vol. 22, No. 2, pp 108-114.

Hoyos, L.R., Ordonez, C.A., Puppala, A.J., and Hossain, MD.S. (2008). Engineering characterization of cement-fiber treated RAP aggregates. *Proceedings of Sessions of GeoCongress*, ASCE Geo-Institute Geotechnical Special Publication, No. 179, pp 613-621.

Huang, Y., Bird, R.N., Heidrich, O. (2007). A review of the use of recycled solid waste materials in asphalt pavements. Resources, Conservation and Recycling, Vol. 52, No. 1, pp 58-73.

Jovicic, V., Coop, M.R., and Simic, M. (1996). Objective criteria for determining $G_{max}$ from bender element test. Geotechnique, Vol. 46, No. 2, pp 357-362.

Kung, T.C., Ou, C.Y., and Hsieh, P.G. (2004). Measurement of shear modulus of soil using bender elements. Geotechnical Engineering, Vol. 35, No. 1, pp 1-7.

Landers, K. (2004). Selecting a portable concrete crushing plant. Better Roads, Vol. 74, April, pp 60-67.

Leong, E.C., Yeo, S.H., and Rahardo, H. (2005). Measuring shear wave velocity using bender elements. Geotechnical Testing Journal, Vol. 28, No. 5, pp 488-498.

Lim, S., Kestner, D., Zollinger, D.G., and Fowler, D.W. (2003). Characterization of crushed concrete materials for paving and non-paving applications. pp 1-162.

Lohani, T.N. and Imai, G. (1999). Determination of shear wave velocity in bender element test. Procedding of Earthquake Geotechnical Engineering, Rotterdam, pp 101-106.

Merritt, F.S., Loftin, M.K., and Ricketts, J.T. (Eds.). (1996). *Standard Hanbook for Civil Engineers,* 4th Ed., New York, McGraw-Hill.

Minnesota Department of Transportation (2007). Pavement Design Manual.

Nash, P.T., Jayawickrama, P., Tock, R.W., Senadheera, S., Viswanathan, K., and Woolverton, B. (1995). Use of glass cullet in roadway construction. Texas Tech University College of Engineering Research Reports 0-1331-1 and 0-1331-3.

Nataatmadja, A. (1992). Resilient modulus of granular materials under repeated loading. Proc., 7th Int. Conf. on Asphalt Pavements, Univ. of Nottingham, Nottingham, U.K., 1, pp 172-185.

Nataatmadja, A. and Tan, Y.L. (2001). Resilient response of recycled concrete road aggregates. Journal of Transportation Engineering, Vol. 127, No. 5, pp 450-453.

Poon, C.S. and Chan, D. (2006). Feasible use of recycled concrete aggregates and crushed clay brick as unbound road sub-base. Construction and Building Materials Vol. 20, No. 8, pp 578-585.

Putnam, B.J. and Amirkhanian, S.N. (2004). Utilization of waste fibers in stone matrix asphalt mixtures. Resources, Conservation and Recycling, Vol. 42, No. 3, pp 265-274.

Rathje, E., Trejo, D., and Folliard, K. (2006). Potential use of crushed concrete and recycled asphalt pavement as backfill for mechanically stabilized earth walls. Center for Transportation Research, The University of Texas at Austin, Project 0-4177.

Recycling Technology Assistance Partnership (ReTAP). Quality control for recycled concrete as a structural fill material. January 1998.

Richardson, B.J.E. and Jordan, D.O. (1994). Use of recycled concrete as a road pavement material within Australia. Proceeding 17th ARRB Conference, Vol. 17, No. 3, Australia Road Research Board Ltd., Nunawading, Australia, pp 213-228.

Schroeder, R.L. (1994). The use of recycled materials in highway construction. Road & Transport Research, Vol. 3, No. 4, pp 12-24.

Senior, S. (1992). New development in specification for road base materials in Ontario. 45th Canadian Geotechnical Conference, Canadian Geotechnical Society, pp 99-1 to 99-9.

Shirley, D.J. (1978). An improved shear wave transducer. Journal of the Acoustical Society of America, Vol. 63, No. 5, pp 1643-1645.

Shirley, D.J. and Hampton, L.D. (1978). Shear-wave measurements in laboratory sediments. Journal of the Acoustical Society of America, Vol. 63, No. 2, pp 607-613.

Takallou, H.B. and Takallou, M.B. (1991). Recycling tires in rubber asphalt paving yields cost, disposal benefits. Elastomerics, Vol. 123, No. 7, pp 19-24.

Terrell, R.G., Cox, B.R., Stokoe, K.H., Allen, J.J., Lewis, D. (2003). Field investigation of the stiffness of unbound aggregate base layers in inverted flexible pavements. Transportation Research Board: Journal of the Transportation Research Board, Vol. 1837, pp 50-60.

Texas Department of Transportation (2001). Use of recycled portland cement concrete fines in TxDOT applications, Report 7-4954-1.

Texas Department of Transportation (2004). Standard Specifications for Construction and Maintenance of Highways, Streets, and Bridges.

Viggiani, G. and Atkinson, J.H. (1995). Interpretation of bender element tests. Geotechnique, Vol. 45, No. 1, pp 149-154.

Wang, Y., Wu, H.C., and Li, V.C. (2000). Concrete reinforcement with recycled fibers. Journal of Materials in Civil Engineering, Vol 12, No. 4, pp 314-319.

## BIOGRAPHICAL INFORMATION

Juan Bosquez Jr. was born in Carrizo Springs, Texas. He graduated from Texas A&I University, Kingsville, Texas with a Bachelor's of Science in Civil Engineering in 1992. He also graduated from Texas A&M University-Kingsville, Kingsville, Texas with a Master's of Science in Environmental Engineering in 1995. Since then, he has worked as a construction engineer predominantly in highway construction projects. While continuing to work, he joined The University of Texas at Arlington to pursue his doctorate in Civil Engineering. During the course of his study, his research work was predominantly in areas related to the use of recycled materials as construction materials.